Computerised Accelerometric Machine Learning Techniques and Statistical Developments for Human Balance Analysis

Oseikhuemen Osemekhian Davis Ojie

A thesis submitted in partial fulfilment of the requirements of
Sheffield Hallam University
for the degree of Doctor of Philosophy

January 2022

Declaration

I hereby declare that:

1. I have not been enrolled for another award of the University, or other academic or professional organisation, whilst undertaking my research degree.

2. None of the material contained in the thesis has been used in any other submission for an academic award.

3. I am aware of and understand the University's policy on plagiarism and certify that this thesis is my own work. The use of all published or other sources of material consulted have been properly and fully acknowledged.

4. The work undertaken towards the thesis has been conducted in accordance with the SHU Principles of Integrity in Research and the SHU Research Ethics Policy.

5. The word count of the thesis is 68484.

Name	Oseikhuemen Osemekhian Davis Ojie
Award	Ph.D
Date of Submission	January 2022
Faculty	College of Business, Technology and Engineering
Director(s) of Studies	Professor Reza Saatchi

Abstract

Balance maintenance is crucial to participating in the activities of daily life. Balance is often considered as the ability to maintain the centre of mass (COM) position within the base of support. Primarily, to maintain balance, reliance is placed on the balance related sensory systems i.e., the visual, proprioceptive and vestibular. Several factors can affect a person's balance such as neurological diseases, ageing, medication and obesity etc. To gain insight into the balance operations, studies rely on statistical and machine learning techniques. Statistical techniques are used for inferencing while machine learning techniques proved effective for interpretation.

The focus of this study was on the issues encountered in human balance analysis such as the quantification of balance by relevant features, the relationships between COM and ground projected body sway, the performance of various sensory systems in balance analysis, and their relationships between the directions of body sway (i.e., mediolateral (ML) and anterior-posterior (AP)). A portable wireless accelerometry device was developed, balance analysis methods based on the inverted pendulum were devised and evaluated for their accuracy and reliability against a setup designed to allow manual balance measurements. Balance data were collected from 23 healthy adult subjects with the mean (standard deviation) of the age, height and weight: 24.5 (4.0) years, 173.6 (6.8) cm, and 72.7 (9.9) kg respectively. The accelerometry device was attached to the subjects at the approximate position of the illac crest, while they performed 30 seconds trials of the four conditions associated with a standard balance test called the modified Clinical Test of Sensory Interaction and Balance (mCTSIB). These required standing on a hard (ground) surface with the eyes open, standing on hard surface with the eyes closed, standing on a compliant surface (sponge, 10 cm thick) with the eyes open and standing on a compliant surface with the eyes closed. Statistical and machine learning techniques such as t-test, Wilcoxon signed-rank test, the Mann-Whitney U test, Analysis of variance (ANOVA), Kruskal-Wallis test, Friedman test, correlation analysis, linear regression, Bland and Altman analysis, principal component analysis (PCA), K-means clustering, and Kohonen neural network (KNN) were employed for interpreting the measurements.

The findings showed close agreement between the developed balance analysis methods and the related measurements from the manual setup for balance analysis. The COM was observed to be responsible for differing amount of sway across the subjects and could affect both the angle and ground projected sway. The AP direction was more sensitive to sway than the ML direction. The subjects were observed to depend more on their proprioceptive system to control balance. The proprioceptive system was observed to have a greater impact in controlling the AP velocity of the subjects as compared to their visual system. The proprioceptive system had no impact on the ML velocity. The visual system was responsible for the control of the ML velocity and for reducing the acceleration in both directions.

It was concluded that for comparison of postural sway information, subjects with closely related COM positions should be compared, comparison should be carried out in respect to the base of their support. The sway normalisation by dividing with COM position should be performed to reduce the obscuring effect of the COM. Enhancement of the proprioceptive system should be carried out to reduce the AP velocity while enhancement of the visual system should be used to reduce the ML sway and acceleration in ML and AP directions. The velocity in the AP direction should be used to examine the performance of the proprioceptive system while the ML velocity and acceleration should be used for the visual system. The vestibular system characterised sway more in the AP direction, and hence, the AP direction should be used to examine its performance in balance.

Acknowledgement

My profound gratitude goes to the Almighty God who is the author and finisher of all things good for his grace, protection love and mercy upon life towards the completion of this doctoral research.

My deep thanks go to my director of studies, Professor Reza Saatchi for his expertise, support, supervision, encouragement, suggestions and valuable comments on various aspects of this work, without which this research would have not been a success. Your comments and advice in writing up this thesis has improved the quality of this work. I have learnt a lot of critical thinking from being with you which has made me a better researcher.

My special appreciation goes to my co-supervisors, Dr Samantha Lear and Professor Derek Burke, for their support and advice towards this study. Also, I greatly appreciate all those who work for the Design Futures Group of I3RI most especially Mr Anthony Jones and Mark Phillip for their immerse contribution to this project.

I am grateful to all volunteers who took part in the data recording section of this study.

Finally, I would also like to appreciate my parents, Mr and Mrs. Ojie, my brother, Dr. Ehizojie Ojie and my wife Patrice Ojie for their support towards the completion of this study.

May God immensely bless you all.

Publications

Journals

Ojie, O.D. and Saatchi, R. (2021). Kohonen neural network investigation of the effects of the visual, proprioceptive and vestibular systems to balance in young healthy adult subjects. *Healthcare*, vol. *9*(9), pp. 1219-1236.https://doi.org/10.3390/healthcare9091219

Ojie, O.D & Saatchi, R. (2020). Development and evaluation of an accelerometry system based on inverted pendulum to measure and analyse human balance. *Adv. Asset Manag.* Cond. Monit. *Springer, cham,* vol. *166*, pp. 1129–1141.

Ojie, O.D, Saatchi, R., and Saatchi, M. (2020). Demonstration of the effect of centre of mass height on postural sway using accelerometry for balance analysis. *Technologies*, vol. *8*(2), pp. 20-33. https://doi.org/10.3390/technologies8020020

Ojie, O.D. and Saatchi, R. (2020). Principal component analysis of the modified clinical test of sensory interaction in healthy adult humans. *WSEAS Transactions on Biology and Biomedicine*, vol. *17*, pp. 125-142. https://doi.org/10.37394/23208.2020.17.15

Presentations

Ojie, O.D & Saatchi, R. (2019). Development and evaluation of an accelerometry system based on inverted pendulum to measure and analyse human balance. Paper presented at the 32nd International Congress and Exhibition on Condition Monitoring and Diagnostic Engineering Management, University of Huddersfield, UK.

Ojie, O.D, Saatchi, R., Harrods. J., & Kent N. (2019). Developments of tools to assist with diagnosing balance problems. Creating Knowledge Conference, Sheffield Hallam University UK.

Table of Contents

List of Tables

List of Figures

List of acronyms and their meanings

2D	Two dimension
3D	Three dimension
Acc	Accelerometer
ADC	Analogue to digital converter
ADHD	Attention deficit hyperactivity disorders
ADLs	Activities of daily living
ANOVA	Analysis of variance
AP	Anterior posterior
BOS	Base of support
CDP	Computerised dynamic posturography
CI	Confidence interval
CNS	Central nervous systems
COG	Centre of gravity
COM	Centre of mass
COP	Centre of pressure
CPX	Cardiopulmonary exercise testing
DB	Davies-Bouldin index
DCD	Developmental coordination disorder
df	Degree of freedom
DMP	Digital motion processor
FEC	Foam surface eyes closed
FEO	Foam surface eyes open
fLoS	Functional limit of stability

FoG	Freezing of gait
GEC	Ground surface eyes closed
GEO	Ground surface eyes open
Gyr	Gyroscope
Hz	Hertz
I^2C	Inter-integrated circuit protocol
ICC	Intra-class correlation
IDE	Integrated device environment
IMU	Inertial measurement unit
ISM	Industrial, scientific and medical band
k-NN	k nearest neighbour
KNN	Kohonen neural network
KNN	Kohonen neural network
mCTSIB	modified Clinical Test for Sensory Interaction and Balance
ML	Mediolateral
MS	Multiple Sclerosis
MVPA	Moderate to vigorous physical activity
NFC	Near Field Communication
OA	Osteoarthritis
P. E	Potential energy
PCA	Principal component analysis
PD	Parkinson disease
PT	Physical therapist
pwMS	People with Multiple Sclerosis
RFID	Radio Frequency Infrared Detection
RMS	Root mean square
SB	Sedentary behaviour

SD	Standard deviation
SOM	Self-organising map
SPI	Serial peripheral interface
SVM	Support vector machines
TBI	Traumatic brain injury
TD	Typical development
TUG	Timed Up and Go
UV	Unilateral vestibular
VA	Visual acuity
VCC	Voltage common collector
VEMP	Vestibular evoked myogenic potential
VOR	Vestibular ocular reflex
WHO	World Health Organisation

List of symbols and their meanings

$A_{z_{av}}$	Average acceleration
$D_{z_{RMS}}$	Root mean square of displacement
$V_{z_{av}}$	Average velocity
$RangeA_z$	Range of acceleration
$RangeD_z$	Range of displacement
$RangeV_z$	Range of velocity
d_x	Displacement in the x axis
d_y	Displacement in the y axis
d_{ya}	Average displacement in the y direction
f_c	Cut off frequency
τ_b	Kendall's coefficient of rank correlation
H	Height above the ground

Chapter 1 Introduction

1.1. Background to the study

Balance is a fundamental requirement whose loss in humans has detrimental effects on both physical and social functions. The ability to maintain balance plays an immerse role in independent living. Falls and fear of mobility due to falls, are associated significantly to myriads of psychological problems such as trauma, depression, inactivity, and serious morbidity. Balance problems are caused mainly by ageing, neurological and musculoskeletal disorders.

About 33 to 50 percent of people over 65 years of age have been reported to experience some sort of balance or ambulation difficulties (Mancini & Horak, 2010). The World Health Organisation (WHO) estimates that the number of people over 60 years of age by 2050 is expected to be over 2 billion (Ageing and health, 2018). In Western Europe, the ageing population (65 year or higher) is expected to increase from 18.5% in 2010 to 27.3% in 2035 (Nations, 2012). This introduces a great burden on the independence of the ageing population, of which the ability to maintain balance is a key player. Without independence, as the ageing population increases so does the population and technology required to foster their care. Thus, the independence of older adults in the performance of basic life functions are paramount to the world, most especially to technologically advanced countries as there is a link between advancement in medical technology and ageing (Breyer et al., 2010).

The prevalence of balance disorders has also been reported in both young children, young adults and adults alike. An estimation of 3.3 million children (5.3%) in the United States of America has been reported to have experienced some sort of dizziness and related balance problems (Li et al., 2016). Similarly, an estimate of 50 million people worldwide has been reported to sustains a traumatic brain injury (TBI) every year (Maas et al., 2017) with the age range of TBI generally between 15 and 25 years (Hillier et al., 1997).

Currently, there exist no unanimous definition of the term balance in humans (Pollock et al., 2000). In order to define balance, one has to consider the mechanical definition according to Newton's first law of motion. The state of rest referred to by Newton in his first law of motion is what defines balance. This may be true for inanimate objects and may not be the case for humans, as humans are constantly in motion when alive. In the context of human balance, the definition of stability as the property of restoring to an initial state after disruption (Johansson

& Magnusson, 1991) appears well suited. Thus, the term maintaining balance can be used interchangeably with the term stability. The term stability was what Pollock et al. (2000) referred to as postural control howbeit with the restoration to an initial state referring to the line of gravity within its base of support. This implies that the term postural control and balance ability can be used interchangeably. Thus, the loss of postural control also implies loss of balance ability. In the context of this study the term "loss" as used in balance is not binary in nature but rather varies in degrees. The loss of the state of balance can be categorised into two: intentional and unintentional loss (Bhatt & Pai, 2005). Intentional loss is a loss of balance that can be avoided with prior knowledge. For example, children engaging in 'merry-go-round', tripping over an obstacle, engaging in difficult exercises that involves specialised training etc. Contrarily, unintentional loss occurs because of inadequacies/deficiencies in one or more of the systems responsible for balance leading to inadequate control of the centre of mass (COM) position within the base of support (BOS). The major difference between the two is that the former is not linked with a balance problem while the latter is. The term 'balance problem' is often used in connection with unintentional loss.

Balance is achieved through the integration and coordination of several systems of the body including the auditory, visual, vestibular, motor, and higher premotor systems (Horak, 1997). Primarily, balance in humans is maintained by the integration and interaction of the uninterrupted signal flow from the sensory systems i.e., the visual, vestibular and proprioceptive systems (Fitzpatrick & McCloskey, 1994). Under normal circumstances, the main elements in spatial orientation are the visual system-for spatial orientation and proprioceptive systems-for balance (Bronstein, 2016) while the vestibular system is responsible for the detection of head motion and head position with respect to the gravitational vector (Fernandez & Goldberg, 1976). The reliance on these systems to maintain balance depends on several factors such as age, history of fall, the operational state of the systems (healthy or unhealthy) etc. Redfern et al. (2001) suggested that when the vestibular system becomes defective, reliance on balance is placed on the visual system. Among the elderly, sensorial interaction has been shown to vary according to the history of falls (Ricci et al., 2009). In another study, older adults have been shown to prioritise vision in other to control balance (Yeh et al., 2014) while younger healthy adults have been suggested to depend on their proprioceptive system (Horak, 2006; Peterka, 2002).

Balance can be broadly divided into two: static and dynamic balance. Geuze (2003) defined static balance as the ability to maintain an upright posture and keeping the COM within the

area of the base of support (Geuze, 2003). The term “upright posture” as used in this definition can be considered ambiguous because upright posture can mean having a good posture which may not always be the case even in people with good balance. In this study, we refer to static balance as balance in quiet standing position where the balance is measured by the ability to maintain the COM position within its base of support. Dynamic balance is considered as balance in non-static position (Karimi & Solomonidis, 2011; Neptune & Vistamehr, 2019). In static condition, the base of support is fixed while in dynamic condition the base of support is moveable. Static and dynamic balance are considered as integral parts of functional balance (Ghanavati et al., 2012). The rate of feedback and feedforward control from the sensory systems to the central nervous systems (CNS) and vice-versa is lower for static balance as compared to dynamic balance (Gerasimenko et al., 2017). One can argue that before engaging in dynamic activities, the ability to balance in static position should be prioritised. However, this does not infer that a good static balance is equivalent to a good dynamic balance, although it can give confidence of the expected performance in a dynamic situation.

Balance assessment can be classified into two groups: Qualitative and Quantitative (Mancini & Horak, 2010). In qualitative assessment of balance little or no equipment are used and this leads to tester bias in its procedure (Mancini & Horak, 2010). In quantitative assessment an objective method is introduced to carry out the procedure thus tester bias is reduced. However, the bias that could be present is due to the limitation of the equipment used, the algorithm, the method of analysis, the procedure and whether or not the battery of test is capable of deciphering the balance condition. The objective methods can be divided into two: force-measuring platform and wearable inertial sensors. According to Horak (1987), a clinically quantitative reference tool should:

i. Reflect functional capabilities and the quality of postural strategies
ii. Be sensitive and selective to abnormalities of postural control
iii. Be valid and reliable
iv. Be practical i.e., inexpensive and easy to implement.

Inertial sensors can better meet all these recommendations as compared to the force-measuring platforms. However, inertial sensors have need for suitable signal processing and interpretation methods.

Balance analysis using accelerometry involves the conversion of the digital output obtained from the use of the IMU sensor into meaningful and interpretable information that can aid in

the improvement of balance. Usually, balance analysis is carried out using statistical and machine learning methods. Many methods from machine learning and statistics have been used for making inferences and predictions. Both inference and prediction are the two major goals for the study of biological systems, and this fits well with statistical and machine learning methods (Bzdok et al., 2018). However, statistical methods are geared towards making inferences which are achieved through the creation and fitting of probabilistic models that are project specific in nature (Bzdok et al., 2018). These models enable us to compute quantitatively with a measure of confidence that a discovered relationship is of true effect and not based on random noise (Bzdok et al., 2018). In contrast, machine learning methods are aimed towards prediction using general purpose algorithms to find patterns (Bzdok, 2017; Bzdok et al., 2017).

In this study, accelerometry techniques were devised to accurately measure and quantify body postural sway and analyse balance using statistical and machine learning techniques.

1.2. Aim and objectives

The aim of this study is to further develop computerised accelerometry techniques to facilitate better understanding of human balance.

The objectives are:

(i) Development of a wireless accelerometry system with associated hardware and software to accurately record balance information.
(ii) Representation of accelerometry signals by balance related features.
(iii) Development of accelerometry techniques to accurately quantify body movement, e.g., displacement, velocity, acceleration and tilt and their interpretation.
(iv) Critical analysis and interpretation of accelerometry data to assist with balance related sensory systems' dysfunctions.
(v) Critical evaluations of the devised approaches through trials on healthy adult volunteers.

The main challenge has been accurate computerised quantification of body movement, i.e., acceleration, tilt etc. and their interpretation in the context of the subject's physique and balance related sensory functions.

1.3. Outline of thesis

The outline of the thesis is presented as below:

Chapter two: Literature review. In this chapter, previous related studies in relation to use of accelerometry in balance analysis are reviewed.

Chapter three: Related theory. In this chapter, the theoretical background in the analysis of balance is presented.

Chapter four: Methodology. This chapter presents the research problem, type of data, the data collection method, the subjects' details, and ethical considerations.

Chapter five: Algorithm development and evaluation based on the inverted pendulum model. In this chapter, the algorithm utilised for balance analysis is developed and evaluated using a manual setup. Time domain measures of the accelerometry data were obtained and utilised to better understand relationships between the sensory systems and balance.

Chapter six: The effect of centre of mass position on balance analysis. The effect of varying centre of mass position on balance is investigated.

Chapter seven: Investigation of the sensory interaction in healthy adult subject using principal component analysis. The patterns/behaviour of the sensory systems to balance are investigated. This is carried out using PCA and other statistical methods.

Chapter eight: Investigation of the interaction of the sensory system interaction to human balance using the Kohonen neural network. The sensory systems behavioural characteristics in relation to the direction of sway is investigated.

Chapter nine: Conclusion and further work. The study is summarised and further research work are presented.

1.4. Summary

In this chapter, the general concept of human balance and its importance to human life were introduced. Balance is related to the quality of life of a person. Balance and postural control can be used interchangeably. In humans, an absolute state of rest is non-existent and balance is used as a quantifying term for the state of rest or equilibrium. Because humans are locomotive beings, an expected degree of balance is required in carrying out their daily activities. The

expected degree of balance is considered as the ability for a person to control his/her centre of mass within the base of support and it is task dependent. Balance degenerates as a result of certain factors not limited to age and neurological problems. Balance is assessed either in static or dynamic conditions. Accelerometry and force platform are the two major instruments used for objective balance analysis. However, the benefit of using accelerometry outweighs that of a force platform in cost, weight, size, sensitivity, comfortability and ease of use. Accelerometry suffers from various limitations such as accuracy in algorithm for balance measurement and the interpretability. Statistical and machine learning methods are the two main methods used for balance analysis. Statistical methods are geared towards inference while machine learning methods are used for prediction.

Chapter 2 Literature review

2.1. Importance of balance assessment

The ability to maintain balance is fundamental to human movement. Maintaining balance as well as a proper body posture, during the performance of anti-gravitational activities is primary to the execution of other secondary movement related activities (Panjan & Sarabon, 2010). Balance is important in order to navigate our surrounding environment (Winter, 1995) and to engage in the physical dimensions of life such as physical function, health, energy and vitality which contributes significantly to quality of life (Spirduso et al., 2005). The importance of balance can be readily observed among fray elderly people. The balance of a person is assessed by the amount of his/her postural control during some balance related task. Postural control is the act of maintaining, achieving or restoring a state of balance during any activity or posture (Pollock et al., 2000). Quantitatively, postural control is measured by measuring the movement of the centre of mass (COM), centre of pressure (COP), body segment, electromyographic activities and the evaluation of the contribution of the sensory systems (Paillard & Noé, 2015). Poor postural control in a particular activity may infer poor ability to balance in that activity. Hence, balance is a relative term that is categorised depending on the activity under consideration.

Postural instability has been related to a myriad of problems relating to the systems responsible for maintaining balance. Postural instability and poor balance are features of neurological diseases such as Parkinson's disease (PD) (Kim et al., 2018), Alzheimer's disease (Apostolova, 2016), Multiple sclerosis (Goldenberg, 2012), Huntington's disease (Porciuncula et al., 2020), Cerebellar ataxia (Kashyap et al., 2020), Stroke (Hou et al., 2019), Traumatic brain injury (TBI) (Harrell et al., 2021), Neuropathies (Khan & Andersen, 2021), and Vestibular syndromes (Young et al., 2018). Other factors that can affect a person's balance include ageing, medication and obesity. Ageing has been reported to be a contributing factor to poor balance as it progressively reduces the functions of the sensorimotor which include changes in the structural and functional aspect of the visual, somatosensory and vestibular systems, alongside leads to a decline in the central neural processing system and muscle strength (Sturnieks et al., 2008). Consequently, ageing is a contributing factor to slow reaction time and reduced limit of stability, leading to an exacerbated control of balance especially during cognitive task and unanticipated postural perturbations (Sturnieks et al., 2008; Mileti et al., 2019). Ageing also leads to multimorbidity, a term used to describe the co-existence of two or more chronic health

conditions. Multimorbidity correlates with reduced quality of life, mobility, functional ability, self-rated health, physiological distress, increase in hospitalisation, mortality, cost, and use of health care resources (Caughey et al., 2009; Marengoni et al., 2008; Roughead et al., 2011). Polypharmacy, a term used to describe the use of multiple medicines, is associated with multimorbidity. Polypharmacy is associated with adverse outcomes such as adverse drug reaction, mortality, higher length of stay in hospitals, falls and hospital readmissions (Milton et al., 2008; Caughey et al., 2010; Caughey et al., 2010). The use of benzodiazepine and its relation to falls was investigated among a cohort of 169 elderly tenants in New Jersey with mean age (±SD) of 79.8 (7.3) years, of which 80% were women (Sorock & Shimkin, 1998). They found out that any use of benzodiazepine was related to multiple falls in the persons who fell (Sorock & Shimkin, 1998). They suggested a periodic review for the need of benzodiazepine among the elderly (Sorock & Shimkin, 1998). The effect of obesity and its relation to balance, posture and fear of falling among different genders were studied by Ercan et al. (2020). Their study consisted of 251 subjects (51.4% female and 48.6% male, ages 40 to 60 years) of which 49.8% were obese. Their findings suggested: among obese people gender played a factor as there was a significant difference between the history of stumbling and falls in obese males as compared to obese females ($p<0.05$); no fear of falling or impede confidence to engaging in activities was evident among the obese males ($p>0.05$); restriction to engaging in activities as a result of fear of falling was observed among obese females ($p < 0.05$); and impaired posture was also observed among the 125 obese patients (Ercan et al., 2020). They suggested that balance and postural training should be included in exercise as part of a multidisciplinary approach to obesity (Ercan et al., 2020).

Thus, balance assessment is useful in areas of measuring and detecting neurological diseases; combating ageing constraints; controlling weight and monitoring the impact of medications. Clinical assessment of balance can be divided into two: Qualitative and Quantitative (Mancini & Horak, 2010). In qualitative assessment of balance, little or no equipment are used, and this leads to tester bias in its procedure (Mancini & Horak, 2010). In quantitative assessment an objective method is introduced to carry out the procedure thus tester bias is reduced.

In subsequent sections, the objective methods most especially on the aspect of accelerometry are discussed, the challenges in clinical balance analysis and the commonly used methods of analysis available in the literature are presented.

2.2. Objective clinical balance assessment

The objective clinical assessment of balance can be broadly divided into two, Posturography using: Force platforms and Computerised Dynamic Posturography (CPD), and Accelerometry (Mancini & Horak, 2010)

2.2.1. Force platform and computerised dynamic posturography as a balance evaluation tool

The objective assessment of balance overcomes the limitations of the subjective methods by providing an objective and quantitative measure to posturography, i.e., the measurement of postural sway (Bronstein & Pavlou, 2013). Posturography involves the use of techniques that objectively quantifies balance by providing quantitative measures. These techniques for posturography can be divided into static and dynamic. Static techniques indicate situations where the position is studied under normal condition, i.e., a fixed platform, while dynamic techniques indicate the conditions where the position of the individual studied is in response to an applied perturbation either to the individual or to the individual's support surface (Duarte & Freitas, 2010). The two most commonly used and widely accepted instruments for investigating posturography are the computerised dynamic posturography and the force platform used for the analysis of the individuals' centre of pressure (COP), an important parameter used to monitor premature sensory motor deficit (Moe-Nilssen, 1998).

The equipment usually employed under static condition to quantify balance is the force platform. A force platform consists of sensors attached to a metal plate to give electrical output proportional to the force on the plate (Wardoyo et al., 2016). A force platform measures the centre of pressure (COP) of a subject in the form of three-dimensional ground reaction force. The COP refers to a point on the support surface where the resultant vertical force tends to act. The force platform enables postural evaluation under differing conditions such as standing on a single leg or with both legs, with eyes open or closed, the performance of varying cognitive tasks simultaneously, which supports its use as the chosen instrument for many research studies (Bauer et al., 2008). Thus, this instrument has been considered as the gold standard for the analysis of postural control in static condition.

The use of force platform in balance analysis has been reported in several studies. Jaworski & Kołodziej (2020) utilised a force platform to assess the postural stability of woman aged 60 and above. In their study, the women were divided into two groups: 14 younger (< 70) and 10

older (> 70) group and comparison were made based on their COP sway parameters. The result suggested that the older group had a lower level of postural stability compared to the younger group (Jaworski & Kołodziej, 2020).

Nevertheless, the force platform has been reported to suffer from several limitations such as high cost (around £11,529), weight (around 10 kg for only the platform), considerable testing area (around 2.5 square metre), difficulty to transport, difficult of use, lack of sensitivity to the weight of children (Estévez-Pedraza et al., 2020; Rodríguez-Rubio et al. 2020). Matłosz et al. (2020) compared three different and commonly used force platforms among 111 young healthy adult subjects. They observed a low level of agreement between their measurements in the eyes open and closed conditions (Matłosz et al., 2020). Thus, the analysis obtained from one force platform may differ from those obtained from another force platforms and hence there is low reliability across platforms.

Dynamic posturography refers to the measurement of postural control oscillations over a predefined area which is unstable (Leirós-Rodríguez et al., 2019). In the case of oscillating platforms, the external instability can be permanent when the surface is not flat or can be as a result of a sudden alteration, i.e., rotation or inclination (Leirós-Rodríguez et al., 2019). Internal instability can result from varying movements such as leaning forward, sitting to standing and raising arms etc. (Pérennou et al., 2005). On the other hand, in computerised dynamic posturography, a force platform is used with a combination of different stimuli. A model of the computerised dynamic posturography commonly used in research is the EquiTest, which is made up of an evaluation surface that consists of two independent force platforms in the mid lateral axis (Leirós-Rodríguez et al., 2019). In computerised posturography, the information regarding the type of difficulty faced by the individual in maintaining postural control is not known. The system is capable of only quantifying the degree of functional limitation to stay in balance which is important in predicting fall risk and the evaluation of the sensory systems (Visser, 2008). The main drawbacks of dynamic posturography include the cost of the equipment, space for installation, the time for training and testing, unsuitability for dynamic balance during gait, as well as turning and sit to stand transition (Mancini & Horak, 2010; Visser, 2008).

These methods of evaluation are in theoretical conflict with the widely acceptable concept of balance as the control of the centre of mass (COM) position during movement produced by an individual or an external disturbance (Honeine & Schieppati, 2014; Horak, 2006). However, it

has been shown that the variables obtained from the COP corresponds to that from the COM under static conditions (Winter et al., 1998).

2.2.2. Accelerometry as a balance evaluation tool

An alternative to the force platform in measuring balance is the use of accelerometry. Accelerometry refers to the use of accelerometers to measure and quantify balance. The use of accelerometry for the assessment of human movement was first proposed in the 1950s (Liberson et al., 1962; Saunders et al., 1953). However, due to their high cost, bulkiness and unreliability, they were considered unsuitable for ambulatory monitoring (Culhane et al., 2005). In the past decade the fabrication technology of accelerometers has advanced greatly as a result of the need for its use in various areas in the automotive industry such as air bags release systems (Culhane et al., 2005). These new generational accelerometers were designed to meet the requirement of reliability, high volume and low cost. The benefits of using accelerometers over the force platform include low cost, small size which is suitable for subjects to work without obstruction, diversity of dynamic range and sensitivity, and direct measurement of 3D acceleration (Adlerton et al., 2003; Mayagoitia et al., 2002).

Accelerometry can also be defined as the use of inertial measurement unit (IMU, accelerometers, gyroscope and magnetometers) to quantify postural control. Various applications of IMUs have been reported in clinical monitoring. Gonzalez et al. (2021) utilised a combination of IMU, surface electromyography, and force plates with application of support vector machines in activity recognition task such as walking and running performed by five healthy subjects (Gonzalez et al., 2020). Principal component analysis (PCA) was used to compare similarities across the various tasks and support vector machine was used in order to classify the PCA data into motion categories. The results obtained using the sensors provided a classification accuracy of 90% (Gonzalez et al., 2020). Janc et al. (2021) compared the simultaneous measurements of the IMU (MediPost) placed at the L4 region (penultimate vertebra of the lumber spine) and a force platform of the head shaking posturography (at a frequency of 0.3 and 0.6 Hz) of 38 patients (age 50.6 with standard deviation of 11.6 year) with unilateral vestibular weakness (UV) and those of 65 healthy volunteers (mean age and standard deviation: 48.7 and 11.5 years). The results suggested that both systems were suitable for differentiating between subjects with problems of vestibular pathology although a slightly lower value of velocity was observed in the IMU result for head shaking at 0.6 Hz (Janc et al., 2021). Yu et al. (2021) utilised a waist worn tri-axial accelerometer to assess the functional

balance and mobility of 85 community dwelling adults (mean and standard deviation: 72.12 and 6.99 years) using a short form of the Berg Balance Scale test and Timed Up and Go test (Yu et al., 2021). The result showed a moderate to high predictive accuracy for both test (Yu et al., 2021).

Accelerometry has also been found useful in the quantitative assessment of activities of daily living (ADLs). Quantitative assessment of the activities of daily living has been suggested to play an essential role in the evaluation of the severity of diseases and of the quality of life (Mulas et al., 2020). IMUs have been shown to be important in these aspects as they enable ease of use, long term and remote functioning evaluations. Abdollah et al. (2021) investigated the effectiveness of using a single accelerometer mounted on the head to monitor postural transition and the Timed Up and Go (TUG) test. Two tri-axial accelerometers with a sampling frequency of 100 Hz were attached to 12 able-bodied subjects–one on the right mastoid and the other on the sternum while the subjects performed a battery of activity of daily living task that consisted of varying postural transitions (Abdollah et al., 2021). The results of the head-mounted accelerometer and that of sternum were compared to the result of a video motion capture device. Utilizing their developed systems, the result suggested that a single head mounted tri-axial accelerometer can produce a high accuracy (>95%), sensitivity (>90) and specificity (100%) for detecting events of walking and postural transition (Abdollah et al., 2021). Pau et al. (2021) employed the use of accelerometer worn on the wrist to quantify bilateral upper limb activity and asymmetry in twenty-eight people with multiple sclerosis (pwMS) under free living conditions. Twenty-eight age and sex matched individuals were required to wear the device for two weeks in the same way as the twenty-eight individuals with multiple sclerosis (Pau et al., 2021). The results obtained from the accelerometer attached to the upper limb suggested that significant lower overall activity, extended time period of the dominant limb and superior intensity were characteristics of the people with multiple sclerosis (Pau et al., 2021). Soltero et al. (2021) utilised wrist worn accelerometers to determine the contribution of 24-hour activity and sleep behaviours on type 2 diabetes in Latino adolescents and young adults with obesity. The accelerometer sensors were worn for a period of 24 hours while it assessed moderate to vigorous physical activities, sedentary behaviours (SB), sleep, and sleep regularity in both thirty-eight adolescents (age range: 12-16 years) and twenty-two young adults (age range: 18-22 years) (Soltero et al., 2021). The result suggested that physical activity, reducing sedentary behaviour and improving sleep are critical for reducing type 2 diabetes in young adults and Hispanic adolescent (Soltero et al., 2021).

There is also association between involvement in physical activity and improved health. Shiraishi et al. (2021) investigated the association that exist between an accelerometer worn on the wrist, cardiopulmonary exercise testing (CPX), and the result of the Kansas City Cardiomyopathy Questionnaire in thirty-one heart failure patients that were hospitalised for acute decomposition (Shiraishi et al., 2021). The device was worn for two weeks and a short version of the Kansas City Cardiomyopathy Questionnaire filled by the patients shortly after the removal of the device. The parameters measured consisted of the exercise time, daily step counts and percentage sedentary time. The result showed best correlation between sedentary time, Kansas City Cardiomyopathy Questionnaire overall score and the clinical scores, and suggested that accelerometer could be used as a complement with the Kansas City Cardiomyopathy Questionnaire in assessing physical activity in heart failure patients after hospitalization (Shiraishi et al., 2021).

Accelerometry has also been reported to be useful in assessing physical disabilities. Dostál et al. (2020) utilised 31 time-synchronised accelerometer sensors placed at different locations of the body to recognise the gait motion patterns between twelve ataxic and thirteen healthy aged, matched individuals. Data of the mean power of the frequency band was used as features in the classification algorithms. The result showed high accuracy (77.1% to 98.5%) in differentiating between the healthy and the ataxic individuals (Dostál et al., 2020). The use of accelerometers in assessing Parkinson disease (PD) subjects have also been reported in Barrachina-Fernández et al. (2021). Rovini et al. (2020), employed four wearable IMU devices (two placed on the hands and two placed on the feet) to extract information from 40 healthy adult subjects and 40 aged matched patients with PD. Seventy-eight and ninety-six parameters were measured from the lower and upper limb respectively, which were trained using supervised learning classifiers. The result suggested excellent discrimination between the two groups with accuracy ranging from 0.936 to 1 across classifiers (Rovini et al., 2020).

In the field of medicine and biomedical engineering, various studies have been conducted to improve the ability of people affected by balance problems. In order to assess and evaluate balance problems such as Parkinson disease, the assessment of the functional limit of stability (fLoS) and freezing of gait are usually used (Nutt et al., 2011). The fLoS is defined as the maximum centre of pressure displacement of a person while voluntarily leaning forward and backward (Mancini et al., 2008; Hasegawa et al., 2019). Freezing of gait (FoG) is referred to as an intermittent failure to maintain or initiate locomotion (Giladi & Nieuwboer, 2008; Nutt et al., 2011). The use of wearable sensors such as IMUs have been reported in the measurement

of fLoS and FoG. People with PD have been suggested to have worsen fLoS and FoG. Mancini et al. (2021) investigated FoG in 40 participants with PD using a novel algorithm based on five inertial sensors attached to the feet, shins and lumber regions while the participants were walking (Mancini et al., 2021). The algorithm's performance was compared with the clinical decisions of two experts that examined the number of FoG episodes from the video recordings of the participants walks and turns based on differing duration of times, ranging from very short (< 1 second) to long (> 5 second). The result suggested moderate to good agreement between the results of the algorithm and the clinical decisions for the short and long episodes of FoG (Mancini et al., 2021). In another study, Mancini et al. (2021), also extended the method to 48 PD individuals with and without FoG in an unsupervised home monitoring condition with three sensors worn at the feet and lumber regions for 7 days, while recording the percentage time of freezing and its variation. The result suggested that the percentage time of freezing and its variation were significantly ($p < 0.05$) capable of differentiating between people with and without FoG and that 69 percent of FoG were made up of short FoG episodes (Mancini et al., 2021). Similarly, Hasegawa et al. (2021) investigated the difference in the fLoS during quiet stance between 64 PD individuals with FoG and 80 PD individuals without FoG, and also the difference between the individuals with PD and 79 healthy control subjects. The inertial sensor was worn on the lumber spine while the participants were involved in several balance task such as the fLoS in the forward and backward directions and postural sway while they stood with their eyes open on a firm and foam surface respectively i.e., condition one and three of the modified clinical test of sensory interaction and balance (mCTSIB) test. The result suggested that: (i) participants with PD and FoG showed significantly ($p = 0.004$) smaller fLoS compared to those without FoG and to the healthy controls ($p < 0.001$); (ii) participants without FoG and healthy controls showed no significant difference ($p = 0.48$) in the fLoS; (iii) significant larger postural sway on foam surface was observed between participants with PD and FoG and participants with PD and without FoG as against those of healthy controls ($p = 0.001$) and (iv) no significant difference existed between PD participants with FoG and without FoG on foam surface (Hasegawa et al., 2021).

The use of accelerometers to assess the balance of children and to assess neuro-developmental disorders have been reported. García-Liñeira et al. (2020) investigated the reliability and internal consistency of accelerometric measurements related to static equilibrium and gait in 70 healthy children aged 6 to 12. The accelerometer was placed at the 4th lumbar vertebra while the participants performed three trials while standing on one leg with eyes closed and

eyes open, dynamic balancing on one leg on a foam mat and normal gait. The result suggested that the test on older children had higher internal consistency than those in younger children, test performed in children aged 8 years and above had strong correlation ($r > 0.71$) between trials and that the static test presented more reliability than those obtained in the gait test. Thus, comparison between healthy controls and children that have balance problems are better applied to children above 8 years of age in the static condition as compared to gait condition (García-Liñeira et al., 2020). Examples of neuro-developmental disorders that occur in children are the developmental coordination disorder (DCD) and attention deficit hyperactivity disorders (ADHD). DCD and ADHD, are neuro-developmental disorders which starts at childhood and affect a child's planning of movement and coordination (Ricci et al., 2019). The prevalence of DCD is estimated to be about 6% worldwide (Blank et al., 2012) while ADHD is estimated to be about 5% worldwide (Sayal et al., 2018). The use of wearable IMUs have been reported in the diagnoses of these problems. Ricci et al. (2019) investigated how an IMU can provide objective support in the diagnosis of motor impairments such as DCD and ADHD in 37 school children. The IMU was used to measure the linear and rotational movements of the children (ages 7-10 years), of which 17 of them had DCD and ADHD while the other 20 children were used as healthy controls. The result measured from the movements suggested a significant difference in the linear and rotational movements between children with the motor impairments and healthy control (Ricci et al., 2019). Children with developmental coordination disorders are known to be physically less active as compared to children of typical development (TD). Yu et al. (2021) utilised an accelerometer to investigate the functional movement skill of 73 children with DCD and 99 children of typical development (TD) in the age range of 6 to 10 years. The five components of the functional movement skill (running, catching, kicking and jumping) were assessed by various product and process-oriented approaches using the second edition of Test of Gross Motor Development while measuring the time spent in moderate to vigorous physical activity (MVPA) and sedentary behaviour (SB). The result showed that children with DCD had significantly poorer performance in the functional movement skill when compared to those of TD (Yu et al., 2021).

Despite the usefulness of accelerometry in the analysis of balance and gait, it also has limitations which currently prevent its acceptance as the standard in clinical setting. Some of these challenges are presented in the next section.

2.3. Challenges faced in human balance analysis using accelerometry

In order for acceleormetry to be used as a clinical tool for balance evaluation, it must address the needs in balance evaluation as suggested/required by clinicians. Several clinicians and researchers have given their recommendations on the areas that need to be addressed in order for posturography to be considered as a clinical tool. A summary of their recommendations was presented by Kingma et al. (2011). The first recommendation was the system to meet the aims of posturography. As indicated, the aims of posturography include objective quantification of balance control; identification and adequate description of the deficits and functional loss; quantification of handicap in daily life; prediction of falls and problems with balance; assist with guidance for programs in balance rehabilitation (Kingma et al., 2011). The second recommendation was to determine which measurement technique was optimal and required for the assessment of balance control (Kingma et al., 2011). Some of the widely used methods suggested include the use of a force platform, camera-based method and accelerometry or inertial measurement units (IMUs). The need for a 2 or 3 dimensional evaluation of movement and the need for separation into anterior-posterior and lateral sway (Kingma et al., 2011). The third recommendation was the test conditions and the technique of perturbations required (Kingma et al., 2011). They considered the position of the arms, head and feet; the cognitive task; importance of the postural assessment in regards to eyes open and close or necessary sway reference vision; and optokinetic stimulation; balance during gait; neck and calf muscle vibrations; and adaptation and habitual impact (Kingma et al., 2011). The fourth recommendation was the definition of relevant clinical output parameters and the technique for analysis (Kingma et al., 2011). They suggested spatial orientation of the body; muscle activity; timing between stimulus and response; spectral analysis; the sequence and timing of body movement; and movement perception and psycho-physics (Kingma et al., 2011). The fifth recommendation was in the standardisation of the measurement technique, data analysis, procedure and display (Kingma et al., 2011). They identified the need for the test to be reproducible and individually adaptable; sensitive and specific to various balance problems; identify pathologically responsive patterns, dependent on data of posturgraphy such as experience, motor training, gender and age; practical limitation of the test and methods on dealing with incomplete test (Kingma et al., 2011). Finally, the sixth category identified was in the comparison of posturography with other balance assessment methods such as balance analysis during gait (Kingma et al., 2011).

Posturography should be carried out in such a way that it describes the individual's balance strategies and the dependencies from the various sensory modalities (Kingma et al., 2011). The goal is to tailor the assessment to the sensory and motor deficits in relation to complaints, have discriminative and meaningful estimate of the deficits of an individual patient and not based on merely group differences, and aid in the rehabilitation process of an individual by providing relevant information (Kingma et al., 2011).

In order to address the issues that faces clinical balance analysis, a widely acceptable definition of the view of human balance is required. Several researchers in the study of human balance have suggested that humans sway was likened to the form of an inverted pendulum when in quiet standing. Although other researchers have utilised more complex models to analyse balance (Jacob, 1997; Nicholas et al., 1998) or have refuted the claim of the inverted pendulum (Bloem et al., 2000), the inverted pendulum model has been shown to be simpler to investigate as it requires fewer variables; only one joint axis exist through the ankles and the angular position of the mass of the pendulum can be measured precisely; its balancing strategy illuminates the mechanism used in standing and provides a hypothesis for which standing can be tested (Loram & Lakie, 2002). An inverted pendulum is one in which the COM position is above the pivot point. Thus, for a system to be adequately utilised in balance analysis, it should be able to accurately represent the COM sway while utilizing the inverted pendulum model.

Several challenges prevent the use of accelerometry in balance analysis. Some of the main challenges include the reliability and validity of the metric or a combination of metric used to accurately quantify a person's health outcome as it relates to balance (Shiroma et al., 2018); the transformation of the reference frame of the body fixed sensor to an inertial reference frame (Zijlstra & Aminian, 2007); analysing balance according to the inverted pendulum (Winter, 1998) and the translatability of the outcomes of accelerometry to that of a force platform (Richmond et al., 2021). When deploying an instrument for medical use, priority is placed on how and what the instrument should measure rather than trying to conform to what the instrument measures. In posturography, parameters of body sway are dependent on the head orientation, mental state, visual fixation distance, shoes, foot position and support surface (Kingma et al., 2011). Some researchers have considered balance in relation to the maintenance of the COM position with regards to the base of support (Fujimoto et al., 2015; Suvarna et al., 2021; Rogers & Millie, 2018). This supports the need for the projection of the COM position unto the ground surface. Most algorithms for balance and postural sway analysis using accelerometry depend on integration of acceleration of the accelerometer placed on the centre

of mass position and by making analysis from the angles roll, pitch and yaw derived from the acceleration. These methods do not necessarily produce a reliable information about the sway of the subject as they deviate from the basis of the inverted pendulum. As the body is thought to obey the principle of the inverted pendulum model during balance, it is necessary that the model is used in deriving the algorithm utilised for postural sway analysis. The task to project the COM position to the ground surface have been embarked on by Mayagoitia et al. (2002). However, the algorithm proposed by Mayagoitia et al. (2002) suffers from limitations in modelling of the inverted pendulum which led to a 2-dimensional sway representation rather than a three-dimensional sway representation, limitation in ground projection of the COM position which requires the angle of sway to be relatively small and the occurrence of sway in both directions i.e., the mediolateral (ML) and anterior-posterior (AP) when actually the sway occurred in only one direction. Thus, there is a need for a more accurate representation of the projected COM postural sway.

Accelerometry is also hindered from been the standard of assessing posturography due to unknown accuracy of IMU based evaluations with the gold standard i.e., the force platform (Ghislieri et al., 2019). If proven accurate, the use of IMUs for balance assessment would be ideal, since they are portable and low in cost. Validations of accelerometry with the gold standard i.e., the force platform and clinical score were introduced by several authors to check its validity and sensitivity (Ghislieri et al., 2019). Cabarkapa et al. (2021), investigated the accuracy of an accelerometer sampled at 100 Hz in detecting vertical jump heights in 15 healthy young adult subjects (10 females and 5 males) by comparing its result with that of a laboratory-based force plate (Cabarkapa et al., 2021). They found that the accelerometer was effective in determining the vertical jump heights but produced a result that was 3.1 cm greater than the force plate (Cabarkapa et al., 2021). Pollind & Soangra (2020), investigated the validity of an IMU for sway analysis and its feasibility in detecting slight balance impairments due to reduced proprioception in 10 healthy adult subjects (5 males and 5 females). They found that sway velocity, root mean square and sway path were effective in differentiating postural changes due to varying proprioception and concluded that IMUs can be used for accurate clinical postural assessment and was effective in diagnosing postural impairments (Pollind & Soangra, 2020). Similarly, Noamani et al. (2020) investigated the accuracy of an IMU against an in-lab equipment used for characterizing standing balance. The study was divided into four approaches: camera-based bottom-up approach (reference method), camera-based top-down approach, IMU-based (accelerometer) top-down approach, and IMU-based (accelerometer and

gyroscope) top-down approach, were used to evaluate the inter-segmental moments and the COP position. In their study, ten young healthy adult individuals stood on a force platform for 2 minutes. They observed that camera-based top-down approach and IMU-based (accelerometer and gyroscope) top-down approach resulted in high accuracy as compared to the reference method and no significant difference was observed between using only an accelerometer and a combination of an accelerometer and a gyroscope (Noamani et al., 2020). The validation of accelerometry based on these studies has either been due to a force platform, a camera-based method or based on clinician assessment. The force platform, camera-based method and clinician assessment have limitations and may not be considered as the standard method for sway comparison. A gold standard should produce the same result under similar condition, it should be limited to tester bias and design considerations. Different force platform has different sensitive and measurement accuracy. Rodríguez-Rubio et al. (2020), using healthy adult subjects, investigated the validity and reliability of the Satel 40 Hz stabilometric force platform for measuring quiet stance and dynamic balance. They observed that the validity of the device was directly proportional to the weight measured i.e., lower weight resulted in lower validity and higher weight resulted in higher validity (Rodríguez-Rubio et al., 2020). This implies that the system would produce a lesser valid result for children as a result of their lesser weight. Although the weight of a person can affect his/her balance, balance is not the measure of weight rather the excursion of the COM position with regards to the base of support under specific conditions. The force platform suffers from standardisation. The interpretation of the result of sway using a force platform varies and it is subject to the systems design or outcome report (Croarkin & Zampieri, 2021). Thus, a high amount of sway on one platform may not be considered as a high amount of sway on a different platform. A problem of validating a system against another when the other system is not the actual process to be measured or has limitations is that it may be considered accurate especially if they both have excellent reliability even when they may both share the same limitation. The algorithm proposed by Mayagoitia et al. (2002) when evaluated against a force platform, showed closely related results (Mayagoitia et al., 2002). Thus, there is a need for accelerometry to be validated against the physical unit of length and not based solely on the force platform, video-based system and the expertise of clinicians. Physical unit of measurement helps to make necessary adjustments and to act when designing systems that could counter the sway reaction and prevent fall. It also aids in evaluating the accuracy of the system before deployment on a human subject. The representation of postural sway with physical unit creates a holistic approach to a subject's balance analysis i.e., the subject can be used as his/her own control.

Another important consideration is in the investigation of balance in the mediolateral (ML) and anterior-posterior (AP) direction (Kingma et al., 2011). Varying pathologies and balance conditions have been suggested to lead to variation of sway in differing directions (Kingma et al., 2011). Ibara et al. (2021), using the sway of the hip, investigated the relationship between the kinematic and centre of pressure (COP) parameters of the time series scaling component (α) in hip osteoarthritis (OA) patients that were involved in a one leg standing task. The COP parameters were used to measure the scaling exponent (α), the standard deviation (SD), the maximal change in acceleration of the hip sway, and balance performance, and was compared during a one leg standing task between the OA and the control group using regression analysis (Ibara et al., 2021). The result for the OA group suggested a smaller α in the ML direction, larger SD and maximal change in the anterior-posterior acceleration, significantly negative and positively associated COP parameter with α in the ML and AP directions respectively, limited hip sway in the ML direction and greater movement in the AP direction (Ibara et al., 2021). Using a sit to stand activity, Annor et al. (2021) investigated the influence of the local tendon vibration of the lower limb in 10 elderly subjects (mean age of 76 and standard deviation of 1.7 years) and also examined whether postural control can be improved by using a specific vibration frequency (Annor et al., 2021). In particular, comparison was carried out between the elderly subjects and 15 healthy young adults (mean age and standard deviation: 25.5 and 1.5 years). The result suggested that the elderly subjects exhibited larger COP sway area and higher ML displacement than the healthy young adult subjects, and that local tendon vibration helped to reduce the ML displacement and sway area (Annor et al., 2021). Balance is primarily maintained by the interaction of the sensory systems i.e., the visual, proprioceptive and vestibular systems. Thus, examination of their respective postural responses would help determine and isolate balance related problems and deficits and understand their contributions to postural sway. For example, Masani et al. (2003), reported that the sway velocity reflects the proprioceptive system (Masani et al., 2003; Sun et al., 2019).

2.4. Overview of commercially available IMUs and smartphone technologies for human balance

2.4.1. Commercially available IMUs

The most commonly used commercially available sensors include: Opal System by APDM Inc. (APDM, Portland,OR,United States), G-Walk System (BTS Bioengineering® S.p.A., Garbagnate Milanese, Italy), Xsens MTx Enschede (MTx, XSens Inc, Eschende, Netherlands) and the Shimmer 3 (Shimmer, Dublin, Ireland) (Donisi et al., 2021; Ghislieri et al., 2019).

The Opal system is composed of a tri-axial accelerometer, a tri-axial gyroscope, and a tri-axial magnetometer (Donisi et al., 2021). The accelerometer consists of a 14-bits analogue to digital (ADC) resolution and a sensitivity scale range of ±16 to ± 200 g. The gyroscope consists of a 16-bits analogue to digital (ADC) resolution and sensitivity scale factor of range ± 2000 deg/s. The magnetometer consists of a 12-bit analogue to digital (ADC) resolution and ± 8 Gauss range. The sensor uses Bluetooth 3.0 technology for wireless communication.

The G-Walk system is composed of a single wearable sensor equipped with four inertial platforms which is run by sensor fusion technology. The sensor consists of a 16-bit tri-axial accelerometer with a sensitivity scale factor of up to ±16 g, a tri-axial gyroscope of 16-bit with range of sensitivity up to 2000 degrees/second, a tri-axial magnetometer of 13-bit with a sensitivity scale factor of up to 1200 μT, where T is Tesla. The wireless mode of connection is based on Bluetooth 3.0 technology.

The MTX Xsens Enschede consists of a 16-bit tri-axial accelerometer with a sensitivity scale factor of up to ±50 g, a 16-bit tri-axial gyroscope with a range of sensitivity up to ±1200 degrees/second, a 16-bit tri-axial magnetometer with a sensitivity range of ±75 μT. The wireless mode of connection is based on Bluetooth 3.0 technology.

The Shimmer-Shimmer 3 consists of a 16-bit tri-axial accelerometer with a sensitivity scale factor up to ±16 g, a 16-bit tri-axial gyroscope with a range of sensitivity up to ±2000 degrees/second, a 16-bit tri-axial magnetometer with a sensitivity range of ±400 μT. The wireless mode of connection is based on Bluetooth 3.0 technology.

Dugan et al. (2021), utilised Xsens MVN Analyse system to examine the gait and balance of 38 patients who were undergoing treatment of concussion. The sensor consisted of 17 wireless sensors with a sampling frequency of 60 Hz attached to the feet, sacrum, thighs, scapulae,

sternum, upper arms, lower arms, head and hands. The patients were assessed in two phases: the initial arrival testing phase and the leaving or clearance testing phase. The motion of the mediolateral COM and gait velocity were measured. Also, during eyes open and closed condition of balance, postural sway velocity and jerk index were also measured. The result obtained suggested a significant decrease in ML sway from initial to clearance testing, a significant increase in gait velocity from initial to clearance testing, a significant increase in complexity index from the initial to clearance testing in the eyes closed condition and a significant decrease in jerk from initial to clearance testing for eyes open and eyes closed condition (Dugan et al., 2021). Thus, suggesting the system was effective in assessing the progress of concussions.

However, the repeatability of these systems did not agree. The repeatability of the G-WALK System was assessed on 40 patients with neurological and orthopaedic pathologies (Pagano et al., 2021). The pathologies included fractured femur, hip replacement, knee replacement and hemiparesis. Two trials of the Timed Up and Go (TUG) test was used for each patient. The patients were asked to stand from a chair, walk for 7 m along a straight path, turn around a pin, go back and sit on the chair (Pagano et al., 2021). Seven kinematic parameters were analysed such as: test duration, duration of the raised phase, vertical acceleration during the raised phase, vertical acceleration during the sitting phase, duration of the sitting phase, mean rotation speed during the intermediate rotation phase and the mean rotation speed during the final rotation phase, with the sensor placed above the iliac crest at the L2 level (Pagano et al., 2021). Intra-class correlation coefficient (ICC) was used to measure the repeatability. The result showed different repeatability for the motion parameters assessed and the repeatability changed based on the type of pathology (Pagano et al., 2021).

The interchangeability of the Opal and G-Walk systems was investigated on twenty-one pathological subjects (mean age of 49.5 and standard deviation of 17.4 years) and thirty-two healthy subjects (mean age: 45.4 years and standard deviation of 14.2 years), that were involved in gait related task with seven spatiotemporal parameters recorded (Donisi et al., 2021). The result of the study showed a good repeatability and a non-perfect agreement between the two systems (Donisi et al., 2021). Thus, they suggested that the two systems should not be interchangeable during test.

2.4.2. Smartphones technologies

Smartphones have also been found useful in gait and balance analysis as most smartphones have embedded IMUs. The accuracy of a smartphone's gyroscope for measuring dynamic stability was investigated in 85 healthy adult subjects, 37 women (mean age ± SD: 22.1±1.6 years) and 48 men (mean age ± SD: 22.4±1.7) (Polechoński et al., 2019). To assess the accuracy of the smartphone, stabilometric measurement was recorded simultaneously with a Sigma balance platform. The sampling frequency of the device was 30 Hz (Polechoński et al., 2019). A total of 170 measurements of postural stability were recorded in the frontal and sagittal plane. The result of the measurement showed a significantly strong correlation between both devices for the frontal (r = 0.997) and sagittal (r = 0.990) plane (Polechoński et al., 2019). In Borzì et al. (2020), a smartphone was used to assess the postural instability of 42 PD patients (31 males and 11 females, mean age ± SD: 68.6 ± 10.7 years) and 7 young healthy adult subjects (5 males, 2 females, mean age ± SD: 27.2 ± 2 years). The subjects were asked to maintain a 30 second quiet stance with the smartphone attached to the lower back, L3-L5 level. A total of 414 features that were representation of the time and frequency domain were extracted and used to train a support vector machine (SVM). The model produced a 100% accuracy in differentiating between the healthy control, patients with mild and severe postural instability (Borzì et al., 2020). Similarly, Mansson et al. (2021) utilised a mobile phone application (Mybalance) to assist with the self-assessment of balance for older people. The device has been developed and evaluated on 31 older adult individuals against a clinical standard instrument (Mansson et al., 2021). Although the device is still in its initial testing phase, the device was shown to be reliable and valid against clinical instruments used in a physiotherapist setting (Mansson et al., 2021). The limitations of using a smartphone is the cost of the system and the interruptions due to text messages or calls.

2.5. Common parameters in balance measurement

Body sway is a representation of deviations in the location of the centre of gravity (COG) in space and centre of pressure (COP) on the support surface (Peterka, 2000). Similarly, body sway can also be defined as the slight movement in posture made by individuals in order to maintain a position of balance and can be estimated by the total displacement of the centre of mass (COM) in relation to the base of support (BOS) (Wang et al., 2010). The use of accelerometry entails recording of the COM sway in the form of acceleration (using accelerometers) and angular rate of change (using gyroscope) converting it into both linear and

angular displacements. The raw data is usually low pass filtered using a digital low pass filter with a frequency range of 0.5 to 10 Hz (Ghislieri eta al., 2019). The conversion to displacement is usually carried out by integration of the raw signals i.e., accelerations from the accelerometer sensor, although using the inclinometer capability of the IMU and algebraic calculations, the signal can also be converted into ground displacement (Mayagoitia et al., 2002). When accelerometry is projected to the ground surface, it utilised similar variables to a force platform for its sway analysis (Mayagoitia et al., 2002). Thus, the COM sway can thus be effectively analysed using the COP variables.

The technique used to study the body sway in a standing position using a force platform is known as stabilomentry (Kapteyn et al., 1983). Usually, the force platform is connected to a computer which records the COP displacement for a defined period forming the COP signal. The COP signal can be considered in two forms: stabilogram and statokinesigram. Stabilogram refers to the representation of the COP displacement signal in only one direction (anterior posterior or mediolateral) as a function of time and statokinesigram is a representation of the COP displacement signal graphically in a horizontal plane (Prieto et al., 1996). Differing COP variables can be obtained from the raw COP data to evaluate/quantify postural sway. However, there is no agreement on the COP variables that should be extracted for balance assessment (Błaszczyk, 2016; Błaszczyk et al., 2016). The commonly used variables for postural sway are obtained from the COP displacement raw data. Because many variables of COP exist, it is often necessary to consider the characteristics of the postural task and the variables characteristics. These variables can be classified into global and structural variables (Duarte & Freitas, 2010; Baratto et al., 2002; Ihlen et al., 2013; Rhea et al., 2015). Global variables characterise the COP traces by the magnitude of the resultant components of the ML and AP in the time and frequency domains. Researchers usually consider the magnitude or deviations of these variables such that the greater the magnitude or deviations the lower the postural stability. However, some researchers have argued that global variables may not be sensitive to the structure of variation which harbours insightful information about the postural control process (Baratto et al., 2002; Ihlen et al., 2013). As a result, they suggested structural variables to be considered. Structural variables decompose the patterns of COP sway into smaller units correlating them with motor control processes (Baratto et al., 2002; Chen et al., 2021; Collins & De Luca, 1993, Duarte & Freitas, 2010; Ihlen et al., 2013; Rhea et al., 2015).

The commonly used global variables that are synonymous to the IMU and force platforms include displacements (path length and amplitude), velocity, acceleration, standard deviation

and root mean square (Lapointe et al., 2021; Majcen Rosker et al., 2021; Zhu et al., 2021; Zhou et al., 2021). The path length examines the magnitude of the two-dimensional displacement based on the total distance travelled. The path length has been applied in various cohorts of subjects and has been considered a valid measure. Often, the smaller the path length the better the postural stability or balance. However, the path length may not be sensitive to the behaviour of the sensory systems as it affects the respective direction of sway due to it combining the measures. The amplitude of displacement is calculated by considering the distance between the maximum and the minimum COP displacement for each direction. Usually, the greater the value the lesser the stability. The amplitude variable was used to examine the differences in lower extremity reach performance, static posturography and gait outcomes between young (20–39 years), middle-aged (40–59 years) and older (60–79 years) adults using identical tests and parameters (Hill et al., 2020). The findings suggested reduced lower extremity reach distance was found in older adults compared to intermediate-aged (Cohen's d = 1.28–3.60) and young (Cohen's d = 2.09 – 3.87) adults ($p < 0.001$), while young adults demonstrated greater reach distances than intermediate (Cohen's d = 0.64–1.74) aged adults ($p < 0.001$) (Hill et al., 2020). The amplitude measure has been found useful in diagnosing patients with neurological disorders (Pavão et al., 2014). The velocity is obtained by dividing the COP excursion with the time duration of the trial. The velocity measure quantifies the efficiency of the postural control system while characterising the total neuromuscular activity required for balance maintenance. The velocity measure has been described as the most effective and reliable measurement among trials (Duarte & Freitas, 2010). Other researchers have also considered the COP velocity to have greater sensitivity in comparing people from differing age groups and with differing neurological conditions (Raymakers et al., 2005; Masani et al., 2014). In Siragy & Nantel (2020), information of the velocity variable was utilised in investigating the effect of arm swing on balance in twenty people with Parkinson disease (age: 63.78 ± 8.97). Average and standard deviation of the trunk linear and angular velocity were obtained from the subjects who walked with two arms conditions (absent and normal) on a split belt treadmill CAREN Extended-System (Motek Medical, Amsterdam, NL) in all three axes. The result suggested that trunk anteroposterior instantaneous angular (least affected leg) and linear velocity (bilaterally) were reduced by the absent arm swing (Siragy & Nantel, 2020). The acceleration measure has also been found useful in balance analysis. The acceleration is the first derivative of the velocity. The root mean square obtained by taking the mean of the square root of the samples. The standard deviation is the total deviation from the mean and it is equal to the RMS if the COP signal has zero mean. The RMS and SD has been reported to provide good reliability in

differentiating between old and young subjects and between subjects that have pathologies and healthy subjects (Duarte & Freitas, 2010; Ozinga & Alberts, 2014; Zhang et al., 2021).

2.6. Methods of data analysis

Data analysis method refers to methods that enables inference, deduction and learning from the data (Bzdok et al., 2018). In balance analysis, the global or structural parameters are utilised as inputs in carrying out data analysis. Broadly speaking, data analysis in balance studies can be divided into statistical and machine learning methods.

2.6.1. Statistical methods

Statistical tests are used for comparing the differences between groups and for finding relationships. These can be broadly classified as parametric and non-parametric models (Orcan, 2020; Van Buren & Herring, 2020). Parametric tests refer to those models where the number of parameters is fixed while non-parametric models refer to the case where the number of parameters increases as the available data increases (Orcan, 2020; Van Buren & Herring, 2020; Zhou et al., 2020). Parametric models can be defined by the assumption of the shape of the probability distribution of the data. The model is parametric if the distribution is normal and the mean and standard deviation are known. In parametric test, the mean is used as the representative measure for the normally distributed continuous variable and the median is used for non-parametric conditions (Mishra et al., 2019). In other to determine which model to employ, test of the distribution of the data are usually carried out. The commonly used statistical tests for normality are the Shapiro-Wilk test and the Kolgomorov-Smirnov test (Miot, 2017; Orcan, 2020). Other methods include the construction of histogram combined with skewness and kurtosis statistic (Jun & Yanling, 2021), boxplot, probability to probability plot (Miot, 2017; Mishra et al., 2019). Several parametric and non-parametric models have been used in balance analysis depending on the task and the number of groups considered. The most common of these include the methods of testing hypothesis and inferences such as the t-test, Wilcoxon signed-rank test, the Mann-Whitney U test, Analysis of variance (ANOVA), the Kruskal-Wallis test and Friedman test; the methods of measuring association such as correlation analysis, linear regression, and methods of agreement such as Bland and Altman analysis, intra-class correlation and kappa statistic (Ranganathan et al., 2017). The principle of hypothesis testing is a decision on whether the data sample is a representative or not a representative of the population assuming the formulated hypothesis is true about the population (Mishra et al., 2019). In hypothesis testing, a null hypothesis and its alternative are

stated (Mishra et al., 2019). The null hypothesis states that no difference exist between the population and the sample in accordance with the parameter being measured (Mishra et al., 2019). On the other hand, the alternative hypothesis states that in accordance with the parameter being measured, the population is different from the sample (Mishra et al., 2019). A probabilistic value also called the p-value is used to measure this difference. Typical values for the p-value varies from 5% to 1%, implying that there is 5% and 1% chance respectively of rejecting the null hypothesis (Emmert-Streib & Dehmer, 2019). The t-test is a parametric test that is used to compare the difference of means between two groups (Mishra et al.,2019). The t-test can be broadly divided into two: the independent sample t-test and the paired sample t-test (Yan et al., 2017; Mishra et al., 2019). The independent sample t-test is used to test if a significant difference existed between two unrelated groups. The paired sample t-test is used to compare two related groups to investigate whether a significant difference existed or not. The non-parametric alternative of the independent t-test is known as the Wilcoxon rank-sum test or the Mann-Whitney U test (Yan et al., 2017; Mishra et al., 2019). The non-parametric alternative of the paired sample t-test is the Wilcoxon signed rank test. The two-sample t-test was used to examine the difference between the gait and balance parameters of 16 patients (sex: 10 males and 6 females; mean age ± standard deviation: 70.4 ± 7.1 years) with progressive supranuclear palsy (PSP) and those of 25 healthy adult controls (sex: 25 females; mean age ± standard deviation: 72 ± 6.6 years) (Ali et al., 2021). The result showed that gait parameters such as: kinematics, spatiotemporal and kinetic gait measures were significantly different between both groups ($p < 0.05$) (Ali et al., 2021). The paired sample t-test was used to evaluate the pre and post treatment data obtained from thirty-eight Diabetes Mellitus Type-II patients (sex: 20 males; mean age ± standard deviation: 63.08 ± 3.3 years) with diagnosis of diabetic neuropathy (Daud et al., 2021). The Berg Balance Scale and Time Up and Go test were used to collect pre and post treatment data from the participants who were involved in 12 sessions (two sessions per week) of balance training on Biodex stability system. The result from the pre and post test suggested that balance training with Biodex Balance System can significantly improve balance function in Diabetes Mellitus Type-II patients with diabetic neuropathy (Daud et al., 2021). The self-reported change in physical activity dose and deterioration in balance performance, gait speed, and self-rated health (SRH) in One hundred and eighty-six older women (ages 69–79 years) between two time points were investigated using the Wilcoxon signed-rank and the Mann–Whitney U test (Papp et al., 2021). The result suggested that greater physical activity was important for maintaining physical functions and self-rated health.

Hypothesis testing is not limited only to two groups. There are conditions were more than two groups are required for comparison. In such a case, repetition of the t-test between the groups increases the chances of type 1 error (Gray et al., 2017). Type 1 error refers to the error of incorrectly rejecting the null hypothesis. That is, stating that the null hypothesis is false when indeed it is true. In a situation when more than two means are compared, the analysis of variance (ANOVA) is used (Mishra et al., 2019). There are two main types of ANOVA: the one-way ANOVA and the one-way repeated measures ANOVA (Mishra et al., 2019). The one-way ANOVA analysis is the extension of the independent sample t-test howbeit with more than two groups. Similarly, the one-way repeated measures ANOVA is the extension of the paired sample t-test howbeit with more than two groups. ANOVA states whether a significant difference exist between the groups but cannot tell which pairs are different. Thus, further analysis also called post hoc analysis are required (Mishra et al., 2019). The use of ANOVA in balance analysis have been reported in the literature. The Kruskal-Wallis test is the non-parametric equivalent of the one-way ANOVA and the Friedman test is the non-parametric equivalent of the one-way repeated measures ANOVA. The Kruskal-Wallis test and the Mann-Whitney U test were used to investigate whether a significant difference existed in the ocular and cervical vestibular evoked myogenic potential (VEMP) in regards to the balance between 30 Parkinson disease (PD) patients, 16 patients with atypical parkinsonism (AP) and 30 healthy controls (Klunk et al., 2021). The VEMP was induced by a mini head shaker and its latency recorded using a non-invasive surface electromyography (EMG) while the subjects balance were investigated using a pressure platform. The latency (n10 and p15 for the ocular VEMP and p13 and n23 for the cervical VEMP) and peak to peak amplitude obtained was used for statistical analysis (Klunk et al., 2021). The results suggested that patients with PD had a prolong ocular VEMP n10 as compared to healthy controls and extended p15 in comparison to both healthy controls and AP patients (Klunk et al., 2021). Patients with AP showed reduced ocular VEMP amplitudes in comparison to healthy controls and PD patients. There were no differences in cervical VEMP between groups (Klunk et al., 2021).

The measures of association are used to measure the direction and magnitude between two variables (Franco & Di Napoli, 2017). Several type of correlation coefficient have been reported in literature. The most commonly used correlation coefficient measure include: Pearson correlation coefficient (r), Spearman rank correlation coefficient (ρ), Kendall's coefficient of rank correlation (τ_b) (Janse et al., 2021). Pearson correlation coefficient (r), Spearman rank correlation coefficient (ρ), Kendall's coefficient of rank correlation (τ_b), have

been used in several studies to measure association. The choice of correlation analysis to use depends on certain factors such as the level of measurement and the result of the distribution of the variable (Khamis, 2008; Janse et al., 2021). The Pearson correlation is mainly used for normally distributed data while the Spearman and Kendall's tau correlation are suitable for non-normally distributed data (Janse et al., 2021). The Pearson correlation coefficient was used to investigate the relationship between balance confidence, core muscle strength and trunk control in 177 (110 males and 67 females, median age = 57 years and interquartile range (IQR) = 46-64 years) community dwelling patients with chronic stroke (Karthikbabu & Verheyden, 2020). The balance confidence, core muscle strength and trunk control were measured using the activity specific balance confidence scale, handheld dynamometer and the trunk impairment scale 2.0 (TIS 2.0) respectively. The result of the correlation analysis showed that trunk control was highly correlated with balance confidence ($r = 0.66$, $p < 0.001$) and overall core muscle strength ($r = 0.61 – 0.70$, $p < 0.001$) (Karthikbabu & Verheyden, 2020). Spearman rank correlation coefficient was used to investigate the association between dizziness and falls in 187 (85 males and 102 females, mean age = 77.75 years with standard deviation = ±14.14 years) institutionalised older adults (Lima Rebêlo et al., 2021). The instrument used for data collection were the questionnaires for assessing variables related to falls and the socioeconomic and demographic questionnaire. The result showed significant association between dizziness and the number of morbidities ($p < 0.05$), and dizziness and history of falls ($p < 0.05$) (Lima Rebêlo et al., 2021).

The measures of agreement are used to investigate the accuracy and precision between two different methods, two different operators using the same method, or a repeated measure by the same operator (Watson & Petrie, 2010). The agreement between measurement is the degree of concordance between the measurements. The most common of these measures include the Bland and Altman's method, intra-class correlation (ICC) analysis and the kappa statistic (Watson & Petrie, 2010; Taffé et al., 2020; Ranganathan et al., 2017). The Bland and Atlman's method is used to measure the degree of agreement between two methods when one is considered as the gold standard (Watson & Petrie, 2010). The kappa statistic is also used in the same manner but operates only on categorical data (Watson & Petrie, 2010). The intra-class correlation coefficient (ICC) is used to measure the concordance between two readings. While the Bland and Altman's is mainly used to compare two methods with one of the methods being considered as the reference, the intra-class correlation coefficient (ICC) is used without consideration of a reference (Ranganathan et al., 2017). The Bland and Altmans method,

weighted kappa (κ) and the intraclass correlation coefficient (ICC) were used to investigate for home use the reliability and validity of a modified version of the community balance and mobility scale (CBMS-Home) in 55 people (mean age and standard deviation: 77.2 ± 6 years). The subjects completed the full original CBMS, home based CBMS, the functional reach test and the step test. The result from the Bland and Altman analysis and the weighted kappa suggested a moderate to almost perfect agreement (weighted $\kappa = 0.45–0.84$) between the CBMS-Home and the CBMS. The intra-class correlation coefficient showed excellent test-retest reliability (ICC = 0.95) of the distribution scores of the CBMS-Home based test (Ng et al., 2021).

2.6.2. Machine learning methods

The use of machine learning for gait and balance analysis is a fairly recent development. Machine learning techniques are aimed at designing algorithms that either can learn from the experience of the labelled data or can learn patterns automatically from the input data set (Prakash et al., 2016). Machine learning technique utilised for gait and balance analysis can be divided into supervised, unsupervised, reinforcement, evolutionary, probabilistic and hybrid approaches, and rule based (Prakash et al., 2016; Kabade et al., 2021). However, the most widely used for balance analyses include the supervised methods such as the neural network, the k-nearest neighbour (k-NN), ensembles (random forest, bagging and boosting) and the support vector machines and unsupervised methods or clustering methods such as the fuzzy c means, k means, hierarchical and the self-organising map (SOM); fuzzy logic, reinforcement learning and evolutionary approaches (Wright & Jordanov, 2014). Bao et al. (2019) explored supervised machine learning technique and trunk sway data to automatically evaluate balance. Sixteen participants (5 males, 11 females, mean age and standard deviation: 68.2 and 8.0 years) participated in a standing balance exercise while their trunk sway data were being recorded, and rated by a physical therapist (PT), rating their performance on a scale of 1 to 5. Applying support vector machines to 61-dimensional feature vectors representing performance of each exercise, an accuracy of 82% was achieved and the SVM outputs were significantly closer to PT ratings (Bao et al., 2019). Kamran et al. (2021) also utilised a supervised approach (convolutional neural network and random forest) to automatically evaluate balance in older adults and observed a good classification performance in comparison to that of physical tests (Kamran et al. 2021). Sun et al. (2019) suggested that the random forest algorithm showed good classification performance in differentiating controls and Multiple Sclerosis (MS) among individuals (153 participants (50 healthy controls and 103 MS individuals), 108 females and

45 males, with MS using their sway metrics obtained from standing upright for 30 seconds on a force platform) with an accuracy of 86.3 to 92.3%, sensitivity of 76.5 to 85.7% and specificity of 92.0 to 96.0% (Sun et al., 2019). Savadkoohi et al. (2021) showed that a one-to-one deep neural network used to process an open-sourced force plate sway data of (163 females and males aged 18-86) involved in the four conditions of the modified clinical test of sensory interaction and balance (mCTSIB) test were able to provide an accuracy of 99.9%, precision of 100% and a sensitivity of 100% in differentiating between fall risk individuals and healthy controls (Savadkoohi et al., 2021).

Often the actual label of the dataset may not be known. In that case, the unsupervised method is used. The unsupervised method helps to reveal the patterns inherent to the data set and is suitable for understanding the systems under consideration. Rodrigo et al. (2012) applied the Kohonen neural network to classify the inter-subject gait variability of 60 normal individuals (mean age and range: 63.3 and range 37 to 86 years, 28 men) and 60 patients with idiopathic Parkinson's disease (mean age and range: 68.8 and range 45 to 84 years, 37 men) based on a databased force platform obtained dataset. The result of the clustering obtained from the Kohonen map agreed with those of the classification carried out by experts (Rodrigo et al., 2012).

Araugo et al. (2018) utilised competitive neural network to access body steadiness in older adults (age range 60 to 80) by finding out the quiet standing point of equilibrium of their body sway. Stabilometry was used to obtain the values of the centre of pressure (COP) of the subjects. The result suggested that competitive neural network was a feasible alternative to compute the global centre of pressure and contributed to the postural steadiness and equilibrium condition analysis of the elderly (Araugo et al., 2018).

Thus, machine learning techniques are task dependent. The supervised methods are mainly used for classification and prediction, while the unsupervised are used for finding hidden patterns.

2.7. Summary

In this chapter, the importance of balance assessment, the methods commonly used for the assessment of balance in a clinical setting, the challenges faced in the assessment of balance, the common parameters and common methods for analysis were briefly discussed. The commonly used methods for balance analysis are the force platform, computerised dynamic posturography and accelermetry. Accelerometry overcomes the limitations of the other two

methods due to its low cost, sensitivity to lesser weight, ease of use, ease of mobility and suitability in dynamic conditions. However, accelerometry also faces challenges such as the need for suitable algorithms to accurately depict the widely acceptable notion of balance i.e. the inverted pendulum model, interpretation of the results obtained in the mediolateral (ML) and (AP) directions for an understanding of the various sensory systems i.e. the visual, vestibular, and the proprioceptive system and its use for a comprehensive understanding of the balance of an individual. These challenges are addressed in this study.

To gain insight into balance analysis, statistical and machine learning methods are used. The most widely used statistical methods can be grouped into three based on the task required. These are: the methods of testing hypothesis and inferences, methods of testing associations and methods of testing agreement. The most commonly used machine learning methods in human balance analysis can be grouped into two: supervised and unsupervised. These machine learning methods are task dependent. In this study, these methods are utilised for balance analysis.

In the following chapter, the theories relevant to this study are presented.

Chapter 3 Related theory

3.1. Introduction to the process of human balance

The balance system comprises of complex organs and mechanisms which control the displacement of the centre of gravity (COG) from the equilibrium position. This is done by generating counter postural reactions and eye movements to maintain a stable image of the environment (Olchowik et al., 2015). The location of the body's COG is determined by the information from the visual, proprioceptive and vestibular systems (Peterka, 2002). This information is received by the central nervous system (CNS) via a network of neurons which activates the musculoskeletal system in a way that prevent the COM from extending beyond the base of support, formed by the area of the feet (Alghwiri & Whitney, 2020; Richmond et al., 2021). The balance control mechanism of the human body is shown in Figure 3.1. It consists of three layers: the sensory input, the input integration and the motor output. These layers are interdependent in their functions; hence, their interactions and correct functioning are paramount to the maintenance of balance and postural control.

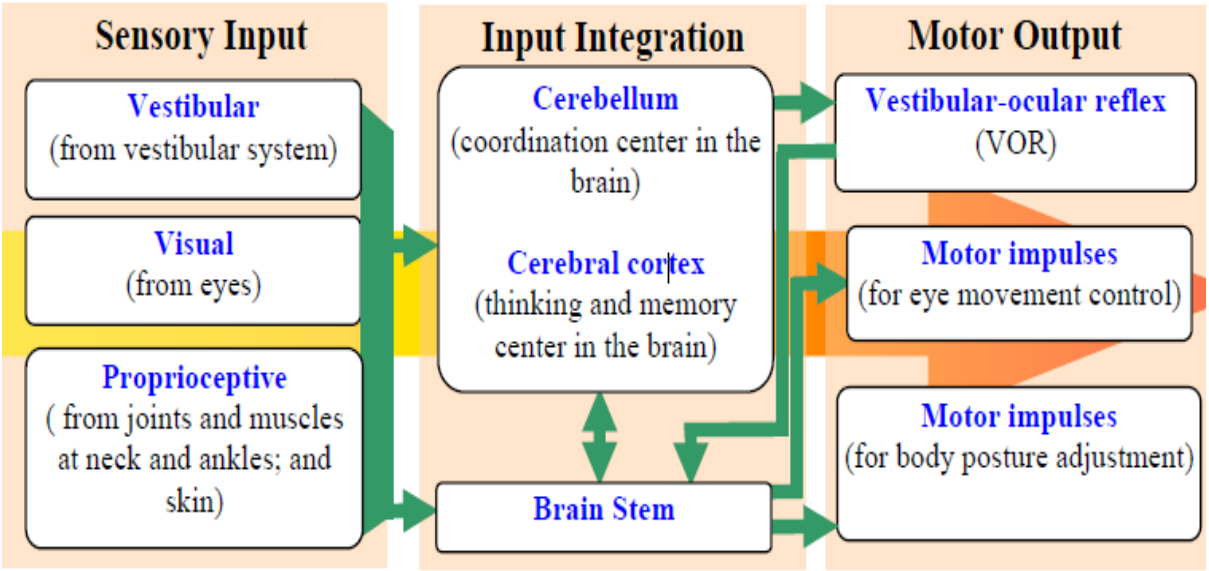

Figure 3.1. Balance control in human body (Vestibular Disorders Associations, 2020).

3.2. Balance related sensory systems

The sensory systems mainly associated with balance are the visual, proprioceptive and the vestibular systems.

3.2.1. Vestibular system

The vestibular system is often referred to as the primary sensory organ of movement. Its origin can be traced back to 500 million years ago (Graf & Klam, 2006) and it is involved in all levels of the brain. The vestibular system consists of three semi-circular canals and two otolithic sensors, these are located in the inner ear close to the cochlear organ. The canals encode the angular head acceleration in three dimensions and the sensors encodes linear and gravitational related linear acceleration (Besnard et al., 2018). This information is vital to the central nervous system (CNS) in order to maintain balance. The position of the head and neck is regulated by the vestibular system via two outputs: the vestibular ocular reflex (VOR) and the vestibular spinal reflex (Alghwiri & Whitney, 2020). Whilst the head is in motion, the vestibular ocular reflex is used for the stabilization of visual images on the retinal. The vestibular spinal reflex allows for the reflex control of the muscles of the neck and lower extremities so that the motion of the head and trunk can be maintained accurately and correlatively with the movement of the eye (Alghwiri & Whitney, 2020). The vestibular system provides support for brainstem functions (Vidal et al., 2004) and has recently been recognised for high level functions in spatial cognition (Besnard et al., 2015; Smith, 2017). The outermost portion of the vestibular system acts as a miniaturized accelerometer and gyroscope and reports information continually regarding the position and motion of the head and body. This information is sent to integrative units situated in the brainstem, cerebellum and somatic sensory cortices (Purves & Williams, 2001). The vestibular system is a key component in both reflexes of posture and eye movement. When the head is in motion, a damaged vestibular system adversely affects balance, eye movement control and the sense of orientation. The assessment of the damage done to the vestibular system is important in brainstem injury evaluation. The brainstem consists of a large part of the vestibular circuitry, of which simple clinical examination of the vestibular function can be performed to examine its involvement in patient's orientation. The primary symptoms of vestibular problems include dizziness, vertigo, vestibulovisual symptoms and postural symptom (Bisdorff et al., 2015). Dizziness is the sensation of an impaired spatial orientation which does not occur from a false sense of motion (Bisdorff et al., 2015). Vertigo is the sensation of a false sense of the motion of the head or body (Bisdorff et al., 2015). The

vestibulovisual symptoms are symptoms associated with the visual system such as visual distortion and false sensation of motion or tilting of the visual surround. These symptoms occur as a result of the interplay between the vestibular and the visual system or a vestibular pathology (Bisdorff et al., 2015). Postural symptoms are balance symptoms related to the maintenance of postural stability which occurs while in an upright position i.e., seated, standing, or walking (Bisdorff et al., 2015). Disorders of the vestibular system manifest in any of the above symptoms. Dizziness has been reported as one of the symptoms that occurred at the time of concussion (Alkathiry et al., 2018), and also in chronic unilateral vestibular hypofunction (Morimoto et al., 2019). Vertigo has been reported as a symptom of Ménière's disease (Phillips et al., 2020) and it is said to have a duration between 20 minutes and 12 hours (Lopez-Escamez et al., 2015).

The vestibular-ocular reflex (VOR) is responsible for integrating the vestibular and ocular systems to maintain gaze during head motion. It is often negatively affected following sport-related concussion (Quintana et al., 2020).

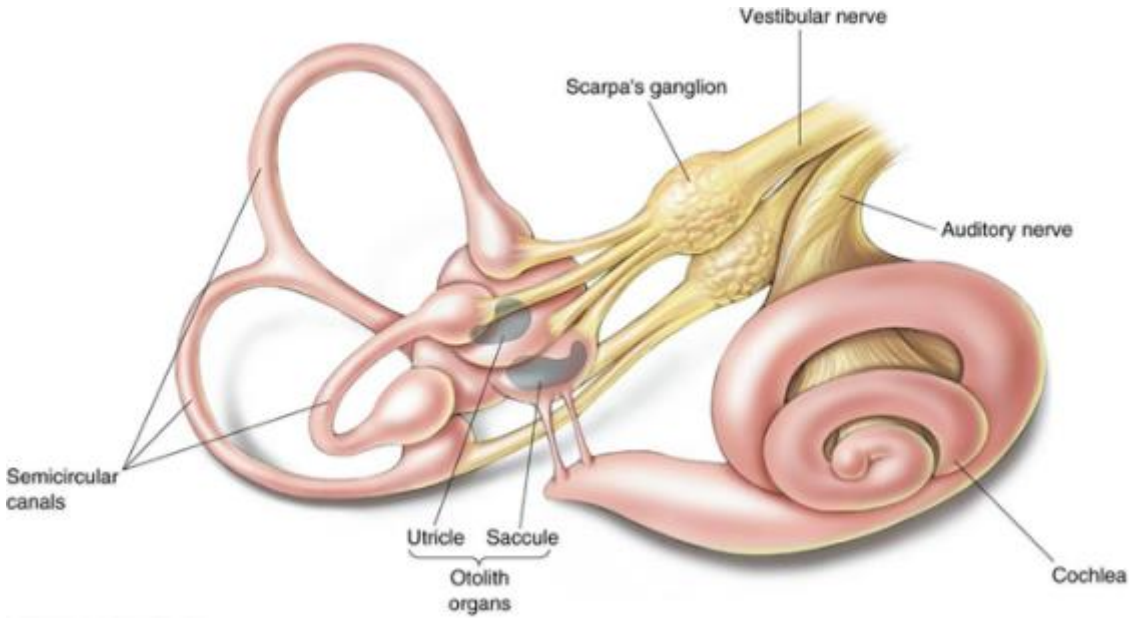

Figure 3.2. Vestibular system (Vision Therapy Children, 2018)

3.2.2. The visual system

The visual system is one of the primary systems responsible for balance. The visual input provides the CNS with the information necessary to maintain a vertical position in relation to the environment (Chiba et al., 2016). The visual function is known to deteriorate with age and this deterioration has been reported to increase the risk of falls (Amir et al., 2021). In older adults, the major reasons for the decline in visual functions are attributed to anatomical changes of the eyeball (Saftari & Kwon, 2018). Structural changes to the eye occur as a result of ageing (Saftari & Kwon, 2018). Throughout the life span of the eye, the weight and cross-sectional area of its lens decreases. The lens of the eye, responsible for the change of focal distance, becomes thicker, heavier and loses its elasticity (Saftari & Kwon, 2018). Ageing also leads to changes in the ciliary muscle, a smooth muscle, responsible during accommodation for changing the shape of the lens when viewing objects at varying distances (Hipsley & Hall, 2021). Glasser & Campbell (1999) compared the biometric, optical, and physical properties of 19 pairs of isolated human eye-bank lenses obtained from people of ages 5 to 96 years. A scanning laser apparatus was used in measuring the lens focal length and spherical aberration, the lens thickness and the lens surface curvatures, were measured by digitizing the lens profiles. This data was used to calculate the equivalent refractive indices for each lens. The result obtained suggested that the optical and physical properties of the lens changed substantially with age in a complex manner (Glasser & Campbell, 1999). Although anatomical changes affect the visual functions by reducing the quality of the sensory input of higher-level processing (Alghwiri & Whitney, 2020; Saftari & Kwon, 2018), it is not solely responsible for the decline of the visual functions. Reduction in visual functions can also occur as result of a decline in the computational efficiency and compensatory heuristic in the higher-level processes (Alghwiri & Whitney, 2020).

Ageing also leads to functional changes of the visual system (Saftari & Kwon, 2018). Some of these functional changes that are affected by age include, but are not limited to visual acuity, contrast sensitivity, glare sensitivity, and visual field (Rubin et al., 1997). Visual acuity (VA) is a measure of the eye's ability to distinguish the details of objects and shape at a given distance (Alghwiri & Whitney, 2020; Saftari & Kwon, 2018). VA testing is a vital assessment of visual function and a screening tool for ocular pathology (Samanta et al., 2020). Contrast sensitivity is the ability to detect fine differences in patterns and shading (Alghwiri & Whitney, 2020). It is an important function necessary for detecting objects without clear outlines and for discriminating objects from their background (Alghwiri & Whitney, 2020). The balance of the

oculomotor (a nerve responsible for the coordination of eye muscle) and contrast sensitivity are known to be impaired after an intake of a single dose of lorazepam (Giersch et al., 1996). Glare sensitivity refers to the loss of visual acuity in bright lighting (Marié et al., 2021). The conditions of light could produce discomfort and pain without necessary affecting the visual perception (Boyce, 2017). Aartolahti et al. (2013) investigated the relationship between functional vision, balance, and mobility performance in a community-based sample of 576 older adults, aged 76 to 100 years. Balance and mobility were measured by the Timed Up and Go (TUG) test, maximal walking speed, Berg balance scale (BBS), and the chair stand test. Depressive symptoms, self-reported fear of falling, cognition and physical activity were also assessed with the participants placed into poor, moderate, or good functional vision groups. Compared to the participants with moderate (N = 222) or good functional vision (N = 259), the participants associated to the poor functional vision group (N = 95) had more comorbidities (multiple illness), depressed mood, fear of falling, cognition decline, and reduced physical activity (Aartolahti et al., 2013). By addressing problems of the visual system, the risk of falls can substantially decrease. For example, peripheral field deficits can be addressed by using glasses with prisms, contrast sensitive can be increased by tinted glasses and problems with bifocals can be addressed by glasses for near and far vision (Alghwiri & Whitney, 2020).

3.2.3. The proprioceptive system

The receptors of the joints, muscles, and tendons provides the somatosensory information to the central nervous systems (CNS). This information is about the body's: segment position, movement in space and the amount of force generated for the movement (Alghwiri & Whitney, 2020). Clinically, the assessment of somatosensory function is carried out in two distinct phases: the primary and cortical sensory modality (Klingner & Witte, 2018). The primary sensory modalities include touch, vibration, pressure, pain, position sense of joint and temperature (Klingner & Witte, 2018). The cortical sensory modality are experiences that occurs from the fusion of the primary sensory modalities by the parietal cortex (Klingner & Witte, 2018). Examples of cortical sensory modalities include stereognosis (the ability to understand an object by touch), graphesthesia (the ability of a person to recognize a letter written on the person's skin without seeing it), two-point discrimination (the ability to distinguish the cutaneous stimulation of one point from the stimulation of two points), tactile localization (the ability to accurately identify the site of tactile stimulation), muscle spindle activity, proprioception, cutaneous receptors in the lower extremities and changes in vibration

sense (Klingner & Witte, 2018). These functions are known to decrease with age. Lower extremities vibration perception has been found to be the main determinant of postural control in older adults (Kristinsdottir et al., 2001). The postural control of the younger adults was found to be comparable with that of older adults who had good vibration perception, while an increase in frequency was observed in older adults with impaired vibration perception (Kristinsdottir et al., 2001). The testing of the primary and cortical sensory modality provides an indication of where a possible lesion exists and whether the parietal cortex is affected (Klingner & Witte, 2018). The primary sensory information required to maintain balance has been found to be proprioception and cutaneous input (Bacsi & Colebatch, 2005). The information of the somatosensory function that includes proprioception, cutaneous input and vibration, have been found to be primarily important in the assessment and intervention processes of older adults who are at risk of postural instability (Alghwiri & Whitney, 2020). Clinically, proprioception (sense of position and movement) is assessed by a joint positioning matching test (Alghwiri & Whitney, 2020). The test starts distally with the "toe up/down" test with eyes closed and moves proximally to the ankle and knee, if impairments are observed in the toes (Alghwiri & Whitney, 2020). A proprioceptive normal patient should be capable of detecting the subtle movement of the big toe (Alghwiri & Whitney, 2020). Vibration sense can be assessed by placing a tuning fork (normally 128 Hz) at the first metatarsal (the bones of the foot) head (Alghwiri & Whitney, 2020).

3.2.4. Sensory organisation test

The sensory systems (visual, vestibular and proprioceptive) interaction can be evaluated using different methods. However, the most common method used with accelerometry is the modified Clinical Test of Sensory Interaction and Balance (mCTSIB) test. The test is designed to assess a person's ability to utilise his/her sensory systems (visual, vestibular and proprioceptive) for balance (Wrisley & Whitney.,2004). The mCTSIB test was proposed by Cohen et al. (1993). It is a modified version of the Clinical Test of Sensory Interaction and Balance (CTSIB) developed by Shumway-Cook & Horak. (1986). The CTSIB test is made up of six conditions: (i) standing on a firm surface with eyes open, (ii) standing on a firm surface with eyes closed, (iii) standing on a firm surface with visual conflict dome, (iv) standing on a compliant surface with eyes open, (v) standing on a compliant surface with eyes closed and (vi) standing on a compliant surface with a visual conflict done. However, the mCTSIB test consists of four conditions which are obtained after eliminating the two conditions where the visual conflict dome were used in the CTSIB test, as no significant difference were observed

with the eyes open conditions. The four conditions of the mCTSIB test include standing on a firm surface with eyes open, standing on a firm surface with eyes closed, standing on a compliant surface with eyes open, and standing on a compliant surface with eyes closed. The mCTSIB dynamic platform test has been suggested to have a moderate validity and reliability to evaluate balance in older women living in the community (Antoniadou et al., 2020). Shaikh & Joshi (2020) observed that gender had no effect in the performance of static balance while using the mCTSIB test.

3.3. Motor control system

Motor control refers to the regulation of movement in organisms that have a nervous system (Li et al., 2018). This consists of reflexes and controlled movement (Li et al., 2018). Motor control is an important property required to perform the activities of daily living (ADLs) and for the regulation of stability and balance. The activities of daily living (ADLs) is a term used to describe the fundamental skills required to independently care for oneself (Bieńkiewicz et al., 2014). The central nervous system (CNS) and the peripheral nervous system (PNS) play an important role in motor control. The CNS integrates the input from the sensory system, coordinates and implement the orders required for the neuromuscular system to provide the necessary and accurate motor output (Alghwiri & Whitney, 2020). The CNS is defined as the brain and the spinal cord and it is usually considered to consist of seven basic parts: the spinal cord, the pons, the medulla, the midbrain, the cerebellum, the cerebral hemisphere and the diencephalon (Purves et al., 2001). The pons, midbrain and the medulla are collectively referred to as the brainstem; the cerebral hemisphere and diencephalon are collectively referred to as the forebrain (Purves et al., 2001). The brainstem consists of the cranial nerve nuclei. The cranial nerve nuclei are responsible for receiving input from the cranial sensory ganglia via the various cranial sensory nerve and to give rise to axons that form the nerves of the cranial motor (Purves et al., 2001). The brainstem is also considered as the channel for various crucial areas in the CNS (Purves et al., 2001). These areas are responsible for relaying sensory information from the spinal cord and brainstem to the midbrain and forebrain and vice versa (Purves et al., 2001). The cerebellum has been suggested to play an important role in timing, sensory acquisition and in the prediction of the sensory consequences of action (Manto et al., 2011). In humans, the cerebellum constitutes 10% of the brain volume but accounts for more than 80% of the neurons of the CNS (Herculano-Houzel, 2009). Its function is well known in motor control. However, recent studies have suggested that the cerebellum also aids in non-motor functions (Welniarz et al., 2021). Impairments of the cerebellum results in disorders relating to

speech, eye movement, limb movement, posture and gait, and cognition (Manto et al., 2011). The PNS is responsible for relaying information from the brain to the rest of the body and vice versa (Irimia & Van Horn, 2021). The peripheral nerves reside outside of the brain and spinal cord and can be divided into two: The autonomic nervous system and the somatic nervous system (Bradley, 1989). The autonomic nervous system regulates glands and control involuntary body function such as digestion, blood pressure and heart rate etc. (Maltese et al., 2020). The somatic nervous system is responsible for controlling motor movement and for relaying information from the sensory systems to the central nervous system (Bradley, 1989). Problems with the CNS and PNS affects balance in various ways. For example, severe COVID-19 was reported in four male subjects (ages 50 - 70 years) which affected their CNS and PNS, and resulted in confusion, psychiatric disorders (hallucinations and paranoid delusion), pyramidal signs, swallowing dysfunctions, upper limbs myoclonus, cognitive dysfunctions and fasciculation and focal muscle atrophy (Chaumont et al., 2020). In another study, twenty individuals that have suffered from stroke were compared against aged matched sixteen healthy controls to identify postural control impairment. Their centre of mass (COM) and centre of pressure (COP) information obtained from quiet standing and voluntary stepping response were used for comparison (Moisan et al., 2021). The result suggested that in quiet standing position, post stroke individuals showed greater maximal COP displacement in the mediolateral direction, greater displacement in the vertical direction and greater COM speed excursions compared to healthy controls. While during the voluntary stepping response, post-stroke individuals showed smaller step length, posterior foot placement in relation to the pelvis and COM anteroposterior excursions compared to those of heathy controls (Moisan et al., 2021). The link between the disorders of the CNS and vertigo has been reported (Saha, 2021).

3.4. Postural strategies

The strategies used to respond to unexpected postural disturbances can be grouped into five: the ankle strategy, hip strategy, stepping strategy, reaching strategy and suspension strategy (Alghwiri & Whitney, 2020). The strategy used by a person is based on the size of the base of support (BOS) and the amount of force created by the disturbance (Alghwiri & Whitney, 2020). Ankle strategy is used for small disturbances and involves the activation of muscles around the joint of the ankle while standing on a normal support surface (Alghwiri & Whitney, 2020). The ankle strategy has been suggested to consist of a delayed activation of the ankle, thigh and trunk muscles with this delay starting distally to proximally on the ventral position of the body (Nashner & McCollum, 1985; Horak & Nashner, 1986). The mobility and the strength of the

ankle is important for the successful implementation of the ankle strategy. The mechanical perspective of the ankle strategy is considered as a single segment inverted pendulum that is directed by the torque of the ankle joint. It involves the rotation of the body about the ankle joint with less movement about the superior joint (Nashner & McCollum, 1985). The latency i.e., the delay from the time of impulse to the time of action, is considered to be between 73 to 110 millisecond (Horak & Nasher, 1986).

Hip strategy is used for sudden and forceful disturbances of the BOS while the subject is standing and results in the activation of the muscles around the hip (Alghwiri & Whitney, 2020). Contrary to the ankle strategy, a delayed activation of the trunk and thigh muscles that occurs in a proximal to distal fashion is observed in the hip strategy (Alghwiri & Whitney, 2020). However, the hip strategy has the same latency as the ankle strategy (Alghwiri & Whitney, 2020). Mechanically, the hip strategy consists of the forward and downward rotation of the upper body which imposes on the lower body a backward rotation, while resulting in a decrease of the moment of inertia about the ankle (Runge et al., 1999). The hip strategy is limited by the friction of the surface and the horizontal force produced against the support surface (Nashner & McCollum, 1985; Horak & Nashner, 1986). The hip and ankle strategy are considered as the most widely used strategies for assessing postural control. Horak & Nashner (1986), suggested that people can learn how to implement/execute the ankle and hip strategy through a training paradigm. Smith et al. (2012), investigated the effect of a six-week strength training protocol on force sense and strength development in forty participants with functional ankle strategy, with a mean and standard deviation of ages 20.9 ± 2.2 years. The participants were divided into two groups of equal sizes and sex representing the control and experimental group. The participants in the experimental group performed strength exercises with their injured ankle three times per week for six weeks using strengthening methods that were clinically accepted for ankle rehabilitation with a load used to measure the strength and force sense. The result suggested that strength training at the ankle increased strength but does not improve force sense (Smith et al., 2012). Similarly, Hall et al. (2018), investigated the effect of strength training on balance and functional performance in thirty-nine young adult subjects aged 23.5 ± 6.5 years with chronic ankle instability. The subjects were divided into three groups: balance training protocol, strength training protocol and control, with each group performing 20 minutes of session, three times per week, for six weeks. The result suggested both training protocols improved strength, balance and functional performance (Hall et al.

2018). In both the ankle and the hip strategies, the generated muscle activities maintain the centre of gravity (COG) within the base of support (BOS).

When more forceful disturbances occur, other movements different from the ankle and hip movements, must occur to change the BOS in order to prevent falling (Alghwiri & Whitney, 2020). For forceful distances the stepping strategy is usually implemented (Alghwiri & Whitney, 2020). The stepping strategy involves the rapid movement of the forward and backward step in order to gain equilibrium in situations where the COG is displaced beyond the limits of the BOS (Alghwiri & Whitney, 2020). Im et al. (2021) investigated the effects of cerebellar disease on compensatory balance control in response to postural perturbation. In their study, comparison was made between ten healthy adult controls and ten aged-matched patients living with degenerative cerebella ataxia, and the recovery reactions to balance were assessed using a lean and release postural perturbation method while variables of the spatiotemporal characteristics of stepping movement and COM associated with the torso were obtained and analysed using a 3D motion capture system. The result suggested that patients with cerebellar disease utilised multiple steps to recover balance following perturbation while healthy controls used only a single step. Also, patients with cerebellar disease exhibited higher COM velocity, shorter foot to COM distance and less flexion of the trunk than the healthy controls (Im et al., 2021).

The reaching strategy involves the movement of the arm to grasp an object for support (Alghwiri & Whitney, 2020). The movement of the arm is important in the maintenance of stability as it alters the COG or protect against injury (Alghwiri & Whitney, 2020). The stepping and reaching strategies are the only strategies utilised to compensate for large perturbations and as such important in prevention of falls. The suspension strategy is used for maintaining a stable position during perturbation and it involves bending the knees during standing or ambulation (Alghwiri & Whitney, 2020). By bending the knee, the COG is lowered in respect to its distance from the base of support hence promoting better balance.

3.5. Key components in balance analysis

3.5.1. Centre of mass position and centre of pressure

The centre of mass (COM) is an imaginary point in the body where all the weight is said to be concentrated. It is obtained as the three-dimensional weight average position of each segment of the body (Corriveau et al., 2000). The vertical projection of the COM position on the ground is referred to as the centre of gravity (COG) (Boughen et al., 2013). The centre of pressure (COP) is a representation of the centre of distribution of the resultant applied force on the support surface (Corriveau et al., 2000; Zemková et al., 2021).

Direct information about postural sway and postural control in relation to balance is obtained by considering the movement of the COM position. Close relationship exists between the COM and COP movements with COM considered as a more valid measure of levels of equilibrium in movements requiring high velocity (Benvenuti et al., 1999). Despite the close relationship between the COM and COP especially when averaged, partially distinct aspect of movement and neural control is reflected by the instantaneous COM and COP position (Richmond et al., 2021). Recent modelling study by Safavynia & Ting (2013), suggested that the CNS may be more predisposed to the movement (position, velocity and acceleration) initiated by the COM position (Safavynia & Ting, 2013). During postural control the COM position is the key variable controlled by the central nervous system (CNS) (Scholz et al., 2007). Palmieri et al. (2002) suggested that the COP outcome reflects the CNS response to the COM (Palmieri et al., 2002). In other word, the COP movement reflects the neuromuscular response to maintain stability. Comparing the sway obtained from an inertial measurement unit and that from a force plate, Soangra & Lockhart (2013) observed that the sway obtained from the trunk does not provide the same physiological time series information as the COP sway. Fall risk is directly influenced by the increase in the COM variability. This variability manifests itself in the form of an increased range of velocity of the COM position in relation to the BOS and in turn results in periods of low margin of stability (Hof et al., 2005). Small margin of stability results in difficulty in withstanding a large perturbing force (van Emmerik et al., 2016). The area of the BOS is of immerse importance when evaluating the excursion of the COM position. Within a larger BOS, the COM and COP have greater room for postural stability while a small BOS limits the maximum stable excursion of the COM position. Constant movement of the COM requires the range of the COP to be greater than that of the COM to prevent a fall occurrence

(Winters, 2009). To constrain the movement of the COM, the COP attempts to reach the boundaries of the BOS before the COM.

The uncontrolled movement of the COM reflects the challenge faced in balance while the movement of the COP represents the response of nervous and musculoskeletal systems to counter the challenge (Richmond et al., 2021). Thus, while there is a close relationship between these measures, there exists differences in what they measure. The recognition of this distinction may be valuable to clinicians in keeping track of the changes in patients' performance.

3.5.2 Planes and axes of movement

The ground in which we stand can be considered as a two-dimensional shape consisting of the horizontal and vertical axes. The horizontal axis also known as the abscissa/x axis, is drawn from left to right while the vertical axis also known as the ordinate/y axis is drawn from top to bottom. The meeting point of these two axes is referred to as the origin. However, in other to completely describe the shape of a person a three-dimensional shape is often used. In addition to the above two axes, a z-axis can be obtained by drawing a line in space to meet the x and y axes of the ground. Utilizing the three-dimensional representation, the planes of movement and the axes of movement can be described with the origin of these planes and axes usually expressed as the centre of mass. The planes of movement can be divided into three: sagittal, frontal and transverse (Cury et al., 2021). The sagittal plane is the plane that runs from the front to the back starting from the head to the toe or superior to inferior and divides the body into two equal halves left and right (Grimshaw et al., 2019). The transverse/frontal axis of rotation is perpendicular to the sagittal plane and extends from left to right (Grimshaw et al., 2019). Body movement in this plane occurs about the transverse axis i.e., the direction of which it is perpendicular. Examples of motion in this direction include flexion and extension movement or anterior and posterior movements examples include somersault, walking, jumping, squatting. The frontal plane runs from side to side and superior to inferior orientation while dividing the body into the equal front (anterior) and rear (posterior) portions (Grimshaw et al., 2019). The axis perpendicular to the frontal plane is called the sagittal or the anterior-posterior axis. Example of movement about the sagittal axis and in the frontal plane is the cartwheel. A cartwheel is an activity in which a person performs a lateral handspring with arms and legs extended i.e., similar to rolling a coin from side to side while looking at it from the front. The transverse plane runs from side to side and anterior to posterior orientation and divides the

body into two equal parts: upper (superior) and lower (inferior) portions. The axis perpendicular to the transverse plane is called the longitudinal axis. Example of a movement in this plane and a rotation about this axis is the pirouette (Grimshaw et al., 2019). The anatomical position (facing forward, arms by the side, palms forward with fingers extended and feet forward and parallel) with the planes and axes of movement is shown in Figure 3.3**.**

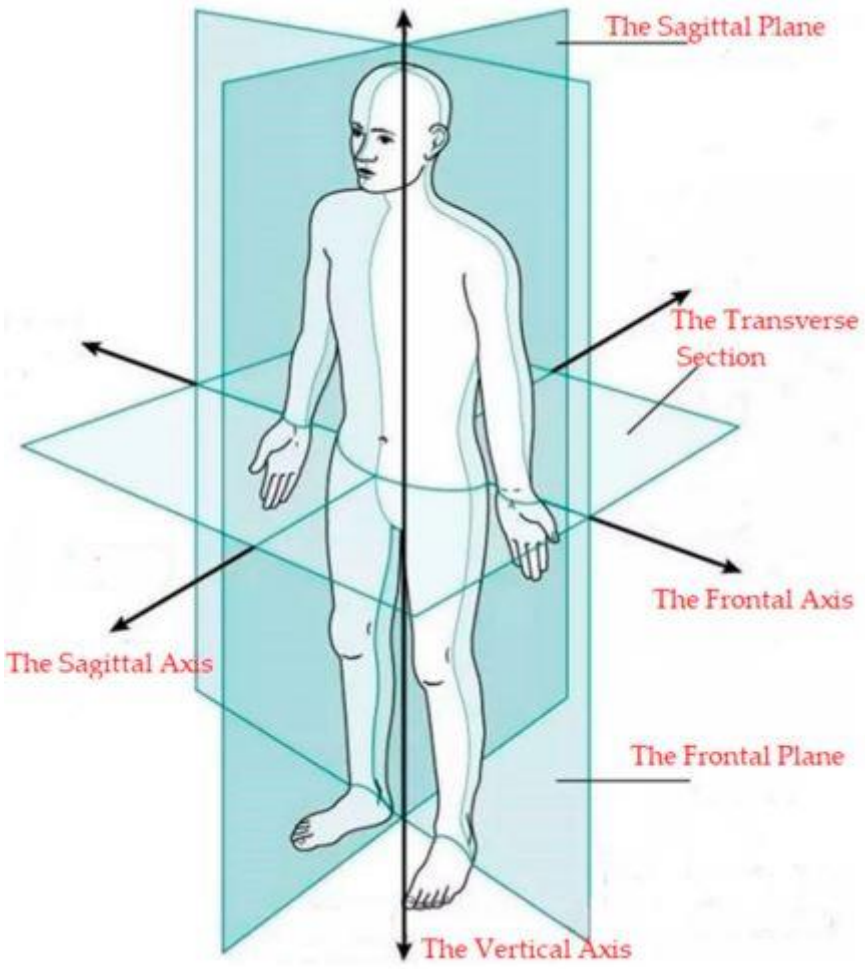

Figure 3.3. Planes and axis of motion (Duan et al., 2020)

In the analysis of human balance while in quiet standing position, two axes are often used for the quantification of the postural sway: the anterior-posterior (AP) or the sagittal axis and the mediolateral (ML) or the transverse axis. Using the centre of pressure velocity and standard deviations of the AP and ML axes, gender and age-related differences were investigated among 47 older adults (70% women) and 38 younger adults (58% women) in their control of balance during and after stair descent on a foam mat (Kováčiková et al., 2021). The result showed

significant COP sway and velocity in both directions for older women as compared to older men where only significantly higher values were observed in the AP direction in relation to the younger counterparts. The result suggested that advancement in age, results in higher risk of women falling forward and sideways while men were prone to fall forward (Kováčiková et al., 2021).

3.5.3. Types of movement

In other for humans to navigate their environment and participate in activities various type of movement are used. These include extension, abduction/adduction and rotation.
During extension movement, the angle between two adjacent segments of the body increases as the ventral surfaces of the segments move away from each other (Uppal, 2020). This movement occurs in a sagittal plane about a frontal axis. However, the extension of the thumb is an exception to the direction of movement of extension as it takes place in the frontal plane and about the sagittal axis (Uppal, 2020).

Flexion movement occurs in the sagittal plane, about the frontal axis and results in a decrease of the angle between two adjacent segments in the body as the ventral surfaces approximate each other. The extension of the thumb is an exception to the direction of movement of flexion as it takes place in the frontal plane and about the sagittal axis (Uppal, 2020).

Abduction is movement in the frontal plane about the sagittal axis and involves moving the body part away from the midline of the body (Uppal, 2020; Hamill et al., 2021). Adduction occurs in the frontal plane, about the sagittal axis and is a return movement of the segment of the body that occurred during abduction back towards the midline position of the body. Abduction and adduction occur in the body parts of the foot (metatarsophalangeal), hip, shoulder, wrist, and hand (metacarpophalangeal) joints.

Rotational movements include any twisting motion and occurs in the transverse plane. A rotation can either be medial (internal) or lateral (external) (Hamill et al., 2021). Rotational movement is carried out using the hip and shoulder. These joints are referred to as ball and socket joints. Through the use of smaller joints, our necks and backs can be rotated. The pivot joint in the neck between the first two vertebrae (C1 and C2) called the atlanto-axial joint is also used for rotation (Delleman et al., 2004). Rotation of the hip and shoulder are also considered as internal (medial) or external (lateral) rotation.

3.5.4. Types of motion

In humans, there are two types of motion: translational and rotational motion (Hamill et al., 2021). In translational motion, the motion of the centre of mass of the body from one position to the other is along a straight line. Rotational motion is also known as angular motion and refers to motion in which all parts of the body segment, travel through the same angle simultaneously and in the same direction about the axis of rotation but having varying distances e.g., the movement of a body segment about a joint such as the elbow (Hamill et al., 2021).

3.6. Accelerometry in balance analysis

Accelerometry refers to the technique of using inertial measurement unit (IMU) to quantify human movement (Ojie & Saatchi, 2020). An IMU consists of an accelerometer, gyroscope and magnetometer. However, the magnetometer is not often used due to its sensitivity to the magnetism of ferrous metals.

3.6.1. Accelerometer

An accelerometer is an inertial sensor that measures the acceleration of a moving system. They are useful in other motion sensing applications such as tilt, shock and for detecting vibration (Analogue Device Incorporation, 2009; Senturia, 2001). Accelerometers have been a major contributor to the MEMS market since 2012 due to their varied application in areas such as smartphones, flight control and navigation, air bag control unit etc. (Perlmutter & Breit, 2016; Yazdi et al., 1998). The MEMS accelerometer have the advantages of low power, small size, easy integration with existing systems and high precision (Yazdi et al., 1998). The sensing mechanisms utilised by accelerometers are capacitive type, piezo-resistive and piezoelectric (Mukhiya et al., 2020). The capacitive accelerometer is preferred to other types due to its low noise and high sensitivity, low power dissipation, and compatibility with CMOS (Mukhiya et al., 2019). The underlying operational mechanism for the accelerometer is often described using the mass-spring system which is explained using the principle of Hooke's law and newton's second law of motion. Hooke's law states that within the limits of proportionality, the extension of a spring is directly proportional to the force applied to it ($F = kx$) (Mustafazade et al., 2020). On the other hand, Newton's second law states that the acceleration of a body is directly proportional to the force applied to it but inversely proportional to the mass of the object ($F = ma$). When movement occurs on a mass-spring system it leads to the compression

of the spring which produces a restoring force proportionate to the movement (Kavanagh & Menz, 2008).

In practice, the class of the accelerometer determines the technique used to quantify the acceleration (Kavanagh & Menz, 2008). In capacitive accelerometer, the mass element made of silicon is surrounded by an array of paired capacitors that is placed on the opposite sides of the housing of accelerometer. During movement, an imbalance is created between the opposing capacitor. This imbalance is due to the reaction of the mass element to the movement. Subsequently, the imbalance created results in an electrical output signal that is proportional to the magnitude of the acceleration applied (Kavanagh & Menz, 2008). The schematic diagram of the basic principle of operation of a parallel plate capacitor is shown in Figure 3.4.

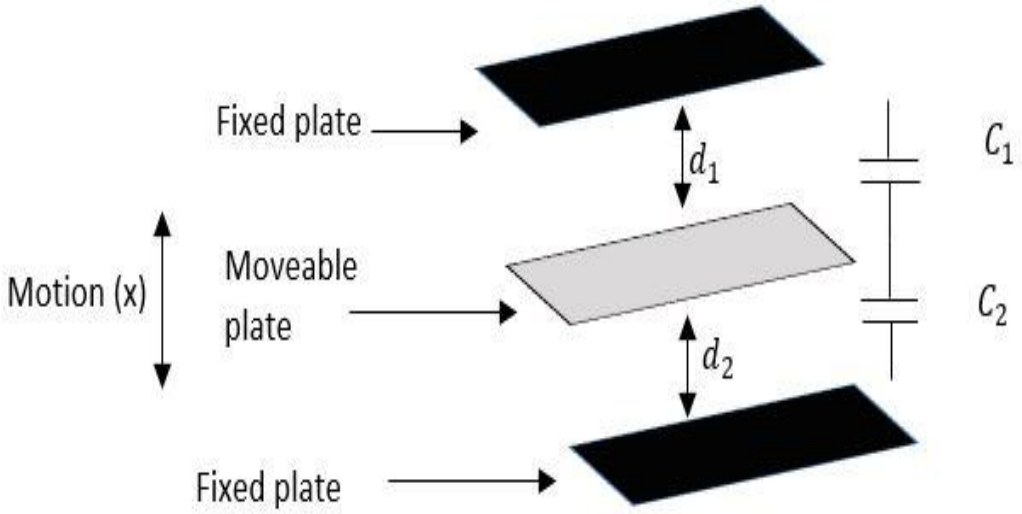

Figure 3.4. Principle of operation of accelerometer (Dadafshar, 2014).

The motion of the moveable plate results in a change in the capacitance c_1 and c_2, whose difference result in the displacement and direction of the moveable mass. The acceleration is obtained from the displacement. The capacitance of a parallel plate capacitor can be obtained using Equation (3.1) (Dadafshar, 2014).

$$C = \varepsilon_0 \varepsilon_r \frac{A}{d} \tag{3.1}$$

where ε_0 is the permitted free space with an approximate value of 8.85 × 10−12 F/m, ε_r is the relative permittivity between the plates, *A* is the area of overlap between the electrodes and *d* is the separation between the plates.

Irrespective of the accelerometer class, calibration is required to match the corresponding electrical output and the reference value of the acceleration. The calibration is performed under

specific conditions (Kavanagh & Menz, 2008). According to Kavanagh & Menz (2008), the calibration of an accelerometer can be carried out in two ways: static and periodic calibration. In static calibration, the output of the stationary accelerometer is compared with a known constant of acceleration (Kavanagh & Menz, 2008). For example, when aligned to gravity or the global vertical, the output of the sensing axis of the accelerometer should correspond to 1g and -1g when inverted respectively. Once the accelerometer raw output has been established for static conditions, a two-point linear calibration can be used to transform the raw output to units of acceleration (Kavanagh & Menz, 2008). Other forms of calibration which assumes linearity such as zero-span and slope intercept method can also be used (Kavanagh & Menz, 2008). Alternatively, periodic calibration can be used although it is more time consuming and requires a specialised equipment. In periodic calibration, the relationship between the raw accelerometer output and the known acceleration harmonics is obtained by harmonic forcing of the accelerometer (Kavanagh & Menz, 2008). Periodic calibration has the advantage of enhancing the accuracy of the accelerometer measurement especially at a range of amplitude and frequencies that would be expected in real world situations (Kavanagh & Menz, 2008).

In general, the fundamental characteristics in selecting an accelerometer are based on the bandwidth, sensitivity, voltage noise density, zero-g voltage, frequency response and dynamic range (Dadafshar, 2014). The bandwidth of an accelerometer in units of Hertz (Hz), refers to the range of vibration frequency to which the accelerometer will respond. The bandwidth is a critical consideration for data collection. The frequency range of body movement is contained below 20 Hz (Bianchi et al., 2010; Karantonis et al., 2006). However, for static posture, the frequency range of movement is below 5 Hz and as such a sampling frequency of 10 Hz is sufficient (Bao & Intille, 2004). The sensitivity of an accelerometer refers to the change in the electrical output signal per unit mechanical change (Dadafshar, 2014). It is a measure of the minimum detectable signal and the higher its value the more responsive the accelerometer to small changes in motion. The sensitivity of an analogue accelerometer is given in units of millivolt per acceleration due to gravity (mV/g). For digital accelerometers, the sensitivity is given in least significant bit per acceleration due to gravity (LSB/g). The voltage noise density changes with the inverse of the square root of the bandwidth. The accuracy of the signal is affected by the speed at which the accelerometer readings are obtained (Dadafshar, 2014).

3.6.2. Gyroscope

Gyroscopes are sensors used for motion detection. Basically, it transforms the angular movement of an object or body from its physical quantity into electrical signal (Chen, 2005). There are various types of gyroscopes: mechanical, micro electrical mechanical sensors (MEMS) and optical (Abdelzaher et al., 2021). The mechanical gyroscope is made up of a free wheel that occupy a 3-dimensional space. The operation of the wheel is based on the principle of the conservation of angular momentum. This principle which is also referred to as the rotational equivalent of Newton's third law of motion states that: in a system that is closed, the exerted torque on an object is equal and opposite to the torque exerted on another object (Krishna, 2021). In the case of the mechanical gyroscope, the orientation angle is obtained by using an angle acquisition unit. The transformation of angular motion into an electrical signal is carried out using Coriolis effect and is based on the movement of a metal sphere connected to a group of springs. This has led to the development of the micro-electro-mechanical system (MEMS) (Bergh et al., 1984; Abdelzaher et al., 2021). The MEMS gyroscope is made up of a mass that is attached to a solid frame by springs. It is constructed using silicon micro-machining technique. Based on the construction material, the MEMS gyroscope is divided into two types: silicon and non-silicon (Miller et al., 2007; Witvrouw et al., 2004). Among the non-silicon types, the quartz gyroscope is of great interest because of its measuring ease and high-quality factor (Madni et al., 2003). However, the quartz gyroscope is expensive, and its fabrication process is complex. Compared to the quartz gyroscope, the advantages of the silicon MEMs gyroscope include low cost, high sensitivity, high precision, good linearity, small size and low power consumption (Liu et al., 2009). The silicon MEMs gyroscope is used in a large variety of settings such as information and communication, aeronautics and astronautics, medical treatment, national defence, industry, navigation, environment and bioengineering (Guo et al., 2015). A diagram illustrating a simple working principle of the MEMS gyroscope is shown in Figure 3.5**.**

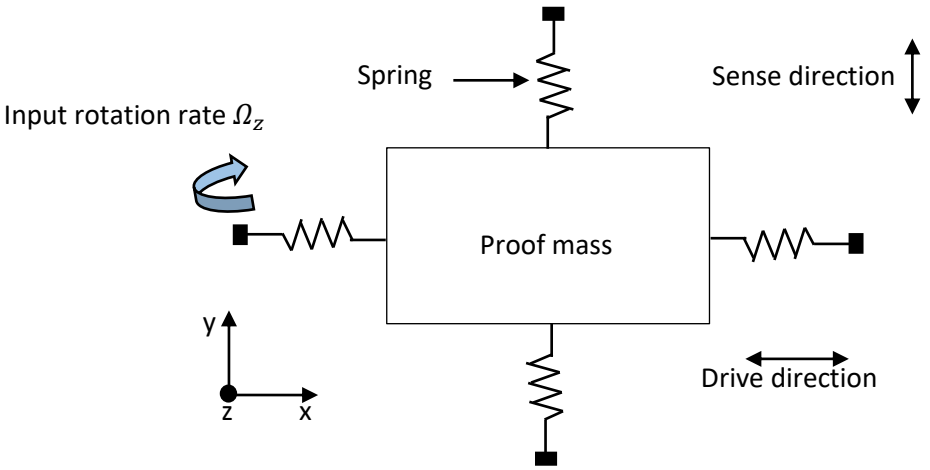

Figure 3.5. The typical mechanics model of the Coriolis effect gyroscope (Guo et al., 2015)

The sensor consists of a drive system, a sense element and a proof mass. The drive system and the sense element could be supported by a spring-like system and a suspended beam is used to support the proof mass. The drive system initiates a constant motion of the proof mass which reciprocates back and forth in the x direction. The displacement of the proof mass (x) is shown in Equation (3.2) (Guo et al., 2015).

$$x = A_x \cos(\omega_x t) \tag{3.2}$$

where A_x, is the amplitude of the movement of the displacement; ω_x, is the angular speed of the driving system (Guo et al., 2015). An angular rate applied to the sensor in the Z direction results in a Coriolis force along the *Y* direction. The force in the *Y* direction (F_y) is expressed in Equation (3.3) (Guo et al., 2015).

$$F_y = 2m\Omega \times v = -2m\Omega A_x \omega_x \sin(\omega_x t) \tag{3.3}$$

where Ω is the applied angular speed; v is the linear speed of the proof mass (Guo et al., 2015).

3.6.3. Placement of the sensor

The placement of the sensor refers to the location of the body where the sensors are placed and the way it is attached to that location (Yang & Hsu, 2010). The ergonomic guideline of the wearability for the description of the interaction between the wearable object and the human body have been proposed by Gemperle et al. (1998). The locations proposed for wearing an IMU sensor include the collar area, rear of the upper arm, waist, forearm, front and rear sides of the ribcage, thighs, top of the foot and shin (Gemperle et al., 1998). These locations are common for both sexes, have a large surface area for attachment, and are less flexible. In most

cases, the sensor is placed on the sternum, lower back and waist to measure the entire body movement. Nguyen et al. (2021) proposed an algorithm for the estimation of the trunk acceleration using an IMU worn at the sternum. Lyu et al. (2019) investigated the difference in sway for a sensor placed at the sternum against the sensor placed at the waist level of twenty-six (twelve males and fourteen females) healthy adults and found no difference between the sway obtained from the sternum and the waist level (Lyu et al., 2019). However, there is a possibility of inaccuracies in the result as less sway is expected for healthy adult subjects and the sway at the sternum has a different ground projection from that of the waist. Adamová et al. (2018) investigated the postural stability of patients with cerebellar disorder during quiet stance using three-axis accelerometer placed at the lower back at the L region. Alkathiry et al. (2018) reported the use of accelerometer placed at the lower back to record postural sway in adolescents with concussions. Baracks et al. (2018) utilised the use of accelerometer placed at the lower back to investigate acute based sport related concussion.

In most studies, the waist placement of the motion sensor is usually adopted as the torso occupies most of the mass of the human body and it is close to the centre of mass position of the entire body (Yang & Hsu, 2010). This ensures that the acceleration measured by a single sensor is a representation of the major part of the human motion (Yang & Hsu, 2010). Ergonomically, the weight bearing capacity of the torso is greater than most part of the body and can bear extra weight of wearable devices (Yang & Hsu, 2010). The waist also provides easy attachment and detachment of sensors and causes less restrain in body movement while minimizing discomfort.

Another issue to consider in wearable sensors is the mode of attachment to the human body. The attachment of wearable sensors can be made directly to the skin (Najafi et al., 2003; Lindemann et al., 2005); using an indirect method such as a pant belt, wristband, straps or other accessories (Liszka-Hackzell & Martin, 2005; Menz et al., 2003; Menz et al., 2003) and integrated into clothing (Noury et al., 2004). It is necessary that the accelerometer is securely attached to the human body to prevent unintended movements that could affect its accuracy. In this study, the waist attachment method using a belt is utilised due to its ease of attachment, closeness to the centre of mass and reliability.

3.6.4. Mode of transmission

Accelerometers can be connected either wired or wirelessly. Wired connection consists of only one system which is attached to the subject using a cable to a computer. The main problem with wired connection is that it restricts the movement of the subject as the range is limited to the length of the physical connection to the computer. On the contrary, the wireless connection consists of two sections: the transmitter and receiver sections. The transmitter section usually contains the accelerometer and the wireless transmitting unit and is attached to the subject. The dominant wireless technologies include ZigBee (Mu & Han, 2017) and Bluetooth. Low et al. (2020) utilised the XBee as a medium for communication of postural sway related data. Clark et al. (2021) utilised Bluetooth as the medium for collecting postural sway data (Clark et al., 2021). The ZigBee module are expensive in comparison to other standards such as Bluetooth, Radio Frequency Infrared Detection (RFID) and Near Field Communication (NFC) (Saha et al., 2017). However, the aforementioned standards are limited by their area of coverage (Saha et al., 2017). A new technology that is easy to configure and cheaper called the nRF24L01+ has been added to these technologies. The nRF24L01+ has been compared to a version of the ZigBee called the XBee and found to provide better throughput than the XBee (Saha et al., 2017). The rate of transmission has also been determined to be higher than the XBee in multi-hop networks (Saha et al., 2017). Thus, in this study, the nRF24L01+ module is used to implement the wireless capability of the device.

3.6.5. Signal filtering

Most sensors are plague with some limitations in their performance and the accelerometer and the gyroscope are no exception. The accelerometer has been reported to be affected by noise and this noise results in inaccuracies in its reading. Similarly, limited by the current fabrication technology, the precision level of the gyroscope is usually low (Diao et al., 2013). The output of the gyroscope sensor is affected by drift and noise which result in a decline in its accuracy with time (Diao et al., 2013). The noise in the accelerometer is known to be of high frequency while the noise in the gyroscope is known to be of low frequency. Filtering and sensor fusion techniques are usually applied to produce accurate readings. Filtering is the process of removing unwanted frequencies from a signal (de Cheveigné & Nelken, 2019). The goal of signal filtering is to process the signal so that the result is more suitable than the original signal for a specific application (de Cheveigné & Nelken, 2019). Fourier transform is used to reflect the frequency of the periodic part of the signal. A filter can be considered as a matrix whose

components vary from 0 to 1. When the component is 1, the frequency is allowed to pass and when 0, the frequency is removed (Guo et al., 2015). A large variety of signal processing can be implemented through the application of differing filters. Examples of these filters include low pass filter, high pass filter and band pass filter (de Cheveigné & Nelken, 2019). A low pass filter attenuates high frequencies while passing low frequencies. A high pass filter allows high frequency signal to pass through while attenuating lower frequency. The cut-off frequency is the main determining factor of both filters. Frequencies below the cut-off frequency are considered as low frequencies while frequencies above the cut-off frequencies are called high frequencies. The band pass and band reject filter allow specific frequencies to pass through i.e., for a band pass filter, the cut-off frequencies are frequencies outside the specified range, while for a band reject filter, the cut-off frequencies are frequencies in the specified range (de Cheveigné & Nelken, 2019). However, these filters are not ideal in nature because in practical implementation they behave in a causal fashion i.e., the output cannot be determined by the input in the future but are based on the present and past input. This creates a delay which result in a phase change that is inconsistent with the frequency response specification for an ideal filter. An ideal filter has zero transition from the pass-band to the stop-band. The filtering techniques used in this study are the Butterworth low pass filter and the complementary filter.

3.6.5.1. Butterworth low pass filter

The Butterworth filters are referred to as maximally flat filters. They are called maximally flat because for a given order, they have the sharpest roll off possible (Ellis, 2012). The second-order Butterworth filter is the two-pole filter with a damping ratio of 0.707. Butterworth filters are commonly used because they do not have peaking (Ellis, 2012). The general formula for the Butterworth filter depends on whether the filter order is odd or even. The amplitude response of the Butterworth filter is given by Equation (3.4) (AlHinai, 2020).

$$|H(j\omega)| = \frac{1}{\sqrt{1+\left(\frac{\omega}{\omega_c}\right)^n}} \tag{3.4}$$

Where n is the order of the filter, ω is the frequency of the signal and ω_c is the cut-off frequency.

3.6.5.2. Complementary filter

The complementary filter is a sensor fusion technique that consists of a low-pass and a high pass filter. The accelerometer has noise (unwanted signal that does not represent the true vibration) produced by the mechanical vibrations of the polysilicon springs, signal conditioning circuitry, and the measurement system (Mohd-Yasin et al., 2003). The gyroscope drift is mainly due to integration of the bias instability and the angular random walk (Guo et al., 2015). The dynamics of the gyroscope is complementary to the that of the accelerometer i.e., combining in such a way as to enhance the qualities of each other. The basic structure of the complementary filter is shown in Figure 3.6.

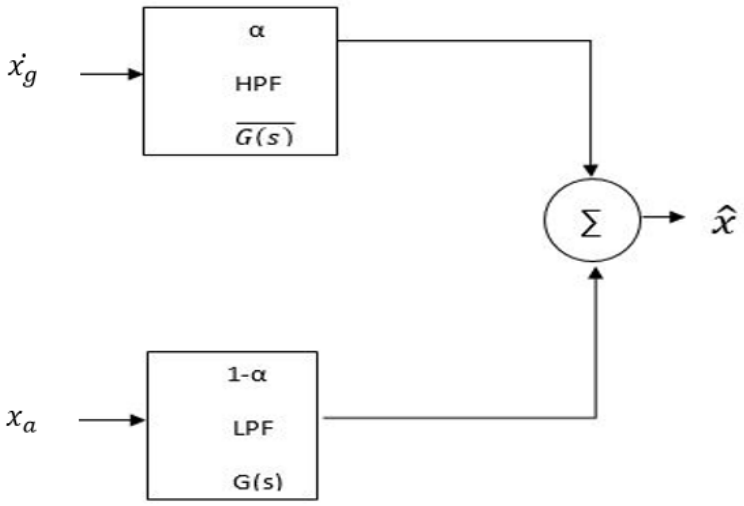

Figure 3.6. Basic structure of the complementary filter (Narkhede et al., 2021)

The figure consists of two inputs x_a and $\dot{x_g}$, where x_a is the accelerometer angle which could either be roll or pitch and $\dot{x_g}$ is the corresponding gyroscope rate of change of the angle, $G(s)$ is the transfer function of the low pass filter, $\overline{G(s)}$ is the transfer function of the high pass filter, $\hat{x}$ is the complementary filter output and $G(s)+\overline{G(s)}=1$.The complementary filter output $\hat{x}$ is given by Equation (3.5) (Narkhede et al., 2021).

$$\hat{x} = G(s)\, x_a + \overline{G(s)}\dot{x_g} \tag{3.5}$$

Analytically, the angle ($\hat{x}$) is given by Equation (3.6) (Narkhede et al., 2021).

$$\hat{x} = \alpha \times \left(\int \dot{x_g} dt\right) + (1-\alpha) \times x_a \tag{3.6}$$

The parameter α also known as the scaling factor varies from 0 to 1 and determines the weight given to the gyroscope and the accelerometer. The scaling factor is usually between 0.7 and

0.98, dt represents the sampling period. The scaling factor and the time constant τ is given by the Equation (3.7) (Narkhede et al., 2021), dt is the sampling rate and f_c is the desired cut-off frequency.

$$\alpha = \frac{\tau}{\tau + dt}, \tau = \frac{1}{2\pi f_c} \tag{3.7}$$

The estimate of the filter angle in terms of the transfer function in the frequency domain ($dt = 1/s$) is given by Equation (3.8) (Narkhede et al., 2021).

$$\hat{x} = \frac{\tau s}{\tau s + 1}\left(\frac{\dot{x}_g}{s}\right) + \frac{1}{\tau s + 1}(x_a) \tag{3.8}$$

3.7. Statistical and machine learning methods for human balance analysis

3.7.1. Statistical methods

Statistical methods involve the testing of hypothesis based on information provided by the samples and to draw conclusions for the population based on the result of the hypothesis (Emmert-Streib & Dehmer, 2019). In carrying out hypothesis testing, the sample under consideration is usually divided into a minimum of two groups considered as the experimental and the control group. The experimental group is the group under test and it is given the treatment while the control group is usually given a placebo or left alone (Emmert-Streib & Dehmer, 2019). The methods used for statistical testing is based on the level of measurements and the type of statistical inference (Fisher & Marshall, 2009).

3.7.1.1 Level of measurement

The level of measurement refers to the mechanism by which a variable is scored (Allanson & Notar, 2020). Generally, there are three main levels of measurement: nominal, ordinal and continuous. The nominal level of measurement refers to the scoring of cases into broad categories. In nominal levels of measurement, the categories must be sufficient for the cases, and mutually exclusive (Fisher & Marshall, 2009). The categories do not have hierarchical meanings i.e., considering sex, male is not different from female in terms of hierarchy (Fisher & Marshall, 2009). Examples of nominal levels of measurement include sex, religion and diagnosis etc. Ordinal level of measurement refers to the scoring of research participants into categories that have hierarchical meaning (Fisher & Marshall, 2009). Ordinal levels are used for variables that cannot be directly measured for example anxiety, pain and satisfaction. Like nominal data, ordinal categories are mutually exclusive and exhaustive, however unlike the

nominal levels, the categories have numerical hierarchy (Fisher & Marshall, 2009). For example, the Likert scale is numbered from low score to high score with each score having a numerical meaning. Continuous level of measurement refers to the measurement based on infinite scales where increments on the scales are of equal distance (Fisher & Marshall, 2009). Examples of continuous level data include pressure in mmHg, volume in millimetres and weight in grams etc. Continuous level of measurement can be divided into interval and ratio level of measurement. The data measured on the ratio scale have an absolute zero i.e., a zero score implies the absence of existence (Fisher & Marshall, 2009). Interval level of measurement does not have an absolute zero. An example of interval level of measurement is temperature, where an absolute zero does not mean nonexistence.

3.7.1.2. Type of statistical inference

Several parametric and nonparametric methods exist in literature. However, the most popularly employed methods are utilised in this study and consists of the t-test, Wilcoxon signed rank test, Mann-Whitney U test, Pearson and Spearman correlation, one-way analysis of variance, Kruskal Wallis test and the Friedman test.

3.7.1.2.1 T test

The t-test is a parametric method used to compare the mean of two groups (Kim, 2015). The t-test is used when the samples satisfy the condition of normality, independence and equal variance. The test of equal variance can be carried out using the Levene's test or the Bartllet's test and the test for a normal distribution can be carried out based on the Shapiro's test or the Kolmogorov-Smirnov test. The t-test can be divided into two: the independent t-test and the paired sample t-test (Kim, 2015). The independent t-test is used when the two groups under consideration are independent of each other while the paired sample t-test are used when the two groups under consideration are dependent on each other. In the independent t-test, the experimental subjects are divided into two independent groups, with one group given a particular treatment different from the other, while the dependent variable is measured on a continuous scale (Kim, 2015). In the paired sample t-test, the same group is treated with different treatment at differing times. The formula for calculating the t statistic between two groups of an independent sample with the assumption of a normal distribution and equal variance (independent sample t-test) is given by Equation (3.9) (Kim, 2015). Where $\bar{X}_1$ and $\bar{X}_2$

represents the mean of the samples of the two groups, $s_{(1+2)}$ represent the standard deviation of the samples of the two groups, n_1 and n_2 represents the number of samples in each group.

$$t = \frac{\bar{X}_1 - \bar{X}_2}{s_{(1+2)}\sqrt{\frac{1}{n_1}+\frac{1}{n_2}}} \sim t\,(n_1 + n_2 - 2) \tag{3.9}$$

In situations where the assumption of equal variance cannot be met and/or the sample size differ the Welch's t-test method is used.

In the paired sample t-test, the same sample is used which could lead to correlations in the variance and hence, the variance of the paired sample t-test differs from those of the independent sample t-test as a result of these correlations (Kim, 2015). In cases where the samples are not independent, the variance can be given by Equation (3.10) (Kim, 2015), where ${\sigma_1}^2$ is the variance of variable A and ${\sigma_2}^2$ is the variance of variable B, ρ is the correlation coefficient of the two variables. For an independent sample, the correlation coefficient (ρ) is zero. Since the samples are the same, the t statistic for the paired sample t-test is given by Equation (3.11) (Kim, 2015).

$$\mathrm{Var}(\mathrm{A} - \mathrm{B}) = {\sigma_1}^2 + {\sigma_2}^2 - 2\rho\sigma_1\sigma_2 \tag{3.10}$$

$$t = \frac{\bar{X}_1 - \bar{X}_2}{\sqrt{\frac{{s_1}^2 + {s_2}^2 - 2\rho s_1 s_2}{n}}} \tag{3.11}$$

3.7.1.2.2. Mann-Whitney U test and Wilcoxon signed rank test

The Mann-Whitney U test and Wilcoxon signed rank test are nonparametric alternatives of the independent sample t-test and the paired sample t-test. In contrast to the independent samples t-test, the Mann-Whitney U test also known as the Wilcoxon rank sum test, is used to test for the differences between two groups on a single ordinal variable when the data does not conform to a normal distribution (Mann & Whitney, 1947; MacFarland & Yates, 2016; Mesároš et al., 2019; Wilcoxon, 1945). The calculation of the Mann-Whitney U test is carried out using Equation (3.12) Where U is Mann–Whitney U test, n_1 is sample size one, n_2 is sample size two, R_i is the rank of the sample size.

$$U = n_1 n_2 + \frac{n_2(n_2+1)}{2} - \sum_{i=n_i+1}^{n_2} R_i \tag{3.12}$$

The Wilcoxon signed rank test is used when the parametric condition required for the paired

sample t-test are not met. The design criteria require that the samples are paired, the data are not subjected to the conditions of normality but at least of an ordinal scale. Rosenblatt & Benjamini (2018), evaluated the performance of the Wilcoxon signed rank test and the paired sample t-test under mixture alternatives. They observed that Wilcoxon signed rank test is more useful than the t-test in conditions where normality cannot be obtained. The Wilcoxon signed rank test is calculated using Equation (3.13).

$$W = \sum_{i=1}^{N_r}[sgn(x_{2,i} - x_{1,i}).R_i] \quad (3.13)$$

Where W is the test statistic, N_r is the sample size, sgn is the sign function, $x_{1,i}$ and $x_{2,i}$ are the corresponding ranked pairs from two distribution and R_i is the rank i.

3.7.1.2.3. Analysis of variance

The Analysis of variance (ANOVA) is a statistical technique for comparing the means of more than two groups. The ANOVA test can be broadly classified into two: the one-way ANOVA and the one-way repeated measures ANOVA (Mishra et al., 2019). The one-way ANOVA is used for independent samples, and it is considered as the extension of the independent sample t-test onto three or more groups (Mishra et al., 2019). The one-way repeated measures of ANOVA is used for dependent samples and it is considered as the extension of the paired sample t-test. The repeated measures design consists of multiple measures of the same variable taking under different conditions or time period on the same or matched subjects (Mishra et al., 2019). A significant p-value in this test leads to further pair-wise multiple comparisons to determine the significant pair. This further pair-wise comparison is also referred to as post-hoc analysis (Mishra et al., 2019). When post-hoc analysis is carried out correction for multiple testing is required (Smalheiser, 2017). The simplest method is to use Bonferroni correction. This involves dividing the p-value by the number of pairwise test conducted (Smalheiser, 2017). The general idea for the calculation of the ANOVA is to compare the variability across the groups with that of the variability within the groups (Smalheiser, 2017). When the variability within groups is much smaller than the variability across groups, at least one of the groups has a mean that is different from the others (Smalheiser, 2017). If the ratio of the across group variability and the within group variability is greater than 1, then at least one group is significantly different from the others. The ratio is indicated in Equation (3.14) (Smalheiser, 2017).

$$\frac{Across\ group\ variability}{within\ group\ variability} = \frac{SS_a/\mathrm{df}_a}{SS_w/\mathrm{df}_w} \tag{3.14}$$

Where SS_a is the across group sum of squares, SS_w is the within group sum of squares, df_a is the across groups degree of freedom and df_w is the within groups degree of freedom. $\mathrm{df}_a = k - 1$ and $\mathrm{df}_w = nk - k$, where k is the number of groups and n is the total number of data points in each group. A ratio of variance follows the F distribution.

The ANOVA is a parametric statistic test and is used if the assumptions of parametric statistics are meant such as conformity to a normal distribution, equal variance of each group, and each data point of the same group are independent of each other, randomly sampled and follows the same underlying distribution (Mishra et al., 2019). The Kruskal-Wallis test is the nonparametric equivalent of the one-way ANOVA and it is based on ranks. The Friedman test is the nonparametric equivalent of the one-way repeated measures ANOVA. A detailed account of the calculation of these tests can be found in Hoffman (2019).

3.7.1.2.4. Correlation analysis

Correlation analysis examines the strength of the relationship between two variables. The choice of the measure of correlation depends on the scale of measurement and the distribution of both variables (du Prel et al., 2010). Pearson correlation (r) is a parametric variant that exclusively test for the linear relationship between two variables (Liu et al., 2020).

The assumptions for Pearson correlation are: linear relationship, independence of the variables and normality (Deshpande et al., 2016). The spearman correlation (ρ) is a nonparametric variant that tests for the monotonous relationship between two variables and has the advantages of robustness to outliers and suitable for skew distributions (du Prel et al., 2010; Gogtay & Thatte, 2017). The null hypothesis to be tested claims no linear or monotonous relationship exist between the variables. The correlation coefficient is a single value that determines the relationship between the two variables under consideration (Gogtay & Thatte, 2017). The values of the correlation coefficient can vary between -1 to +1 with -1 representing the maximum inversely proportional relationship and +1 representing the maximum directly proportional relationship (du Prel et al., 2010; Gogtay & Thatte, 2017; Liu et al., 2020). A correlation coefficient of 0 indicates that no linear or monotonous relationship exist between the two variables under consideration (Gogtay & Thatte, 2017). The calculation of the correlation coefficient gives the sample correlation coefficient of which test of significance is

required to see how the value compare with the true population value i.e., the population correlation coefficients (Gogtay & Thatte, 2017). By squaring the value of the correlation coefficient, the coefficient of determination (r^2) is obtained, which when expressed in percentages gives the percentage variability in one of the variables that is accounted for by the other variable. The Pearson (r) and Spearman (ρ) correlation coefficient can be obtained by Equation (3.15) (Saccenti et al., 2020).

$$r_N = \frac{\sum_{i=1}^{N}(x_i-\bar{x})(y_i-\bar{y})}{N s_x s_y} \tag{3.15}$$

Where $\bar{x}$ and $\bar{y}$ are the sample mean of the variables x and y over N observations, s_x and s_y are their corresponding standard deviations.

3.7.1.2.5. Bland and Altman's analysis

The bland and Altmans method is used to describe the agreement between two quantitative measurements by constructing limits of agreement (Bland & Altman, 1999). The statistical limits are calculated by using the mean and standard deviation (SD) of the differences between the measurements. The graphical approach was used to check the assumption of normality. The resulting graph is an XY scatterplot, with the differences in the Y axis and the means of the two measurements in the X axis. Bland and Altman recommend that 95% of the data points should lie between ± 2 SD in order to indicate agreement (Giavarina, 2015).

3.7.1.2.6. Regression

Unlike correlation analysis that focuses on the strength of the relationship between two variables without the assumption of one been dependent or independent, regression analysis measures a causal relationship between one or more independent variable and the dependent variable (Gogtay et al., 2017). Both correlation and regression analysis are often conducted together with correlation used to identify the strength of the relationship while regression is used to model the relationship for prediction purpose. In regression analysis one variable is considered as the dependent variable while the other(s) is/are considered as the independent variable(s). An independent variable is one that remains unaffected and whose effect is studied. The dependent variable is one that responds to the effect of the independent variable by measuring its alteration/changes and it is the one of interest to the researcher. In medical research, there are three common types of regression: linear, logistic and Cox regression (Gogtay et al., 2017). The type of regression to be employed depends on the number and nature

of the independent and dependent variable and the shape of the regression line. Linear regression can be divided into simple linear or multiple linear regression. Simple linear regression is used when there in a one-to-one relationship between the dependent and independent variable while multiple linear regression is used where there is a one-to-many relationships between the dependent variable and independent variables (Gogtay et al., 2017). In linear regression both the independent and dependent variable must be continuous in nature. The logistic regression is used when the dependent variable is binary (categorical) in nature. The independent variable can be either quantitative or qualitative in nature. Unlike linear regression, logistic regression does not require a linear relationship. The criteria for using logistic regression include no correlation between the independent variables and an adequate sample size (Gogtay et al., 2017). Cox regression is used when the analysis is based on survival or time to die analysis (Gogtay et al., 2017). Regression analysis is conducted in three steps: analysing the correlation, fitting the regression line and evaluating and validating the regression line and its usefulness (Gogtay et al., 2017). The linear regression is used in this study and it is presented in Equation (3.16) (Gogtay et al., 2017).

$$Y = B_0 + \sum_{n=1}^{m} B_n X_n \tag{3.16}$$

Where Y is the dependent variable, B_0 is the Y intercept, m is the number of independent variables, B_n is the gradient of the independent variable X_n and the dependent variable Y.

The evaluation and validation of the regression analysis can be carried out using graphical and numerical method. The graphical method requires the analysis of the residuals that uses graphs to visually inspect the robustness (Gogtay et al., 2017). On the other hand, the numerical method can be carried out by looking at the value of the coefficient of determination. The value of the coefficient of determination determines the variation accounted for by the line. The higher this value the better the fit (Gogtay et al., 2017).

3.7.1.2.7. Principal component analysis

Principal component analysis (PCA) is a technique that is mainly used for data reduction. It preserves a high amount of information that was originally contained in the data while reducing its dimensions. The principal components and the magnitude of the variance are represented by eigenvectors and eigenvalues.

The eigenvectors and eigenvalues are obtained from the covariance or correlation matrix by eigenvalue decomposition. The eigenvector with the greatest eigenvalue is known as the first

principal component and subsequent principal components are obtained in the descending order of the eigenvalues. Before applying principal component to a dataset, the dataset is normalised to prevent variables of larger magnitude from suppressing those with lower magnitudes. The commonly used standardisation methods include the z-score and the minimum-maximum techniques. However, standardisation is not required when PCA is performed using the correlation matrix (Jolliffe & Cadima, 2016). In PCA, the first few components with the largest eigenvalues are usually selected to represent the entire data set as they represent most of the variance in the dataset. The scree plot analysis and/or the eigenvalue criterion are used to decide which of the principal component(s) to retain (Cattell & Vogelmann, 1977). The sum of the eigenvalues is a representation of the number or variables entered into the PCA. This implies that an eigenvalue of one explains approximately one variables worth of the variability (Larose, 2006). The rationale behind the use of the eigenvalue criterion is that at least for a component to be retained as principal, it should explain at least one variable worth's of variability (Larose, 2006). Thus, the eigenvalue criterion states that components with eigenvalues greater than one should be retained. The scree plot is a graphical plot of the eigenvalues against the components. Its representation follows a downhill fashion as the first few principal components usually explains much of the variability i.e., has higher eigenvalues (Larose, 2006). The scree plot criterion states that the components that should be extracted from conducting a PCA are those prior to where the plot begins to flatten out into a horizontal line (Larose, 2006). A pictorial view of the eigenvalue and scree plot criterion is shown in Figure 3.7.

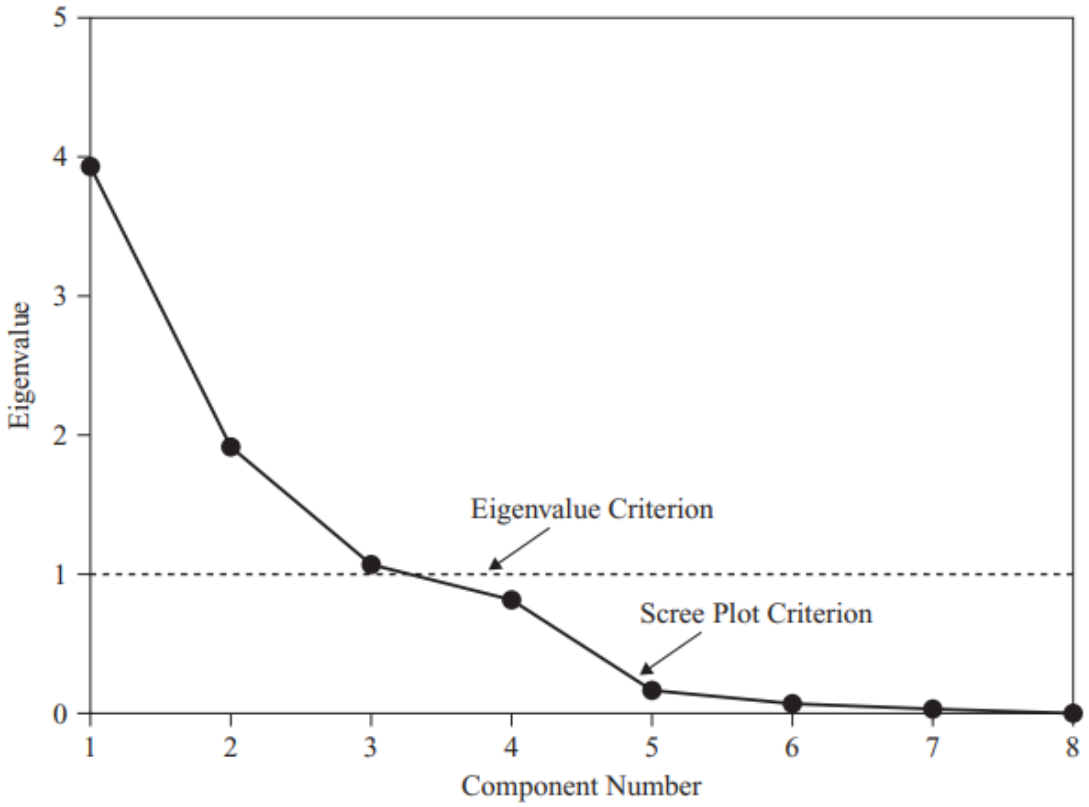

Figure 3.7. Eigenvalue and scree plot criterion (Larose, 2006)

The component matrix is the matrix that represents the correlation of the components with the variables and it is often rotated to achieve a simple structure. A simple structure is one where only one variable correlate highly unto a component. Various type of rotation exists, however, in this study the rotation used is the varimax rotation. The varimax rotation is a rotation that is orthogonal in structure and maximises the sum of the variances of squared coefficient within each eigenvector (Kaiser, 1958). The relationship between the components with the correlations of the variables are often used for inference. The coefficients of these correlations are known as factor loadings. Variables with closely related factor loadings have similar relationships (Hair et al., 1998). The variables with high correlations are referred to as the representatives of the principal component. Factor loadings greater than 0.4 have been considered to reach the minimal significance level of loading (Ho, 2006). However, there is no unanimous agreement for the threshold used for loading. The widely reported ranges for loading varies from 0.3 to 0.7 (Maskey et al., 2018). For interpretive purposes, Stevens (1992) suggested a threshold of 0.4. However, the purpose of this study was to observe the pattern of the distribution of the factors across the principal components, where closely related patterns showed close similarities between the conditions under investigation. In this study, 0.4 was

selected based on the recommendations of Stevens (1992). However, irrespective of the threshold used, the overall pattern observed remained unchanged.

Principal components can be described mathematically (Larose, 2006) as follows: Let *C* be a matrix of the size *m*×*n*, with *m* representing the observations and *n* representing the variables. In this study, *m* is used to indicate the number of participants while *n* represent the number of variables.

$$C_{m\times n} = \begin{pmatrix} c_{1,1} & \dots & c_{1,n} \\ \vdots & \vdots & \vdots \\ c_{m,1} & \dots & c_{m,n} \end{pmatrix}$$

The *i*th principal component of the standardised data matrix $C = [C_1, C_2, \dots, C_n]$ is given by $Y_i = e_i'C$, where e_i refers to the ith eigenvector and e_i' is the transpose of e_i. The principal components are linear combination $Y_1, Y_2, \dots Y_k$ of *C* such that the variance of Y_i are as large as possible and Y_i are uncorrelated. The eigenvalues can be obtained by solving for the lambdas in $|B - \lambda I| = 0$, where B is a square matrix obtained from the standardised matrix *C* and *I* is an identity matrix of size equal to *B*. Similarly, if λ is an eigenvalue of *B*, then its eigenvector (*e*) is a column vector such that $Be = \lambda e$.

3.7.2. Machine learning methods

The machine learning methods utilised in this study for balance analysis can be divided into two: supervised and unsupervised methods (Khera & Kumar, 2020).

3.7.2.1. Supervised learning approach

Supervised learning is regarded as a task-based approach in which the input and desired output are available (Prakash et al., 2016). In supervised learning, a mathematical model is designed that maps the input to the desired outputs. Data outside of the training set should be assigned to an accurate class by the model. The main objective of supervised learning approach is to minimize error. However, this method relies on the expert knowledge of the clinician or a predetermined truth. Examples of supervised machine learning methods include the neural network, decision tree, K nearest neighbour, radial basis function, ensembles, and support vector machines (Prakash et al., 2016). The neural network aims to replicate the operation of the biological neural network. The first mathematical modelling research to formulate artificial neurons was conducted in 1943 by Warren Mculloch and Walter Pitts. Other more enhanced models have since been developed by various researchers. The process of the neural network

continues until a certain minimum error, or a predefined epoch is reached. Through training using the existing data, a learning model is developed and the validation of the model is carried out using either the known or unknown data. The leave one out, K-fold validation approaches etc. can be used for validation (Prakash et al., 2016). The radial basis function is considered as the simplest variant of neural network. Naïve Bayes is a probabilistic approach employed when prior knowledge is available and hence is considered as a supervised learning method (Prakash et al., 2016). The Naïve Bayes assumes for each class a Gaussian distribution of values. The conditional probability for each feature $d_i \in D$ class is learnt for a given set of training data having class name $e \in$ class label set E (Prakash et al., 2016). Ensembles are employed for prediction models and for clinical analysis (Prakash et al., 2016). Support vector machine is a part of supervised learning that is based on the concept of optimally separating hyper planes (Prakash et al., 2016). It projects non-linearly the input space unto a high-dimensional feature space and it is non-probabilistic (Prakash et al., 2016). It defines the distribution of data points inside the feature space using a kernel function (Prakash et al., 2016). In the availability of labelled training data points, supervised learning method is the dominant method used.

3.7.2.2. Unsupervised learning method

In unsupervised learning methods, the model is trained without the use of labelled examples. These methods find the similarity between the attributes of the given data points using set of similarity measure. Based on the measure of the similarity also known as distance measures each of the data point is grouped into a cluster. Distance measures play an important role in the clustering process. Distance measures refers to the way the similarity between two points will be determined. Several distance measures exist, however the most widely used in clustering include the Euclidean distance, Manhattan distance, Minkwoski distance, Hamming distance, bit vector distance, Jaccard index, cosine index and the Dice index (Pandit & Gupta, 2011). The objective is to minimise the within cluster distance and maximise the between cluster distance. Examples of some well-known clustering method include fuzzy c mean, K-means, hierarchical clustering and the self-organising map. However, the K-means and self-organising map (SOM) are utilised in this study. The K-means is selected due to its efficiency and suitability, its empirical success, ease of implementation and its simplicity (Gesicho et al., 2021; Jain, 2010). The SOM is selected due to its effectiveness in the representation of the data,

illustrating the hidden patterns inherent to the characteristics of the data as a specific data distribution (e.g., normal) is not expected (Kim et al., 2002; Samsonova et al., 2006).

3.7.2.2.1. K-means clustering

The K-means clustering is considered as the oldest and most popular partitioning clustering method. Several studies in literature have utilised the K-means clustering with varying extensions and in differing areas. However, the K-means clustering is affected by initialization and issues relating to the selection of the number of clusters (K). Several validity indices have been proposed for determining the number of clusters (K) such as Davies-Bouldin index (DB), Dunn's index, Akaike information index, Bayesian information criterion, silhouette width, Gap statistic, Calinski and Harabasz index, modifield Dunn's index and the generalized Dunn's index (Sinaga & Yang, 2020). In this study the Davies-Bouldin index is used for validating the number of cluster (K). The similarity measure used for the K-means algorithm is the Euclidean distance. The operation of the K-means algorithm is as follows:

I. The initial centroid for the clustering is defined by k points
II. The distance of each point to be clustered is measured against the centroids. The point is placed in the centroid with least distance. This process is done for all the points that needs to be clustered.
III. When all the points have been assigned to a cluster, the centroids are recalculated based on the points in its cluster.
IV. Steps ii and iii, are repeated until no more changes between the points in their clusters.

The aim of the K-means clustering is to minimize an objective function i.e., the overall sum of square error function. The objective function (W) is given in Equation (3.17) (Kodinariya & Makwana, 2013).

$$W(S,C) = \sum_{k=1}^{K} \sum_{i \in s_k} \|y_i - c_k\|^2 \tag{3.17}$$

where S is the K cluster partition, c_k is the k^{th} centroid of the partition s_k, y_i is the i^{th} data point in the cluster s_k, k varies from 1 to number of clusters (K).

3.7.2.2.2. Kohonen neural network

The Kohonen neural network (KNN) was developed in the 1980s by the Finnish researcher Tuevo Kohonen (Kohonen, 1990) and has been widely used in data exploration applications (Kohonen, 2013). The KNN is an unsupervised clustering method that represents an input space of high dimensions unto a low regular grid of low dimension that can effectively visualize and explore the relationships present in the data (Vesanto & Alhoniemi, 2000). Its operation is based on competitive learning, that is, each neuron competes with other neurons to be a representative of the input example (Larose & Larose, 2014). It has been used in various balance related studies for balance related analysis. The information in high dimensional balance strategies for young adult subjects, before and after a 6-week slackline training intervention were extracted and visualized using the KNN. The result showed that the pre and post-test coordination pattern for the slackline task were significantly different (Serrien et al., 2017). A two-dimensional Kohonen map of size 10 by 10 neurons is shown in Figure 3.8.

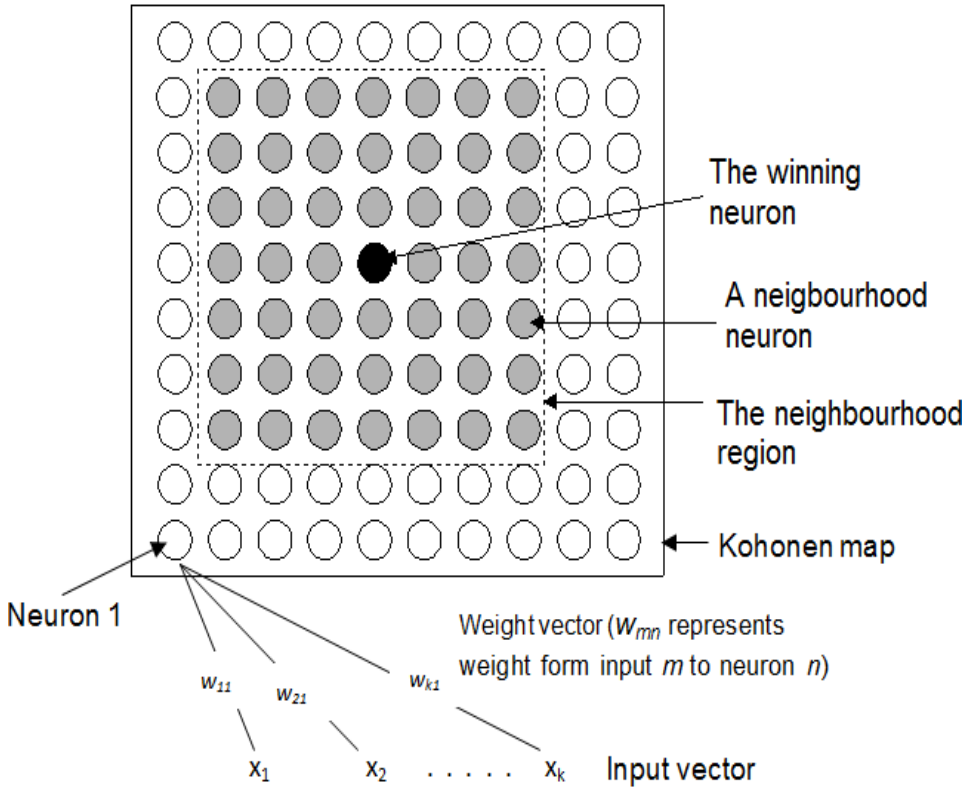

Figure 3.8. Kohonen neural network with a 10 ×10 output map (Ojie & Saatchi, 2021)

The operation of the Kohonen neural network is summarized below in the following 4 steps:

I. Initialization

In this stage, the weights associated to each neuron is initialized. The initialization of the weights of the neurons can be based on prior information or randomly selected. The n^{th} neuron is connected to the m^{th} feature of the input vector (representing an input example) by the connection weight w_{mn}. The number of features of the input vector is the same as the number of weights of each neuron. The neighborhood size and the learning rate are also initialized as defined in step iii. The point of termination of the learning process is also initialized as described in step iii.

II. Competition

In this stage, the j^{th} training input vector (Xj) is presented to the Kohonen network. Each neuron competes by calculating its distances of its weight to the j^{th} training input vector. The neuron with the smallest distance is determined to win the competition. With the Euclidean distance, the distance (d_n) for each neuron n is calculated using Equation (3.18).

$$d_n = \sqrt{(x_1 - w_{1n})^2 + (x_2 - w_{2n})^2 + \cdots + (x_k - w_{kn})^2} \tag{3.18}$$

III. Adaptation

This stage is defined in two steps. The first step involves identifying the neighbors of the winner neuron while the second stage involves updating the weight of the winning neurons and those of its identified neighbors (Ojie & Saatchi, 2021). The winner neuron (black dot) is surrounded by the neighborhood neurons as shown in Figure 3.8 above. The neighborhood size is defined as the number of neurons on each side of the winner neuron. In Figure 3.8, the neighborhood size is defined as 3. The operation of adaptation is carried out using the Kohonen learning rule as defined by Equation (3.19).

$$W_{j\_updated} = W_{j\_current} + \mu\left(X_j - W_{j\_current}\right) \tag{3.19}$$

where the current and updated weight vectors for the winning neurons are represented by $W_{j\_current}$ and $W_{j\text{-}updated}$ respectively. The amount of weight changes taking place during each iteration is controlled by the learning rate and varies from $0 < \mu \leq 1$. Smaller values of μ leads to slower learning but may improve adaptation effectiveness while larger values of μ leads to faster learning, but may reduce adaptation effectiveness. Its initial value is typically chosen heuristically (Ojie & Saatchi, 2021). To improve

learning, the neighborhood neurons are also updated to a lesser extent than that of the winner neuron. In most cases, the Gaussian function is used to adjust the extent of the update with smaller weights changes for the neurons farther from the winner neuron. This ensures the transition from coarse adjustments of the weight to finer adjustments.

IV. Termination of iterations

The processes of stages (ii) and (iii) are repeated until the desired iteration or the magnitude of the predefined weight value is reached

The implementation of the KNN can be carried out either by the sequential or the batch process. In the sequential process, the update of the neurons takes place after the presentation of each input vector to the network. In contrast, the update using the batch process takes place after an epoch – a single pass through the entire input data set (Lawrence et al., 1999). The batch process has the advantages of no dependence upon the order in which the input is presented to the network (Lawrence et al., 1999) and the elimination of issues regarding poor convergence as the coefficient of the learning rate is absent (Ceccarelli et al., 1993).

3.8. Summary

In this chapter, the theories relevant to this study were briefly discussed in order to give an understanding about the work.

Human balance system is primarily comprised of the sensory input, the sensory integration and the motor output. The sensory input comprises of the visual, proprioceptive and the vestibular systems. The information from these systems is integrated by the central nervous system (CNS) which gives control to the necessary motor system.

In accelerometry, balance analysis is carried out by using inertial measurement unit (IMU) to measure the centre of mass (COM) sway. Its control within the base of support is important to prevent a fall. The sway from a subject is reflected mainly in two directions: mediolateral (ML) and anterior-posterior (AP) directions. These directions reflect the patterns inherent in understanding the balance of a subject. Signal filtering (low pass and complementary filter), statistical (t-test, analysis of variance, PCA, linear regression, correlation, and Bland and Altman analysis) and machine learning (K-means and Kohonen neural network) methods used in this study for data processing and balance analysis were presented.

In the following chapter, the research methodology is presented.

Chapter 4 Research methodology

4.1. Introduction

In this chapter, the methodology that is general to the results obtained in this study is described. For clarity and ease of reading, the research methodologies specific to the studies in the respective chapters are explained in the chapters related to them. This chapter is divided into two sections: human balance evaluation and the design of the hardware and software.

Section one describes the procedures for carrying out balance analyses on the human participants. Section two describes the system (hardware and software) used in the study. The system consisted of two units: the transmitter and receiver unit.

A detailed description of the procedures and processes are presented in the following sections.

4.2. Human balance evaluation

4.2.1. Ethical approval

Ethical approval was obtained from Sheffield Hallam University's Ethics Committee prior to carrying out the study. The research was not deemed invasive in its application and structure, and posed low risk to human subjects. Refer to appendix 1 for ethical approval.

4.2.2. Risk assessment

The study was adequately risk assessed and it adhered to appropriate guidelines. All necessary forms were submitted to the designated authority.

4.2.3. Information sheet

Information sheet about the study was provided to the participants. The information sheet was prepared in such a way as to allow easy comprehension and understanding. Refer to appendix 5 for the participant information sheet.

4.2.4. Informed consent

Informed consent was obtained from the participants through a signed consent form. The consent form gave the participants the leverage to withdraw from the study at any time if they so wished. Refer to appendix 6 for the participant consent form.

4.2.5. Inclusion and exclusion criteria

The participants had to meet certain conditions for them to take part in the study: no current or history of balance problems or falls; no intake of any substance that could affect a person's balance 48 hours prior to participating in the study; participants must be between ages 18 and 60 years; the ability to maintain balance unaided; corrective lenses must be worn by those who needed them; ability to read and understand the instructions and demonstrations of the mCTSIB test. Those who did not meet the inclusion criteria as stated above were excluded.

4.2.6. Participants' information

Twenty-three healthy adult subjects participated in this study. Their mean age and standard deviation were 24.5 and 4.0 years; their mean height and standard deviation were 173.6 and 6.8 cm; and their mean weight and standard deviation were 72.7 and 9.9 kg. The participants performed the four conditions of the mCTSIB test. The demography of the participants is shown in Table 4.1.

Table 4.1. Demography of the participants

Parameter	Value
Sex	Males:10 males; Females: 13
Mean age (SD) (years)	24.5 (4.0)
Mean weight (SD) (kg)	72.7(9.9)
Mean height (SD) (cm)	173.6(6.8)
Mean COM location (SD) (cm)	109.9 (5.45)

4.2.7. Anonymity

In accordance to the guidelines of the ethical approval of the study, unique identification numbers were used to identity each participant.

4.2.8. Algorithm for balance analysis

The algorithm used in this study for postural sway analysis will be developed and evaluated in chapter 5.

4.2.9. Balance assessment test

The test used for balance analysis was the modified Clinical Test of Sensory Interaction and Balance (mCTSIB). The mCTSIB test was proposed by Cohen et al. (1993). It consists of four

conditions: (i) standing on a firm surface with eyes open, (ii) standing on a firm surface with eyes closed, (iii) standing on a compliant surface with eyes open and (iv) standing on a compliant surface with eyes closed. In this study, the compliant surface utilised was a sponge of dimension 10 cm height, 50 cm length and 50 cm width. The test duration for each condition was 30 seconds.

4.3. Design of the hardware and software

4.3.1. Hardware

The device consisted of two sections: the transmitter and the receiver unit. These sections are discussed below.

4.3.1.1 The hardware components

The components used for the development of the transmitting and receiving unit consisted of the inertial measurement unit (IMU) (type: MPU 6050), the microcontroller unit (type: Arduino Nano and Arduino Uno) and the wireless transceiver module (type: nRF24L01+).

The MPU 6050 is designed for low power, low cost and high-performance requirements for wearable sensors. It consists of a 3-axis accelerometer and a 3-axis gyroscope embedded on the same silicon die, with an on-board Digital Motion Processor (DMP) which processes complex 6-axis motion fusion algorithms (Invensense, n.d.). The dimension of the device was 4 mm × 4 mm × 0.9 mm with an accuracy of ±1% over the operating temperature range. The device voltage (VCC) is specified to operate between the range of 2.375 V to 3.46 V. The current drawn by the accelerometer and the gyroscope when in operation are 500 µA and 3.6 mA respectively. The sensor is integrated with a 16-bit analogue to digital converter (ADC). Thus, the device can produce a resolution from 0 to 2^{16} steps. The digital output of the three axes has a user programmable range of ±2g, ±4g, ±8g and ±16g for the accelerometer and an angular rate of ±250, ±500, ±1000, and ±2000 °/sec for the gyroscope, where g represents acceleration due to gravity and is approximately equal to 9.8 m/s^2 (Invensense, n.d.).

This programmable ranges are obtained from the sensitivity scale factors, where an increase in the sensitivity results in a reduction in the range. In this study, the ±2g range was used to provide suitable sensitivity, the digital output was divided by the sensitive scale factor of 16,384 i.e., 65536/16384 = 4 g, which was further divided into its two complements of ±2g.

The higher the resolution the greater the sensitivity of the accelerometer but the lesser the range of coverage of the device.

The nRF24L01+ is a low-cost transceiver module which operates on the 2.4 GHz industrial, scientific and medical band (ISM). It has a channel spacing of 1 MHz resulting in 125 possible channels from the range of 2.4 GHz to 2.525 GHz ("Nrf24L01-2.4GHz-HowTo - ArduinoInfo", 2021). Channel 76 was utilised in this study. The module was interfaced to the microcontrollers (Arduino Uno and Nano) on both the receiving and transmitting section using the SPI interface. The Arduino platform was used for the programming of the microcontroller. An excellent open-sourced library RF24 developed by TMRH20 was used in this study ("Nrf24L01-2.4GHz-HowTo - ArduinoInfo", 2021). The communication between the nRF24L01 modules is carried out using a logically shared pipe. Pipe 1 was utilised in this study. The addresses for both the transmitter and receiver were the same and consisted of a 40-bit address.

The Arduino Nano is a small microcontroller board based on the ATmega328. It has 22 digital I/O pins of which 6 of them are used for pulse width modulation. Its operating voltage is 5 volts with a recommended input voltage of 7-12 volts. It has a clock speed of 16 MHz, a PCB size of 18 × 45 mm, a weight of 7 g, and a power consumption of 19 mA. It was used in the transmitter unit because of its small weight and size. The Arduino Uno is a robust microcontroller board that is based on the ATmega328P. It consists of a quartz crystal of 16 MHz, a power jack, a USB connection, an ICSP header, a reset button, 6 analogue input pins and a 14 digital input and output pins ("Arduino - ArduinoBoardUno", 2021). It can be powered directly from a PC using its USB interface or from an external DC power supply using its AC-to-DC adapter. Its operating and recommended input voltage is 5v and 7-12v respectively with a 50mA DC current for its 3.3v pin ("Arduino - ArduinoBoardUno", 2021). It has a flash memory of 32 KB of which 0.5 KB is used by its bootloader. It has a clock speed of 16 MHz, a weight of 25 g, a length of 68.6 mm and a width of 53.4 mm. It is programmed using the Arduino IDE ("Arduino - ArduinoBoardUno", 2021). It was used in the receiver unit. The diagram of these components are shown in Figure 4.1.

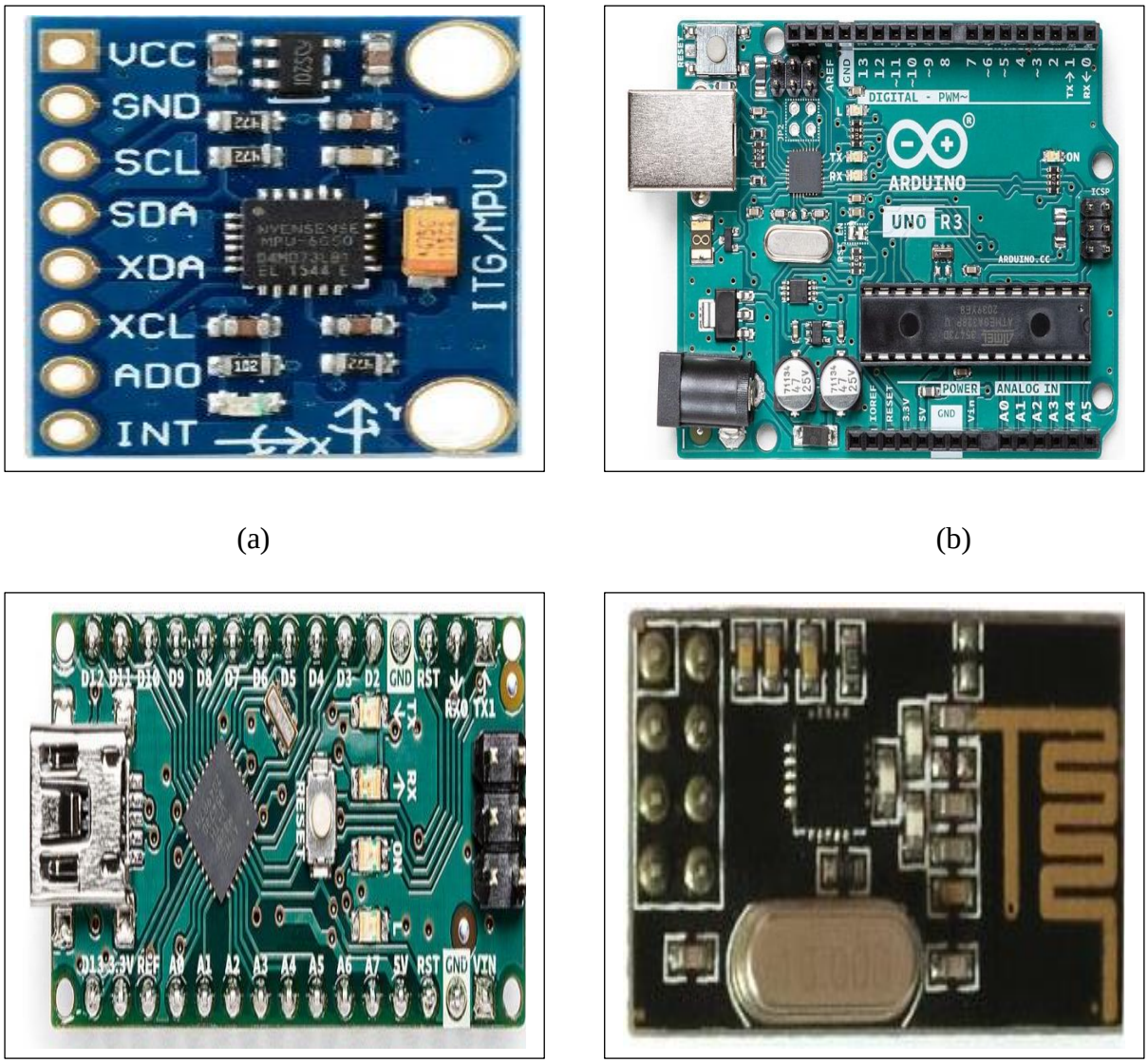

(a) (b)

(c) (d)

Figure 4.1. The hardware components: (a) MPU 6050 (source: "Arduino Playground - MPU-6050", 2021), (b) Arduino Uno (source: ("Arduino Uno Rev3", 2021)), (c) Arduino Nano (source: "Arduino Nano", 2021), (d) nRF24L01 transceiver module

4.3.1.2. The transmitter unit

The transmitter unit was designed to be comfortably worn by the subjects at the approximate COM position as this region has been suggested to represent the entire body's sway. For comfortability, the enclosure was designed to have a flat surface for easy attachment to the back of the human body. The schematic and actual diagram of the device and its associated dimensions are shown in Figures 4.2 (a) and (b) respectively. The device was designed to be attached to the back of the subjects using a Velcro elastic band.

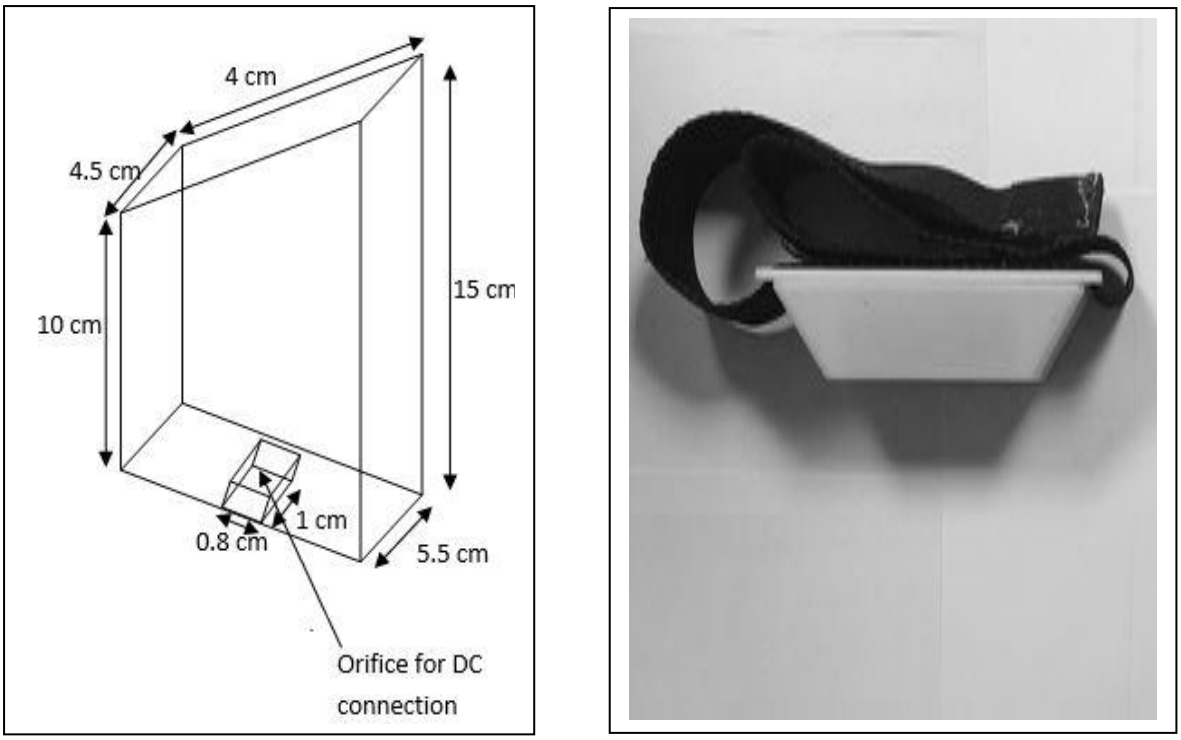

(a) (b)

Figure 4.2. Diagram of the casing of the transmitter device: (a) Schematic diagram, (b) Actual device with belts for attachment onto a subject's back.

The internal circuitry of the transmitter section consisted of an inertia measurement unit (IMU, type: MPU 6050), a wireless transceiver module (type: nRF24L01), a microcontroller (type: Arduino Nano), and a rechargeable battery for power supply. The communication between the IMU and the microcontroller was enabled using the inter-integrated circuit protocol (I^2C). The transmitter unit was responsible for measuring sway or movement related data. This data was in the raw form which was then transmitted by the nRF24L0l transmitter via I^2C communication to the receiver. The communication between the wireless transceiver and the microcontroller was enabled via the serial peripheral interface (SPI) protocol. The recorded movement signals were communicated wirelessly to the receiver unit using the nRF24L01 module. The transmitting range of the device was 100 m. The internal circuitry of the device is shown in Figure 4.3.

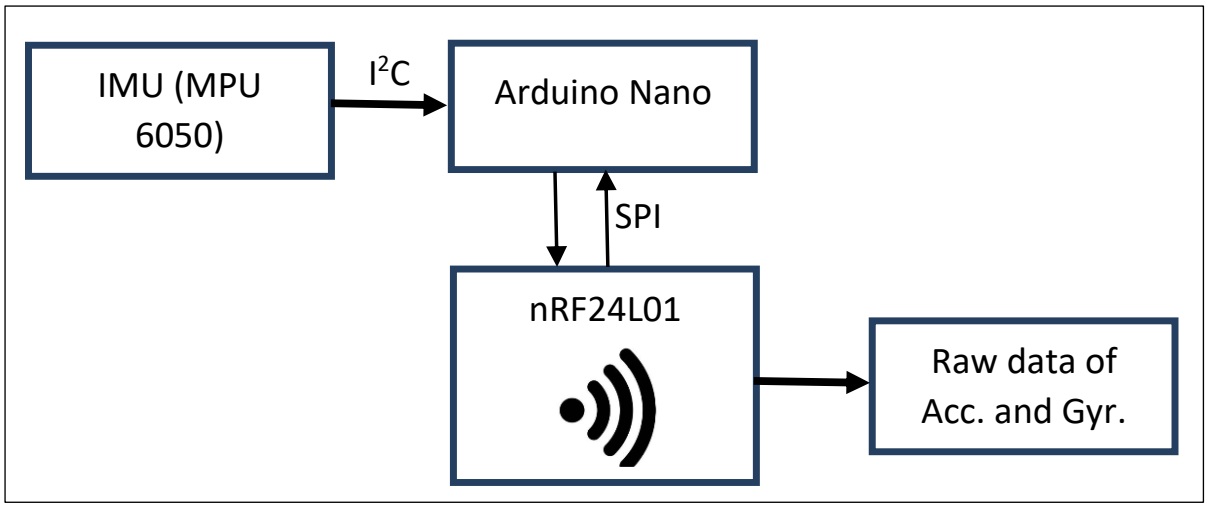

Figure 4.3. The internal circuitry of the transmitting unit. Where Acc. and Gyr. are abbreviations for accelerometer and gyroscope readings

4.3.1.3. The receiver unit

The schematic and actual diagram of the receiving device and its associated dimension are shown in Figures 4.4 (a) and (b) respectively.

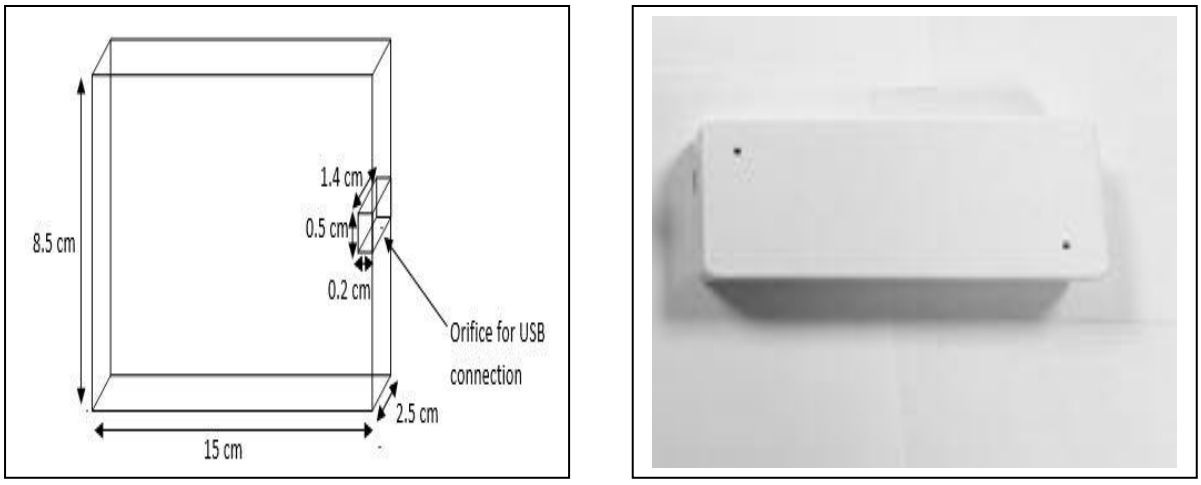

(a) (b)

Figure 4.4. Diagram of the casing of the receiving device: (a) Schematic diagram, (b) Actual device attached to the computer

The receiving unit consisted of a wireless transceiver module (type: nRF24L01), a microcontroller (type: Arduino Uno) and a laptop computer. The communication of the transceiver module with the microcontroller occurred via the serial peripheral interface (SPI) while the communication between the microcontroller and the laptop was facilitated using a

USB cable. The internal circuitry of the device is shown in Figure 4.5. The signal from the transmitter unit was received using the wireless transceiver module which has been programmed to be a receiver. The Arduino Uno serves as the microcontroller that organises the instructions from the laptop computer and the wireless device, and vice versa. The signal was further communicated to the laptop computer. The power source of the device was obtained directly from the laptop computer via its USB interface.

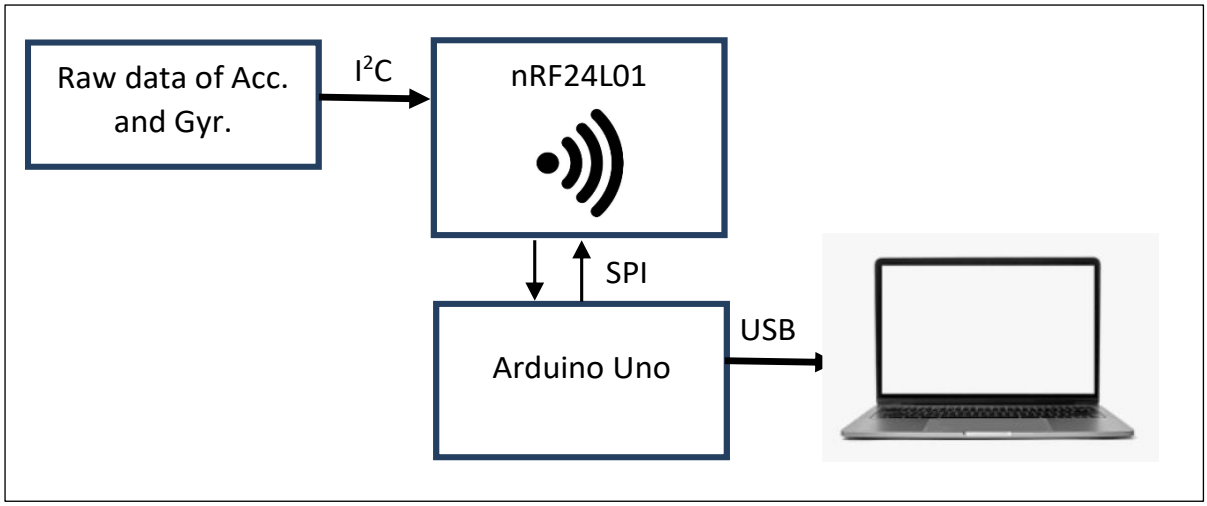

Figure 4.5. The internal circuitry of the receiving unit. Where Acc. and Gyr. are abbreviations for accelerometer and gyroscope readings.

4.3.2. Software

The software section consisted of four types used for various purposes namely Arduino®, Processing®, SPSS® and MATLAB® software. The Arduino® software was used for programming the hardware systems i.e., the Arduino Uno and Nano microcontrollers. The Arduino® software is an open-source programming language used for writing codes and uploading them into microcontrollers. It runs on various operating systems: Windows, Mac OS X, and Linus. The integrated device environment (IDE) is written in C++ and based on Processing and other open-source software.

The Processing® language was used for data recording, and real-time processing of the data based on the developed algorithm. The Processing® language is an open-source computer programming language. It was designed to give a visual appeal to programming. It can easily be interfaced with the Arduino® programing language. It was designed using the java language although its syntax is more simplified (Visual Information for Advocacy, 2021).

SPSS® is a statistical software used for the analysis of data and understanding of large complex data.

MATLAB® programming language developed by MathWorks®. It stands for Matrix Laboratory and is used for the manipulation of matrixes, implementation of data algorithms, and function plotting etc. while presenting an appealing user interface (Wallisch et al., 2014). It can easily interface with other programming languages such as C, C++, C#, java and Python. It was used for post processing of the recorded data from the inertial measurement unit.

4.3.3. Operation of the system

The device was worn by the subjects at approximately the centre of mass position as shown in Figure 4.6 while performing various balance analysis procedures.

Figure 4.6. The accelerometer device worn by a subject while performing a balance task

Processing of data from the device was carried out via a dialogue box as shown in Figure 4.7. The user has the option of real time analysis of the sway or recording of the data for future use. It accepts a keyboard input from numbers 1-5 which performs different tasks and the corresponding program is displayed. Option 1, indicates the display of the accelerometer sway, option 2 indicates the COM plot in the *x* and *y* axes in units of centimetre (cm), option 3 was used to display the polar plot of the subjects in units of centimetre for the radius and degrees for the angle, option 4 created a rectangular sway of the subjects in the *x* and *y* axis simultaneously and option 5 was used for recording the data into the computer hard disk for future use.

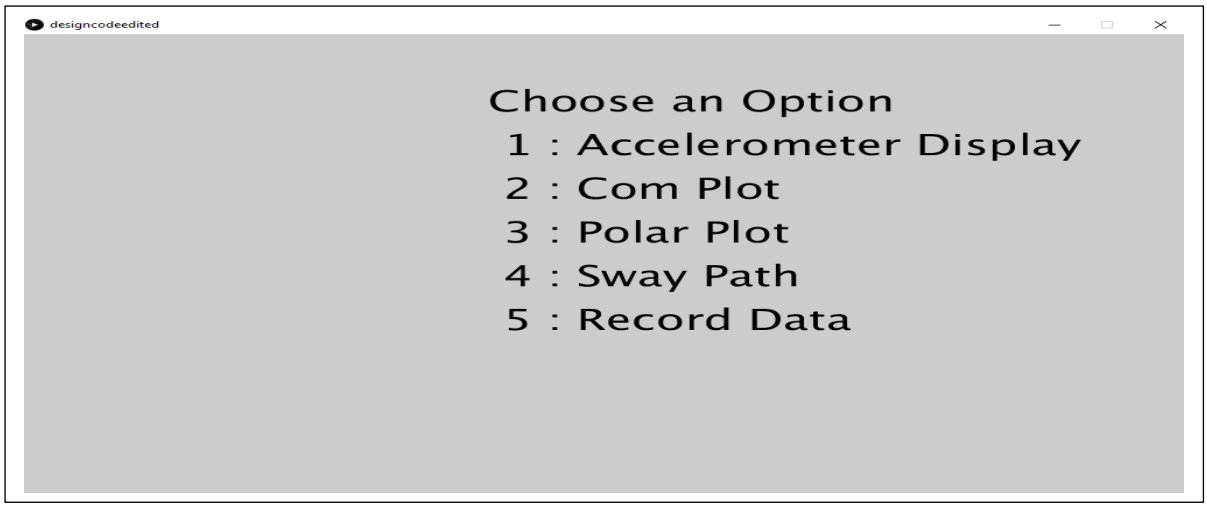

Figure 4.7. Dialogue box for the performing various processing task

The start and stop time of the data recording process is recorded as well as the data and utilised in calculating the sampling rate of the device. The baud rate of the device was set at 19200 bits per second and device sampling rate was 60 Hz. The sampling rate could be increased further by increasing the baud rate; however, the sampling rate of 60 Hz was sufficient for the experiment. The available baud rate varies from 300 bits per second to 115200 bits per second.

During the recording process, the data was saved in rows and columns with the first three columns corresponding to the data from the three axes of the accelerometer and the last three columns corresponding to the data from the three axes of the gyroscope. The data was saved in a text file format (.txt) with the first and last sample time stamped. The time stamp was used to obtain the duration of the recording process which was used in calculating the sampling rate. The sampling rate was obtained by dividing the total number of samples by the recording duration. The recording duration was obtained from the difference between the time stamps of the last and first recorded samples.

4.3. Summary

In this chapter, the methodologies general to the study such as ethical approval, recruitment procedure, design consideration of the system, the associated hardware and software were discussed. Twenty-three healthy adult participants of mixed sex were recruited in this study. The test utilised to assess their balance is a well-known test referred to as the modified Clinical Test for Sensory Interaction and Balance. The test duration for each condition was 30 seconds. Prior to the participation of the subjects in the study, ethical approval was obtained from the

university ethical committee, information sheet was provided to the participants and informed consent of the participants were obtained.

The accelerometry system developed consisted of two sections: the transmitter unit and receiver unit. Wireless mode of communication is used between the two systems. The transmitter unit contains the inertial measurement unit (IMU) and is attached to the subjects to capture postural sway. The receiver unit is connected to a laptop computer for data recording. In the following chapter, the developed device will be evaluated to determine its accuracy. The device will be utilised in subsequent chapters to carry out analysis on the balance of healthy human subjects.

Chapter 5 Algorithm development and evaluation based on the inverted pendulum model

5.1. Introduction

In this chapter, the algorithms developed to analyse human balance are described and evaluated. In order to carry out the evaluations, three methods were considered: method A, method B and method C. Method A consisted of a manual setup constructed using the principle of the inverted pendulum, method B represents the algorithm developed in this study and method C refers to the algorithm developed by Mayagoitia et al. (2002). The limitation of the algorithm developed by Mayagoitia et al., 2002 (method C) are: limitation in modelling of the COM position which led to the reduction of a three-dimensional sway i.e., sway in the *x*, *y* and *z* axes to only two dimensions (sway in the *x* and *y* axes); small angular deviation in order to maintain sway accuracy; and occurrence of sway in both directions when only one direction is actually involved.

In all the three methods, the centre of mass (COM) is projected to the ground. Method A was considered as the reference method as it consists of physical units that can be measured manually. Comparison between the methods were conducted based on the paired sample t-test and the Bland and Altman's analysis. The result showed that the algorithm developed in this study correlated strongly with the manual setup and accurately represented sway based on the principles of the inverted pendulum as compared to the algorithm developed by Mayagoita et al. (2002). The setup of the system, algorithm and the results obtained are presented in the following sections.

Furthermore, the developed algorithm was evaluated on 15 healthy adult subjects (9 males, 6 females; mean age (standard deviation) of their ages, weight and height were: 22.5 (3.4) years, 70.9 (7.5) kg, 173.5 (9.8) cm respectively) who were involved in the balance evaluation of the sensory system based on the modified Clinical Test for Sensory Interaction and Balance (mCTSIB) test in order to examine the time domain measures that could differentiate effectively between the sensory systems. The ground projected sway in both the mediolateral (ML) and anterior-posterior (AP) directions were obtained and used in deriving various time domain measures. The time domain measures in both directions were evaluated using statistical methods to determine their suitability in differentiating between the various balance-related sensory information. The result suggested that measures of the root mean square (rms) velocity

and acceleration, average velocity and acceleration, and the range of the velocity in the AP direction, were more sensitive in differentiating between the sensory systems.

5.2. Chapter specific methodology

5.2.1. Development of the human balance algorithm

Several studies have suggested that during quiet standing, the body sway can be compared to the motion of the inverted pendulum (Masani et al., 2006; Winter et al., 2003; Gage et al., 2004; Madigan et al., 2006). An inverted pendulum is a pendulum whose COM position is located above its pivotal point. Thus, an accurate projection of the COM sway is important in the analysis of human balance. A method to project a body's COM to the ground surface has been reported in Mayagoitia et al. (2002). The method is shown in Figure 5.1 and can be described using Equations (5.1) to (5.3) respectively.

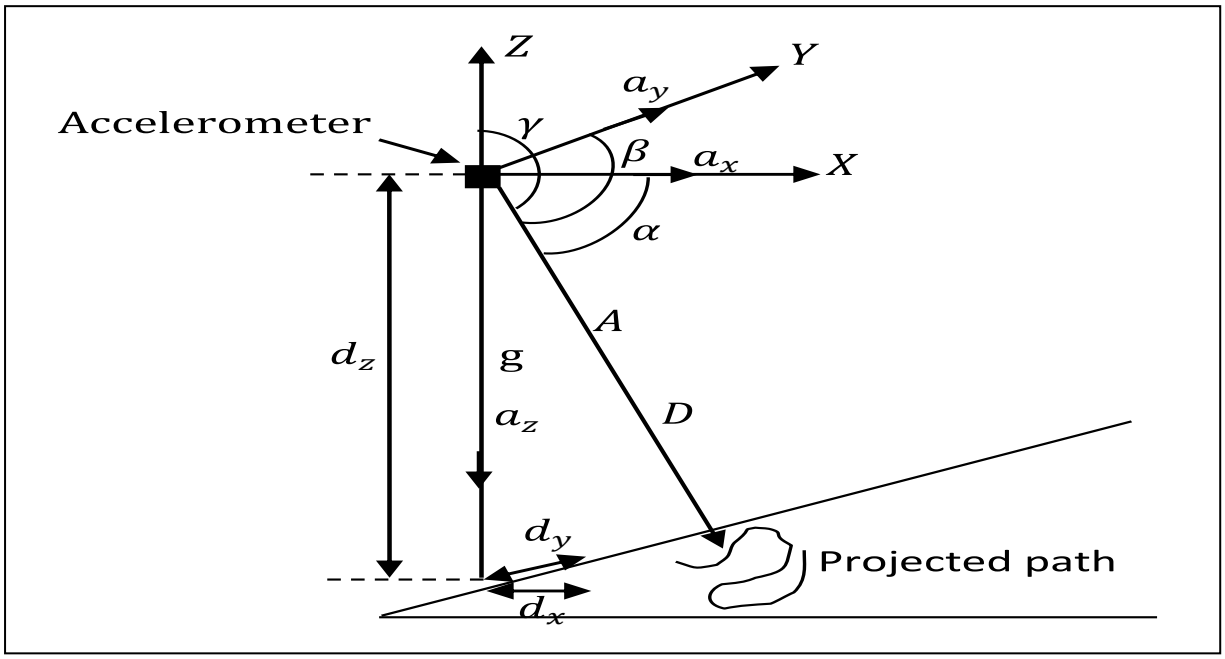

Figure 5.1. Ground displacement of the tri-axial accelerometer (Mayagoitia et al., 2002)

$$A = \sqrt{{a_x}^2 + {a_y}^2 + {a_z}^2} \tag{5.1}$$

$$\cos\alpha = \frac{a_x}{A}, \quad \cos\beta = \frac{a_y}{A}, \cos\gamma = \frac{a_z}{A} \tag{5.2}$$

$$D = -\frac{d_z}{\cos\gamma}, d_x = D\cos\alpha\,, \; d_y = D\cos\beta \tag{5.3}$$

The resultant acceleration is represented by *A*, the directional cosines of the accelerations a_x, a_y, and a_z of the *x*, *y* and *z* axes are represented by $\cos\alpha$, $\cos\beta$ and $\cos\gamma$ respectively, *D* is

the ground projected height of the COM, d_z is the position of the sensor above the ground surface and represents the COM position, d_x and d_y are the ground positional displacement in the *x* and *y* axes respectively. All distances and accelerations are of the units of cm and cm/s^2 respectively. The first limitation of this algorithm was in the design not conforming to the inverted pendulum model. This has a major implication as it eliminates the deviation of the centre of mass height above the ground surface. This results in the reduction of a 3-dimensional sway i.e., sway in the *x*, *y* and *z* directions to 2 dimensions (sway in the *x* and *y* direction). The second limitation is that if sway was occurring in only one direction (say the *y* direction), it was being reflected onto the other direction (*x* direction) and vice-versa. Thus, the accuracy of the result of a subject's postural sway is affected. This is as a result of the component *D* present in both equations for obtaining the ground displacement in the *x* and *y* axes i.e., Equation (5.3). Thirdly, as a result of this limitation the algorithm may not be used for dynamic balance analysis as the angle of sway has to be very small for the measurements to be accurate (Mayagoitia et al., 2002). The inverted pendulum model is shown in Figure 5.2 and described using Equations (5.4) to (5.11).

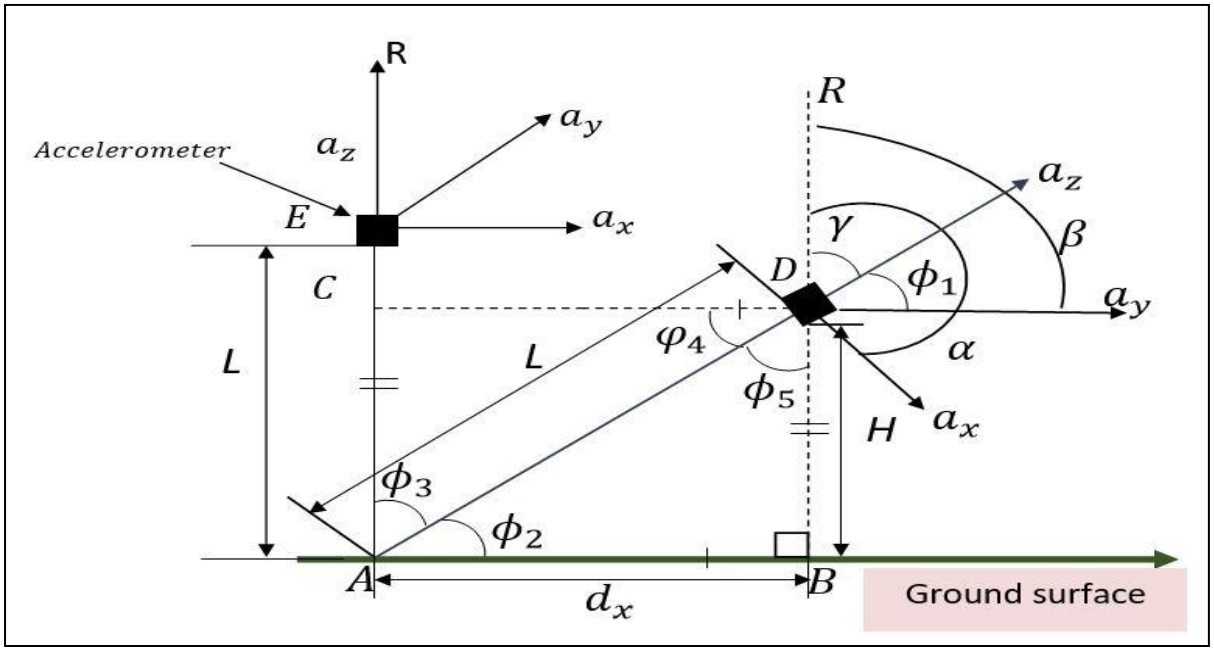

Figure 5.2. Inverted pendulum model (Ojie & Saatchi., 2020)

The resultant acceleration (*R*) in Figure 5.2 is the same as the resultant acceleration (*A*) in Figure 5.1 above.

$$R = \sqrt{{a_x}^2 + {a_y}^2 + {a_z}^2} \tag{5.4}$$

$$\cos\alpha = \frac{a_x}{R}, \ \cos\beta = \frac{a_y}{R}, \cos\gamma = \frac{a_z}{R} \tag{5.5}$$

The inclined accelerometer at position *B* has the following mathematical relationship:

$$\varphi_1 = 90 - \gamma, \gamma = \alpha - 90, \varphi_1 = 180 - \alpha \tag{5.6}$$

The line *CD* is parallel to the line *AB* i.e., $\overline{CD}$ // $\overline{AB}$, and the line *CA* is parallel to the line *BD* i.e., $\overline{CA}$ // $\overline{BD}$, and serves as a transversal to the parallel lines *CD* and *AB*. Mathematically, parallel lines are represented by the symbol // and the symbol – represents a line. Hence, $\varphi_2 = \varphi_1$, $\varphi_3 = \gamma$ (corresponding angles) and $\varphi_4 = \varphi_2$, $\varphi_5 = \varphi_3$ (alternate angles). Replacing all the angles by their corresponding and alternate equivalents in terms of the angles α and γ, the ground position in the *x* axis (d_x) and the height of the sensor above the ground surface (H) can be obtained. Using similar operation and using the trigonometry identity $\cos(180 - \beta) = -\cos\beta$, the ground position in the *y* axis (d_y) can also be obtained. The equation for the ground position in the *x* axis (d_x) and *y* axis (d_y), and the height of the sensor above the ground surface (H) is given by Equation (5.7).

$$d_x = -L\cos\alpha, \ d_y = -L\cos\beta, \ H = L\cos\gamma \tag{5.7}$$

Rotational information can be obtained by making use of the yaw angle of the gyroscope as shown in Figure 5.3.

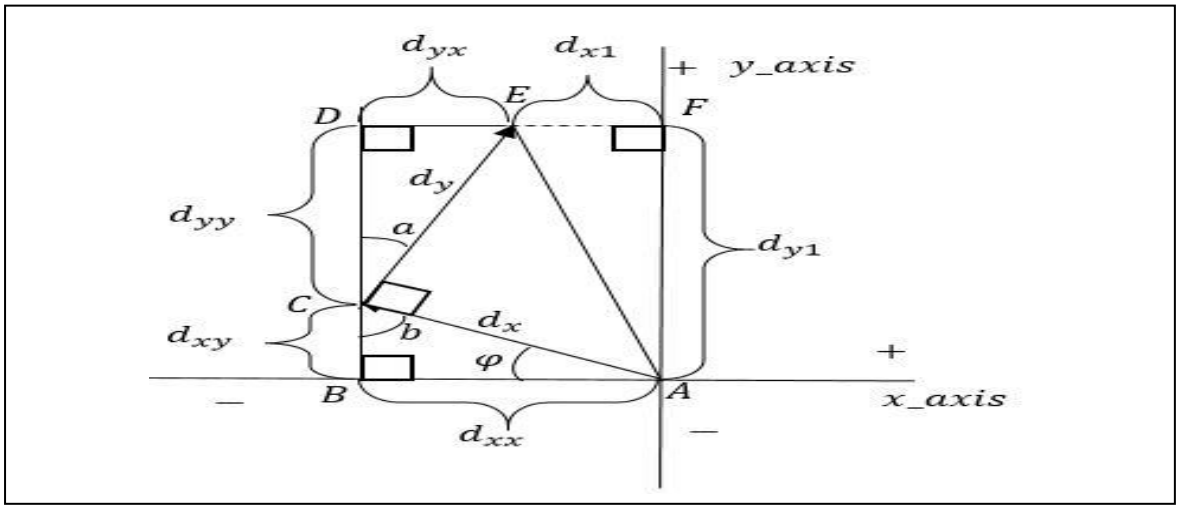

Figure 5.3. Inverted pendulum model with gyroscope rotational angle (Ojie & Saatchi., 2020)

The mathematical algorithm to obtain the displacement, if rotational motion is assumed, is summarised by equations (5.8) to (5.11).

$$\hat{b} = 90 - \hat{\varphi}\ , \hat{\varphi} = 90 - \hat{b}\ ,\ \hat{a} = 90 - b, \hat{a} = \hat{\varphi} \tag{5.8}$$

$$dx_x = d_x cos\varphi\ ,\ dy_y = d_y cos\varphi,\ dy_x = d_y sin\varphi,\ dx_y = d_x sin\varphi \tag{5.9}$$

$$dx_1 = dx_x - dy_x = d_x cos\varphi - d_y sin\varphi \tag{5.10}$$

$$dy_1 = dy_y + dx_y = d_y cos\varphi + d_x sin\varphi \tag{5.11}$$

dx_1 and dy_1 are the resultant displacements in the x and y axes due to the rotational angle φ in unit of degrees. d_{xx}, $d_{xy,}$ d_{yy}, and $d_{yx,}$ are coordinate displacements of the *x* and *y* axes of $d_{x,}$ and $d_{y,}$ respectively. d_x and d_y are displacements of the accelerometer. The symbols with a caret (^) are angles used for mathematical justifications.

It may be necessary to zero the sensor when placed on the subject's back to resolve error due to its placement. Thus, we defined new angles for the inclination angles α, β, and γ known as α_2, β_2, and γ_2 respectively. Where α_2, β_2, and γ_2 are given by Equation (5.12).

$$\alpha_2 = \alpha - \alpha_1 + 90, \beta_2 = \beta - \beta_1 + 90, \gamma_2 = \gamma - \gamma_1 \tag{5.12}$$

Where α_1, β_1, γ_1 is the first value or the mean of the first values of their respective angular measurement. The mean of the first values of the angular measurement may be preferable because of the noise in the system.

5.2.2. Evaluation of the algorithm

The system devised for the evaluation of the algorithm consisted of the transmitter unit, metal rod (length of 134 cm and a diameter of 2 cm), a plumb bob, a string, a vice, a protractor, rechargeable power supply and a measuring tape as shown in Figures 5.4 (a) and (b).

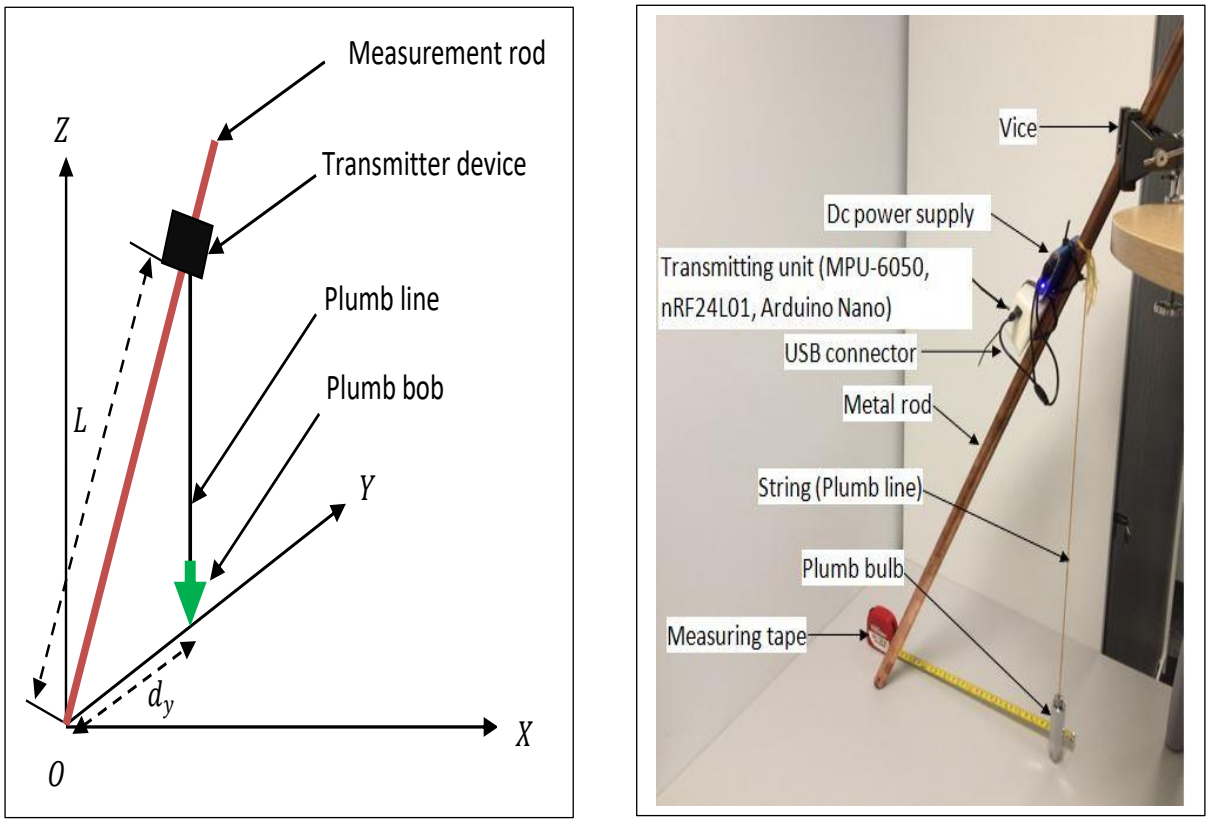

(a) (b)

Figure 5.4. Apparatus used for evaluation (a) schematic diagram, (b) actual apparatus (Ojie & Saatchi., 2020)

A hole was drilled on the metal rod at 100 cm from one of its ends (the end that made contact with the ground), and a string attached with the plumb bob attached at its base, was knotted to the hole. The accelerometer transmitting unit and its power supply were fastened to the metal rod at the position of 100 cm and 110 cm respectively from the end that made contact with the ground using a plastic tie strap. The metal rod was held by a vice which allowed it to be inclined to any angle measured by a protractor. The metal rod was inclined from 0 to 90 degrees and the corresponding *y* axis position of the plumb bob on the ground were recorded using a measuring tape while simultaneously recording the accelerometer and gyroscope sway data. The *y* position (d_y) was obtained by taking the average of the readings over the recording duration using

Equation (5.13). The inclination angle (γ) of the metal rod was obtained by taking the average of the readings over its recording duration using Equation (5.14).

$$d_{ya} = \frac{1}{N}\sum_{n=1}^{N} d_y(n) \tag{5.13}$$

$$\gamma_a = \frac{1}{N}\sum_{n=1}^{N} \gamma(n) \tag{5.14}$$

The sampling rate of the device was 60 samples per seconds and 60 seconds of data recording were conducted for each angle of inclination. The data was transmitted wirelessly to the receiver unit and stored in a laptop computer for further processing.

5.2.3. Experimental procedure for data collection on the healthy adult subjects using the developed system and algorithm

Ethical clearance was obtained from Sheffield Hallam University before conducting the experiment. The experimental procedure was to examine the performance of the subjects on the conditions of the mCTSIB test and to examine the time domain measures capable of differentiating between the information of the sensory systems. Fifteen healthy adult volunteers (9 males, 6 females with mean (standard deviation) of age, weight and height: 22.5 (3.4), 70.9 (7.5) kg, 173.5 (9.8) cm respectively, participated in the study. The accelerometer transmitter unit was placed on the subjects back at approximately the position of the iliac crest. The subjects performed the four conditions of the modified clinical test of sensory interaction and balance (mCTSIB), condition 1: the subjects stood on a firm surface with eyes open; condition 2: the subjects stood on a firm surface as in condition 1 but with eyes closed; condition 3: the subjects stood on a flexible surface (sponge of dimension 10 cm height, 50 cm length and width) with their eyes open; condition 4: the subjects stood on a flexible surface as in condition 3 but with eyes closed. For the eyes open test conditions (conditions 1 and 3), a point of focus for the subjects was marked on the wall. An area of 30 cm wide, was marked on the ground to ensure similarity of the standing position of the subjects. This area was 1 metre from the wall. The recording duration for each test condition was 30 seconds. This provided sufficient data without making the subjects tired. The data was stored on the laptop computer for further analysis.

5.2.4. Data analysis

5.2.4.1. Data filtering

The software used for carrying out data analysis was MATLAB® (version 2017a, MathWorks®, Massachusetts, USA) and SPSS® (version 24, IBM, Armonk, NY, USA). The signals obtained from both the gyroscope and accelerometer were combined using the complementary filter algorithm as shown in Equation (5.15) to obtain the roll and pitch angle respectively. θ_c and θ_{c-1} corresponds to the current and previous roll or pitch angle in degrees respectively, θ_g is the gyroscope's rate of rotation i.e., angular rate in degrees per seconds, dt is the sampling interval in units of seconds, a is the parameter of the filter and φ corresponds to the accelerometers roll (α) or pitch (β) angle. The parameter of the filter (a) was set to 0.8, where $a = \frac{\tau}{dt+\tau}$, τ is the time constant. Thus, with a = 0.8, dt= 1/60 s, τ = 0.066 s and the cut-off frequency f_c = 1/2$\pi\tau$, f_c = 2.39 Hz. The angles from the complementary filter were used to calculate the displacement as shown in Equation (5.7).

$$\theta_c = a \times \left(\theta_{c-1} + \theta_g \times dt\right) + (1 - a) \times \varphi \tag{5.15}$$

5.2.4.2. Algorithmic evaluation

Test of normality of the data was conducted to determine which statistical test (parametric or non-parametric) was more suitable for carrying out the test for significant differences between the results obtained by the methods. Bland and Altman analysis was carried out to compare the values of the displacements of methods B and C with that of method A (the reference method).

5.2.4.3. Human subjects sway analysis

Time domain measures such as the positional displacement (displacement with respect to the origin), velocity and acceleration were used for analysis. The analyses were to examine which time domain features can differentiate between the conditions of the mCTSIB test and to examine the relationship between the conditions. Subsequent time domain measures such as the averages of the measures, the range of the measures and the root mean square values of the measures were obtained. The formulae for these measures are presented in Equations (5.16) to (5.24).

$$D_{ML_n} = D_{ML_n} - D_{ML_1}, D_{AP_n} = D_{AP_n} - D_{AP_1}, V_{ML_n} = \frac{D_{ML_n} - D_{ML_{n-1}}}{T} \tag{5.16}$$

$$V_{AP_n} = \frac{D_{AP_n} - D_{AP_{n-1}}}{T}, A_{ML_n} = \frac{V_{ML_n} - V_{ML_{n-1}}}{T}, A_{AP_n} = \frac{V_{AP_n} - V_{AP_{n-1}}}{T} \quad (5.17)$$

$$D_{ML_{av}} = \frac{1}{N}\sum_{n=1}^{N}\left|D_{ML_n}\right|, D_{AP_{av}} = \frac{1}{N}\sum_{n=1}^{N}\left|D_{AP_n}\right| \quad (5.18)$$

$$V_{ML_{av}} = \frac{1}{N}\sum_{n=1}^{N}\left|V_{ML_n}\right|, V_{AP_{av}} = \frac{1}{N}\sum_{n=1}^{N}\left|V_{AP_n}\right| \quad (5.19)$$

$$A_{ML_{av}} = \frac{1}{N}\sum_{n=1}^{N}\left|A_{ML_n}\right|, A_{AP_{av}} = \frac{1}{N}\sum_{n=1}^{N}\left|A_{AP_n}\right| \quad (5.20)$$

$$Range = |maximum - minimum| \quad (5.21)$$

$$D_{ML_{RMS}} = \sqrt{\frac{1}{N}\sum_{n=1}^{N} D_{ML_n}}, D_{AP_{RMS}} = \sqrt{\frac{1}{N}\sum_{n=1}^{N} D_{AP_n}} \quad (5.22)$$

$$V_{ML_{RMS}} = \sqrt{\frac{1}{N}\sum_{n=1}^{N} V_{ML_n}}, V_{AP_{RMS}} = \sqrt{\frac{1}{N}\sum_{n=1}^{N} V_{AP_n}} \quad (5.23)$$

$$A_{ML_{RMS}} = \sqrt{\frac{1}{N}\sum_{n=1}^{N} A_{ML_n}}, A_{AP_{RMS}} = \sqrt{\frac{1}{N}\sum_{n=1}^{N} A_{AP_n}} \quad (5.24)$$

The test of normality was conducted using the Shapiro-Wilk test of normality. Depending on the result of normality i.e., normally or not normally distributed, the paired sample t-test or the Wilcoxon signed rank test was used respectively to compare the sway measures between each condition of the mCTSIB to examine if a significant difference existed.

5.3. Results and discussion

5.3.1. Results of the comparison of the three methods A, B and C

A comparison between the result of the unfiltered and filtered angle using the complementary filter are shown in Figure 5.5. It represents the vertical inclination angle of the rod at 15 degrees in the direction of the *y* axis.

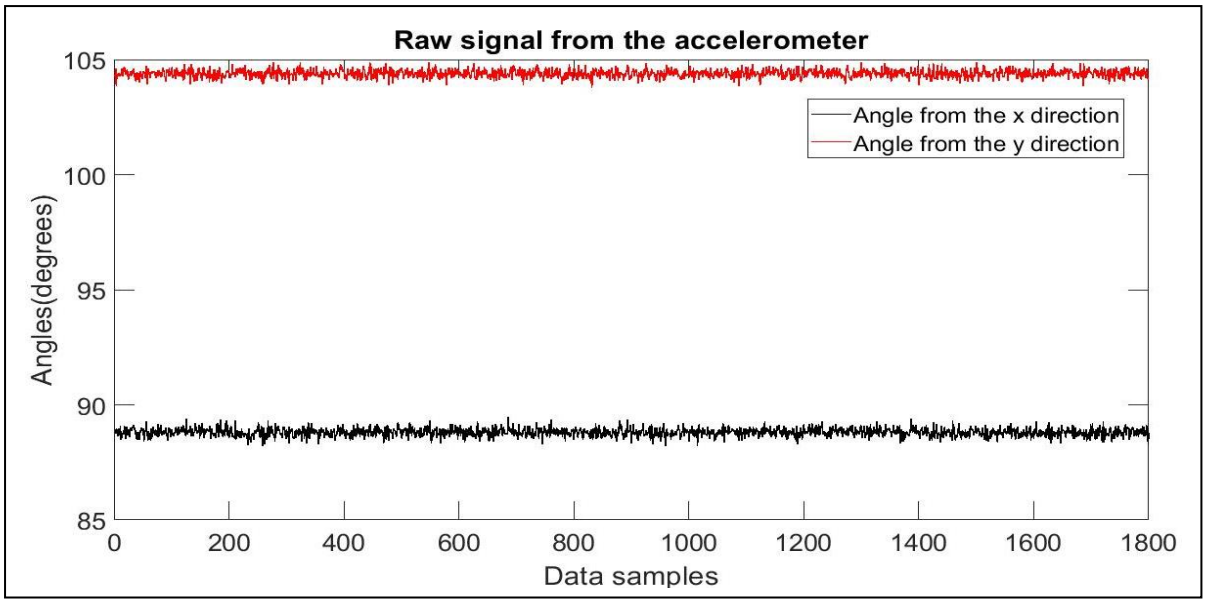

(a)

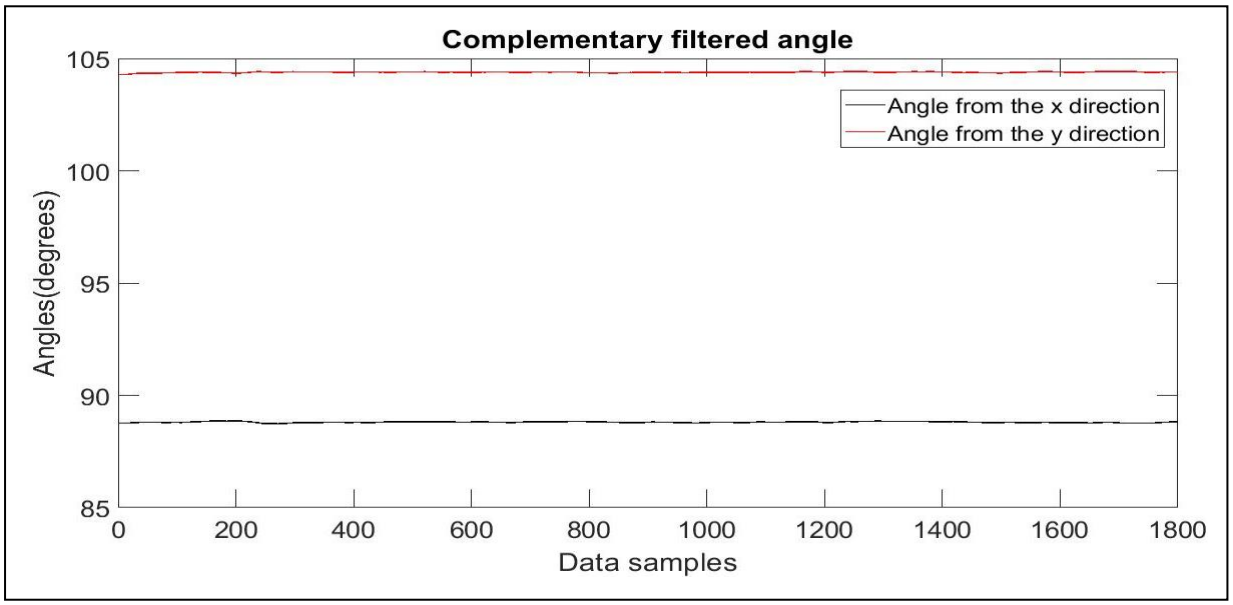

(b)

Figure 5.5. Comparison between: (a) unfiltered and (b) the complementary filtered angle with γ inclined at 15 degrees in the direction of the y axis.

The mean (standard deviation) of the unfiltered and complementary filtered inclination angle were 104.39 (0.181) degree, 104.39 (0.059) degree respectively. The standard deviation of the filtered angle was lower than the unfiltered angle by approximately 0.122 degrees resulting in noise reduction by more than a third.

The results of the displacement and angles of the three methods are shown in Table 5.1. Methods A, B and C represent the manual measurements, the method developed in this study and the method developed in Mayagoitia et al. (2002). Method A was used as the reference for both methods as it is manual and is comparable to physical units. As indicated in Table 5.1, the displacement values for methods A and B are closely related. The displacement values for method C can be observed to deviate largely from those obtained from method A. The graphical representations of the means of the measurement in Table 5.1 are shown in the bar graph of Figure 5.6.

Table 5.1. Displacement and angle measurements between methods A, B and C.

Test number	**Method A**		**Angles (γ) determined using methods B and C (degrees)**	**Method B**	**Method C**
	Angle (degrees)	**Displacement (cm)**		**Displacement (cm)**	**Displacement (cm)**
1	0	0	0.8	1.4	1.4
2	5	9	5.1	8.9	8.9
3	9	17	9.1	15.8	16.1
4	14	26	14.4	24.9	25.7
5	20	34	20.1	34.4	36.5
6	25	43	25.0	42.3	46.7
7	29	50	29.4	49.0	56.2
8	34	58	34.7	56.9	69.1
9	40	65	40.3	64.7	84.7
10	45	70	45.0	70.7	99.9
11	50.00	78.00	50.39	77.10	120.90
12	55.00	82.00	55.65	82.60	146.30
13	60.00	87.00	61.02	87.48	180.60
14	65.00	91.00	65.06	90.68	215.10
15	70.00	93.00	71.02	94.56	290.80
16	75.00	97.00	75.33	96.74	382.00
17	80.00	99.00	80.48	98.62	596.60
18	85.00	99.00	84.17	99.48	979.40
19	90.00	100.00	89.28	99.99	7957.30
Mean (standard deviation)	44.79 (28.32)	63.05 (33.18)	45.07 (28.20)	62.96 (33.32)	595.48 (1799.25)

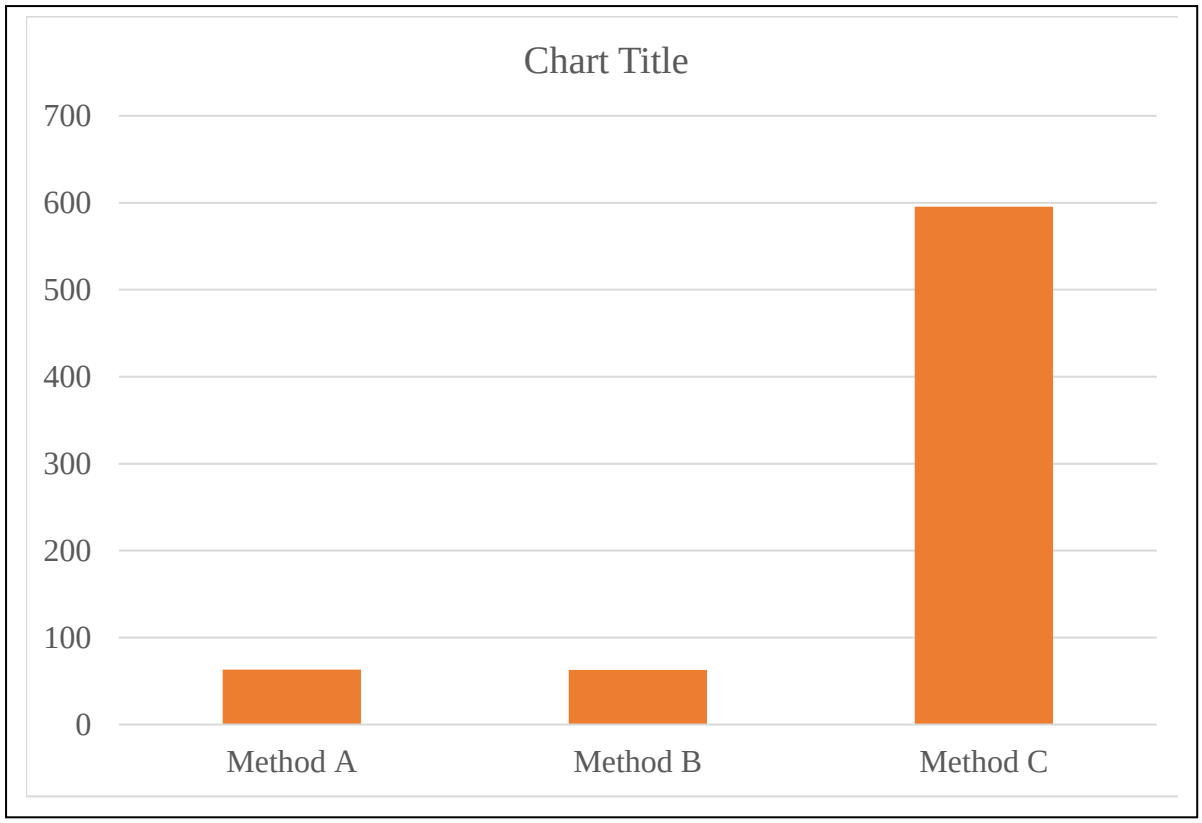

Figure 5.6. Graphical representation of the displacement of method A (manual method), method B (proposed method) and method C (Mayagoitia et al. (2002)) over a range of 90-degree inclination

The results of the test of normality using Shairo-Wilk test showed a p-value of 0.058, 0.051 and 2.47 $\times 10^{-8}$ for the methods A, B and C respectively with the level of significance (α) set to 5%. Based on the results of the p-values, methods A and B conformed to normality while method C did not meet the requirements of normality. Thus, tests of significant differences were carried out using Wilcoxon signed rank test. The result of the test of significant difference between the displacement of the methods A and B showed that no significant difference (p-value = 0.617) existed between the methods. However, the results between method A and C showed that significant difference (p-value = 3.4×10^{-4}) existed between the methods. Test of normality using Shapiro-Wilk test for the values of the inclination angles obtained using methods A, B and C showed that the data conformed to a normal distribution. Their p-values were 0.549 and 0.474 for methods A and methods B and C respectively. The plots of the differences of the displacements and angles of methods B and C with reference to method A are shown in Figure 5.7 (a) and (b). The greater the deviation of the differences from zero, the

greater the disparity between the methods. The angular inclination results show that the protractor and the accelerometery device measurements follow closely.

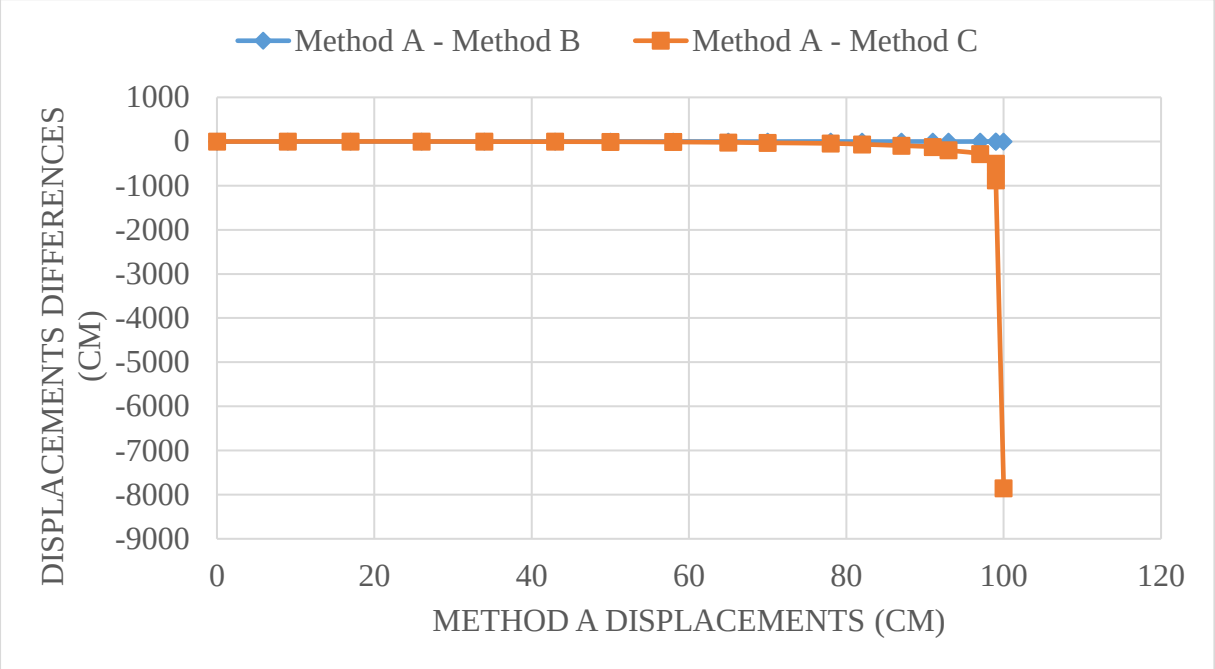

(a)

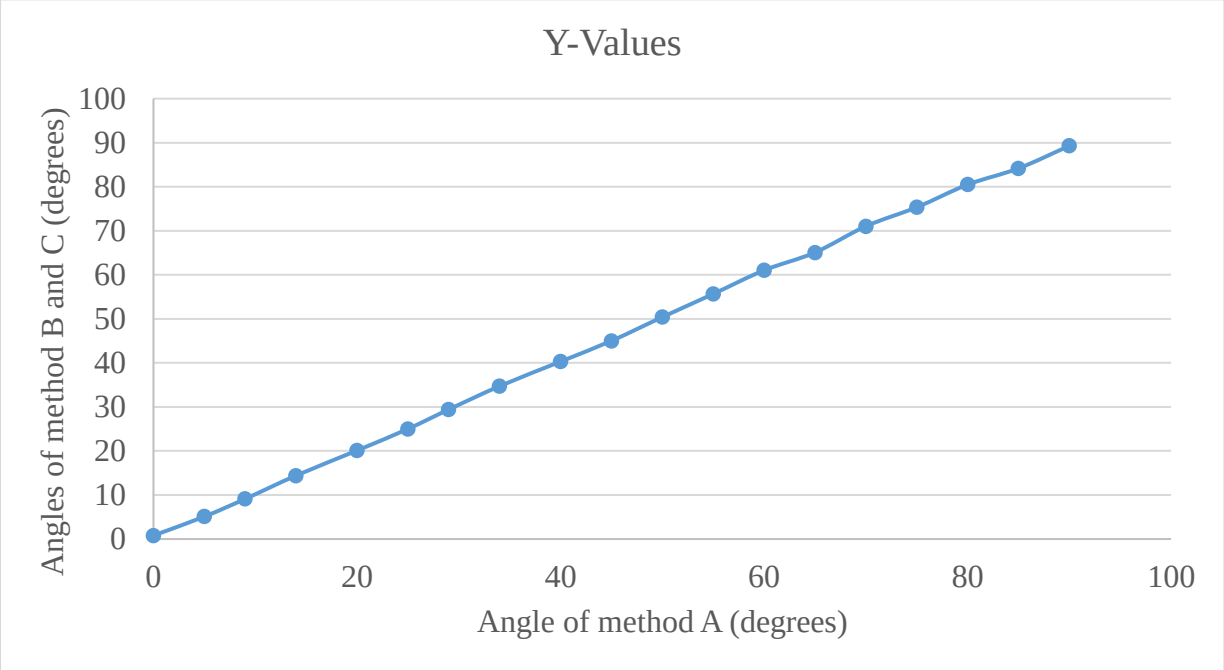

(b)

Figure 5.7. Comparison between the methods: (a) Displacement differences (b) orientation angle

Test and retest reliability were carried out using the Bland and Altman's analysis. The Bland and Altman's analysis was used because the measurements were not repeated (Myles and Cui., 2007) i.e., the measures were simultaneously obtained from the three methods. The Bland and Altman's plot of the differences between the methods A and B against their corresponding means is shown in Figure 5.8.

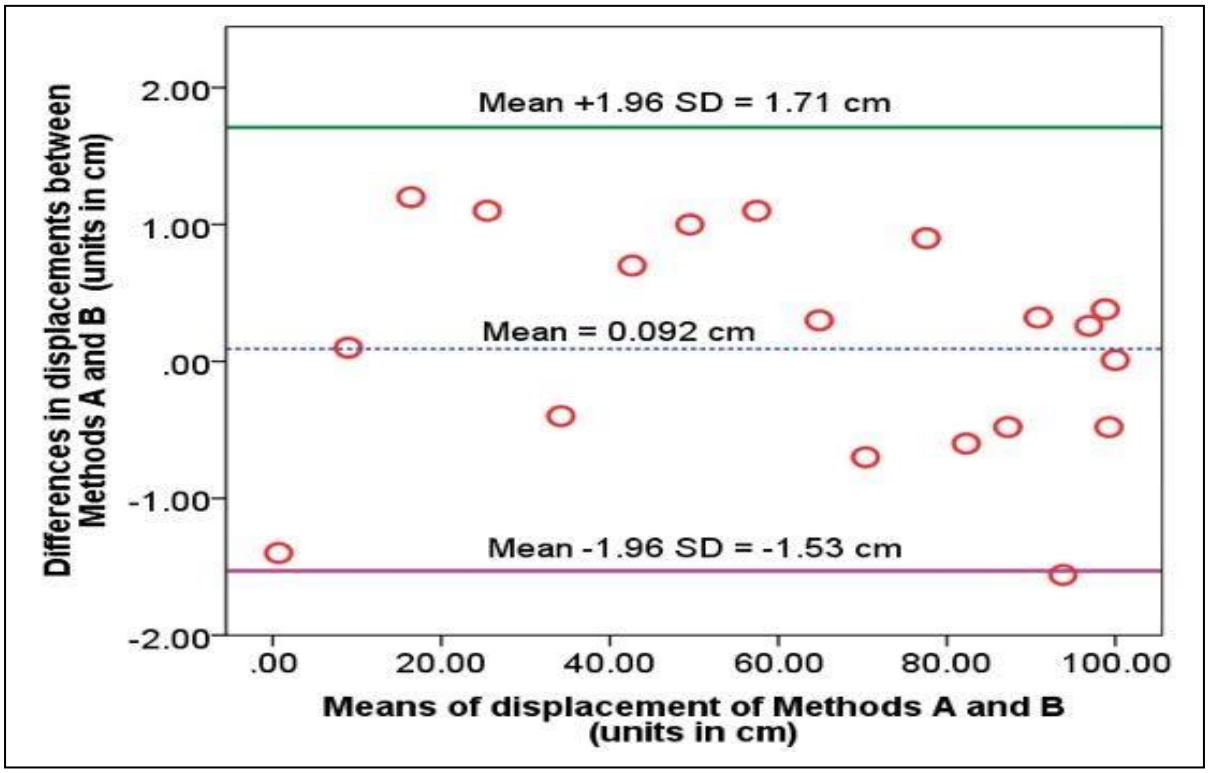

Figure 5.8. Bland and Altman plot for Method A and B data, with the representation of the limits of agreement (Mean ± 1.96 SD)

The *y* axis represents the differences between the methods while the *x* axis represents the corresponding means of each sample entry. The smaller the mean of the difference between the methods (zero representing the least difference) the greater their agreement. The 95% limit of agreement indicated by the line above and below (i.e., the lines representing the Mean ± 1.96 SD) the mean shows the range of variation between the two methods i.e., how well the two methods agree. The smaller the range, the better their agreement. In this case, the range between methods A and B (1.71 cm – (-1.53 cm)) was 3.24 cm. The process of conducting the Bland and Altman's analysis for methods A and B is shown in Table 5.2**.**

Table 5.2. Process of Bland and Altman analysis for methods A and B

Test number	Method A	Method B	Mean ((Method A + Method B)/2)	Differences (Method A – Method B)
1	0.00	1.40	0.70	-1.40
2	9.00	8.90	8.95	0.10
3	17.00	15.80	16.40	1.20
4	26.00	24.90	25.45	1.10
5	34.00	34.40	34.20	-0.40
6	43.00	42.30	42.65	0.70
7	50.00	49.00	49.50	1.00
8	58.00	56.90	57.45	1.10
9	65.00	64.70	64.85	0.30
10	70.00	70.70	70.35	-0.70
11	78.00	77.10	77.55	0.90
12	82.00	82.60	82.30	-0.60
13	87.00	87.48	87.24	-0.48
14	91.00	90.68	90.84	0.32
15	93.00	94.56	93.78	-1.56
16	97.00	96.74	96.87	0.26
17	99.00	98.62	98.81	0.38
18	99.00	99.48	99.24	-0.48
19	100.00	99.99	100.00	0.01
				Mean ($\bar{d}$) = 0.092cm Standard deviation (s) = 0.826 cm

Similarly, the plot of the differences between the methods A and C versus their means are shown in Figure 5.9. The Bland and Altman's plot was not used due to the differences between the methods A and C not conforming to a normal distribution. As indicated by the mean of the differences (Mean ($\bar{d}$) = -532.43cm), method C is 532.43 cm on average greater than method A. The upper and lower limits (i.e., the lines representing the Mean ± SD) show the range of variation between the two methods. In this case, the range between methods A and B (1255.26 cm – (-2320.12 cm)) was 3575.38 cm.

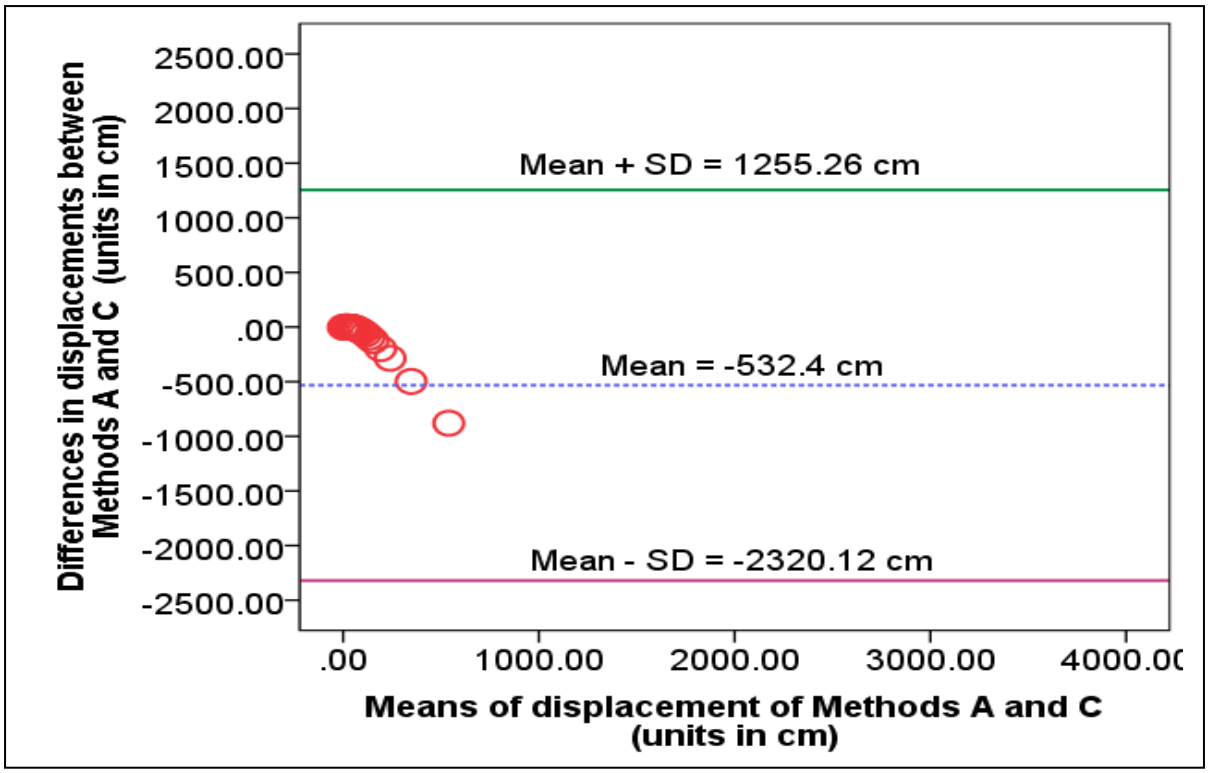

Figure 5.9. The plot of the differences between the Methods A and C against their means (Upper and lower limits (Mean ± SD))

Although method A was more similar to method B than method C, the differences between methods A and C are negligible at inclination angles of less than 20 degrees as indicated in Table 5.1. Thus, method C can still be used for standstill balance analysis as the angle of sway for a human subject is typically low, although care must be taking such that the analysis is limited to only one direction as sway from one direction is reflected unto the other direction even when there is no movement in that direction. The process of the construction of the displacement differences between methods A and C against their means are shown in Table 5.3.

Table 5.3. Process of Bland and Altman analysis for methods A and C

Test number	Method A	Method C	Mean ((Method A+Method C)/2)	Differences (Method A – Method C)
1	0.00	1.40	0.70	-1.40
2	9.00	8.90	8.95	0.10
3	17.00	16.10	16.55	0.90
4	26.00	25.70	25.85	0.30
5	34.00	36.50	35.25	-2.50
6	43.00	46.70	44.85	-3.70
7	50.00	56.20	53.10	-6.20
8	58.00	69.10	63.55	-11.10
9	65.00	84.70	74.85	-19.70
10	70.00	99.90	84.95	-29.90
11	78.00	120.90	99.45	-42.90
12	82.00	146.30	114.15	-64.30
13	87.00	180.60	133.80	-93.60
14	91.00	215.10	153.05	-124.10
15	93.00	290.80	191.90	-197.80
16	97.00	382.00	239.50	-285.00
17	99.00	596.60	347.80	-497.60
18	99.00	979.40	539.20	-880.40
19	100.00	7957.30	4028.65	-7857.30
				Mean($\bar{d}$) = -532.43cm Standard deviation (s) = 1787.70 cm

5.3.2. Analysis of the system on healthy human adult subjects

Typical results of a subject's sway in condition one and four of the mCTSIB test in terms of the time domain measures of position, velocity, acceleration and the polar plot are shown in Figure 5.10 (a) and (b).

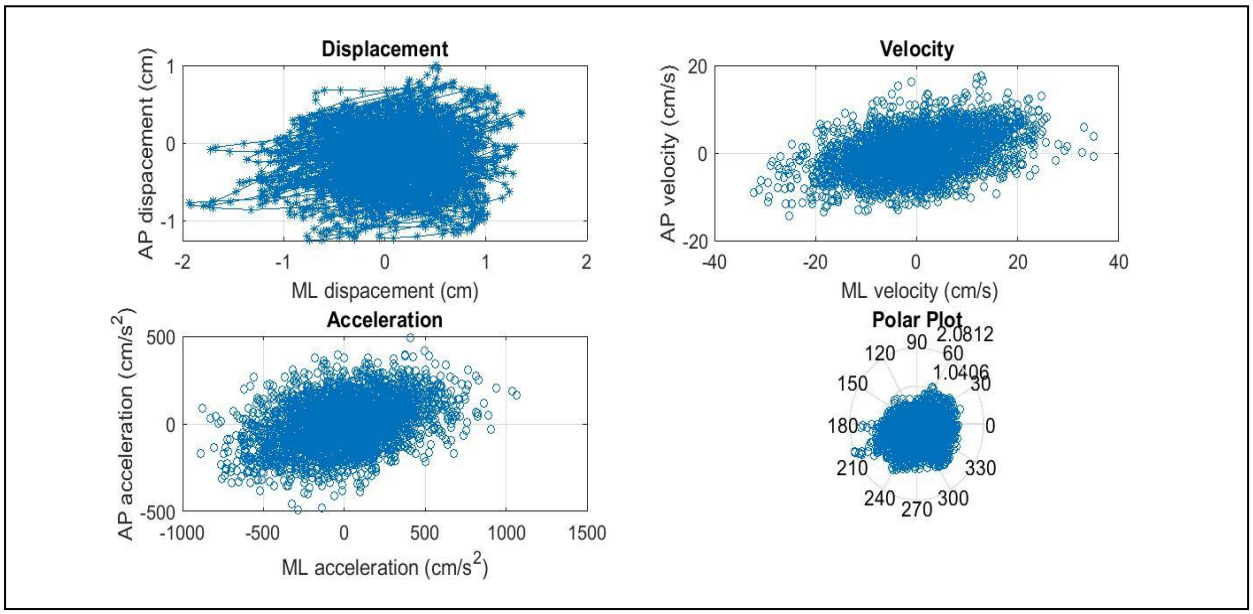

(a)

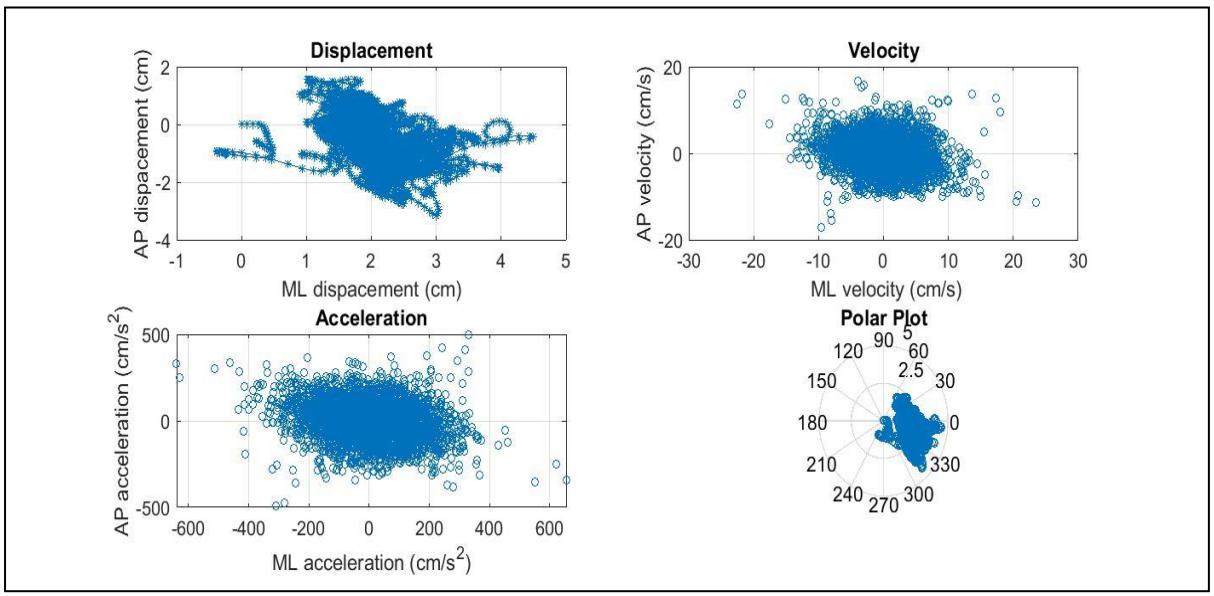

(b)

Figure 5.10. Typical sway of a subject: (a) conditions 1 and (b) condition 4 of the mCTSIB test

The displacement measures the sway of the subject from the origin. The velocity measures the change in the displacement with time. The acceleration represents the rate of change of the velocity. The polar plot is a representation of the subject's displacement in terms of the radius and the angle of the subject. Condition 1 (eyes open standing on ground) represents the scenario when all the balance related sensory systems are working together to maintain balance while condition 4 represents the scenario when only the vestibular system is used to maintain balance. It can be observed from the result of the displacement, velocity, acceleration and polar plot of Figure 5.9, that the sway of condition 4 is greater than condition 1. The mean and standard deviation of the displacement, velocity and acceleration for the mediolateral (ML) direction were 0.4 cm and 0.30 cm, 7.50 cm/s and 5.87 cm/s, 219.92 cm/s^2 and 171.14 cm/s^2 respectively. The mean and standard deviation of the displacement, velocity and acceleration for the anterior-posterior (AP) direction were 0.35 cm and 0.26 cm, 3.81 cm/s and 2.80 cm/s, 109.50 cm/s^2 and 80.48 cm/s^2 respectively. The radius and angle of the polar plot of the displacement for condition 1 are 0.5845 cm and 0.3074 cm, 83.55 degree and 53.60 degree respectively. The mean and standard deviation of the displacement, velocity and acceleration for the mediolateral (ML) direction for condition 4 were 2.06 cm and 0.54 cm, 12.45 cm/s and 6.79 cm/s, 299.46 cm/s^2 and 179.4284 cm/s^2. The mean and standard deviation of the displacement, velocity and acceleration for the anterior posterior (AP) direction were 0.79 cm and 0.55 cm, 6.50 cm/s and 5.60 cm/s, 200.17 cm/s^2 and 101.68 cm/s^2. The radius and angle of the polar plot of the displacement for condition 4 were 2.2541 cm and 0.60 cm, 20.32 degree and 13.74 degree respectively. In the polar coordinate, care must be taking when referring to the angles, as deviation from 90 is an indication of sway in both directions where larger deviations indicate more sway in both directions. Sway in only one direction will have angular values close to 90 degrees. Thus, for the understanding of sway information using polar plot, it is necessary to consider both the radius and the angle.

The time domain sway measures used for analysing the differences between the four conditions are shown in Table 5.3, where a tick mark is used to indicate a significant difference between the respective paired conditions. The test of significant difference was conducted using the Wilcoxon signed rank test or the paired sample t-test, based on the result of the test of normality of the variable. The mean and standard deviation of the sway measures of the various conditions from Table 5.3 that performed best in differentiating between the conditions are shown in Table 5.4. It was observed among all the sway measures that no significant difference existed between conditions 2 and 3. The sway measures that provided the greatest differences as indicated in

Table 5.5 include the root mean square (rms) velocity and acceleration in the AP direction, average velocity and acceleration in the AP direction, and the range of velocity in the AP direction.

Table 5.4. Sway measures used for examining the four conditions of the mCTSIB. A tick mark indicates there was a significant difference between the conditions (source: Ojie & Saatchi, 2020).

Measures	M-CTSIB conditions					
	1 and 2	**1 and 3**	**1 and 4**	**2 and 3**	**2 and 4**	**3 and 4**
RMS displacement-ML						
RMS displacement -AP	✓				✓	✓
RMS velocity-ML						
RMS velocity-AP	✓	✓	✓		✓	✓
RMS acceleration-ML						
RMS acceleration-AP	✓	✓	✓		✓	✓
range of displacement-ML		✓	✓		✓	
range of displacement-AP		✓	✓		✓	✓
range of velocity-ML						
range of velocity-AP	✓	✓	✓		✓	✓
range of acceleration-ML						
range of acceleration-AP		✓	✓		✓	✓
average distance-ML						
average distance-AP						
average velocity-ML						
average velocity-AP	✓	✓	✓		✓	✓
average acceleration-ML						
average acceleration-AP	✓	✓	✓		✓	✓

Table 5.5. The mean (standard deviation) of the most effective sway measures for differentiating between the conditions of the mCTSIB (source: Ojie & Saatchi, 2020).

Measures	M-CTSIB conditions			
	1	**2**	**3**	**4**
RMS velocity-AP	2.3 (0.6)	2.7 (0.8)	2.8 (1.0)	3.6 (1.3)
RMS acceleration-AP	58.6 (15.0)	65.6 (18.8)	69.6(26.9)	85.9 (31.3)
Range of velocity –AP	16.3 (3.5)	23.5 (12.2)	24.1 (11.0)	33.7 (18.0)
Average velocity-AP	1.9 (0.5)	2.2 (0.6)	2.2 (0.8)	2.9 (1.0)
Average acceleration-AP	47.7 (12.8)	53.5 (15.1)	56.8 (21.0)	70.3 (25.2)

5.3. Summary

In this chapter, the accelerometry algorithms for balance analysis based on the model of an inverted pendulum were developed and evaluated using a manual setup designed in similar manner to an inverted pendulum. The system was inclined in the range of 0 to 90 degrees with the manual and accelerometry measurements of the angle and ground projected sway obtained simultaneously. The manual measurements were obtained using a tape rule (to measure the ground displacement) and a protractor (to measure the angle). The measures obtained from the manual setup and accelerometry system were closely related. The algorithms were further utilised in assessing the balance of 15 healthy adult subjects. The ability of the sway measures to differentiate between the four conditions of the modified Clinical Test of Sensory Interaction and Balance (mCTSIB) were investigated. The sway measures investigated consisted of the mediolateral (ML) and anterior posterior (AP) time domain measures of the: root mean square velocity and acceleration, average velocity and acceleration, root mean square of the positional displacement, the average of the positional displacement, the range of the velocity and acceleration and the range of the positional displacement. The results indicated that the AP time domain measures of the: root mean square velocity and acceleration, average velocity and acceleration and the range of the velocity were more effective in differentiating between the conditions.

Chapter 6 The effect of centre of mass position on analysing balance

6.1. Introduction

The centre of mass position plays a fundamental role in analysing a person's balance. The COM position refers to an imaginary point where the entire body mass can be considered to act (Richmond et al., 2021). In balance analysis when using inertial measurement units, the sensor is usually placed at the position of the COM to capture the entire sway of the body (Aguilera-Castells et al., 2020). The COM sway can be used to determine the sensory systems contribution to postural control and to estimate their functionalities. When the goal is to examine the functionalities of the sensory system for diagnostic reasons, the COM position plays an important role in comparing postural sway between people. Since standstill sway analysis is a representative of angular deviation, we hypothesised that the same angular sway would result in the same ground displacement and similar balances. This hypothesis is made for the purposes of comparing the sway of people with balance dysfunction for diagnostic reasons such that similar angular sway can imply similar extent to a particular dysfunction and in turn produce similar sway on ground. Sway comparison could be carried out between a patient and another patient, a patient and a healthy control, and a healthy control and a healthy control.

To investigate this hypothesis, a system was developed to analyse the effect that varying COM position has on postural sway and in turn their balance. The system consisted of 3 plumb bobs attached to a metal rod, at one end, at the position of 50 cm, 75 cm and 100 cm above the ground surface. The accelerometer transmitting unit was attached onto the metal rod using a tie strap and inclined from 0 to 90 degree. Manual measurements of the angle of the rod and the projection of the plumb bobs on the ground surface were obtained using a measuring tape and protractor respectively. The data from the accelerometer were recorded simultaneously with the manual measurements and analysed to determine the angular sways and ground displacements. The results obtained was in support of the alternative hypothesis, that the same angle of sway does not produce the same ground projected displacement. The displacements on ground were in a direct proportional relationship to the COM positions for the same angle of inclination. This implies that methods of analysis using either the angle of sway or the integration of acceleration to carry out balance analysis without reference to the COM position may not produce accurate results. However, normalisation with the COM position can help reduce the disparity for comparison purposes although it may affect the accuracy of the results.

A greater base of support may be required for people with higher COM positions to maintain balance, in the event of a balance problem, in comparison to people with a lower COM.

In accordance with these findings, we suggest that people of relatively equal COM positions are compared; normalisation of sway with the COM position is considered for comparison purposes; and greater base of support is provided for people with greater COM positions in the event of a balance dysfunction.

6.2. Chapter related methodology

6.2.1. Measurement apparatus and data collection

The devised measurement apparatus consisted of a metal rod, 3 plumb bobs and lines, the accelerometry units, a vice, a measuring tape and a protractor. The metal rod was of length 134 cm and diameter 2 cm. The 3 plumb lines-plumb bobs system were attached to one of its ends, at position 1 = 50 cm, position 2 = 75 cm and position 3 = 100 cm to represent the centre of mass positions of 50 cm, 75 cm and 100 cm respectively. These positions were chosen as they are close to COM positions in children and adults. The accelerometry transmitter unit was attached to the metal rod at the height of 105 cm and the metal rod was held by a vice which was clamped to a table and enabled the rod to be inclined vertically from 5 to 90 degrees in the *y* axis of the accelerometer. The measuring tape was used to measure the ground projected displacement made by the plumb lines-plumb bobs system for each angle of deviations and the protractor was used to obtain the angular deviation of the metal rod. Simultaneously with the manual movement of the metal rod to predefined inclination and using the inter-integrated transmission protocol (I^2C), the data from the accelerometer transmitting unit were sent wirelessly to the device's receiver unit which was connected to a laptop computer via a USB connection, for storage and analysis. The data transmitted were the three axes of the accelerometer device (*x,y,z*) and the sampling rate was 60 Hz. The recording duration lasted for 60 seconds. The diagram of the device setup with all the necessary components as discussed above is shown in Figure 6.1.

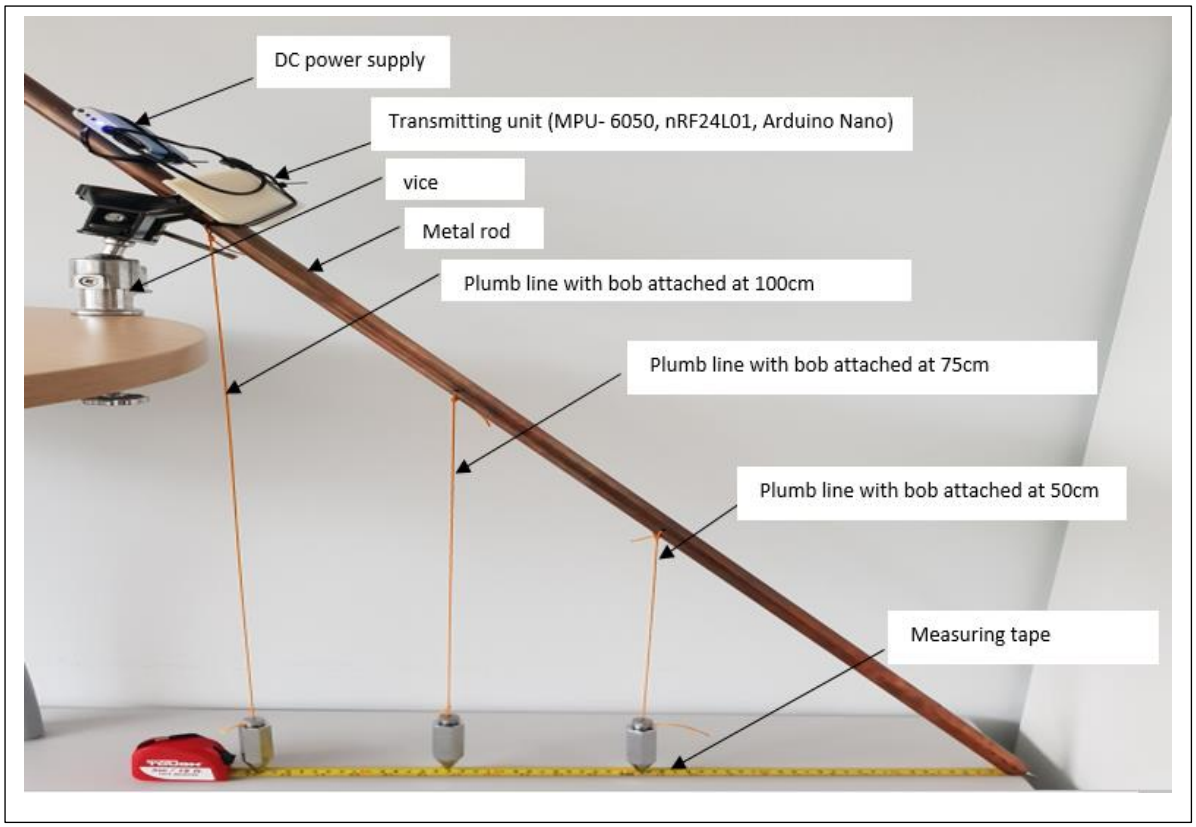

Figure 6.1. Test measurement apparatus (source: Ojie et al., 2020)

6.2.2. Data analysis

The raw data of the tri-axial accelerometer were digitally low-pass filtered in software using a 0.5 Hz second-order low pass Butterworth filter. After filtering, the raw data of the tri-axial accelerometer were converted to the units of acceleration (i.e., g = 9.8 ms^{-2}) with a full-scale range of ±2 gs^{-2} by dividing by the sensitivity scale factor of 16,384 least significant bit/g. The tri-axial accelerations (a_x, a_y and a_z) obtained were converted into directional cosines i.e., cos α, cos β and cos γ using Equation (5.2). Using Equation (5.3), the sway displacement on the ground in the *y* directions (d_y) with respect to the origin, were obtained and averaged over the number of measured samples, *N* (*N* = 60 seconds × 60 samples per second = 3,600 samples) using Equation (6.1), where d_{ya} is the average of the displacement. The inclination angle of the accelerometer was obtained from Equation (5.2) by solving for γ and the average for all the samples were obtained using Equation (6.2), where γ_a is the average of the angle of inclination.

$$d_{ya} = \frac{1}{N}\sum_{n=1}^{N} d_y(n) \tag{6.1}$$

$$\gamma_a = \frac{1}{N}\sum_{n=1}^{N} \gamma(n) \tag{6.2}$$

Data analysis was carried out using MATLAB® and SPSS® statistical packages. Test of normality was conducted using the Shapiro-Wilk test of normality with p-value set to 5%. Depending on the result of normality i.e., normally or not normally distributed, the paired sample t-test or the Wilcoxon signed rank test was used to compare the measures of the displacements to examine if a significant difference existed between the manual measurements using the physical apparatus and the algorithm's calculations. Depending on the result of normality, Pearson or Kendall tau correlation analysis was used, and linear regression analysis were performed to interpret the measurements.

6.3. Results and discussion

6.3.1 Results of the manual and accelerometry system

In total, nineteen measurements were obtained from the inclination of the metal rod from 0 to 90 degrees in steps of 5 degrees. The accelerometer reading for the displacement at 50 cm, 75 cm and 100 cm for an inclination angle of 5-degree is shown in Figure 6.2. A variance of 0.15 degree can be observed from the accelerometer reading of the inclination angle. This is due to the noise of the accelerometer measurement as the sensor was in a stationary position and the data was filtered using a second order low pass Butterworth filter with a cutoff frequency of 0.5 Hz. A cut of frequency of 0.5 Hz was used because the sensor was in a stationary position.

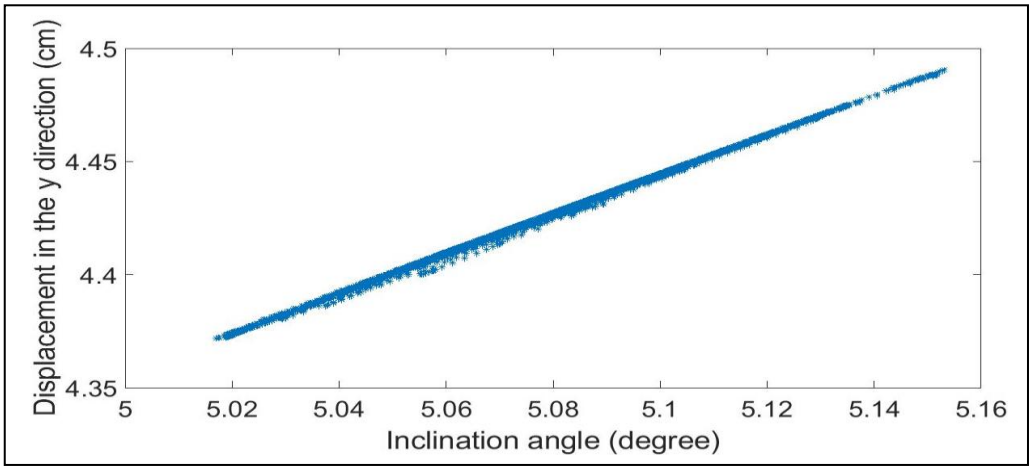

(a)

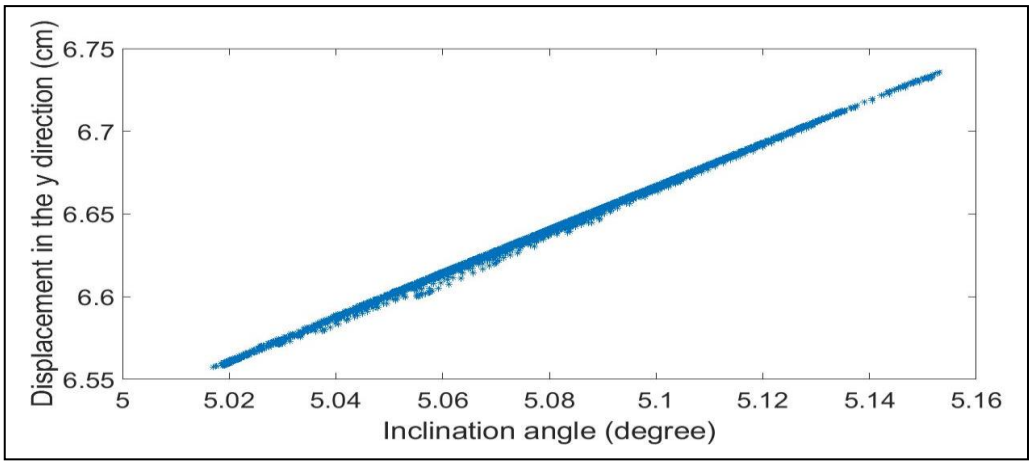

(b)

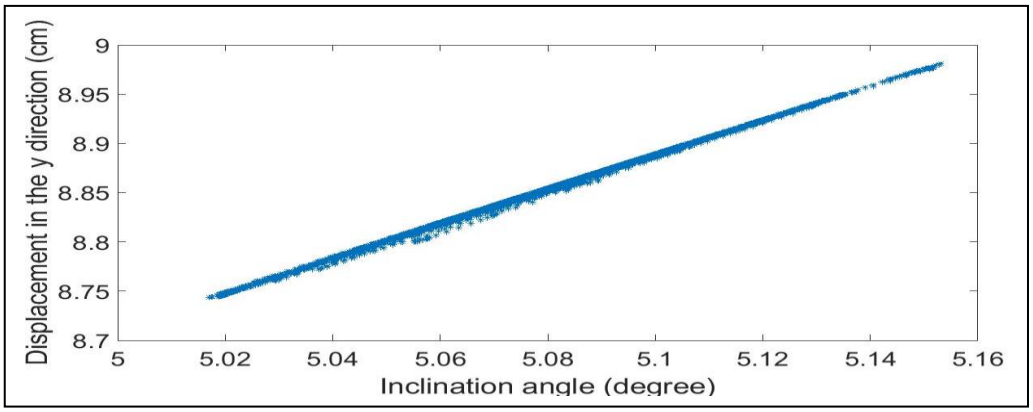

(c)

Figure 6.2. Ground displacement at 5 degrees for position: (a) 50 cm (b) 75 cm and (c) 100 cm respectively

The results of the manual and accelerometry measurements are provided in Tables 6.1 and 6.2 respectively. The displacements in Table 6.1 correspond to the displacements of the plumb

lines-plumb bobs on the ground (positions 1: 50 cm, 2: 75 cm and 3: 100 cm) with respect to the origin that were obtained by the measuring tape and the angles corresponds to the inclination angle made by the metal rod which were obtained by the protractor. The displacements in Table 6.2 corresponds to averages of the displacements of the plumb lines-plumb bobs on the ground (positions 1: 50 cm, 2: 75 cm and 3: 100 cm) with respect to the origin that were obtained by the accelerometer and the angles correspond to the averages of the inclination angles made by the metal rod as obtained by the accelerometer.

Table 6.1. Manual measurements of the displacements and angles obtained by the measuring tape and the protractor (source: Ojie et al., 2020)

Measurement Number	**Angle, γ (degrees)**	**Position 1 (Displacements at COM=50 cm)**	**Position 2 (Displacement at COM= 75 cm)**	**Position 3 (Displacement at COM=100 cm)**
1	0	0	0	0
2	5	5	7	9
3	10	9	13	17
4	15	12	19	25
5	20	17	25	34
6	25	21	31	42
7	30	25	36	50
8	35	29	43	56
9	40	32	50	65
10	45	35	52	70
11	50	39	58	77
12	55	41	60	82
13	60	44	65	87
14	65	45	68	90
15	70	48	70	95
16	75	48	72	97
17	80	49	73	98
18	85	49	74	99
19	90	50	75	100
		Mean=31.5 cm Standard deviation =16.6 cm	Mean=46.9 cm Standard deviation =24.8 cm	Mean=62.8 cm Standard deviation =33.3 cm

Table 6.2. Accelerometry measurements of the averages of the displacement and the inclination angles (source: Ojie et al., 2020).

Measurement Number	**Angle, γ (degrees)**	**Position 1 (Displacements at COM=50 cm)**	**Position 2 (Displacement at COM=75 cm)**	**Position 3 (Displacement at COM=100 cm)**
1	0.80	0.69	1.04	1.39
2	5.09	4.44	6.66	8.87
3	9.12	7.93	11.89	15.85
4	14.42	12.45	18.68	24.90
5	20.05	17.14	25.72	34.29
6	25.01	21.14	31.72	42.28
7	29.35	24.51	36.76	49.02
8	34.66	28.44	42.65	56.87
9	40.27	32.32	48.47	64.63
10	44.96	35.33	52.78	70.66
11	50.39	38.52	57.78	77.05
12	55.65	41.28	61.92	82.57
13	61.02	43.74	65.61	87.48
14	65.06	45.34	68.01	90.68
15	71.02	47.28	70.92	94.56
16	75.33	48.37	72.55	96.74
17	80.48	49.31	73.97	98.62
18	84.17	49.74	74.61	99.48
19	89.28	50.00	74.99	99.99
Statistics		Mean=31.5 cm Standard deviation =16. 7 cm	Mean=47.2 cm Standard deviation =25.0 cm	Mean=62.9 cm Standard deviation =33.3 cm

The means (M) and standard deviations (SD) of the displacements of the manual measurements for the plumb line-plumb bob at positions 1 to 3 were: M= 31.5 cm and SD=16.6 cm, M= 46.9 cm and SD= 24.8 cm, M= 62.8 cm and SD= 33.3 cm respectively. For the accelerometry measurements the means and standard deviations of the displacements for the plumb line-plumb bob at positions 1 to 3 were: M=31.5 cm and SD=16.7 cm, M=47.2 cm and SD= 25.0 cm and M= 62.9 cm and SD= 33.3 cm respectively. For the 19 measurements the results of the accelerometry and manual measurements as inferred from their means and standard deviations gave close readings for all three respective positions. The plots of the displacements against the angles of the accelerometry measurements of Table 6.2 are shown in Figure 6.3. The

maximums of the displacements for each position corresponds to their COM heights of placement.

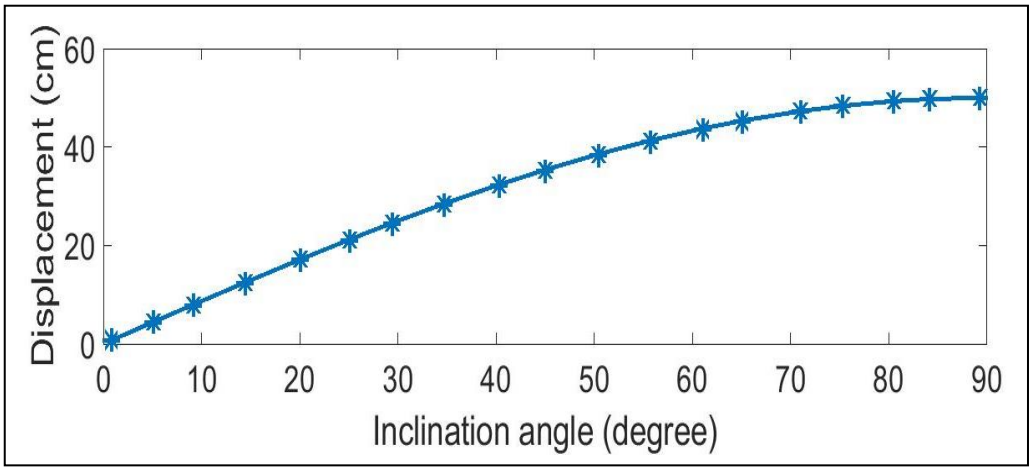

(a)

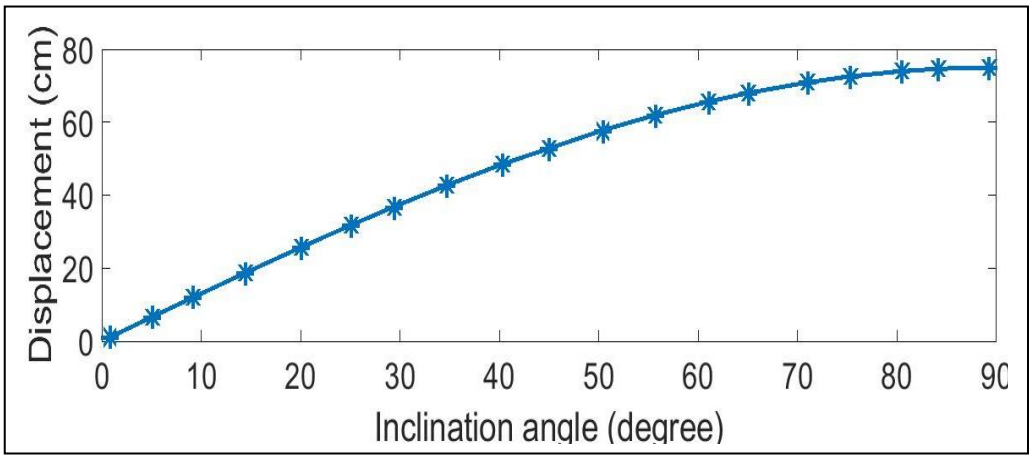

(b)

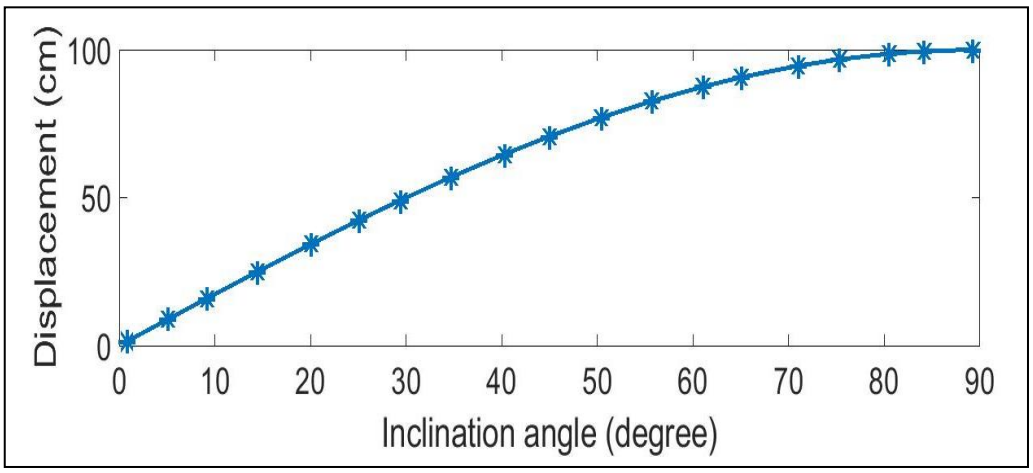

(c)

Figure 6.3. Plot of the displacements vs the angles obtained from the accelerometry unit (a) COM of 50 cm (b) COM of 75 cm (c) COM of 100 cm.

6.3.2. T-test analysis

The Shapiro-Wilks test with a p-value of 0.05 was used to determine the distribution of the displacement values of the respective COM positions. The result showed that the distribution of the data from each group were normal ($p > 0.05$). Paired sample t-tests ($\alpha = 0.05$) were used to establish whether significant differences existed between the displacement values from the three positions i.e., position 1 and 2, position 1 and 3 and position 2 and 3. The results of the paired sample t-test showed significant differences existed between the measurements ($p < 0.01$), suggesting that the position of the COM has implications on the ground displacements. This finding has implications when comparing the sway displacements between individuals of different COM heights, with those of greater COM height producing a greater sway displacement projected on the ground surface. Similarly, falls due to a balance dysfunction will result in taller subjects to be more affected by the impact with the ground as suggested by the potential energy (P.E) given in Equation (6.3).

$$P.E = mgh \tag{6.3}$$

Where m is the mass of the subject, g is the gravitational acceleration (usually 9.8 m/s^2) and h is the height above the ground surface.

6.3.3. Correlation and linear regression analysis

Pearson correlation (r) with confidence interval of 95% ($\alpha = 0.05$) and linear regression were used to investigate the relationships between the three positions of the manual and accelerometry displacement measurements. The results of the manual measurements showed strong positive correlation between the measurements between positions 1 and 2, r (17) = 0.999 and $p < 0.05$, positions 1 and 3, r (17) = 1 and $p < 0.05$, and positions 2 and 3, r (17) = 1 and $p < 0.05$ (Pearson correlation is represented by the symbol r the number (17) in parenthesis is the degree of freedom (df), given by $df = n$-1, where n is the number of samples). Similarly, the results for the accelerometer measurements showed strong positive correlation between positions 1 and 2, r (17) = 1 and $p < 0.05$, positions 1 and 3, r (17) = 1 and $p < 0.05$, and positions 2 and 3, r (17) = 1 and $p < 0.05$. Figure 6.4 shows the relationship between the displacement obtained from each position for the manual and accelerometer data. The related gradients can be observed for all the plots of the positions i.e., positions 1 to 3, given as 1.49 cm, 2.00 cm and 1.34 cm for the manual measurement and 1.50 cm, 2.00 cm and 1.33 cm for the accelerometer setup. The equation of the regression line of the displacement measurements from both methods suggested that the displacement measurements of position 2 could be

obtained from that of position 1 using the formula: 1.5*x* - 0.003 (where *x* is the displacement measurement of position 1). Similarly, the displacement for position 3 could be obtained from position 1 using the equation of the regression line 2.0*x* - 0.001 (where *x* is the displacement measurement of position 1).

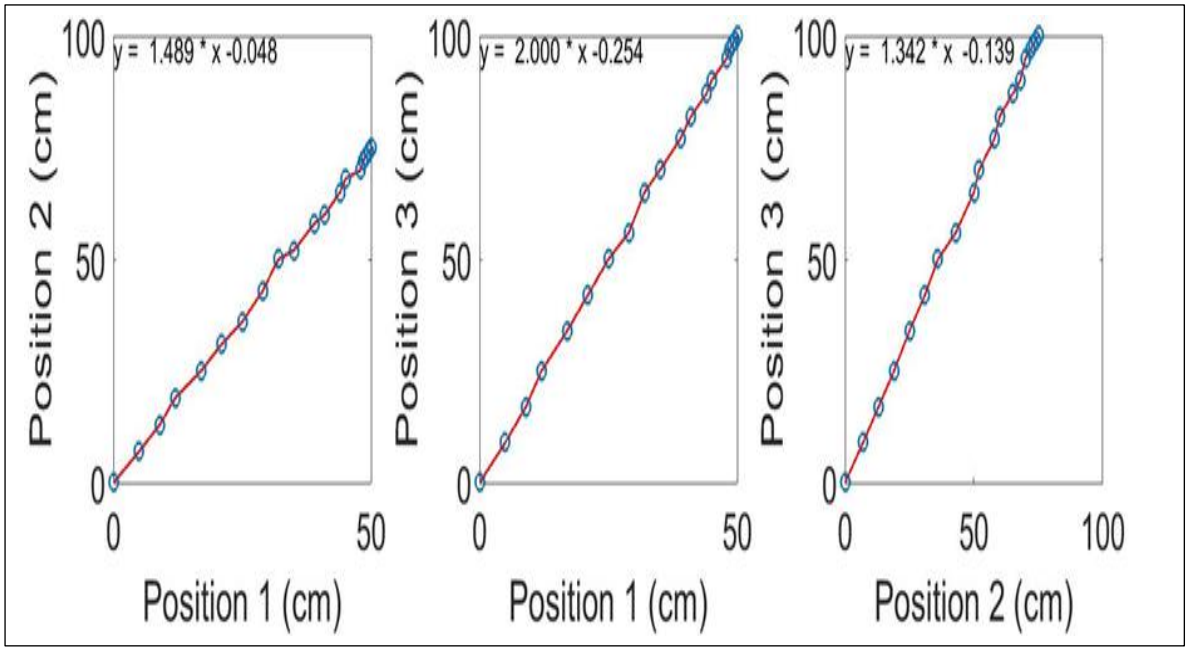

(a)

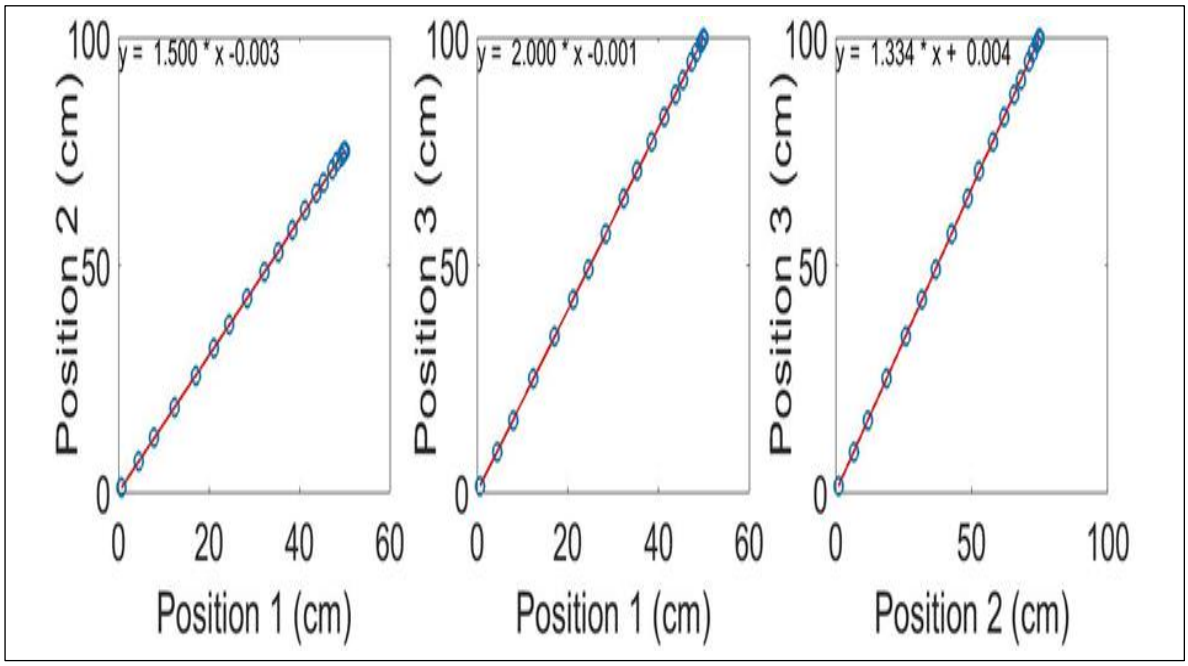

(b)

Figure 6.4. The relationship between the displacements of COM positions: (a) manual, (b) accelerometry (source: Ojie et al., 2020)

Thus, in order to obtain the displacement of position 3, the displacement of position 1 is multiplied by 2 and 0.01 subtracted from the result of the multiplication. Similarly, to obtain the displacement of position 3 from position 2, the displacement values of position 2 is multiplied by 1.334 and 0.004 added to the result of the multiplication as stated by the regression line: 1.334 x + 0.004. The comparison across the positions as shown in each of the above plots suggested that the gradients were a representation of the ratio of the position of COM heights: 75/50 =1.50 for positions 1 and 2, 100/50 = 2.00 for positions 3 and 1 and 100/75 = 1.33 for positions 3 and 2 respectively. This indicates that for the same angular sway, the higher the COM position, the greater the ground projected sway. For a difference of 25 cm, 50 cm, between the COM positions of 2 and 1, a gradient of 1.5 cm was observed. Similarly, for a difference of 25 cm, 50 cm and 25 cm between positions 2 and 1, 3 and 1 and 3 and 2, the gradients were 1.5 cm, 2.00 cm and 1.33 cm respectively. Note that although the difference between positions 2 and 1 and positions 3 and 2 were the same i.e., 25 cm, their gradients were different i.e., 1.5 cm and 1.33 cm respectively. These variations can introduce a bias in the interpretation of postural sway and in sway path measurements as the relationship is not linear. The relationships between the accelerometer measurement for the various COM positions i.e., positions 1, 2 and 3 for both the manual and accelerometer measurement are further illustrated using a box plot as shown in Figure 6.5 (a) and (b). The measurement statistics of the box plot i.e., the median (the horizontal bar inside each box) and interquartile range are in relation to the heights of the COM positions. The median and interquartile range value for position 1, position 2 and position 3 are 35.33 cm and 30.14 cm, 52.78 cm and 45.2 cm and 70.66 cm and 60.27 cm respectively. If similar base of supports where to be considered for all the positions, the balance for position 1 will be greatest, followed by the balance at position 2 and finally the balance at position 3. Thus, an underlying balance condition which produces the same angular deviation will result in differing balances across subjects based on their COM positions if all other factors that can affect balance are kept constant.

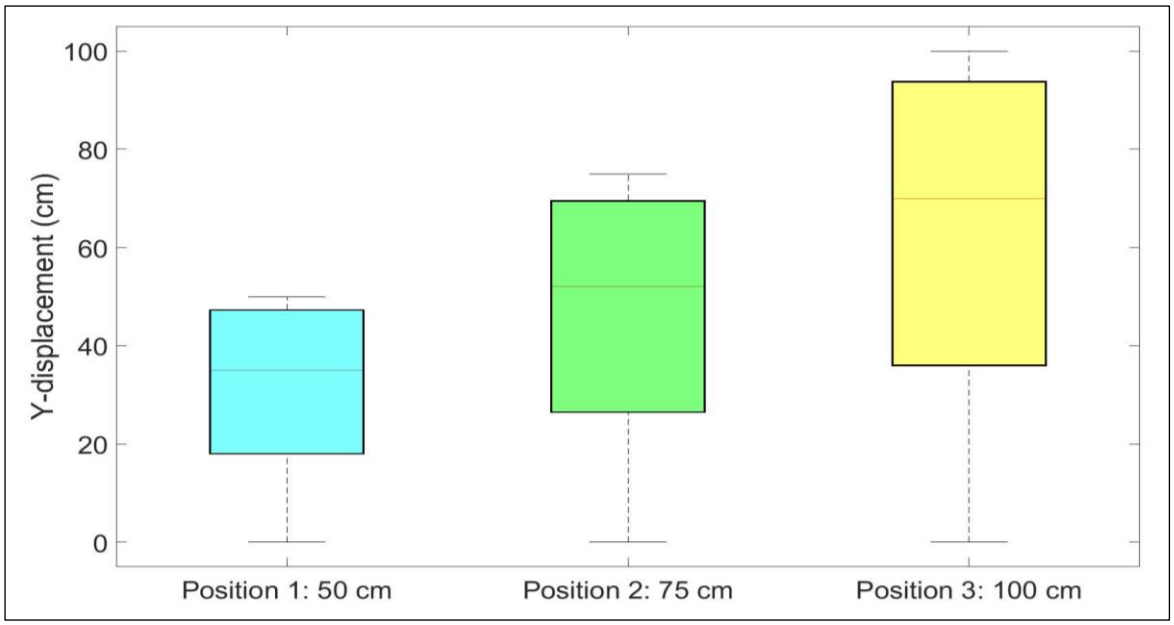

(a)

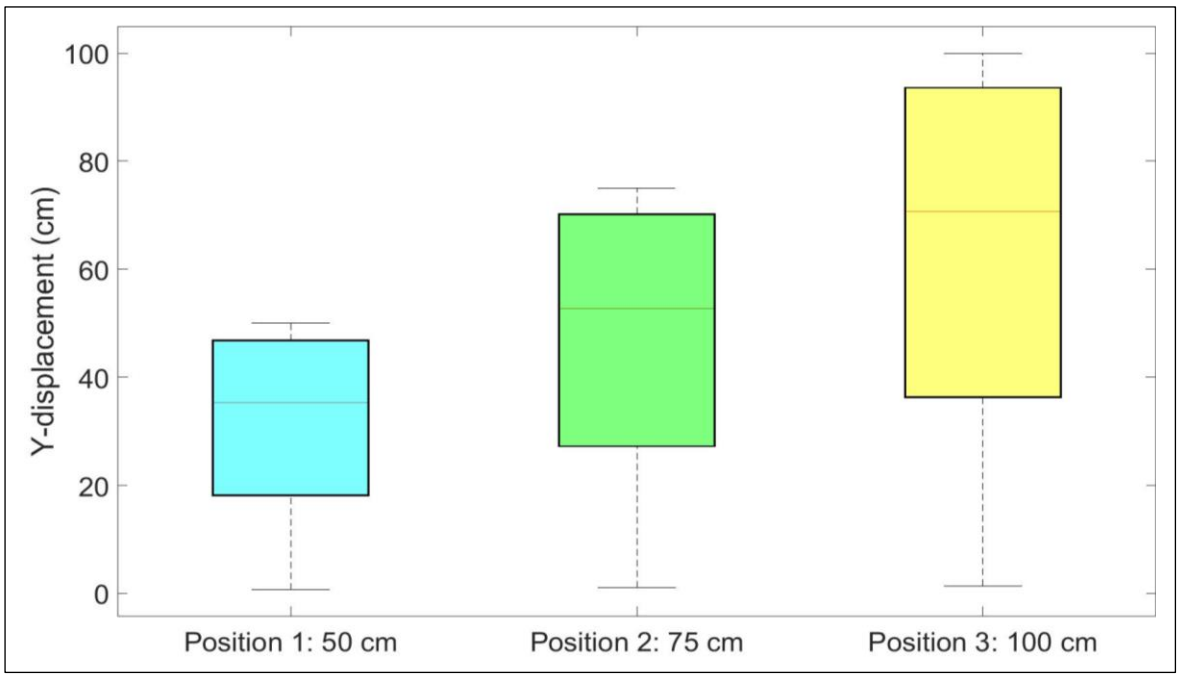

(b)

Figure 6.5. Box plots representations for the displacements: (a) manual, (b) accelerometry measurements (source: Ojie et al., 2020)

Therefore, the COM position can be considered as a factor whose presence affects the postural sway, balance of a subject and the comparison across subjects. Thus, balance may better be treated as a holistic approach where each individual serves as his/her own control. The methods that consider sway only at the COM position without projection unto the ground surface may not be a suitable representation for an accurate analysis of balance. For comparison purpose

across subjects, the bias introduced by the height of the COM position can be reduced by comparing subjects of similar COM positions and by normalization, although normalization may not produce an accurate assessment of balance. The process of normalization is shown in Figure 6.6. In this case the COM position is set to unity i.e., by setting the value of *L* in Equation (5.7) to 1 cm. This results in the same sway across all the positions for a given inclination angle.

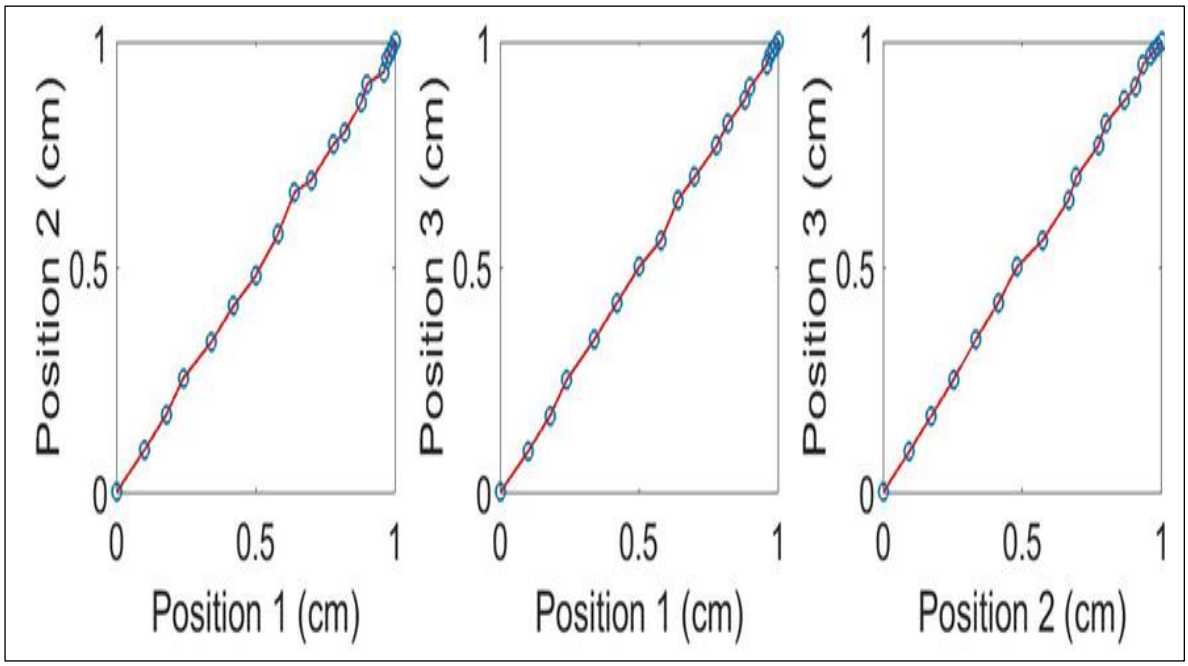

(a)

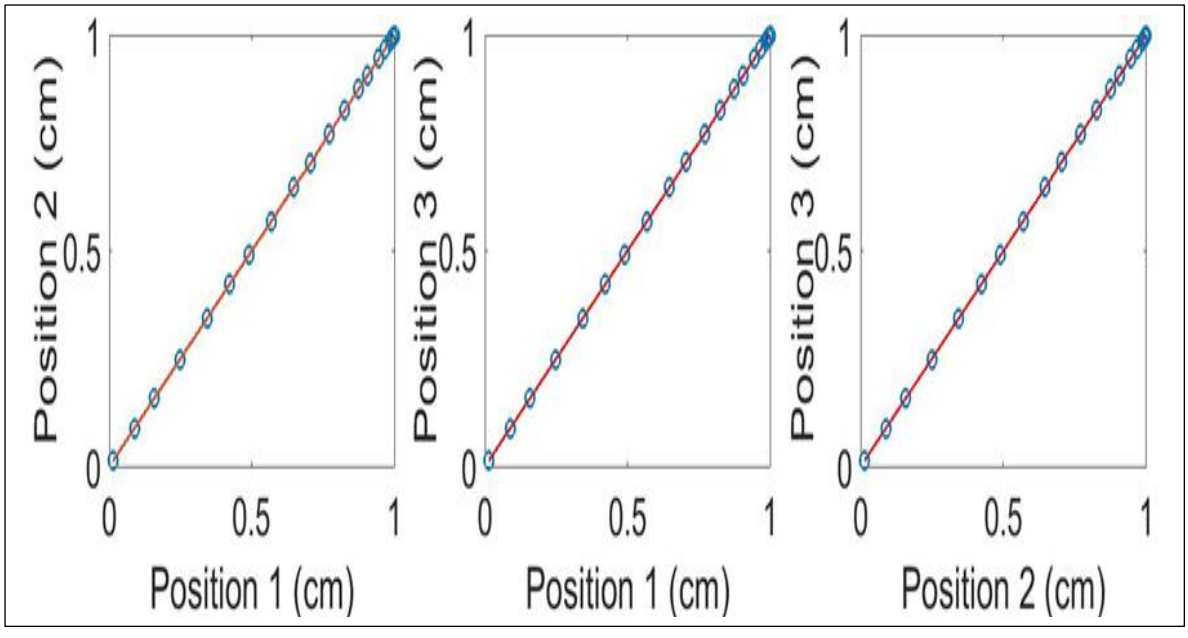

(b)

Figure 6.6. The relationship of the normalised displacements between the COM positions: (a) manual, (b) accelerometry (source: Ojie et al., 2020)

The COM position has an inverse relationship with the angle of sway as shown in Equation (5.7). For a dysfunctional sensory system, a higher COM height could put more strain on the sensory systems as compared to a lower COM height. In this regard, the COM height could affect both the sway angle and the ground displacement. Conversely, although a higher COM position produces a greater displacement, it is not the case that a person with higher COM will produce greater sway than a person with lower COM as many factors affects a person's balance. Thus, the COM height has a double effect which is non-linear on the sway displacement of a subject as it can both affect the angle of inclination and the displacement on ground.

6.4. Summary

The effect that varying centre of mass (COM) positions has on postural sway and balance was discussed in this chapter. A setup was developed to investigate the effects of varying centre of masses. The setup consisted of a metal rod of length 134 cm with a diameter of 2 cm, three plumb bobs, three plumb lines and a vice. The plumb bobs were attached to each plumb line and tied to the metal rod at the position of 50 cm, 75 cm and 100 cm. These positions corresponded to the COM positions of 50, 75 and 100 cm respectively. The rod was inclined from 0 degree to 90 degrees with a 5-degree difference between consecutive measurement making a total of 19 measurements. Simultaneously, the accelerometer transmitter unit developed in chapter 5 was attached to the metal rod to transmit the inclination movement data of the rod to the receiver unit. The receiver unit was connected to a laptop computer for recording and storing of the data. The recorded data was processed to provide the angle of inclination and it corresponding ground displacements.

The result of the manual measurement and the accelerometry system agreed closely for all the three positions respectively. The result suggested that COM height affects postural sway angle and sway displacement on ground. Thus, for accurate analysis of balance the projection unto ground surface should be considered. Similarly, for comparison across subjects, closely related sway should be considered. Although normalisation of the COM height may be considered to reduce the bias introduced by the COM position, it may result in inaccuracies in a subject's balance analysis.

Chapter 7 Investigation of the sensory interaction in healthy adult subjects using principal component analysis

7.1. Introduction

Primarily, balance is maintained by the interaction between the sensory systems i.e., the visual, proprioceptive and vestibular systems (Mohammadi et al., 2021). A problem with any of these systems could lead to balance dysfunctions. For accurate analysis of balance dysfunctions, information from the patient's data is often compared with those of healthy adult individuals – where deviations in the pattern or information can be likened to a dysfunction (Ojie & Saatchi, 2020). Thus, the aim of this chapter was to investigate the patterns inherent in healthy adult subjects using principal component analysis (PCA). Twenty-one healthy adult subjects, with mean (standard deviation) of age, height and weight: 24.5 (4.0) years, 173.6 (6.8) cm, and 72.7 (9.9) kg respectively, participated in the study. The subjects performed the four conditions of modified Clinical Test of Sensory Interaction and Balance (mCTSIB). These conditions are usually used to assess the behaviour/contribution of the sensory systems to balance. Condition one of the test consists of all the sensory systems (i.e. standing on ground surface with eyes open), condition two consists of the proprioceptive and the vestibular systems (i.e. standing on ground surface with eyes closed, excluding the visual system), condition three consists of the visual and the vestibular systems (i.e. standing on a sponge surface with the eyes open, excluding the proprioceptive system) and condition four consists of only the vestibular system (i.e. standing on a sponge surface with the eyes closed, excluding the visual and proprioceptive system). The acclerometry device was attached at the subject's back at approximately the iliac crest. The mediolateral and anterior posterior ground projected sway were recorded and eighteen-time domain measures were further obtained from the sway that quantified the body's position, velocity and acceleration. PCA was used to determine the observed patterns in the sway variables. Based on the observed patterns, further analysis was carried out on the root mean square (RMS) velocity using the Bland and Altman's analysis and other statistical related analysis to verify the structures. The study's results showed that: in a well-lit environment, healthy young adult subjects rely more on their proprioceptive system as compared to their visual system, the anterior-posterior direction was more sensitive to postural sway of the sensory system as compared to the mediolateral direction and a greater coherence in sway information and greater stability was observed in the interaction between the proprioceptive and vestibular systems as compared to the interaction between the visual and vestibular systems.

7.2. Chapter related methodology

7.2.1 Participants' information

Twenty-one healthy adult participants (11 females and 10 males) with no balance dysfunction with mean (standard deviation) of age, height, and weight: 24.5 (4.0) years, 173.6 (6.8) cm, and 72.7 (9.9) kg took part in the study. The participants declared not to have ingested any substance that could affect their balances 48 hours prior to their participation in the data recording process and not to have any balance dysfunction. Corrective lenses were worn by participants who required them before participating in the exercise. Ethical approval was obtained from the university ethical committee and informed consent was provided by all the participants.

7.2.2 Recording device

The devised accelerometry system described in chapter 4 was used here in collecting balance information from the subjects.

7.2.3 Procedure for data recording

The participants wore the transmitting unit part of the device at the position of approximately the iliac crest using a belt that was integrated into the device. Figure 7.1, shows a participant with the device at the position of approximately the iliac crest.

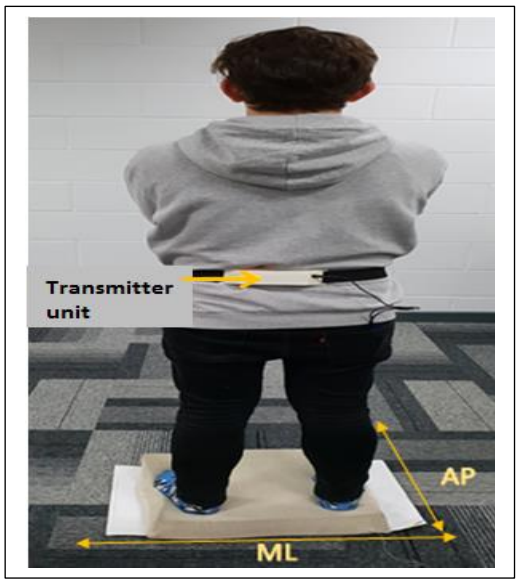

Figure 7.1. The transmitter unit worn by one of the subjects. The subject stood on a soft sponge pad as part of carrying out mCTSIB's conditions 3 and 4 tasks (Ojie & Saatchi, 2020)

During the recording process, the participants stood with their shoes off and with their feet 30 cm apart. The participants were instructed to look at a point on a wall located at a distance of 1 m at the eyes' level while performing the tasks associated to the mCTSIB test. The data recording for each test condition of the mCTSIB lasted for 30 seconds. The participants were provided with a time to rest between each test. During the recording for mCTSIB conditions three and four, the subjects were required to stand on a flexible foam surface. The flexible surface was used to remove the effect of the proprioceptive system and consisted of dimensions 10×50×50 cm corresponding to its thickness, length and width in units of centimetre (cm). The sampling rate of the device was 60 samples per seconds and the data consisted of the *x*, *y* and *z* directions of the accelerometer's axes contained in 3 columns with each column containing 1800 samples of recording i.e., 30 seconds recording at 60 samples per second. The data were transmitted wirelessly and stored in the hard disk of the laptop computer for further processing.

7.2.4. Data processing and analysis

The sampling interval $T = \frac{1}{f_s}$, where f_s is the sampling frequency. The sampling frequency of the device was 60 samples per second. Filtering of the recorded accelerometer signals were performed using a 4th order low pass Butterworth filter with cut-off frequency of 4 Hz to remove the unwanted frequency components that could have obscured the analysis. For further analysis, the signal was converted to the units of accelerations in g = 9.8 ms^{-2} by dividing the signal by the sensitivity scale factor. In this study, a full-scale range of ±2 g corresponding to a sensitivity scale factor of 16,384 least significant bit/g was used. A lower full-scale range was used such that the highest sensitivity is obtained that is capable of measuring the small changes in postural sway associated to healthy adults. The tri-axial accelerations (a_x, a_y and a_z) obtained were converted into directional cosines: cos α and cos β using Equation (5.5). Similarly, after the integration of the gyroscope signal to obtain the angle in degrees from the *x* and *y* axes i.e. pitch and roll angles, the angles were filtered using the high pass Butterworth equivalent of the filter used for the accelerometer signal. The angles from the accelerometer (α and β) were combined to that of the gyroscope (roll and pitch) complementarily using Equation (5.15) with the parameter (a) set to 0.7049 for a cut-off frequency of 4Hz. The result of the filtering is shown in appendix 7.

Using Equation (5.7), the sway positions on ground in the *x* and *y* directions, d_x and d_y were obtained. Time domain measures in the ML and AP directions associated to positions,

velocities and accelerations were obtained using Equations (5.16) to (5.24) above. The measures include the ranges of the displacements ($RangeD_z$), velocities ($RangeV_z$) and accelerations ($RangeA_z$), the averages of the displacements ($D_{z_{av}}$), velocities ($V_{z_{av}}$) and accelerations ($A_{z_{av}}$), and the root mean square (RMS) of the displacements ($D_{z_{RMS}}$), velocities ($V_{z_{RMS}}$) and accelerations ($A_{z_{RMS}}$), where the subscript z can be substituted for either ML or AP, depending on the direction under consideration. The units of position, velocity and acceleration are: cm, $\mathrm{cm/s}$, $\mathrm{cm/s^2}$ respectively.

PCA was applied to these time domain features obtained from the 4 conditions associated with the mCTSIB. Utilizing PCA, the structural relationships (patterns) of each condition were examined and compared based on their similarities and dissimilarities observed from their correlated matrices. Condition one was considered as the reference since it represents the sway information with all balance-related sensory systems unaffected. The Bland and Altman's analysis was used to further investigate the magnitudes of the relationships. For ease of reference, the conditions were represented by their respective acronyms, where GEO represented standing on the ground surface with the eyes open (condition one), GEC represented standing on the ground surface with the eyes closed (condition two), FEO represented standing on a sponge surface with the eyes open and FEC represented standing on a sponge surface with the eyes closed. For the purpose of analysis, a linear relationship was assumed between the 4 conditions. However, their interaction may not necessary be linear in nature. The Shapiro-Wilk test was used for normality testing to determine the distribution of the data. The mean or median based Levene's tests was used when the data met the criteria of normality or not. Analysis of significant differences were conducted based on the one-way analysis of variance (ANOVA) when the condition of normality and homogeneity of variance was met otherwise the Friedman's test was used. Post hoc analysis was carried out using the Wilcoxon signed rank test when the condition of symmetry was satisfied otherwise the Sign test was used.

7.3. Results and discussion

The results for the displacement (cm), velocity ($\mathrm{cm/s}$) and acceleration ($\mathrm{cm/s^2}$) of the sway of a subject involved in the performance of the four conditions of the mCTSIB are shown in Figure 7.2. Indicated by visual inspection of the variables, there was a greater sway in the ML direction as compared to the sway in the AP direction for conditions one and two. In contrast, although the displacement for conditions three and four appeared to have shown greater sway

occurring towards the ML direction, the velocity and acceleration showed otherwise i.e. greater sway occurring in the AP direction as compared to the ML direction. Notwithstanding, the displacement variable may not be an accurate estimator of sway information as it indicates displacements with respect to the origin.

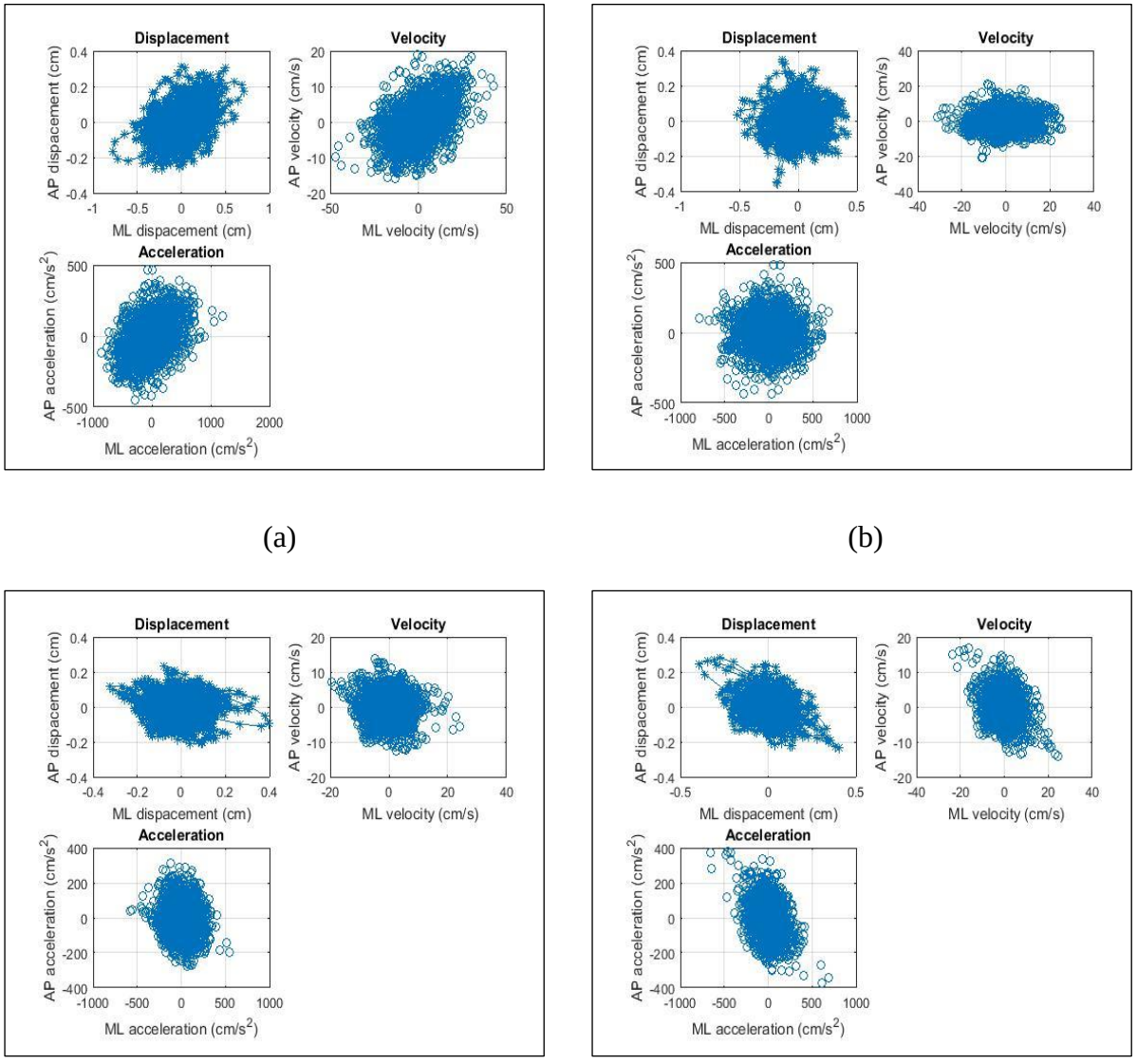

Figure 7.2. A subject's representation of the sway variables of displacement, velocity and acceleration for the four conditions ((a) - (d)) of the mCTSIB (Ojie & Saatchi, 2020)

Eighteen variables from each subject were obtained from the above three variables i.e. displacement, velocity and acceleration and processed using PCA. The scree plots from the application of PCA to the variables are shown in Figure 7.3. This plot assists in determining the number of principal components (PCs) that provide great majority of the variance of the

original data. The selection point is where the plot has its knee. The components utilised for analysis were those with eigenvalues above the knee of the plot. Three components were extracted considering the plot. The variance represented by each component i.e., PC1, PC2 and PC3 for the conditions were: condition one, 67.7%, 14.1%, and 9.1%; condition two, 65.9%, 14.3%, and 9.2%; condition three, 60.9%, 18.3%, and 9. 4% and condition 4, 69.1%, 11.4% and 10.4% respectively.

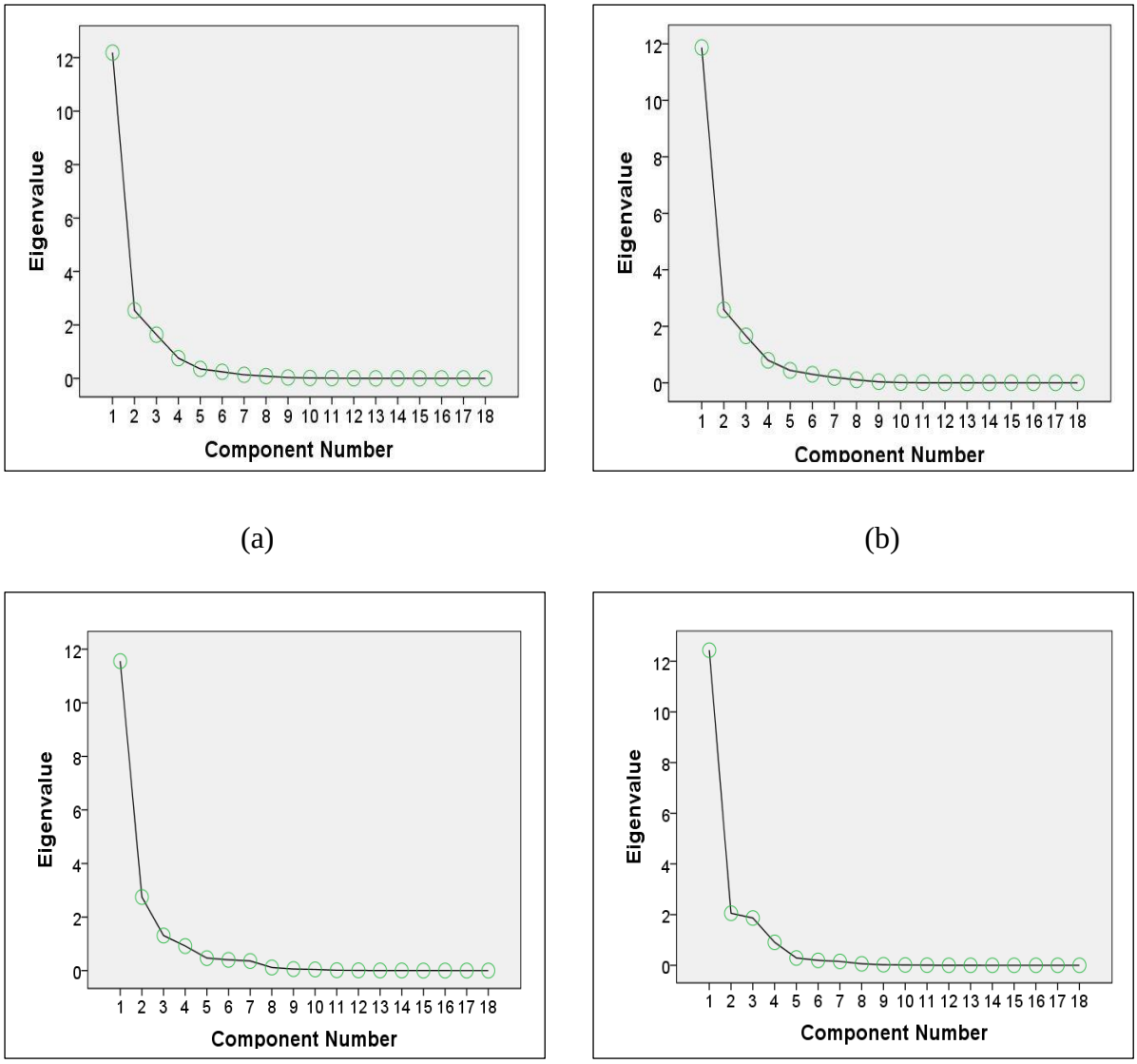

Figure 7.3. The scree plots showing the 18 principal components: (a) condition one, (b) condition two, (c) condition three and (d) condition four of mCTSIB (Ojie & Saatchi, 2020)

7.3.1. Comparison between conditions one (GEO) and two (GEC)

Table 7.1, shows the rotated component matrices for the mCTSIB conditions for the eighteen variables for conditions one and two.

Table 7.1. Rotated component matrix for conditions one and two (Ojie & Saatchi, 2020)

mCTSIB							
		Condition 1			Condition 2		
Number	**Variables**	PC1	PC2	PC3	PC1	PC2	PC3
1	$\mathrm{RangeD_{ML}}$	0.780	0.503	-0.064	0.661	0.661	0.097
2	$\mathrm{RangeD_{AP}}$	-0.114	-0.081	0.857	-0.102	0.794	0.327
3	$\mathrm{RangeV_{ML}}$	0.843	0.399	-0.222	0.700	0.632	0.174
4	$\mathrm{RangeV_{AP}}$	0.175	0.934	-0.096	0.241	0.892	0.240
5	$\mathrm{RangeA_{ML}}$	0.774	0.541	-0.199	0.701	0.614	0.180
6	$\mathrm{RangeA_{AP}}$	0.172	0.946	-0.100	0.372	0.798	0.348
7	$\mathrm{D_{ML_{av}}}$	0.459	0.693	-0.050	0.739	-0.224	0.476
8	$\mathrm{D_{AP_{av}}}$	-0.163	-0.050	0.956	0.071	0.317	0.897
9	$\mathrm{V_{ML_{av}}}$	0.946	0.258	-0.163	0.938	0.238	0.043
10	$\mathrm{V_{AP_{av}}}$	0.609	0.733	-0.070	0.620	0.419	0.596
11	$\mathrm{A_{ML_{av}}}$	0.921	0.336	-0.169	0.946	0.215	0.126
12	$\mathrm{A_{AP_{av}}}$	0.461	0.866	-0.056	0.657	0.274	0.573
13	$\mathrm{D_{ML_{RMS}}}$	0.491	0.689	-0.047	0.767	-0.166	0.466
14	$\mathrm{D_{AP_{RMS}}}$	-0.180	-0.081	.0962	0.060	0.358	0.890
15	$\mathrm{V_{ML_{RMS}}}$	0.941	0.278	-0.165	0.918	0.346	0.027
16	$\mathrm{V_{AP_{RMS}}}$	0.586	0.757	-0.088	0.561	0.576	0.533
17	$\mathrm{A_{ML_{RMS}}}$	0.911	0.363	-0.169	0.933	0.296	0.121
18	$\mathrm{A_{AP_{RMS}}}$	0.449	0.876	-0.071	0.628	0.374	0.564

Thirteen variables in the ML and AP directions were correlated with the first principal component (PC1), with 0.4 utilised as the threshold for minimal correlation significance. As a result of their high correlations, the first principal component was considered as the representative of the variations in the ML directions i.e. the range of the position (RangeD_{ML}), velocity (RangeV_{ML}), and acceleration (RangeA_{ML}), the root mean square (RMS) of the velocity ($\mathrm{V_{ML_{RMS}}}$) and acceleration ($\mathrm{A_{ML_{RMS}}}$), the average velocity ($\mathrm{V_{ML_{av}}}$) and acceleration ($\mathrm{A_{ML_{av}}}$).

The second principal component (PC2) was observed to be correlated with nine variables in the ML and AP directions, i.e. the range of the displacement (RangeD_{ML}), acceleration (RangeA_{ML}) and the RMS displacement in the ML direction ($\mathrm{D_{ML_{RMS}}}$), the range of the velocity (RangeV_{AP}) and acceleration (RangeA_{AP}) in the AP direction, the average

displacement in the ML direction ($D_{ML_{av}}$), the average velocity ($V_{AP_{av}}$) and acceleration ($A_{AP_{av}}$), the RMS velocity ($V_{AP_{RMS}}$) and acceleration ($A_{AP_{RMS}}$) in the AP direction. Since PC2 is correlated most strongly with the variables in the AP direction, it may be considered as a representative of the variation in the AP direction. Similarly, the third principal component (PC3) was a representative of the variation in the AP direction using similar deduction.

Condition one of the mCTSIB comprises of all balance related sensory systems and as such it was considered as the reference since it is expected to produce the lowest amount of sway due to the presence of all the sensory systems. The underlying structural relationships were examined based on the correlation differences across the conditions. Similar correlation across the conditions indicates structural similarities. One component may be sufficient for analysis since the variables were rotated. The first principal component represented the highest amount of variance across the conditions and as such the comparisons of its loadings/correlations across the conditions are used for analysis. The variables whose correlation ranges appeared to be similar with respect to PC1 across both conditions i.e. range of 0.461 to 0.609 for $A_{AP_{av}}$ and $V_{AP_{av}}$, range of 0.459 to 0.491 for $D_{ML_{RMS}}$ and $D_{ML_{av}}$, range of -0.114 to -0.180 for the $\text{Range}D_{AP}$, $D_{AP_{av}}$, and $D_{AP_{RMS}}$, range of 0.172 to 0.175 for $\text{Range}A_{AP}$ and $\text{Range}V_{AP}$, range of 0.911 to 0.946 for $V_{ML_{av}}$, $A_{ML_{av}}$, $V_{ML_{RMS}}$, and $A_{ML_{RMS}}$, range of 0.449 to 0.586 for $V_{AP_{RMS}}$ and $V_{AP_{RMS}}$, and range of 0.774 to 0.843 for $\text{Range}D_{ML}$, $\text{Range}V_{ML}$, and $\text{Range}A_{ML}$ among subjects showed less variations in their standardised equivalents and as such had closely related correlations.

The additional variables that showed significant loadings for condition two of the mCTSIB in respect to PC1 are: average displacement ($D_{ML_{av}}$) and root mean square displacement ($D_{ML_{RMS}}$) in the ML direction, average acceleration ($A_{AP_{av}}$) and root mean square acceleration ($A_{AP_{RMS}}$) in the AP direction. The variables that loaded with PC2 include the range of the displacement ($\text{Range}D_{AP}$) in the AP direction and the range of the velocity in the ML direction ($\text{Range}V_{ML}$). For PC3, the variables that loaded with it were the average velocity and acceleration ($V_{AP_{av}}$and $A_{AP_{av}}$) and the RMS acceleration ($A_{AP_{RMS}}$) in the AP direction. Based on their correlations, PC1 describes the sway in the ML direction, PC2 and PC3 describes the sway in the AP direction. Significant changes occurred in the loading of the variables in the AP direction of conditions one and two in comparison to the variables of the

ML direction. This was an indication of the effectiveness of the AP direction to represent the absence of the sensory information, in this case the visual system. However, due to the small changes in the correlations between conditions one and two, a close relationship between the conditions can be inferred. Thus, a close relationship in terms of sway exist in the conditions where the subjects were standing on a firm surface i.e., conditions one and two.

The first principal component described the sway in the ML direction, while the second and third were defined by the AP direction, based on the strongest correlations. More changes in the loadings of a number of variables were observed mainly in the AP direction in the first and third principal components. This indicated the effectiveness of the AP direction to capture the sensory information of the visual system and highlighted an underlying difference in structure. Nonetheless, the component matrix represents the underlying structure of the variables in the dataset and does not represent the magnitude. That is variables may have similar correlation coefficients in the component matrix and have differing magnitudes. As a result, further investigations into the variables were carried out using the Bland and Altman plot. For simplicity, the RMS velocity was selected and used for further investigations based on its strong correlations with other variables in both the ML and AP direction and its sensitivity to sensory information. The similarities between the ML and AP directions for conditions one and two are shown by the Bland and Altman's plot of Figures 7.4 (a) and (b).

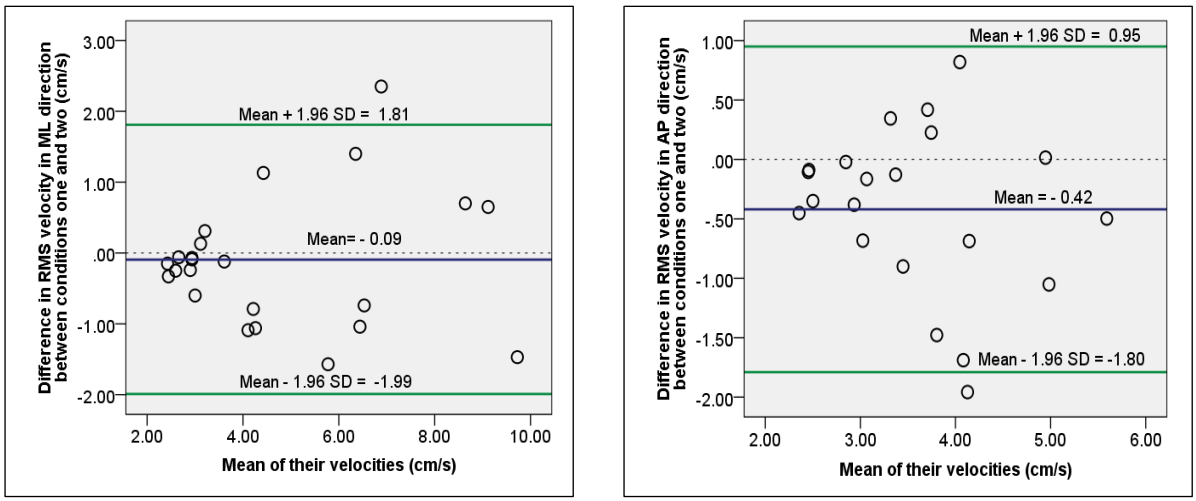

(a) (b)

Figure 7.4. Bland and Altman plot of the correlations of variables of the RMS velocity for conditions 1 and 2 (a) mediolateral direction and (b) anterior posterior direction (Ojie & Saatchi, 2020)

The vertical axis represents the differences between the conditions and the horizontal axis represents their means. The smaller the mean difference between the variables of the respective direction i.e., the RMS velocity in the ML and AP directions, the greater the similarity and the lesser the sensitivity of the direction. In this case, the mean difference of the RMS velocity between the ML direction of the two conditions were smaller than that of the AP direction highlighting that the ML direction was less sensitive to the changes in sway introduced by the exclusion of the visual system. The ML direction showed no consistency of bias as there were roughly equally distributed points above and below the zero line as compared to the bias consistency of the AP direction. Thus, the ML direction suggested with less certainty that the sway obtained from both conditions were different. In contrast, the AP direction suggested that more sway difference was observed between the two conditions and that the sway in condition two of the mCTSIB was more than that in condition one. The negative value of the mean difference is an indication that the sway in condition one is less than the sway in condition two by its respective values i.e., 0.09 cm/s for the ML direction and 0.42 cm/s for the AP direction. The range of the limits of agreement indicates the amount of variation between the directions. A greater variation was observed in the sway obtained from the ML direction (3.80 cm/s) in comparison to that obtained from the AP direction (2.75 cm/s). This was an indication of a lower agreement between the sway information obtained from the ML direction as compared to that of the AP direction. Comparing the ratio of their means, the AP direction was 4.67 times greater than that of the ML direction indicating a greater sway occurred in the AP direction as compared to that observed in the ML direction.

7.3.2. Comparison between conditions one (GEO) and three (FEO)

The result of the rotated component matrix for the conditions one and three of the mCTSIB is shown in Table 7.2. The correlated variables in condition three shown in Table 7.2 are similar to those observed in conditions one and two as indicated by Table 7.1. However, the correlations in the AP direction were observed to be stronger as compared to those of the previous conditions i.e., conditions one and two. This indicated more structural changes in the variation of the sway between both conditions one and two respectively. The ML direction showed smaller changes in the correlated variables between the two previous conditions and in comparison, to those observed in the AP direction. The first principal component (PC1) was strongly correlated with both the sway variables of the ML and AP directions. The strong correlation of the variables was due to their pattern of variation rather than the magnitudes as

the variables were all standardised. The variables in the AP direction correlated strongly with the second and third principal component (PC2 and PC3) suggesting close similarities to condition one. The percentage variation represented by PC1 was highest (60.87%) among the principal components and as such its comparison across both conditions was considered. Utilizing the correlation of its ML and AP variables for analysis, a greater variation can be observed in the AP direction as compared to the ML direction and as such the AP direction indicates more sensitivity to the presence/absence of the sensory input information from the proprioceptive system.

Table 7.2. Rotated component matrix for conditions one and three (Ojie & Saatchi, 2020)

mCTSIB Conditions							
		Condition 1			**Condition 3**		
Number	**Variables**	**PC1**	**PC2**	**PC3**	**PC1**	**PC2**	**PC3**
1	$\mathrm{RangeD_{ML}}$	0.780	0.503	-0.064	0.568	0.220	-0.002
2	$\mathrm{RangeD_{AP}}$	-0.114	-0.081	0.857	0.396	0.173	0.834
3	$\mathrm{RangeV_{ML}}$	0.843	0.399	-0.222	0.694	0.669	0.065
4	$\mathrm{RangeV_{AP}}$	0.175	0.934	-0.096	0.284	0.880	0.230
5	$\mathrm{RangeA_{ML}}$	0.774	0.541	-0.199	0.634	0.719	0.099
6	$\mathrm{RangeA_{AP}}$	0.172	0.946	-0.100	0.331	0.885	0.203
7	$\mathrm{D_{ML_{av}}}$	0.459	0.693	-0.050	0.049	0.171	0.167
8	$\mathrm{D_{AP_{av}}}$	-0.163	-0.050	.0956	-0.117	0.143	0.964
9	$\mathrm{V_{ML_{av}}}$	0.946	0.258	-0.163	0.955	0.208	-0.071
10	$\mathrm{V_{AP_{av}}}$	0.609	0.733	-0.070	0.960	0.139	0.123
11	$\mathrm{A_{ML_{av}}}$	0.921	0.336	-0.169	0.963	0.205	-0.078
12	$\mathrm{A_{AP_{av}}}$	0.461	0.866	-0.056	0.965	0.116	0.096
13	$\mathrm{D_{ML_{RMS}}}$	0.491	0.689	-0.047	0.097	0.156	0.158
14	$\mathrm{D_{AP_{RMS}}}$	-0.180	-0.081	0.962	-0.085	0.099	0.978
15	$\mathrm{V_{ML_{RMS}}}$	0.941	0.278	-0.165	0.939	0.266	-0.055
16	$\mathrm{V_{AP_{RMS}}}$	0.586	0.757	-0.088	0.857	0.416	0.180
17	$\mathrm{A_{ML_{RMS}}}$	0.911	0.363	-0.169	0.942	0.292	-0.055
18	$\mathrm{A_{AP_{RMS}}}$	0.449	0.876	-0.071	0.881	0.388	0.149

The Bland and Altman's plots for comparing the RMS velocities between conditions one and three in the ML and AP directions are shown in Figures 7.5 (a) and 7.5 (b).

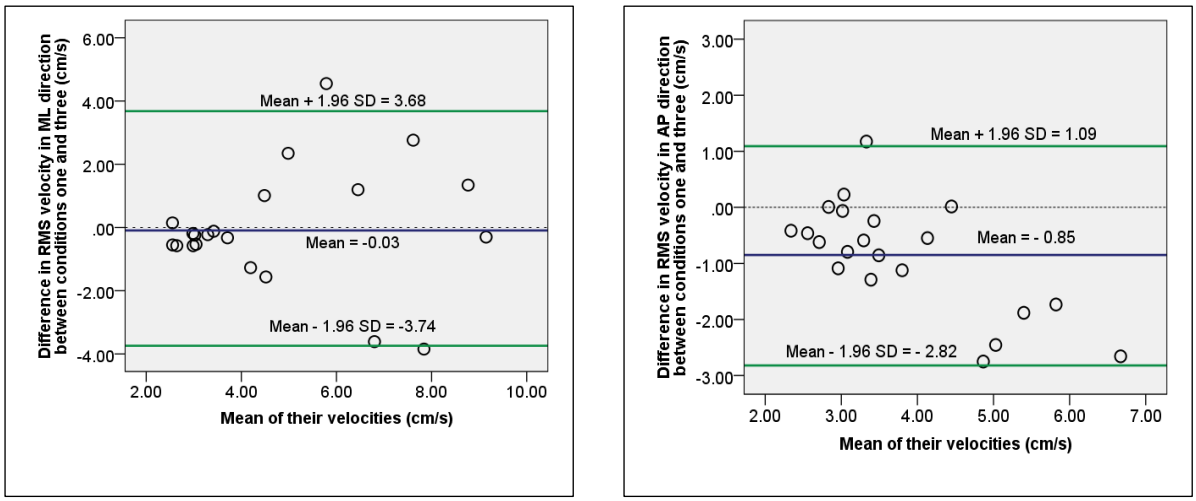

(a) (b)

Figure 7.5. Bland and Altman plots of the correlations of variables with their components for (a) condition one (GEO) and (b) condition three (FEO) (Ojie & Saatchi, 2020)

The vertical axis represents the differences between the two corresponding variables and the horizontal axis shows their respective means. Greater similarities were observed between the ML direction as compared to the AP direction as its mean difference (0.03 cm/s) was smaller than that of the AP direction (0.85 cm/s). Taking the ratio of their means for comparison, the ML direction was 28.33 times less than that of the AP direction.

Similar to the result of conditions one and two above, the ML direction showed a smaller bias consistency between the conditions indicative of the points being evenly distributed above and below the zero line (indicated with the thin dash lines). Thus, presenting less demarcation that the sway in condition one was less than the sway in condition three.

As indicated by the range of the limits of agreement, there existed a larger variation in the ML direction (7.42 cm/s) as compared to that of the AP direction (3.91 cm/s). The comparison of the mean differences of the AP direction across conditions one and two (0.42 cm/s), and conditions one and three (0.85 cm/s) showed that the vestibular system had a greater interaction with the proprioceptive system as compared to its interaction with the visual system in maintaining standstill balance. Similarly, based on the range of the limits of agreement there appeared to be more coherence in the proprioceptive system (2.75 cm/s) as

compared to the visual system (3.91 cm/s) as indicated by the interaction of conditions one and two, and conditions one and three respectively.

7.3.3 Comparisons between conditions one and four of the mCTSIB

The sensory system under consideration in condition four of the mCTSIB test is the vestibular system. Its rotated component matrix shown in Table 7.3 indicates greater differences in structure (indicated by the correlation coefficients of the variables that loaded with the components) as compared to the mCTSIB conditions two and three in relation to condition one. However, correlations of the variables in the ML direction of the first principal component appeared to indicate small changes, thus suggesting a similar structure exist between the conditions. This indicated that the ML direction may be less sensitive to the contribution of the vestibular sensory system.

Table 7.3. Rotated component matrix for mCTSIB's conditions one and four (Ojie & Saatchi, 2020)

mCTSIB Conditions							
		Condition 1			Condition 4		
Number	Variables	PC1	PC2	PC3	PC1	PC2	PC3
1	$RangeD_{ML}$	0.780	0.503	-0.064	0.657	0.627	0.145
2	$RangeD_{AP}$	-0.114	-0.081	0.857	0.484	0.356	0.582
3	$RangeV_{ML}$	0.843	0.399	-0.222	0.850	0.294	0.275
4	$RangeV_{AP}$	0.175	0.934	-0.096	0.825	0.216	0.232
5	$RangeA_{ML}$	0.774	0.541	-0.199	0.880	0.260	0.190
6	$RangeA_{AP}$	0.172	0.946	-0.100	0.838	0.153	0.166
7	$D_{ML_{av}}$	0.459	0.693	-0.050	0.143	0.977	0.051
8	$D_{AP_{av}}$	-0.163	-0.050	0.956	0.123	0.018	0.972
9	$V_{ML_{av}}$	0.946	0.258	-0.163	0.934	0.262	0.141
10	$V_{AP_{av}}$	0.609	0.733	-0.070	0.950	0.104	0.106
11	$A_{ML_{av}}$	0.921	0.336	-0.169	0.946	0.194	0.139
12	$A_{AP_{av}}$	0.461	0.866	-0.056	0.976	0.054	0.057
13	$D_{ML_{RMS}}$	0.491	0.689	-0.047	0.191	0.972	0.068
14	$D_{AP_{RMS}}$	-0.180	-0.081	0.962	0.146	0.048	0.981
15	$V_{ML_{RMS}}$	0.941	0.278	-0.165	0.923	0.269	0.173
16	$V_{AP_{RMS}}$	0.586	0.757	-0.088	0.951	0.125	0.153
17	$A_{ML_{RMS}}$	0.911	0.363	-0.169	0.939	0.196	0.152
18	$A_{AP_{RMS}}$	0.449	0.876	-0.071	0.977	0.072	0.085

The similarities/dissimilarities of the ML and AP directions for RMS velocities between conditions four and one are shown by the Bland and Altman's plots of Figures 7.6 (a) and (b).

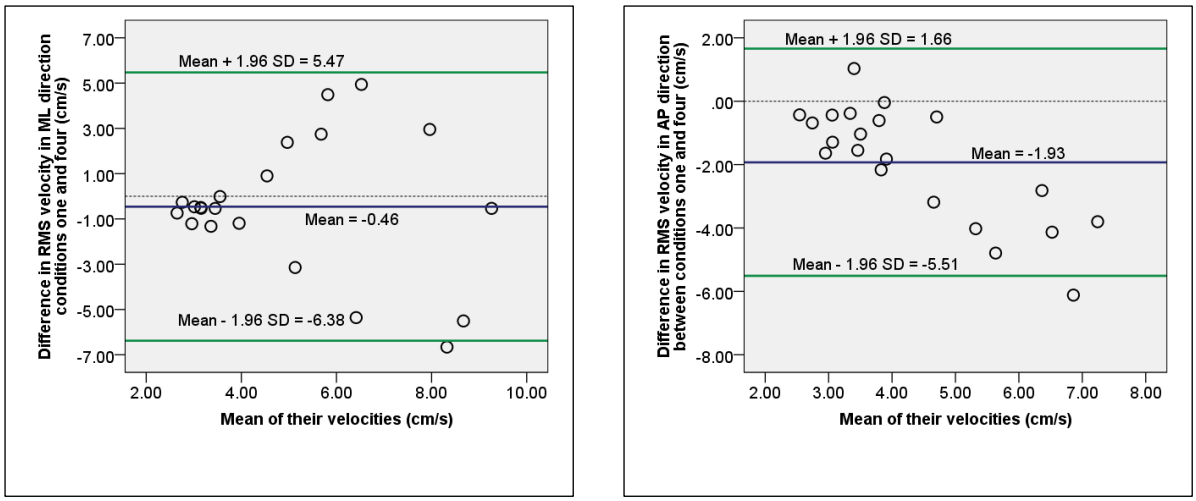

(a) (b)

Figure 7.6. Bland and Altman plots of the correlations of variables with their components for (a) the mCTSIB condition one (GEO) and (b) the mCTSIB condition four (FEC) (Ojie & Saatchi, 2020)

The ML direction showed greater similarity as compared to the AP direction as indicated by their respective mean differences of 0.46 cm/s and 1.93 cm/s. This suggested that the ML direction was less sensitive in differentiating the sway between the two conditions and may produce less information concerning the performance of the vestibular system in comparison to the AP direction. Comparing the ratio of their mean differences, the ML direction was approximately 4.20 times lower in magnitude than that of the AP direction, suggesting a greater sway occurred in the AP direction as compared to the ML direction.

The consistency of the bias as indicated by the scattering of the points i.e., above and below the zero line (indicated by the thin dash line), observed in the ML direction was smaller as more points were scattered above and below the zero line in comparison to that obtained in the AP condition. This highlighted with lower certainty as compared to the information of the AP direction that the sway in condition four was greater than that in condition one. The range of the limits of agreement of the ML direction (11.85 cm/s) in comparison to that of the AP direction (7.17 cm/s) suggested that there were more variations in the ML direction as compared to the AP direction. Based on the analysis of all the sensory systems, the vestibular system in comparison with the proprioceptive and visual systems showed smaller coherence of sway across the subjects as indicated by the range of the limits of agreement (7.17 cm/s). The less coherence of the vestibular system shows that even among healthy subjects, the

performance of the vestibular system to balance varies and that this incoherence should be taken into consideration when comparing vestibular functions.

The median and interquartile ranges of the RMS velocities for the four conditions of the mCTSIB are shown in Table 7.4. Considering the AP direction, the values of the medians and the interquartile ranges (IQR) are in ascending order of magnitude from conditions one to four. The IQR indicated that a closely related characteristics of sway were exhibited by subjects in condition one as compared to the other three conditions of the mCTSIB. Similarly, condition two had less variations as compared to condition three, with the greatest variation observed in condition four of the mCTSIB.

Table 7.4. The median and interquartile range (IQR) of the RMS velocity in ML and AP conditions of the mCTSIB (Ojie & Saatchi, 2020).

Conditions of the modified clinical test for sensory interaction with balance (mCTSIB)	**RMS velocity in the ML direction**		**RMS velocity in the AP direction**	
	Median	**IQR**	**Median**	**IQR**
Condition one (all balance-related sensory systems)	3.56	3.77	3.15	1.18
Condition two (proprioceptive and vestibular systems)	3.86	3.73	3.50	1.74
Condition three (visual and vestibular systems)	3.81	2.84	3.59	2.37
Condition four (vestibular systems)	4.02	3.11	4.24	3.93

The median based Levene's test showed homogeneity of variance for the ML direction ($F(3,80) = 0.066$, $p = 0.978$) across the conditions of the mCTSIB test. In contrast the result of the median based Levene's test for the AP direction showed heterogeneity of variance across all conditions ($F(3,80) = 3.61$, $p = 0.017$). The test of statistically significant difference using the Friedman test across the four conditions of the mCTSIB showed that no statistically significant difference existed for the ML direction ($x^2(3) = 6.52, p > 0.05$) while for the AP direction, the result showed that a significant difference existed ($x^2(3) = 32.71, p < 0.01$). This highlighted that the ML direction was less sensitive to postural sway in comparison to the AP directions.

Using the Sign Test, Post hoc analysis was conducted between the paired conditions (i.e., conditions 1 and 2, 1 and 3, 1 and 4, 2 and 3, 2 and 4, 3 and 4) using the RMS velocities in the AP direction. The Bonferroni correction was used, resulting in a significant level that was

set at $p < 0.0083$ ($\alpha = \frac{0.05}{6} = 0.0083$) for significance. The result for the median (IQR) for the four conditions were 3.15 (2.71 to 3.89), 3.50 (2.99 to 4.73), 3.59 (2.97 to 5.34) and 4.24 (3.62 to 7.55) respectively. The result of the Sign test showed no significant difference for the paired conditions of one and two ($p = 0.027$), and two and three ($p = 0.383$). However, the Sign test showed significant differences for the paired conditions of one and three ($p = 0.007$), one and four ($p < 0.001$), two and four ($p < 0.001$) and three and four ($p = 0.001$). This indicated that condition one (vestibular, proprioceptive and visual systems) was more similar to condition two (vestibular and the proprioceptive systems) as compared to condition three (vestibular and visual systems) and four (vestibular system) respectively.

7.4. Summary

In this chapter, principal component analysis (PCA) was used to investigate the structural relationship (patterns) between the four conditions of the mCTSIB based on the sway measures obtained from the mediolateral (ML) and anterior-posterior (AP) sway of 21 healthy adult subjects. The measures were obtained from the centre of mass (COM) projected sway in standstill position. Using the root mean square (RMS) measure of the velocity and acceleration, the actual magnitude of the sway from the various directions were investigated using statistical methods such as the Bland and Altman's method and analysis of variance methods to measure their relationship. The results of the study suggested that the interaction of the vestibular system with the proprioceptive system contributed more in maintaining balance in standstill position than the interaction between the vestibular and visual systems. The finding in this study is in agreement with those obtained in Peterka (2002). The findings in Peterka (2002) suggested that healthy adults were more dependent on their proprioceptive system as compared to their visual system in a well-lit environment (Peterka, 2002; Horak 2006).

The AP direction was more sensitive to balance related sensory information than their ML counterparts in a standstill position. The finding in this study is in agreement with those obtained in della Volpe et al. (2006). In their study, they observed that the average centre of pressure (COP) velocity and the RMS of COP in the AP direction was capable of differentiating between patients with chronic lower back pain (CLBP) and healthy subjects. However, no significant difference was observed in the ML direction between the two groups using same measures (della Volpe et al., 2006).

The proprioceptive system, showed less variability across the subjects as compared to the vestibular and visual systems. The findings in this study agreed with similar findings in Fukuoka et al. (2001). In their study, less inter-subjects' variability was observed with the proprioceptive system as compared to the visual and vestibular systems in an upright posture using the ankle strategy (Fukuoka et al., 2001).

The findings of the study could assist in better interpreting accelerometry recorded data obtained using mCTSIB test for diagnosing balance dysfunctions and understanding the operation of the sensory systems.

Chapter 8 Investigation of the interaction of the balance related sensory systems for human balance using Kohonen neural network

8.1. Introduction

Balance maintenance is a joint process of the interaction between the balance related sensory systems and the central nervous system (CNS). The CNS in addition to other activities plays an important role of correctly integrating the information from these sensory systems i.e., visual, proprioceptive and vestibular systems (Peterka., 2002). The balance related sensory systems act as sensors in providing the necessary information pertaining to its specific functionality towards maintaining balance (Ojie & Saatchi, 2021). For example, information of visual cues are provided by the visual system (Assländer et al., 2015); information of the position and movement of the limbs and trunk are provided by the proprioceptive system (Proske & Gandevia, 2012); information of the acceleration of the head and spatial orientation are provided by the vestibular system (Zalewski, 2015).

To examine these systems, clinicians commonly use a standstill balance test called the modified clinical test of sensory interaction and balance (mCTSIB) (Wrisley & Whitney, 2004; Cohen et al., 2019). In balance analysis, sway from these systems are usually represented in the medio-lateral (ML) and anterior-posterior (AP) directions. These directions contain information that are necessary in understanding the behavioural patterns inherent to the sensory systems. Most studies have utilised these directions in conducting postural sway analysis. Roh et al. (2021) investigated the differences in postural control between healthy young and old people under various four gaze tasks (fixation, saccade, pursuit, and vestibular-ocular reflex) using their COP mean sway amplitude in the ML and AP directions. The result suggested that postural sway significantly reduces with saccade eye movement for both young and old while the vestibular-ocular reflex results in greater postural sway (Roh et al., 2021). Similarly, Shafizadeh et al. (2020) investigated the effect of age and task difficulty on postural sway, variability and complexity among children, young adults and older adults using their respective COP sway displacement in the ML and AP directions. The result showed that children and older adults had greater sway area and complexity and less postural variability in more difficult tasks (Shafizadeh et al., 2020).

In this chapter, Kohonen neural network (KNN) was utilised to investigate the behaviour and contribution of the balance related sensory systems in maintaining balance. The KNN was used to cluster the respective time domain measures in the ML and AP directions of 23 healthy adult

subjects, who were engaged in the mCTSIB. External measures of clustering performances such as purity, precision, recall and F-measure were used to examine the resulting clustering and to analyse their interactions and behaviours of the sensory systems as it pertains to their direction of sway. The results for the parameters of purity, precision, recall and F-measure were higher in the AP direction as compared to the ML direction by 7.12%, 11.64%, 7.12% and 9.5% respectively, with their differences statistically significant ($p < 0.05$). The result obtained showed that the sensory systems mostly affect the AP direction as compared to the ML direction. However, the visual system was more effective in reducing the sway in the ML direction as compared to the proprioceptive system. Similarly, it was observed that the proprioceptive system was more effective in controlling the velocity in the AP direction as compared to the visual system. Also, it was observed that the visual system was more effective in controlling the acceleration in the AP and ML direction and the ML velocity. Thus, the visual system reduces the ML velocity and the acceleration of subjects, while the proprioceptive system reduces the AP velocity of subjects.

8.2. Chapter related methodology

8.2.1. Data collection

Twenty-three healthy adult subjects (10 males and 13 females) with mean (standard deviation) of age, height and weight: 24.5 (4.0) years, 173.6 (6.8) cm, 72.7 (9.9) kg, took part in the study. The subjects were involved in the mCTSIB while the developed accelerometry transmitter device discussed in chapter four was attached to each subject at the approximate position of the illac crest. The subjects stood on a marked white surface to ensure consistency of the distance from the wall and the distance between the feet placement (30 cm apart). Thirty seconds of accelerometry data in the ML and AP directions were obtained. Ethical approval was obtained from the university ethics committee before carrying out the study. A subject with the device attached to his illac crest is shown in Figure 8.1.

Figure 8.1. A subject standing on a marked white surface with the device attached to the position of the illac crest while performing condition two of the mCTSIB test (source: Ojie & Saatchi, 2021)

8.2.2. Data analysis

The analysis of the data was carried out in three stages: (i) conversion of the raw data from the accelerometry device into sway information, (ii) clustering of the sway information and (iii) interpretation of the clustering results to examine the information present in ML and AP sway directions.

8.2.2.1 Extracting sway information from the accelerometry data

The digital outputs (units of least significant bits (LSB)) of the accelerometry data consisted of the accelerations of the tri-axial accelerometer (x, y and z). The digital outputs were divided by the sensitivity scale factor (16384 LSB/g for the full-scale range of 2gs) in units of LSB/g to obtained the accelerations in units of gravity (g = 9.8/m^2). The accelerometer signals were low pass filtered using a Butterworth filter of second order with a cutoff frequency of 4 Hz. The resultant acceleration R, the directional cosines and the ground position in the ML (d_x) and AP (d_y) directions were obtained using Equations (5.1) to (5.3) respectively. Subsequently, the

RMS values of the position, velocity and acceleration were obtained using Equations (7.6) and (7.7) respectively. The RMS measurements were employed due to its effectiveness in sway differentiation across the conditions of the mCTSIB test (Ojie & Saatchi, 2020).

8.2.2.2. Clustering of the postural sway information

Firstly, correlation analysis was conducted on the RMS measures of the position, velocity and acceleration of the ML and AP sway to identify variables with strong correlation. The threshold for highly correlated variables was 0.85 or greater (Vatcheva et al., 2016). Prior to correlation analysis, the Shapiro-Wilk test of normality with significance level set to 0.05 was used to establish whether the data were normally distributed. Kendall's tau correlation was used when the data deviated from normality while Pearson correlation was used otherwise (de Winter et al., 2016). The clustering of the variables consisted of two stages. The two-stage approach has been shown to be computationally more effective (Vesanto & Alhoniemi, 2000). The first stage involved clustering of the uncorrelated variables and forming prototype vectors using KNN with a 10 by 10 neuron in its output layer. A MATLAB® batch algorithm was used to process the data. Clustering analysis was carried out by pairing each of the three conditions of the mCTSIB with condition one as the reference (as condition 1 incorporated all the balance related sensory systems). Three pairs were formed in the clustering process i.e., conditions: 1 and 2, 1 and 3, and 1 and 4. The number of iterations to train KNN was set to 1000 with the default initial neighborhood size of 3 neurons. The training and test sets were the same and consisted of the entire dataset as the aim was to investigate the interactions and not to use the Kohonen network as a data classifier (Ojie & Saatchi, 2021).

The second stage is defined by the use of the K-means algorithm to cluster the prototype vectors formed in the first stage by the KNN clustering of the data. Using the K-means algorithm, the dataset is divided into K clusters such that the within cluster sum of square distance is minimized (Hartigan & Wong, 1979). To carry out the clustering process, the prototype vectors were represented by their centroids and then clustered. The prototype vectors consisted of neurons which contains at least one input data point. The number of clusters (K) was determined by performing K-means clustering of the centroids for thirty times with K varying from 2 to 30, while evaluating the separation between the clusters using the Davies-Bouldin (DB) index. The DB index is an internal evaluation measure used to evaluate cluster separation

by considering the ratio of within to between clusters (Davies & Bouldin, 1979). The equation for calculating the DB index is shown in Equation (8.1).

$$DB = \frac{1}{k}\sum_{i=1}^{k} DB_i\,, \qquad DB_i = maxDB_{ij}, \qquad DB_{ij} = \frac{\sigma_{c_i}+\sigma_{c_j}}{\left\|\mu_{c_i}-\mu_{c_j}\right\|} \tag{8.1}$$

Where μ_{c_i} is mean of cluster c_i, σ_{c_i} is standard deviation of cluster c_i, μ_{c_j} is mean of cluster c_j, σ_{c_j} is standard deviation of cluster c_j, DB_{ij} is an array of DB indices for cluster i with respect to the j^{th} cluster, where i ≠ j, j = i+1:k, DB_i is DB index for the i^{th} cluster. The number of clusters with the minimum DB was used for external evaluation.

The minimum DB index has been suggested not to be the optimal, hence analysis at other local optimal were conducted with the number of clusters (K) used for the clustering selected based on the highest F-measure (Vesanto & Alhoniemi, 2000). It was assumed that the DB index utilised for the clustering between conditions 1 and 4 would be sufficient for other conditions since lesser differences are expected. The built in K-means algorithm in the MATLAB® software was used for the implementation of the K-means clustering and the default distance metric was Euclidean.

8.2.2.3. Clustering performance evaluation

The K means clustering was conducted using the centroids of the prototype vectors obtained from the clustering of the Kohonen neural network. For clustering evaluation, these centroids were replaced by their actual data points. The data points were assigned to their respective class labels corresponding to the four conditions of the mCTSIB. Each cluster was represented by the class label with the majority of the data points present in the cluster and the selected class label could also be a representative of another cluster, if it was dominant in the cluster. The differences between the conditions of the mCTSIB test were examined using external evaluation measures such as purity, precision, recall and F-measure. The purity measure describes how coherent the data points are in the cluster i.e., the singularity of the cluster (Huang, 2008). The greater the purity measure the more the separation and hence the difference between the categories. The precision of a cluster means the same as the purity of the category. The recall measure describes the number of points of the majority partition that is scattered in other clusters. The higher the recall, the more effective the clustering and hence the greater the separation. With the analysis limited to nonempty clusters, the lowest amount of purity is

obtained when all the samples converged to one cluster (Ojie & Saatchi, 2021). Similarly, the lowest precision is obtained when all the data samples are present in a single cluster. The lowest recall is obtained when only one sample is present in the cluster i.e., the recall varies with the number of clusters (Ojie & Saatchi, 2021). In the case of two clusters and equal number of samples, the lowest attainable value for purity, recall and precision is 0.5 respectively (Ojie & Saatchi, 2021). The formulae for these measures are stated in Equations (8.2) to (8.5).

$$purity = \sum_{i=1}^{r} \frac{n_i}{n} purity_i, \quad purity_i = \frac{1}{n_i} \max_{j=1}^{k} \{n_{ij}\} \tag{8.2}$$

$$prec_i = \frac{1}{n_i} \max_{j=1}^{k} \{n_{ij}\} = \frac{n_{ij_i}}{n_i} \tag{8.3}$$

$$recall_i = \frac{n_{ij_i}}{m_{j_i}} \tag{8.4}$$

$$F_i = \frac{2 \times prec_i \times recall_i}{prec_i + recall_i} = \frac{2n_{ij_i}}{n_i + m_{j_i}} \tag{8.5}$$

where n_{ij} is the number of elements of class j in the i^{th} cluster, n_i is the total number of elements in the i^{th} cluster, n is the total number of elements of the dataset, $purity_i$ is the i^{th} purity of the clustering. n_{ij_i} is the maximum elements of the classes in the i^{th} cluster, $prec_i$ is the i^{th} precision. m_{j_i} is the number of elements of the resulting maximum j^{th} class of the i^{th} cluster, $recall_i$ is the recall of the i^{th} cluster. The F-measure of the clustering was obtained by taking the average over all the clusters as shown in Equation (8.6).

$$F = \frac{1}{r} \sum_{i=1}^{r} F_i \tag{8.6}$$

F_i is the F-measure of the i^{th} cluster. For more details about these measures see Zaki & Meira (2020).

Clustering was carried out 30 times to ensure the reliability of the result and was stoped at 30 as no changes were observed above 30 repetitions. The corresponding external measures were recorded and utilised for further analysis. Statistical test of significance was performed to determine whether or not the result of the external measures was significantly different between the clustering. Independent sample t-test or Mann-Whitney U test was used depending on the result of test of normality. The analysis packages used for clustering and statistical analysis consisted of MATLAB® (version 2021a) and SPSS® (version 24) respectively.

8.3. Results and Discussion

8.3.1 Correlation results and determination of the number of clusters

The correlation results between the variables using the weight planes of the KNN are shown in Figure 8.2.

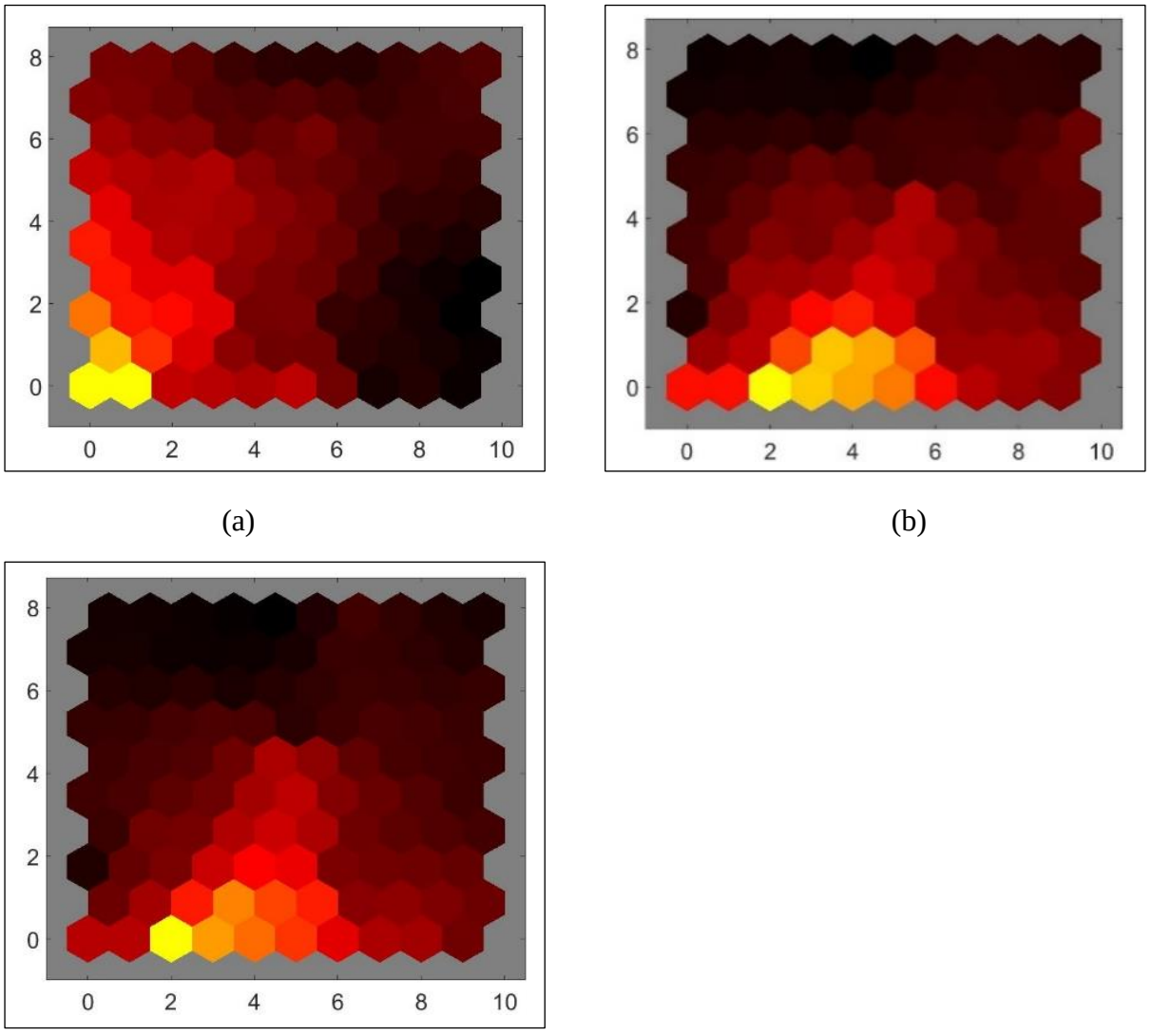

Figure 8.2. Weight planes showing the correlation between the variables. (a) RMS position, (b) RMS velocity, and (c) RMS acceleration respectively. The neuron positions are indicated on the horizontal and vertical axes, with closely related patterns indicating strong correlations (Ojie & Saatchi, 2021).

The most negative connections are represneted by the black colours, the strongest positive connections are represented by the yellow colours and the red colours represented no connections between the input of the neurons. Utilizing KNN, the weights planes are used as indication of correlations between the variables, where strong correlations are indicative of closely related patterns. Strong correlations can be observed between the RMS velocity and acceleration as indicated by their closely related colors. The distribution of each variable was determined using the Shapiro-Wilk test with p-value set to 5%. The test indicated that the variables were not a representative of a normal distribution *($p < 0.05$)*. As a result, correlation analysis was conducted using the Kendall's tau correlation and the result showed a significantly strong positive correlation between the RMS velocity and RMS acceleration (r_τ (21) = 0.929, $p < 0.01$). The correlation between the RMS displacement and RMS velocity showed a significantly weak correlation *(r_τ (21) = 0.344, p = 0.022)*. Similarly, a weak significant positive correlation was observed between the variables of RMS displacement and RMS acceleration *(r_τ (21) = 0.32, p = 0.032)*. Thus several analysis of the clustering relationship was carried out using the variables of RMS displacement and RMS velocity, RMS displacement and RMS acceleration.

The application of the K- means clustering requires the determination of the number of clusters (K). The clustering between conditions 1 and 4 were evaluated using the Davies Boulding (DB) index to determine the number of clusters required for the K-means algorithm. The lower the DB index the better the clustering. The clustering of conditions 1 and 4 was used as the reference because the greatest disparity was expected in these conditions. The results of the DB index for clusters K = 2 to 30 are plotted in Figure 8.3. Figure 8.3 illustrates the averages of 30 repetitions for the clustering with K = 2 to be lowest, although other local minima can be seen to exist at K = 4 and 9. Futhermore, the F-measure was used to determine which cluster K=2, 4 and 9 was most effective. The F-measure was used since it represents the weighted harmonic mean between the recall and the precision.

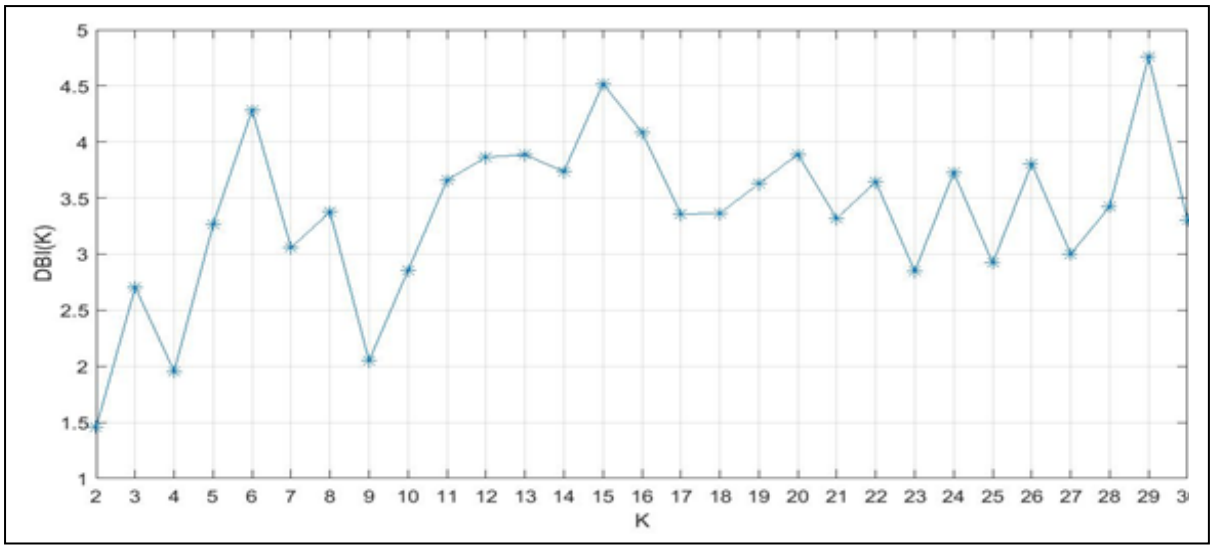

Figure 8.3. Davies-Boulding (DB) index values for clusters K, showing K = 2 as the minimum (Ojie & Saatchi, 2021)

The clustering was repeated 30 times each for the number of clusters (K) equals to 2, 4 and 9, to ensure the reliability of the result, and the F-measure was obtained for each repetition. The mean F-measure for 30 repetitions for the number of clusters (K) equal to 2, 4, and 9 were 0.717, 0.448, and 0.249 respectively for the AP direction. Similarly, for the ML direction, the result of the mean F-measure for 30 repetitions for the number of clusters (K) equal to 2, 4, and 9 were 0.532, 0.356, and 0.246 respectively. Since the F-measure for the number of cluster (K) equal to 2 was higher, subsequent clustering of the K-means were based on two clusters.

8.3.2. Clustering results

8.3.2.1. Conditions 1 and 2

8.3.2.1.1. Clustering using the RMS displacement and acceleration as inputs

Condtion 2 refers to exclusion of the visual system during the balance test. The clustering using the displacement and acceleration variables was carried out due to no strong correlation between the variables as indicated above in section 8.3.1. The number of iteration was set to 1000 and the neighboorhood size was 3 neruon. The result of the clustering using the displacment and acceleration variables for conditions 1 and 2 for both the AP and ML directions are shown in Figure 8.4.

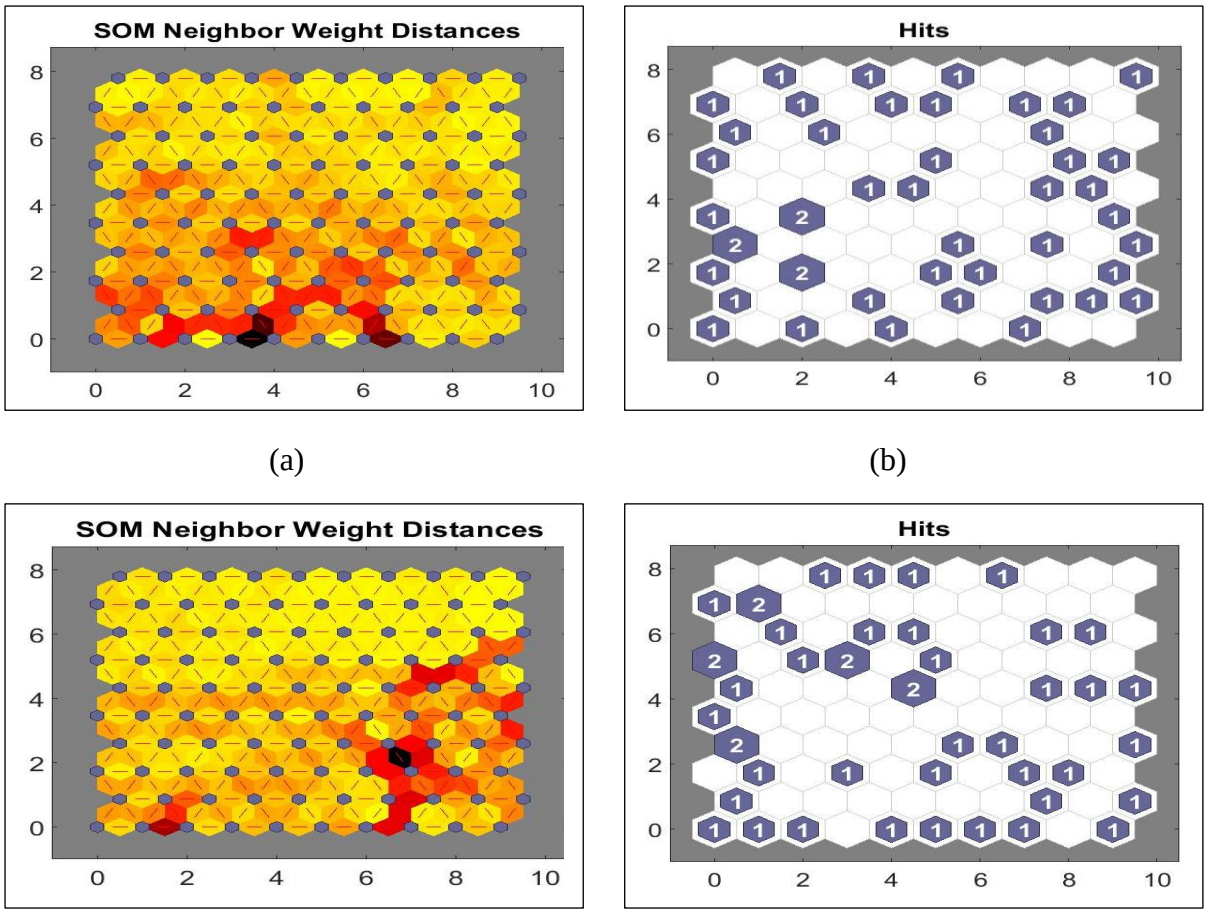

Figure 8.4. Plot of neighbourhood distance and input vector hits of conditions 1 and 2. (a, b) representing the AP direction, (c,d) representing the ML direction. The positions of the neurons are represented by the horizontal and vertical axes.

The map of the neighborhood distance plot of the AP direction suggested a low level of coarseness at the bottom left with a brighter section seen at the top left, top right, and bottom right. As indicated by the input plane, the data samples bounded by the coarse sections of the neighbourhood map are small (approximately 10 data points) in comparirson to the data samples at the finer sections of the map. The brighter/finer sections indicate close similarities among the data points and as such a close similarity between the two conditions is noticeable in the AP direction. The data sample consisted of 46 data points of which 23 data points belong to each condition. However, a mixture of approximately 36 points in the finer section of the map was observed. This is an indication of high level of randomness in the clustering.

Similarly, in the ML direction, it was observed that the clustering as indicated by the neigborhood map is less coarse as compared to the AP clustering. The coarse section is located

at the right most part of the map. As indicated by the input plane (Figure 8.4 (d)), almost all of the data points of the clustering (approximately 42 data points) are situated at the finer section of the map. This is an indication of poor clustering in the ML direction. The poor clustering infers more similarity of the values in this direction and hence infers the occurrence of reduced sway differences in comparison with those of the AP direction. The coarser the clustering, the lower the connection/similarities between the data points of the conditions i.e. conditions one and two. A fine map across almost all the entire data points for both the AP and ML conditions can be observed which suggested that the change in position and acceleration were similar for most of the participants. However the separation could be among the data points of the same group which would infer greater inconsistency in the results. Thus it is necessary to evaluate the clustering using external measures such as purity, precision, recall and F-measure. As already stated in the data analysis section, the values of these measures in this study i.e. purity, precision and recall, varies from 0.5 to 1 for two clusters, with 0.5 been the minimum clustering performance and hence refering to the greatest similarity and 1 been the maximum clustering performance which infers greatest disparity.

A visual representation of the median of the clustering result is shown in the bar chart of Figure 8.5. The median value showed that the external values for the AP direction were higher than those of the ML direction by 0.04, 0.08, 0.04 and 0.072 for the purity, precision, recall and F-measure respectively.

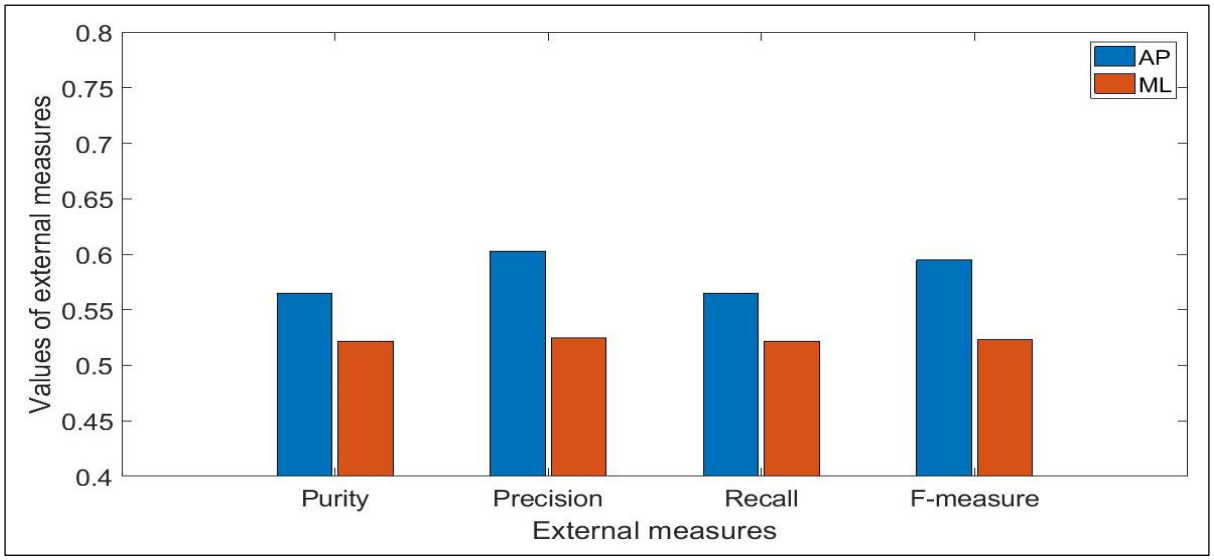

Figure 8.5. Bar chart representation of the external evaluation measures: (a) AP and (b) ML directions from the clustering using RMS position and acceleration.

In comparison to the mimimum possible value of 0.5, it can be observed that exclusion of the visual system affects the change in position and acceleration in both directions, although it produces a higher change in AP direction than ML direction. The interquartile range i.e. the difference between the 75^{th} percentile and 25^{th} percentile, defines the variability in the clustering. The value of the interquartile range for the measures of purity, precision, recall and F-measure were 0.044, 0.032, 0.044, and 0.027 for the AP direction and 0.044, 0.045, 0.044 and 0.044 for the ML direction respectively, thus suggesting similar variability. The result of these values are presented in Table 8.1.

Table 8.1. Values of external measures of the clustering between conditions 1 and 2 using the RMS position and acceleration.

Parameter	AP Direction				ML Direction			
	Purity	**Precision**	**Recall**	**F-measure**	**Purity**	**Precision**	**Recall**	**F-measure**
Minimum	0.544	0.564	0.544	0.554	0.5	0.5	0.5	0.5
Maximum	0.609	0.637	0.609	0.628	0.609	0.612	0.609	0.610
Range	0.065	0.073	0.065	0.074	0.109	0.112	0.109	0.11
Median	0.565	0.603	0.565	0.595	0.522	0.525	0.522	0.523
Interquartile range	0.044	0.032	0.044	0.027	0.044	0.045	0.044	0.044

The test of significant difference between the measures were conducted using Mann-Whitney U test due to non-conformity to a normal distribution using the Shapiro-Wilk test with the p value set to 5%. The result showed that the differences between the external measures of the ML and AP direction were significant ($p < 0.05$).

8.3.2.1.2. Clustering using the RMS position and velocity

To aid easy reading, KNN neighbourhood maps and the input planes associated to the clustering results in this section, have been transferred to appendix 9. The results of the median values of the clustering performance measures between the RMS position and velocity are shown in Table 8.2.

Table 8.2. Values of external measures of the clustering between condition 1 and 2 using the RMS postiton and velocity.

Parameter	AP Direction				ML Direction			
	Purity	**Precision**	**Recall**	**F-measure**	**Purity**	**Precision**	**Recall**	**F-measure**
Minimum	0.522	0.535	0.522	0.528	0.5	0.5	0.5	0.5
Maximum	0.674	0.672	0.674	0.674	0.544	0.576	0.544	0.559
Range	0.152	0.137	0.152	0.146	0.044	0.076	0.044	0.059
Median	0.565	0.580	0.565	0.573	0.522	0.530	0.522	0.526
Interquartile range	0.065	0.063	0.065	0.059	0.022	0.035	0.022	0.028

The median value for the purity, precision, recall and F-measure for the AP direction were: 0.565, 0.580, 0.565 and 0.573 respectively. Similarly, the median values for the purity, precision, recall and F-measure for the ML direction were: 0.522, 0.530, 0.522 and 0.526. This suggested that the change in position and velocity for the AP direction were greater than those for the ML direction. Therefore the AP direction was more sensitive to the exclusion of the visual system. Similarly, the greater the interquartile range the greater the clustering inconsistency between the two conditions. The interquartile range of the measures for the AP direction was 0.065, 0.063, 0.065, 0.059 for the purity, precision, recall and F-measure respectively. The interquartile range for the measures of the ML direction were: 0.022, 0.035, 0.022 and 0.028 for the purity, precison, recall and F-measure. This inconsistency could be as a result of more sway occuring in the AP direction as compared to the ML direction. The values of the median of the external measures are shown in Figure 8.6.

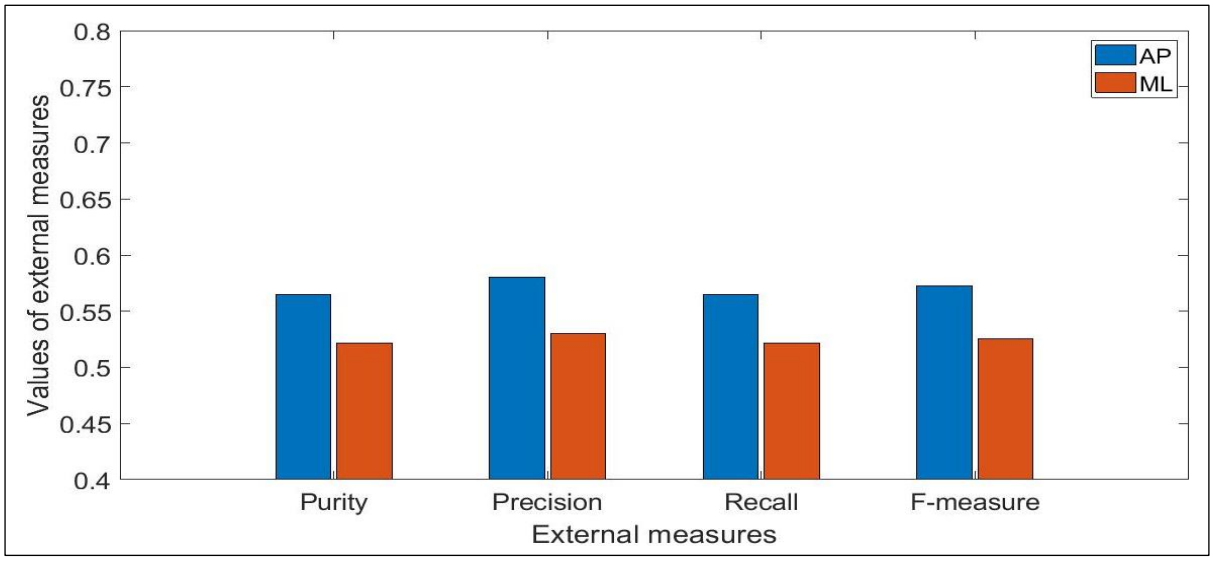

Figure 8.6. Bar chart representation of the external evaluation measures: (a) AP and (b) ML direction from the clustering using position and velocity

In comparison to the median values of the measures of the clustering performance, the acceleration and velocity variables can be seen to produce similar results. However, the acceleration variables appears to be slightly more sensitve than the velocity variable in regards to the AP direction. Since the position variable is constant in both clustering the changes is due to the velocity and acceleration. Thus exclusion of the visual system resulted in a higher acceleration than the velocity in the AP direction. The test of significant difference between the measures were conducted using Mann-Whitney U test due to non-conformity to a normal distribution using the Shapiro-Wilk test with the p value set to 5%. The result showed that the differences between the external measures of the ML and AP directions were significant ($p < 0.05$).

8.3.2.2. Conditions 1 and 3

8.3.2.2.1. Clustering using the RMS displacement and acceleration

Condition 3 is defined by the subject standing on a sponge surface with the eyes open. In this condition the visual and the vestibular system were unaffected while the proprioceptive system was excluded. Thus, this condition is defined by the exclusion of the proprioceptive system. The result of the clustering of condition one and three of the RMS displacement and acceleration are shown in Figure 8.7.

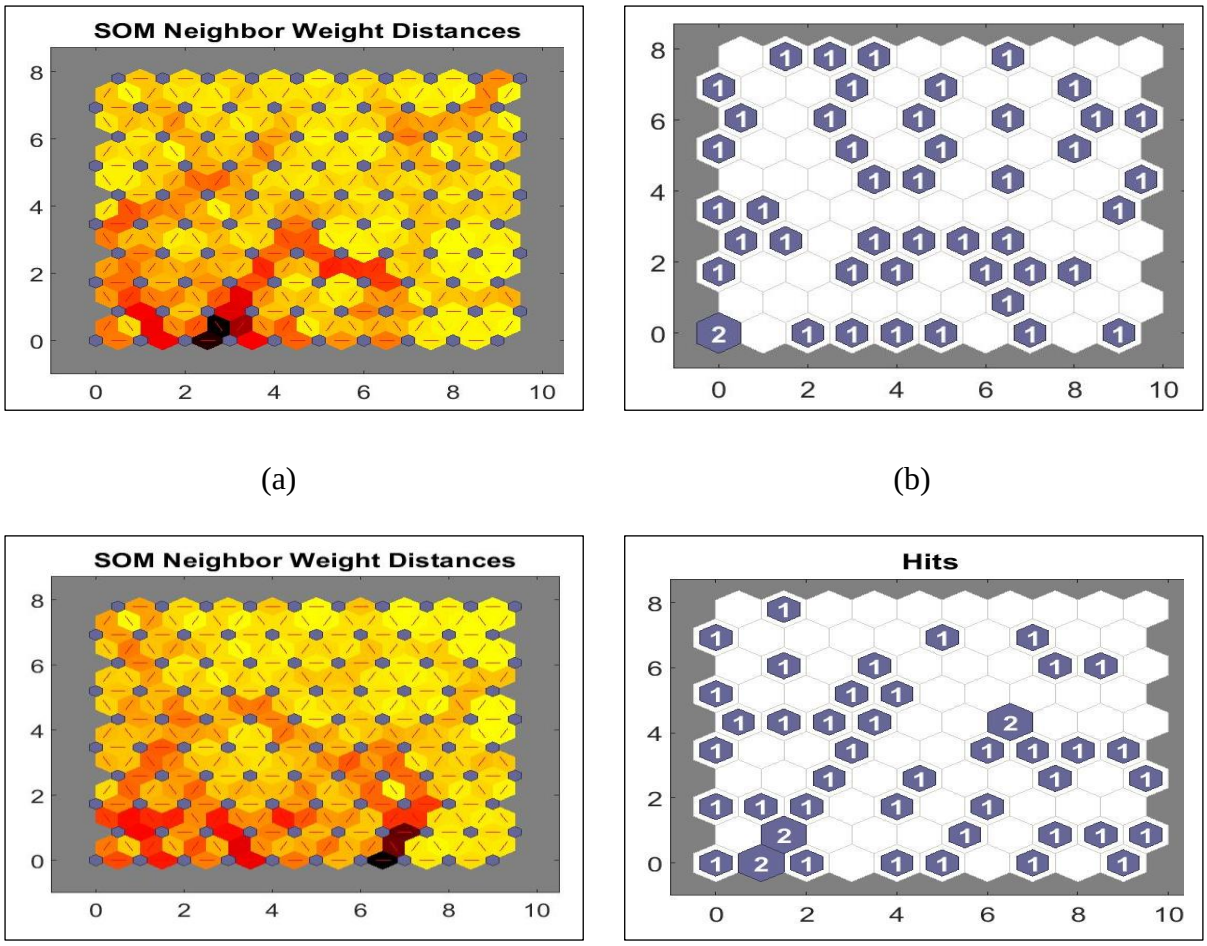

Figure 8.7. Plot of neighbourhood distance and input vector hits of conditions 1 and 3. (a,b) representing the AP direction, (c,d) representing the ML direction. The horizontal and vertical axes are neurons positions.

The clustering of conditions 1 and 3, along the AP direction as indicated by the neighbourhood distance plot, (Figure 8.7 (a)) appear to represent a bright/finer region across the KNN output map with only little shades of coarseness most especially at the middle and the bottom left of the plot. The input plane suggested that a major section of the data points approximately 39 out of 46 are located in the brighter regions. This suggested a poor clustering between conditions one and three as they are both divided into 23 data points each. Poor clustering infers close similarity between the conditions. In comparison with the neighbourhood distance plot of the AP clustering of condition one and two above (Figure 8.4 (a)), a slightly less fine map can be observed. This indicates that reduced differences in the acceleration and position occurred in the AP direction as a result of exclusion of the proprioceptive system. This does not imply that the proprioceptive system results in more acceleration and change in position, but that its

presence with the vestibular system is not as effective in reducing the change in position and acceleration as compared with the interaction of the visual system and the vestibular system. The result implies that the subjects' change in acceleration and position was reduced because of the presence of the visual system.

Similarly, the neighbourhood distance map of the ML direction (Figure 8.7(c)), appears to produce a finer/brighter region across the map, as indicated by only few shades of coarseness at the bottom left region which consists of approximately 7 data points. This suggested greater similarities between the two conditions and infers a reduced change in the position and acceleration values between the conditions in the ML direction. In comparison with the neighbourhood distance of the ML direction of the clustering between conditions one and two (Figure 8.4(c)), a smaller coarse clustering is observed in this condition. This is an indication that the visual system reduces the change in the ML position and acceleration as compared to the proprioceptive system.

The median value shows that the external values for the AP direction was higher than that of the ML direction by 0.022, 0.030, 0.022 and 0.026 for the purity, precision, recall and F-measure respectively. In comparison to the minimum possible value of 0.5, it can be observed that exclusion of the proprioceptive system affects the AP directional sway but not the ML sway as the median value was 0.5. The median values of the external evaluation measures of the resulting clustering are shown in the bar graph of Figure 8.8. The value of the interquartile range for the purity, precision, recall and F-measure were 0.044, 0.076, 0.044, and 0.059 respectively for the AP direction and 0.022, 0.030, 0.022 and 0.026 respectively for the ML direction, thus suggesting a greater variability in the AP direction. The test of significant difference between the measures were conducted using Mann-Whitney U test due to non-conformity to a normal distribution which was obtained by the Shapiro-Wilk test with the p value set to 5%. The result showed that the differences between the external measures of the ML and AP directions were significant ($p < 0.05$). The result of these values are presented in Table 8.3.

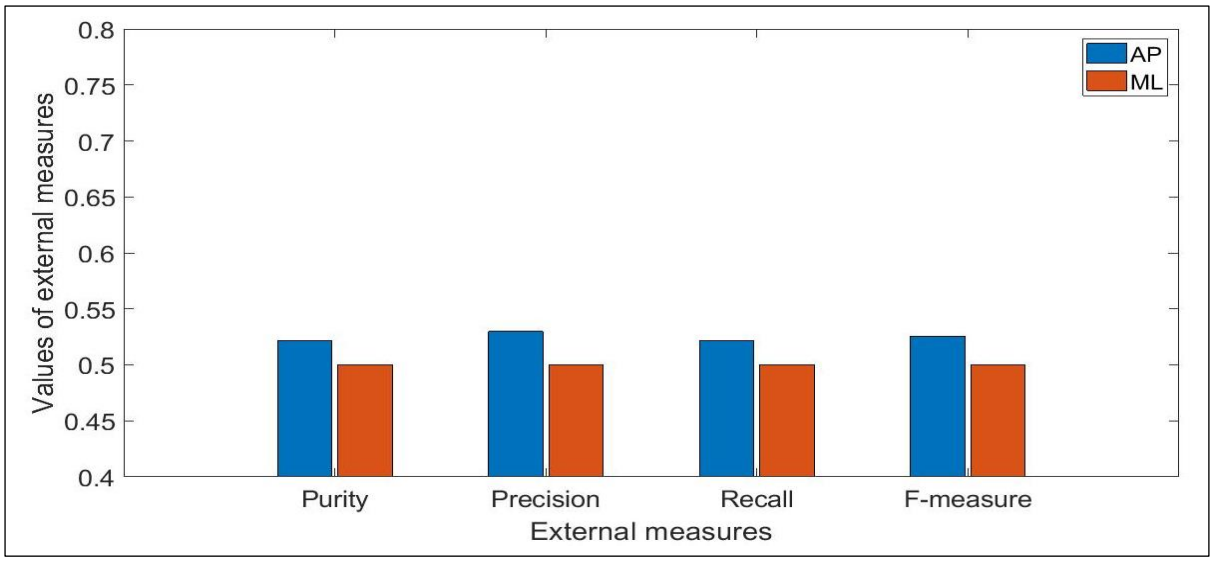

Figure 8.8. Bar chart representation of the external evaluation measures: (a) AP and (b) ML directions from the clustering using RMS position and acceleration.

Table 8.3. Values of external measures of the clustering between conditions 1 and 3 using the RMS position and acceleration.

Parameter	AP direction				ML direction			
	Purity	**Precision**	**Recall**	**F-measure**	**Purity**	**Precision**	**Recall**	**F-measure**
Minimum	0.5	0.5	0.5	0.5	0.5	0.5	0.5	0.5
Maximum	0.545	0.637	0.545	0.587	0.522	0.556	0.522	0.550
Range	0.045	0.137	0.045	0.087	0.022	0.056	0.022	0.050
Median	0.522	0.530	0.522	0.526	0.5	0.5	0.5	0.5
Interquartile range	0.044	0.076	0.044	0.059	0.022	0.030	0.022	0.026

8.3.2.2.2. Clustering using the RMS displacement and velocity

The results of the median values of the clustering performance measures between the RMS position and velocity is shown in Table 8.4.

Table 8.4. Values of external measures of the clustering between conditions 1 and 3 using the RMS position and velocity.

Parameter	AP Direction				ML Direction			
	Purity	**Precision**	**Recall**	**F-measure**	**Purity**	**Precision**	**Recall**	**F-measure**
Minimum	0.522	0.525	0.522	0.523	0.5	0.5	0.5	0.5
Maximum	0.587	0.628	0.587	0.607	0.522	0.556	0.522	0.550
Range	0.065	0.103	0.065	0.084	0.022	0.056	0.022	0.050
Median	0.565	0.613	0.565	0.594	0.5	0.5	0.5	0.5
Interquartile range	0.065	0.070	0.065	0.061	0.022	0.030	0.022	0.026

The median value for the purity, precision, recall and F-measure for the AP direction were: 0.565 0.613, 0.565 and 0.594 respectively. Similarly, the median values for the purity, precision, recall and F-measure for the ML direction were: 0.5, 0.5, 0.5 and 0.5. This suggested that the changes in position and velocity for the AP direction were greater than those for the ML direction. Therefore the AP direction was more sensitive to exclusion of the proprioceptive system. Similarly, the greater the interquartile range, the higher the clustering inconsistency between the two conditions. The interquartile range of the measures for the AP direction were 0.065, 0.063, 0.065 and 0.059 for the purity, precision, recall and F-measure respectively. The interquartile range for the measures of the ML direction were: 0.065, 0.070, 0.065 and 0.061 for the purity, precison, recall and F-measure respectively. The values of the median of the external measures are shown in Figure 8.9.

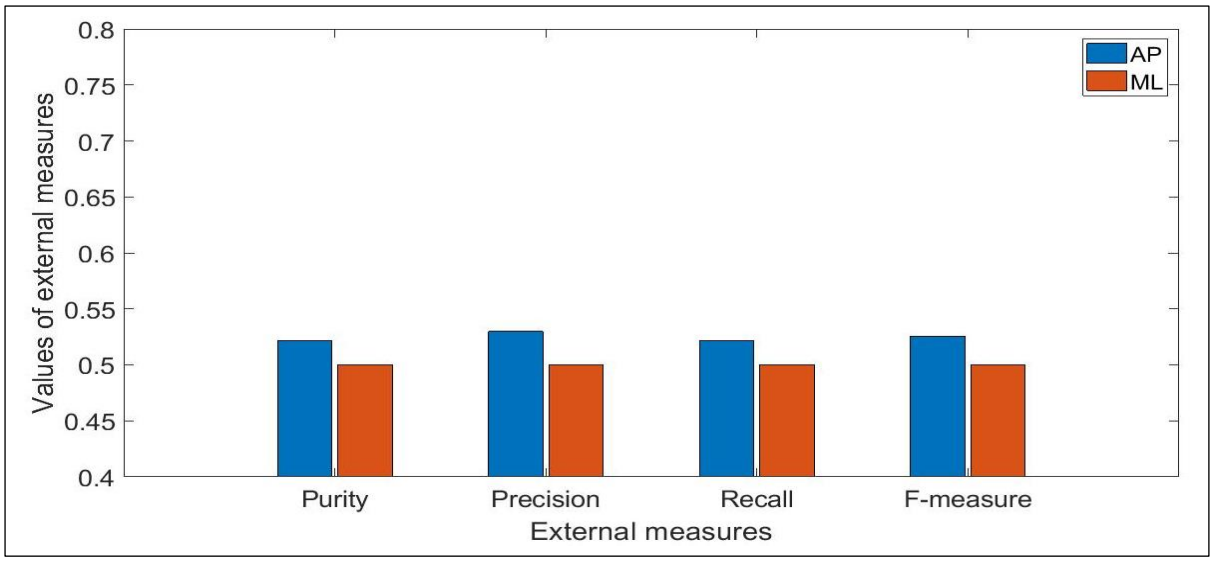

Figure 8.9. Bar chart representation of the external evaluation measures: (a) AP and (b) ML directions from the clustering using RMS position and velocity (Ojie & Saatchi, 2021)

Higher external measures were observed for the precision and F-measure in the AP direction for the clustering of conditions 1 and 3 as compared to those for the clustering between conditions 1 and 2 i.e. 0.613 and 0.594 for the precision of the clustering for conditions 1 and 3, against 0.580 and 0.573 for the clustering between conditions 1 and 2. This suggested that the propriceptive system was more effective in reducing the AP velocity of the subjects as compared to the visual system. However, the values of the external meaures for the clustering of the ML position and velocity were lower for condtions 1 and 3 as compared to those of conditions 1 and 2. This suggested that the visual system was more effective than the proprioceptive system in reducing the ML velocity. The test of significant difference between the measures were conducted usng Mann-Whitney U test due to non-conformity to a normal distribution using the Shapiro-Wilk test with the p value set to 5%. The result showed that the differences between the external measures of the ML and AP direction were significant ($p < 0.05$).

8.3.2.3. Conditions 1 and 4

8.3.2.3.1. Clustering using the RMS displacement and acceleration

Condition four involves the use of only the vestibular system to balance. The clustering results produced by the Kohonen map are shown in Figure 8.10.

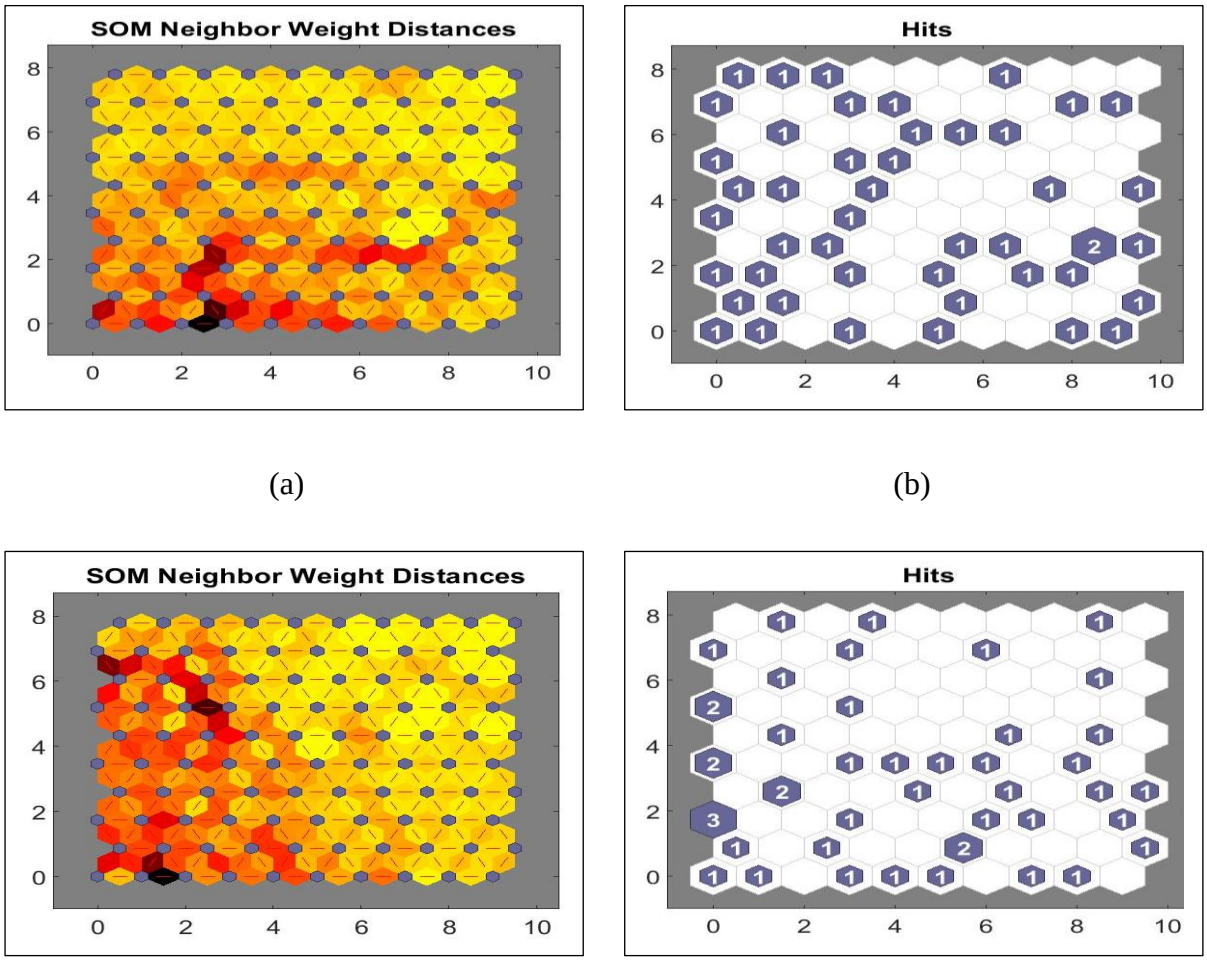

(a) (b)

(c) (d)

Figure 8.10. Plot of neighbourhood distance and input vector hits of conditions 1 and 4. (a,b) representing the AP direction, (c,d) representing the ML direction. The horizontal and vertical axes are neurons positions.

A larger darker section can be seen for the neighborhood distance plot for both the AP and ML directions as shown in Figures 8.10 (a) and (c) in comparison with that of the clustering of conditions one and two (Figures 8.4 (a) and (c)), and conditions one and three (Figures 8.7 (a) and (c)) above. These darker colours shows a coarse clustering for both the AP and ML directions. However, the AP direction appears to be coarser, as there are majority of the data

points (indicated by the input vector hits of Figure 8.10 (b)) located in the coarse region. Thus more disparity is expected for the AP direction as compared to the ML direction. This is an indication of more change in the RMS position and acceleration in this condition. The resulting clustering of the external measures perfomance values are shown in Table 8.5.

Table 8.5. Values of external measures of the clustering between conditions 1 and 4 using the RMS position and velocity

Parameter	AP Direction				ML Direction			
	Purity	**Precision**	**Recall**	**F-measure**	**Purity**	**Precision**	**Recall**	**F-measure**
Minimum	0.609	0.634	0.609	0.621	0.5	0.5	0.5	0.5
Maximum	0.652	0.795	0.652	0.717	0.565	0.626	0.565	0.610
Range	0.043	0.161	0.043	0.096	0.065	0.126	0.065	0.110
Median	0.630	0.795	0.630	0.675	0.544	0.556	0.544	0.544
Interquartile range	0.022	0.068	0.022	0.042	0.022	0.046	0.022	0.033

The median values of the external measures for the clustering in the AP direction were given as: 0.630, 0.795, 0.630, 0.675 for the measures of purity, precision, recall and F-measure respectively. Similarly, the median values of the external measures for the clustering in the ML direction were given as: 0.544, 0.556, 0.544, 0.544 for the purity, precision, recall and F-measure. As indicated by these values, a greater change in the position and acceleration occurs in the AP direction as compared to the ML direction.

In comparison with the measures for the clustering performance for conditions one and two (Table 8.1), it can be observed that the proprioceptive system is effective in reducing the change in acceleration and position in both the AP and ML directions. Similarly, in comparison to conditions one and three (Table 8.3), we observe a greater difference than those obtained in the clustering of conditions one and two. This indicates that the visual system was more effective than the proprioceptive system in reducing the acceleration and position sway. The effect of the visual system is more noticeable in the ML direction, as it results in the reduction of the median value of the clustering performance measures for the purity, precision, recall and F-measure to 0.5 for all the measures. The bar graph of the median values of the external measures are shown in Figure 8.11.

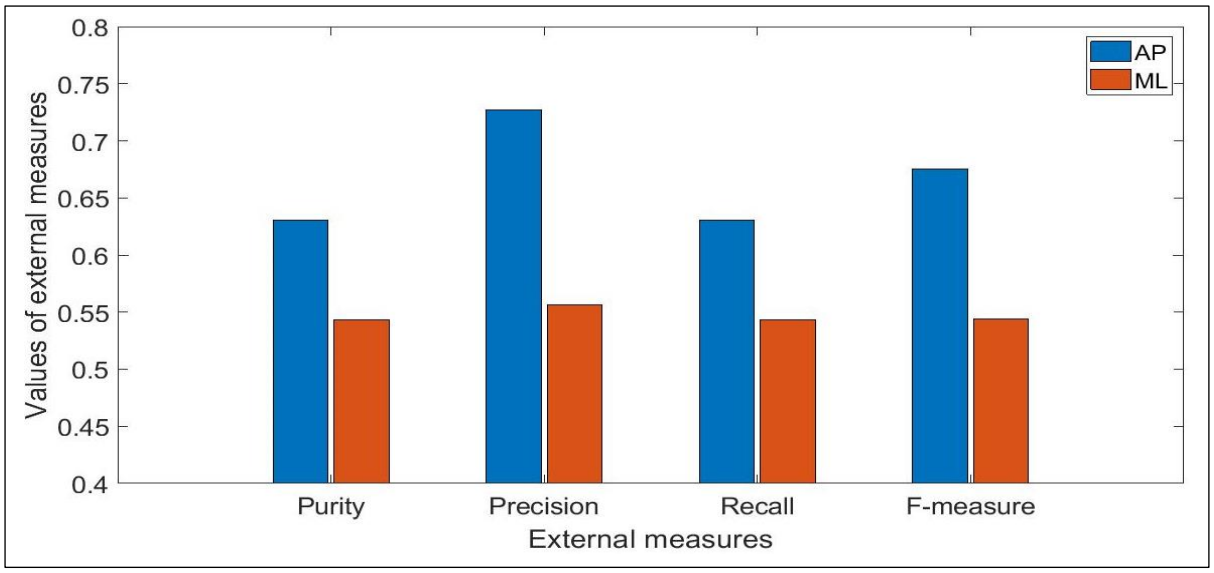

Figure 8.11. Plot of neighbourhood distance and input vector hits of conditions 1 and 4. (a) and (b) representing the AP direction, (c) and (d) representing the ML direction. The horizontal and vertical axes are neurons positions

The bar graph shows an increase in the external measures for both the ML and AP directions. In comparison of this bar graph with that of conditions one and two above, it can be observed that the proprioceptive system helps the control of sway in both the AP and the ML directions. However, the proprioceptive system has greater control over the sway of the AP direction than the ML direction as indicated by the differences between the external measures. This indicates that the other sensory systems i.e., the visual and proprioceptive systems help the vestibular system to maintain a reduction in the change in acceleration and position. However, it can also be observed that a small change occurs across all the measures in the clustering results using only the vestibular system as against its combination with visual and proprioceptive systems. Therefore, a good functional vestibular system can help maintain balance to a great extent. Thus, it is important that the vestibular system is carefully examined in balance dysfunctions.

The test of significant difference between the measures were conducted using Mann-Whitney U test due to non-conformity to a normal distribution using the Shapiro-Wilk test with the p value set to 5%. The result showed that the differences between the external measures of the ML and AP directions were significant ($p < 0.05$).

8.3.2.3.2. Clustering using the RMS displacement and velocity

The results of the median values of the clustering performance measures between the RMS position and velocity are shown in Table 8.6.

Table 8.6. Values of external measures of the clustering between conditions 1 and 4 using the RMS position and velocity.

Parameter	AP Direction				ML Direction			
	Purity	**Precision**	**Recall**	**F-measure**	**Purity**	**Precision**	**Recall**	**F-measure**
Minimum	0.609	0.679	0.609	0.675	0.5	0.5	0.5	0.5
Maximum	0.696	0.795	0.696	0.730	0.565	0.613	0.565	0.600
Range	0.087	0.116	0.087	0.055	0.065	0.113	0.065	0.1
Median	0.652	0.795	0.652	0.717	0.522	0.542	0.522	0.532
Interquartile range	0.044	0.014	0.044	0.033	0.022	0.055	0.022	0.040

The median values for the purity, precision, recall and F-measure for the AP direction were: 0.652, 0.795, 0.652 and 0.717 respectively. Similarly, the median values for the purity, precision, recall and F-measure for the ML direction were: 0.522, 0.542, 0.522 and 0.532 respectively. This suggested that the change in position and velocity for the AP direction were greater than those for the ML direction. Therefore the AP direction was more sensitive to the exclusion of the visual and proprioceptive systems. Similarly, the greater the interquartile range, the greater the clustering inconsistency between the two conditions. The interquartile range of the measures for the AP direction were 0.044, 0.014, 0.044 and 0.033 for the purity, precision, recall and F-measure respectively. The interquartile range for the measures of the ML direction were: 0.022, 0.055, 0.022 and 0.040 for the purity, precison, recall and F-measure respectively. The values of the medians of the external measures are shown in Figure 8.12.

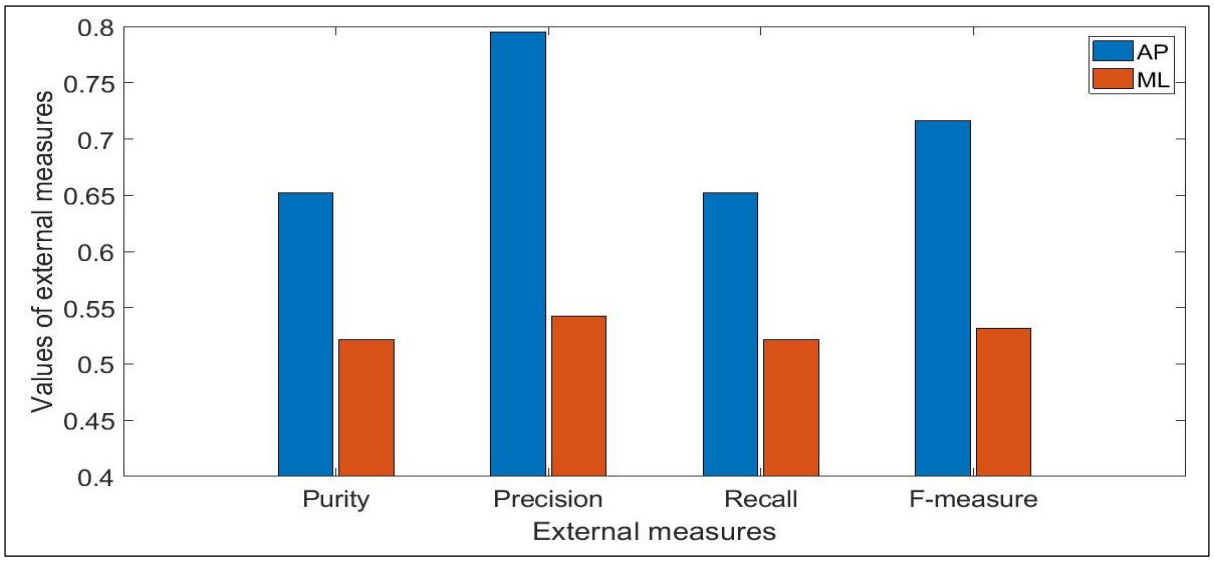

Figure 8.12. Bar chart representation of the external evaluation measures: (a) AP direction and (b) ML direction from the clustering using RMS position and velocity (Ojie & Saatchi, 2021).

The test of significant difference between the measures were conducted using the Mann-Whitney U test due to non-conformity to a normal distribution using the Shapiro-Wilk test with the p value set to 5%. The result showed that the differences between the external measures of the ML and AP directions were significant ($p < 0.05$).

8.3.2.4. Clustering using a combination of the variables of the ML and AP directions

The results of the external measures of the clustering obtained by combining the ML and AP variables of the RMS position and velocity are shown in Figure 8.13. As indicated by the bar graph a reduced overall change was found in conditions 1 and 2, conditions 1 and 3 and finally conditions 1 and 4. The median and interquartile range of the values of the measures are shown in Table 8.7.

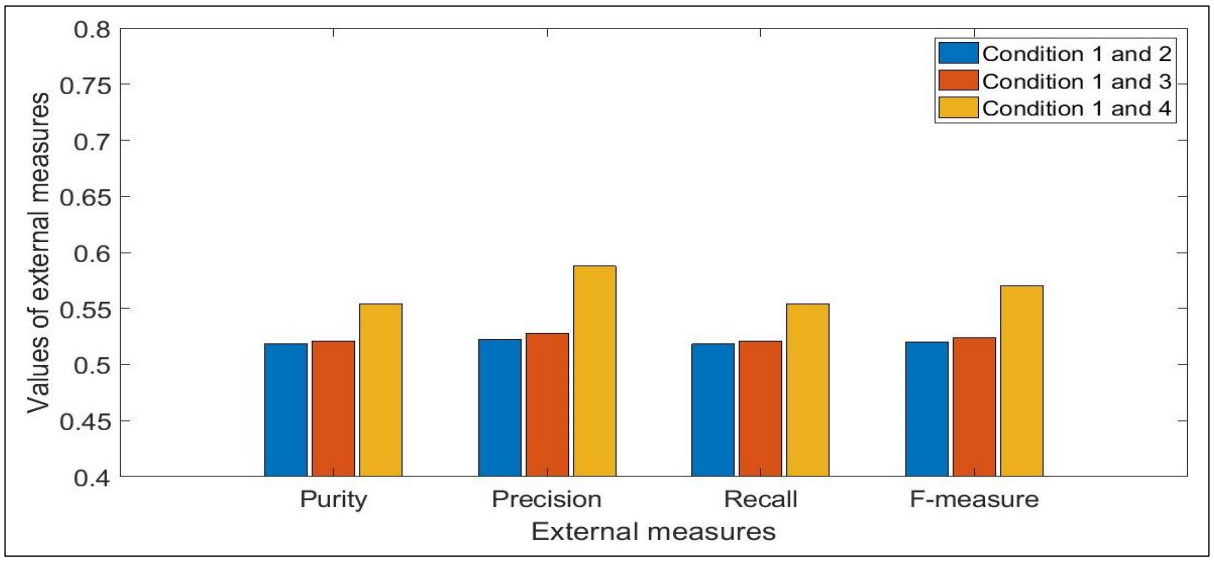

Figure 8.13. Bar chart representation of the external evaluation measures of the combination of the AP and ML position and velocity (Ojie & Saatchi, 2021).

Similarly**,** the result of the external measures of the clustering obtained by combining the ML and AP variables of the RMS position and acceleration are shown in Figure 8.14. As indicated by the bar graph a reduced overall change is noticeable in conditions 1 and 2, conditions 1 and 3 and finally conditions 1 and 4.

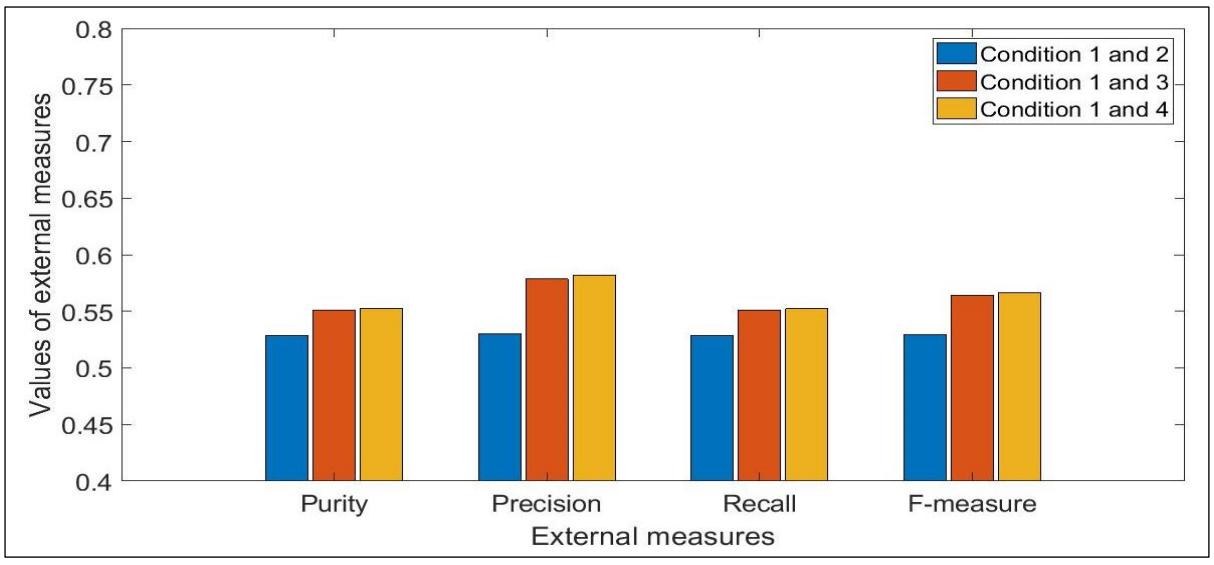

Figure 8.14. Bar chart representation of the external evaluation measures of the combinations of the AP and ML position and acceleration.

Therefore, a combination of the ML and AP variables result in reduced disparities between the conditions. This may be due to the existence of a mutually exclusive relationship between the two directions. As a person is swaying in one direction, say the AP direction, no sway occurs in the ML direction. Similarly, as a person is swaying in the ML direction, no sway occurs in the AP direction. Combining both directions could result in a reduced amount of sway as they counterbalance each other. Thus, it is necessary to determine the direction that represents the majority of the postural sway of the subject rather than combining the results, as this could affect the interpretation of the subject's balance and could hide inherent patterns. However, the major direction of sway does not necessarily mean the direction with the largest magnitude of sway but the direction that represents the COM sway for a longer duration of time.

8.4. Summary

In this chapter, the patterns inherent in the sensory systems based on their direction of sway i.e. the mediolateral (ML) and anterior-posterior (AP) directions, were explored. Twenty-three healthy adult subjects of mean age (standard deviation): 24.5 (4.0) years, mean height (standard deviation): 173.6 (6.8) cm, mean weight (standard deviation): 72.7 (9.9) kg, with no previous history of balance dysfunction participated in the study. Kohonen neural network was used in carrying out the clustering between the conditions of the mCTSIB. The patterns inherent to the sensory systems were examined by using the external clustering performance measures i.e., purity, precision, recall and F-measure. The results obtained suggested that the visual system was more effective in reducing the acceleration of the subjects in both directions and the velocity in the ML direction. However, the proprioceptive system was more effective in reducing the velocity in the AP direction as compared to the visual system but had no effect in the ML velocity.

Chapter 9 Conclusion and further work

9.1. Conclusion

In this study, the applications of accelerometry with machine learning and statistical modelling methods were used to enhance the analysis of human balance. The cohort of subjects involved in the study were young healthy adults with mean (standard deviation) of age, height and weight: 24.5 (4.0), 173.6 (6.8), and 72.7 (9.9) kg respectively. The aim of the study was to develop computerised accelerometry techniques that will facilitate better understanding of human balance.

To achieve the aim of this study, the following objectives were met:

- Evaluated accelerometry based on the inverted pendulum to accurately quantify human balance with respect to actual physical units of length and angle.
- Devised a setup that was used to investigate the effect of the centre of mass (COM) position to balance.
- Obtained time domain balance related data from 23 healthy young adult subjects with the devised setup and algorithms.
- Determined the time domain measures that are sensitive to the information of the sensory system.
- Utilised principal component analysis (PCA), Bland and Altmans analysis method, and hypothesis testing to obtain information about the characteristics of the sensory systems in healthy young adult subjects.
- Applied Kohonen neural network, K-means clustering and clustering evaluation to obtain information about the contribution and behaviour of the sensory systems to balance in subjects included in the study.

9.1.2. Contributions to knowledge

The contributions to the study are:

I. Development of mathematical techniques to project the COM sway of the human body to the ground surface to allow accurate balance analysis. Trigonometry methods were adapted in these developments. Their evaluations were carried out using a devised setup that could compare both the manual measurement obtained from the setup and the calculated accelerometry measurements. Comparison of the methods were conducted using the Bland

and Altmans analysis method, and relevant statistical methods. The results confirmed the accuracy of the devised accelerometry techniques in characterising human balance.

II. The effect of the COM position on postural sway was studied. From this, it was hypothesised that similar angular sways should produce similar ground displacements. To show this effect, an inverted pendulum system consisting of three plumb lines-plumb bobs system attached to a metal rod at 50, 75 and 100 cm at one of its ends, was devised. The devised accelerometry system was also attached to the metal rod and the setup was inclined at angles 0 to 90 degrees with 5 degrees between consecutive measurement. The angles and ground displacements were obtained manually, using protractor and measuring tape, and automatically, using the accelerometry system. The results of the angles and displacements from both methods were similar. The result indicated that for a similar angle of inclination, the displacement on the ground surface differed with respect to the actual COM position of the plumb lines and bobs. This suggested that the COM position can affect the comparison of sway across subjects, with subjects of higher COM position tending to have larger sway and less stability. This in turn suggested that the base of support (BOS) for subjects with a higher COM should be greater than those with smaller COM position. To reduce the obscuring effect of the COM position for comparison purposes, the displacement should be normalised with the COM position, if the inverted pendulum model is employed. The result also suggested that methods of accelerometry that uses the integration of acceleration to obtain velocity and displacement without projection to the ground surface may not accurately represent the balance of a subject.

III. The underling relationship between the interaction of the sensory systems to balance were investigated on 21 healthy adult subjects. The devised acceleromtery method was used to obtain time domain measures with the potential of representing balance while the subjects were involved in the four conditions of the modified Clinical Test of Sensory Interaction and Balance (mCTSIB). Principal component analysis (PCA) and other statistical methods were applied to the time domain measures to investigate the underlying behaviour of the performance and interaction of the sensory systems to balance. For the PCA analysis, the correlations obtained from the rotated component matrix were used in investigating these relationships, where similar correlation inferred close relationships in the behaviour of the sensory systems in the conditions under consideration. The results showed that the interaction of the proprioceptive and vestibular systems resulted in less sway as compared to the interaction of the visual and vestibular systems. The result also suggested that healthy adults relied more on their proprioceptive system to maintain balance in a well-lit

environment; the anterior posterior (AP) direction was more sensitive to the changes in the sensory systems than the mediolateral (ML) direction; and less variability among the subjects was observed in the interaction between the proprioceptive and the vestibular systems as compared to those of the visual and vestibular systems. The highest variability was observed with the vestibular system.

This suggested that the proprioceptive system was more uniform among subjects than the visual and vestibular systems respectively.

IV. The effects of the sensory systems to balance were evaluated on 23 healthy adult subjects using the sway data in the ML and AP directions and the application of Kohonen neural network (KNN), K-means clustering, clustering evaluation methods and related statistical methods. The subjects were engaged in the four conditions of the mCTSIB. Their resulting root mean square (RMS) sway of the position, velocity and acceleration in the ML and AP directions from the four test conditions of mCTSIB were used as inputs for the clustering process. The result suggested that the body sway associated with the sensory systems was more towards the AP direction. However, the ML direction was more sensitive to the inclusion/exclusion of the visual system while the AP direction was more sensitive to all of the balance related sensory systems, most especially the proprioceptive and vestibular systems. It was also observed that the visual system was more efficient in reducing the acceleration of the subjects as compared to the effect of the proprioceptive system. However, the proprioceptive system was more effective in reducing the AP velocity than the visual system. Thus, to examine these systems, the AP velocity sway should mostly be used for the proprioceptive and vestibular systems while for the visual system, the ML velocity sway and accelerations in both directions should mostly be used.

The findings and recommendations of this study are listed in the following headings.

9.1.3. Accelerometry accuracy and time domain measures for balance analysis

The accelerometry devised method in this study when evaluated against the setup used to measure ground projected sway and angles, based on physical units of measurement of cm and degrees respectively, showed excellent agreement between their results. This suggested that accelerometry can be used to measure sway accurately and reliably.

Using the devised accelerometry methods, the time domain measures capable of differentiating between the information of the sensory systems were investigated on fifteen healthy adult subjects with mean (standard deviation) of age, weight and height: 22.5 (3.4), 70.9 (7.5) kg, 173.5 (9.8) cm respectively, using the modified Clinical Test of Sensory Interaction and Balance (mCTSIB). The time domain variables considered were the sways measures of the average, root mean square, and range of the position, velocity and acceleration in the AP and ML directions. The most effective variables for differentiating between the information of the sensory systems were the average, root mean square and range of velocity and acceleration in the AP direction.

It was also observed that no significant difference occurred between the subjects in conditions two and three of the mCTSIB. This infers that healthy adult subjects utilise both the visual and proprioceptive system in similar manner to maintain balance.

9.1.4. Centre of mass effect on postural sway analysis

By analysing the effect of the centre of mass on postural sway using a devised inverted pendulum approach, it was observed that for the same angle of inclination, the ground protected displacement differed. This variation of the ground displacements has implications on the comparison of postural sway responses across subjects and for balance interpretations and interventions.

This also implied that across similar base of supports, the balance of people with higher COM positions are expected to be less stable, if similar conditions existed among them. In this regard, differing interventions may be required. For example, the base of support and mechanical aid could be increased for people with higher COM positions to accommodate the COM interplay. Differing strategies to balance may also be introduced according to the COM position.

For comparison of postural sway across subjects, it may be necessary to investigate people with similar COM positions, standardise the results of sway with the COM position of each subject, and to make comparison with the base of support of each subject. Comparing subjects of similar COM positions ensures the reliability and applicability of the sway analysis. Normalisation with the COM positions reduced the effect that the COM positions had on the results. However, this may affect the accuracy of the analysis as the COM is no longer taking into consideration. Comparison with the base of support is a holistic approach and ensures that the balance of the subject is taking into consideration.

9.1.5. Investigation of the sensory systems interaction

By applying PCA and other statistical methods to investigate the interaction of the sensory system, it was observed that in a well-lit environment, young healthy adult subjects, relied more on the interaction between the proprioceptive and vestibular systems in comparison to the interaction between the vestibular and the visual systems. It was also observed that the AP direction was more sensitive to the information of the sensory systems as compared to the ML direction. Less variability in sway across the subjects was observed for the proprioceptive system as compared to the visual and vestibular systems.

Thus, it may be necessary to enhance proprioceptive perception for young healthy adult subjects. Proprioceptive perception can be improved using proprioception training. With problems with the sensory systems, steps should be taking to accommodate the sway in the AP direction. This may include improving/enlarging the base of support towards the AP direction.

Clinicians should be aware of the variability in these systems when interpreting their results and should following a holistic approach to balance analysis. This can be ensured by making reference to the base of support of the individual in examining these systems.

9.1.6. Behavioural characteristics of the sensory systems

By applying Kohonen neural network (KNN), K-means clustering and clustering evaluation methods on the root mean square time domain measures of position, velocity and acceleration obtained from twenty-three healthy young adult subjects, it was observed that the exclusion/inclusion of the proprioceptive system had no effect on the ML direction of the position velocity and acceleration. However, noticeable changes were observed in the velocity of the AP direction.

This indicated that the proprioceptive system for young adult subjects is a velocity controlling variable in the AP direction. Thus, enhancing the proprioceptive system can help reduce the velocity in the AP direction. Similarly, the examination of the effectiveness of the proprioceptive system to balance can be carried out using the AP velocity.

The result also suggested that the exclusion of the visual system increased the velocity in the ML direction and the acceleration in both the ML and AP directions. In contrast, the exclusion of the proprioceptive system showed no changes on the ML velocity and had a lesser effect on the acceleration in the AP direction. This implies that the visual system is an acceleration controlling variable and reduces ML sway. Thus, enhancement of the visual system is

important to control the acceleration of a subject and to reduce the ML sway. The acceleration and ML sway should be used to assess the functioning of the visual system for balance analysis.

Finally, the result suggested that the vestibular system affects more of the AP velocity and acceleration, as compared to the ML velocity and acceleration. Thus, the AP direction of sway should be used to access the functioning of the vestibular system for balance analysis.

9.1.7. Limitation of the study

Possible limitations of this study include the small sample size, and reduced measurement accuracy due to the manual setup used for evaluating the accelerometry system.

9.2. Further work

In this study, standstill balance analysis was investigated. However, human balance analysis can be considered in both static and dynamic conditions. Thus, further study will evaluate dynamic balance using the algorithms developed in this study. The proposed system will consist of several sensors which will be located at the different segments of the body. Also, in this study time domain measures were used. In further studies, frequency domain and spectral analysis could be used. The behaviour of these measures on healthy adult subjects will be determined and used as the basis for comparison. In further study, inclusion of larger participants can be considered. Similarly, the verification of the methods will be carried out on children and older adult groups to understand their balance characteristics. The study can also be extended to clinical trials to verify the methods on patients.

The validation of the method against existing balance diagnostic methods such as force platform and camera-based methods can also be carried out. The refinement of the accelerometry device for ease of use in clinical environment can be carried out and the commercial aspects of the device, cost and its competitiveness can be explored. The system will require adaptation of medical devices regulatory issues and CE marking. The integration of the accelerometry device into the Cloud for data storage and Internet of Things (IoT) for ease of data access can be explored. The development of a customised software for diagnostic features can be developed. The end goal is to develop a medical device to assist clinicians in diagnosing balance related dysfunctions.

References

1. Aartolahti, E., Häkkinen, A., Lönnroos, E., Kautiainen, H., Sulkava, R., & Hartikainen, S. (2013). Relationship between functional vision and balance and mobility performance in community-dwelling older adults. *Aging Clinical and Experimental Research*, *25*(5), 545-552. https://doi.org/10.1007/s40520-013-0120-z
2. Abdelzaher, H., El-Dokany, I., El-Dolil, S., Oraby, O., Dessouky, M., & El-Fishawy, A. et al. (2021). Noise reduction in optical gyroscope signals based on hybrid approaches. *Journal of Optics*. 1-17. https://doi.org/10.1007/s12596-020-00617-3
3. Abdollah, V., Dief, T. N., Ralston, J., Ho, C., & Rouhani, H. (2021). Investigating the validity of a single tri-axial accelerometer mounted on the head for monitoring the activities of daily living and the timed-up and go test. *Gait & posture*, *90*, 137–140. https://doi.org/10.1016/j.gaitpost.2021.08.020
4. Adlerton, A. K., Moritz, U., & Moe-Nilssen, R. (2003). Forceplate and accelerometer measures for evaluating the effect of muscle fatigue on postural control during one-legged stance. *Physiotherapy research international: the journal for researchers and clinicians in physical therapy*, *8*(4), 187–199. https://doi.org/10.1002/pri.289
5. Ageing and health. (2018). Retrieved 7 April 2021, from https://www.who.int/news-room/fact-sheets/detail/ageing-and-health#
6. Aguilera-Castells, J., Buscà, B., Arboix-Alió, J., McEwan, G., Calleja-González, J., & Peña, J. (2020). Correlational data concerning body centre of mass acceleration, muscle activity, and forces exerted during a suspended lunge under different stability conditions in high-standard track and field athletes. *Data in Brief, 28,* 104912-104926. https://doi.org/10.1016/j.dib.2019.104912
7. Alghwiri, A., & Whitney, S. (2020). Balance and falls in older adults. In D. Avers & R. Wong, *Guccione's Geriatric Physical Therapy* (4th ed., pp. 220-239). Elsevier. Retrieved 11 October 2021, from.
8. AlHinai, N. (2020). Introduction to biomedical signal processing and artificial intelligence. In W. Zgallai, *Developments in Biomedical Engineering and Bioelectronics, Biomedical Signal Processing and Artificial Intelligence in Healthcare* (pp. 1-28). Academic Press. Retrieved 14 December 2021, from.

9. Ali, F., Loushin, S., Botha, H., Josephs, K., Whitwell, J., & Kaufman, K. (2021). Laboratory based assessment of gait and balance impairment in patients with progressive supranuclear palsy. *Journal of The Neurological Sciences*, *429*, 118054-118060. https://doi.org/10.1016/j.jns.2021.118054
10. Alkathiry, A., Sparto, P., Freund, B., Whitney, S., Mucha, A., & Furman, J. et al. (2018). Using accelerometers to record postural sway in adolescents with concussion: A cross-sectional study. *Journal of Athletic Training*, *53*(12), 1166-1172. https://doi.org/10.4085/1062-6050-518-17
11. Allanson, P., & Notar, C. (2020). Statistics as measurement: 4 scales/levels of measurement. *Education Quarterly Reviews*, *3*(3), 375-385. https://doi.org/10.31014/aior.1993.03.03.146
12. Amir, N., Kamaruzzaman, S., Effendi-Tenang, I., Jamaluddin, M., Tan, M., & Ramli, N. et al. (2021). Contrast sensitivity is associated with frailty. *European Geriatric Medicine*, *12*(2), 313-319. https://doi.org/10.1007/s41999-021-00450-2
13. Analogue Device Incorporation. (2009). The five motion senses: using mems inertial sensing to transform applications. https://www.analog.com/en/technical-articles/the-five-motion-senses.html
14. Annor, P., Kwak, K., Kim, H., & Kim, D. (2021). Effect of local somatosensory stimulus on postural sway during sit-to-stand movement in the elderly. *BMC Musculoskeletal Disorders*, *22*(S1), 1-12. https://doi.org/10.1186/s12891-021-04609-7
15. Antoniadou, E., Kalivioti, X., Stolakis, K., Koloniari, A., Megas, P., Tyllianakis, M., & Panagiotopoulos, E. (2020). Reliability and validity of the mCTSIB dynamic platform test to assess balance in a population of older women living in the community. *Journal of musculoskeletal & neuronal interactions*, *20*(2), 185–193.
16. APDM wearable technologies Inc. (2020). User guide mobility lab; APDM wearable technologies Inc.: Portland, OR, USA.
17. Apostolova L. G. (2016). Alzheimer disease. *Continuum (Minneapolis, Minn.)*, *22*(2 Dementia), 419–434. https://doi.org/10.1212/CON.0000000000000307
18. Araujo, E., Bentes, G. E., & Zangaro, R. (2018). Body sway and global equilibrium condition of the elderly in quiet standing posture by using competitive neural networks. *Applied Soft Computing*, *69*, 625-633.
19. *Arduino - ArduinoBoardUno*. Arduino.cc. (2021). Retrieved 17 November 2021, from https://www.arduino.cc/en/pmwiki.php?n=Main/arduinoBoardUno.

20. *Arduino Nano*. Arduino official store. (2021). Retrieved 17 November 2021, from https://store.arduino.cc/products/arduino-nano.
21. *Arduino playground - MPU-6050*. Playground.arduino.cc. (2021). Retrieved 17 November 2021, from https://playground.arduino.cc/Main/MPU-6050/.
22. *Arduino Uno rev3*. Arduino official store. (2021). Retrieved 17 November 2021, from https://store.arduino.cc/products/arduino-uno-rev3.
23. Assländer, L., Hettich, G., & Mergner, T. (2015). Visual contribution to human standing balance during support surface tilts. *Human movement science*, *41*, 147–164. https://doi.org/10.1016/j.humov.2015.02.010
24. Bacsi, A. M., & Colebatch, J. G. (2005). Evidence for reflex and perceptual vestibular contributions to postural control. *Experimental brain research*, *160*(1), 22–28. https://doi.org/10.1007/s00221-004-1982-2
25. Bao L., Intille S.S. (2004). Activity recognition from user-annotated acceleration data. In: Ferscha A., Mattern F. (eds) Pervasive Computing. Pervasive 2004. Lecture Notes in Computer Science, vol 3001. Springer, Berlin, Heidelberg, 1-17. https://doi.org/10.1007/978-3-540-24646-6_1
26. Bao, T., Klatt, B. N., Whitney, S. L., Sienko, K. H., & Wiens, J. (2019). Automatically evaluating balance: A machine learning approach. *IEEE transactions on neural systems and rehabilitation engineering: a publication of the IEEE Engineering in Medicine and Biology Society*, *27*(2), 179–186. https://doi.org/10.1109/TNSRE.2019.2891000
27. Baracks, J., Casa, D., Covassin, T., Sacko, R., Scarneo, S., & Schnyer, D. et al. (2018). Acute sport-related concussion screening for collegiate athletes using an instrumented balance assessment. *Journal of Athletic Training*, *53*(6), 597-605. https://doi.org/10.4085/1062-6050-174-17
28. Baratto, L., Morasso, P. G., Re, C., & Spada, G. (2002). A new look at posturographic analysis in the clinical context: sway-density versus other parameterization techniques. *Motor control*, *6*(3), 246–270. https://doi.org/10.1123/mcj.6.3.246
29. Bardid, F., Vannozzi, G., Logan, S. W., Hardy, L. L., & Barnett, L. M. (2019). A hitchhiker's guide to assessing young people's motor competence: Deciding what method to use. *Journal of science and medicine in sport*, *22*(3), 311–318. https://doi.org/10.1016/j.jsams.2018.08.007

30. Barrachina-Fernández, M., Maitín, A., Sánchez-Ávila, C., & Romero, J. (2021). Wearable technology to detect motor fluctuations in Parkinson's disease patients: Current state and challenges. *Sensors, 21*(12), 4188-203. https://doi.org/10.3390/s21124188
31. Battaglia, G., Giustino, V., Tabacchi, G., Lanza, M., Schena, F., & Biino, V. et al. (2021). Interrelationship between age, gender, and weight status on motor coordination in Italian children and early adolescents aged 6–13 years old. *Frontiers in Pediatrics*, *9*, 1-10. https://doi.org/10.3389/fped.2021.738294
32. Bauer, C., Gröger, I., Rupprecht, R., & Gaßmann, K. (2008). Intrasession reliability of force platform parameters in community-dwelling older adults. *Archives of Physical Medicine and Rehabilitation*, *89*(10), 1977-1982. https://doi.org/10.1016/j.apmr.2008.02.033
33. Benvenuti, F., Mecacci, R., Gineprari, I., Bandinelli, S., Benvenuti, E., & Ferrucci, L. et al. (1999). Kinematic characteristics of standing disequilibrium: Reliability and validity of a posturographic protocol. *Archives of Physical Medicine and Rehabilitation*, *80*(3), 278-287. https://doi.org/10.1016/s0003-9993(99)90138-7
34. Bergh, R., Lefevre, H., & Shaw, H. (1984). An overview of fiber-optic gyroscopes. *Journal of Lightwave Technology*, *2*(2), 91-107. https://doi.org/10.1109/jlt.1984.1073580
35. Besnard, S., Lopez, C., Brandt, T., Denise, P., & Smith, P. F. (2015). Editorial: The vestibular system in cognitive and memory processes in mammalians. *Frontiers in integrative neuroscience*, *9*, 55. https://doi.org/10.3389/fnint.2015.00055
36. Besnard, S., Tighilet, B., Chabbert, C., Hitier, M., Toulouse, J., & Le Gall, A. et al. (2018). The balance of sleep: Role of the vestibular sensory system. *Sleep Medicine Reviews*, *42*, 220-228. https://doi.org/10.1016/j.smrv.2018.09.001
37. Bhatt, T., & Pai, Y. (2005). Long-term retention of gait stability Improvements. *Journal of neurophysiology*, *94*(3), 1971-1979. https://doi.org/10.1152/jn.00266.2005
38. Bianchi, F., Redmond, S. J., Narayanan, M. R., Cerutti, S., & Lovell, N. H. (2010). Barometric pressure and triaxial accelerometry-based falls event detection. *IEEE transactions on neural systems and rehabilitation engineering: a publication of the IEEE Engineering in Medicine and Biology Society*, *18*(6), 619–627. https://doi.org/10.1109/TNSRE.2010.2070807

39. Bieńkiewicz, M. M., Brandi, M. L., Goldenberg, G., Hughes, C. M., & Hermsdörfer, J. (2014). The tool in the brain: apraxia in ADL. Behavioral and neurological correlates of apraxia in daily living. *Frontiers in psychology*, *5*, 353-366. https://doi.org/10.3389/fpsyg.2014.00353
40. Bisdorff, A., Staab, J., & Newman-Toker, D. (2015). Overview of the international classification of vestibular disorders. *Neurologic Clinics*, *33*(3), 541-550. https://doi.org/10.1016/j.ncl.2015.04.010
41. Bland, J. M., & Altman, D. G. (1986). Statistical methods for assessing agreement between two methods of clinical measurement. *Lancet (London, England)*, *1*(8476), 307–310.
42. Bland, J. M., & Altman, D. G. (1999). Measuring agreement in method comparison studies. *Statistical methods in medical research*, *8*(2), 135–160. https://doi.org/10.1177/096228029900800204
43. Blank, R., Smits-Engelsman, B., Polatajko, H., Wilson, P., & European Academy for Childhood Disability (2012). European Academy for Childhood Disability (EACD): recommendations on the definition, diagnosis and intervention of developmental coordination disorder (long version). *Developmental medicine and child neurology*, *54*(1), 54–93. https://doi.org/10.1111/j.1469-8749.2011.04171.x
44. Błaszczyk, J. (2016). The use of force-plate posturography in the assessment of postural instability. *Gait & Posture*, *44*, 1-6. doi: 10.1016/j.gaitpost.2015.10.014
45. Błaszczyk, J. W., Beck, M., & Sadowska, D. (2014). Assessment of postural stability in young healthy subjects based on directional features of posturographic data: vision and gender effects. *Acta neurobiologiae experimentalis*, *74*(4), 433–442.
46. Błaszczyk, J. W., Beck, M., Szczepańska, J., Sadowska, D., Bacik, B., Juras, G., & Słomka, K. J. (2016). Directional measures of postural sway as predictors of balance instability and accidental falls. *Journal of human kinetics*, *52*, 75–83. https://doi.org/10.1515/hukin-2015-0195
47. Bloem, B. R., Allum, J. H., Carpenter, M. G., & Honegger, F. (2000). Is lower leg proprioception essential for triggering human automatic postural responses?. *Experimental brain research*, *130*(3), 375–391. https://doi.org/10.1007/s002219900259
48. Blum, L., & Korner-Bitensky, N. (2008). Usefulness of the Berg balance scale in stroke rehabilitation: A systematic review. *Physical Therapy*, *88*(5), 559-566. https://doi.org/10.2522/ptj.20070205

49. Borzì, L., Fornara, S., Amato, F., Olmo, G., Artusi, C., & Lopiano, L. (2020). Smartphone-based evaluation of postural stability in Parkinson's disease patients during quiet stance. *Electronics*, *9*(6), 919-933. https://doi.org/10.3390/electronics9060919
50. Boughen, J., Dunn, K., Nitz, J., Johnston, V., & Khan, A. (2013). A new method of interpreting the centre of gravity location using the modified Clinical Test of Sensory Interaction on Balance: A reliability study. *Hong Kong Physiotherapy Journal*, *31*(2), 64-68. https://doi.org/10.1016/j.hkpj.2013.04.002
51. Boyce, P. (2017). *Human factors in lighting, Third Edition*. CRC Press.
52. Bradley, P. (1989). The somatic motor system. In P. Bradley, *Introduction to Neuropharmacology* (pp. 35-42). Retrieved 14 December 2021, from.
53. Breyer, F., Font, J., & Felder, S. (2010). Ageing, health, and health care. *Oxford Review of Economic Policy*, *26*(4), 674–690. https://doi.org/10.1093/oxrep/grq032
54. Bronstein A. M. (2016). Multisensory integration in balance control. *Handbook of clinical neurology*, *137*, 57–66. https://doi.org/10.1016/B978-0-444-63437-5.00004-2
55. Bronstein, A., & Pavlou, M. (2013). Balance. In M. Barnes & D. Good, *Handbook of clinical neurology* (100th ed., pp. 189-208). Elsevier. Retrieved 13 December 2021, from.
56. Brunnekreef, J., van Uden, C., van Moorsel, S., & Kooloos, J. (2005). Reliability of videotaped observational gait analysis in patients with orthopedic impairments. *BMC Musculoskeletal Disorders*, *6*(1), 1-9. https://doi.org/10.1186/1471-2474-6-17
57. Bzdok, D. (2017). Classical statistics and statistical learning in imaging neuroscience. *Frontiers in Neuroscience*, *11*, 1-23. https://doi.org/10.3389/fnins.2017.00543
58. Bzdok, D., Altman, N., & Krzywinski, M. (2018). Statistics versus machine learning. *Nature Methods*, *15*(4), 233-234. https://doi.org/10.1038/nmeth.4642
59. Bzdok, D., Krzywinski, M., & Altman, N. (2017). Machine learning: a primer. *Nature Methods*, *14*(12), 1119-1120. https://doi.org/10.1038/nmeth.4526
60. Cabarkapa, D., Fry, A., & Hermes, M. (2021). Accuracy of an experimental accelerometer for assessing countermovement vertical jump height. *Sports Innovation Journal*, *2*, 45-55. https://doi.org/10.18060/24831

61. Cattell, R., & Vogelmann, S. (1977). A comprehensive trial of the scree and kg criteria for Determining the Number of Factors. *Multivariate Behavioural Research*, *12*(3), 289-325. https://doi.org/10.1207/s15327906mbr1203_2
62. Caughey, G., Ramsay, E., Vitry, A., Gilbert, A., Luszcz, M., Ryan, P., & Roughead, E. (2009). Comorbid chronic diseases, discordant impact on mortality in older people: a 14-year longitudinal population study. *Journal of Epidemiology & Community Health*, *64*(12), 1036-1042. https://doi.org/10.1136/jech.2009.088260
63. Caughey, G., Roughead, E., Pratt, N., Shakib, S., Vitry, A., & Gilbert, A. (2010). Increased risk of hip fracture in the elderly associated with prochlorperazine: is a prescribing cascade contributing?. *Pharmacoepidemiology and Drug Safety*, *19*(9), 977-982. https://doi.org/10.1002/pds.2009
64. Caughey, G., Roughead, E., Vitry, A., McDermott, R., Shakib, S., & Gilbert, A. (2010). Comorbidity in the elderly with diabetes: Identification of areas of potential treatment conflicts. *Diabetes Research and Clinical Practice*, *87*(3), 385-393. https://doi.org/10.1016/j.diabres.2009.10.019
65. Ceccarelli, M., Petrosino, A., & Vaccaro, R. (1993). Competitive neural networks on message-passing parallel computers. *Concurrency: Practice and Experience*, *5*(6), 449-470.
66. Chaumont, H., San-Galli, A., Martino, F., Couratier, C., Joguet, G., & Carles, M. et al. (2020). Mixed central and peripheral nervous system disorders in severe SARS-CoV-2 infection. *Journal of Neurology*, *267*(11), 3121-3127. https://doi.org/10.1007/s00415-020-09986-y
67. Chen X. (2005) Adaptive filtering based on the wavelet transform for FoG on the moving base. In: Huang DS., Zhang XP., Huang GB. (eds) Advances in Intelligent Computing. ICIC 2005. Lecture Notes in Computer Science, vol 3644. Springer, Berlin, Heidelberg. https://doi.org/10.1007/11538059_47
68. Chen, B., Liu, P., Xiao, F., Liu, Z., & Wang, Y. (2021). Review of the upright balance assessment based on the force plate. *International Journal of Environmental Research and Public Health*, *18*(5), 2696-2710. https://doi.org/10.3390/ijerph18052696
69. Chiba, R., Takakusaki, K., Ota, J., Yozu, A., & Haga, N. (2016). Human upright posture control models based on multisensory inputs; in fast and slow dynamics. *Neuroscience Research*, *104*, 96-104. https://doi.org/10.1016/j.neures.2015.12.002

70. Clark, R., Szpak, A., Michalski, S., & Loetscher, T. (2021). Rest intervals during virtual reality gaming augments standing postural sway disturbance. *Sensors*, *21*(20), 6817-6827. https://doi.org/10.3390/s21206817

71. Cohen, H. S., Mulavara, A. P., Stitz, J., Sangi-Haghpeykar, H., Williams, S. P., Peters, B. T., & Bloomberg, J. J. (2019). Screening for vestibular disorders using the modified Clinical Test of Sensory Interaction and Balance and tandem walking with eyes closed. *Otology & neurotology: official publication of the American Otological Society, American Neurotology Society [and] European Academy of Otology and Neurotology*, *40*(5), 658–665. https://doi.org/10.1097/MAO.0000000000002173

72. Cohen, H., Blatchly, C. A., & Gombash, L. L. (1993). A study of the clinical test of sensory interaction and balance. *Physical therapy*, *73*(6), 346–354. https://doi.org/10.1093/ptj/73.6.346

73. Collins, J. J., & De Luca, C. J. (1993). Open-loop and closed-loop control of posture: a random-walk analysis of center-of-pressure trajectories. *Experimental brain research*, *95*(2), 308–318. https://doi.org/10.1007/BF00229788

74. Corriveau, H., Hébert, R., Prince, F., & Raîche, M. (2000). Intrasession reliability of the "center of pressure minus center of mass" variable of postural control in the healthy elderly. *Archives of physical medicine and rehabilitation*, *81*(1), 45–48. https://doi.org/10.1016/s0003-9993(00)90220-x

75. Croarkin, E., & Zampieri, C. (2021). On the edge of task force recommendations: computerized balance assessment. *Rehabilitation Oncology*, *39*(1), 64-67. https://doi.org/10.1097/01.reo.0000000000000246

76. Culhane, K. M., O'Connor, M., Lyons, D., & Lyons, G. M. (2005). Accelerometers in rehabilitation medicine for older adults. *Age and ageing*, *34*(6), 556–560. https://doi.org/10.1093/ageing/afi192

77. Cury, A., Pinto, R., Madaleno, F., & Resende, R. (2021). Do older adults present altered pelvic and trunk movement pattern during gait? A systematic review with meta-analysis and GRADE recommendations. *Brazilian Journal of Physical Therapy*,*15*,484-499. https://doi.org/10.1016/j.bjpt.2021.01.003

78. Dadafshar, M. (2014). Accelerometer and gyroscopes sensors: operation, sensing and applications. Retrieved 4 October 2021, from https://www.maximintegrated.com/en/design/technical-documents/app-notes/5/5830.html

79. Larose, D. (2006). *Data mining methods and models*. Wiley.

80. Davies, D., & Bouldin, D. (1979). A cluster separation measure. *IEEE Transactions on Pattern Analysis and Machine Intelligence, PAMI-1*(2), 224-227. https://doi.org/10.1109/tpami.1979.4766909

81. Daud, S., Rahman, M. U., Arsh, A., & Junaid, M. (2021). Effect of balance training with Biodex Balance System to improve balance in patients with diabetic neuropathy: A quasi experimental study. *Pakistan journal of medical sciences*, *37*(2), 389–392. https://doi.org/10.12669/pjms.37.2.2336

82. de Cheveigné, A., & Nelken, I. (2019). Filters: When, why, and how (not) to use them. *Neuron*, *102*(2), 280-293. https://doi.org/10.1016/j.neuron.2019.02.039

83. de Winter, J. C., Gosling, S. D., & Potter, J. (2016). Comparing the Pearson and Spearman correlation coefficients across distributions and sample sizes: A tutorial using simulations and empirical data. *Psychological methods*, *21*(3), 273–290. https://doi.org/10.1037/met0000079

84. della Volpe, R., Popa, T., Ginanneschi, F., Spidalieri, R., Mazzocchio, R., & Rossi, A. (2006). Changes in coordination of postural control during dynamic stance in chronic low back pain patients. *Gait & posture*, *24*(3), 349–355. https://doi.org/10.1016/j.gaitpost.2005.10.009

85. Delleman, N., Haslegrave, C., & Chaffin, D. (2004). *Working postures and movements: Tools for evaluation and engineering* (1st ed.). CRC Press.

86. Deshpande, S., Gogtay, N., & Thatte, U. (2016). Data types. *The Journal of the Association of Physicians of India*, *64*(6), 64–65.

87. Diao, Z., Quan, H., Lan, L., & Han, Y. (2013). Analysis and compensation of MEMS gyroscope drift. In *2013 Seventh International Conference on Sensing Technology (ICST)* (pp. 592-596). Wellington, New Zealand; IEEE. Retrieved 20 October 2021, from.

88. Dostál, O., Procházka, A., Vyšata, O., Ťupa, O., Cejnar, P., & Vališ, M. (2020). Recognition of motion patterns using accelerometers for ataxic gait assessment. *Neural Computing and Applications*, *33*(7), 2207-2215. https://doi.org/10.1007/s00521-020-05103-2

89. du Prel, J., Röhrig, B., Hommel, G., & Blettner, M. (2010). Choosing statistical tests. *Deutsches Aerzteblatt Online 107*(19), 343-351. https://doi.org/10.3238/arztebl.2010.0343
90. Duan, Y., Zhang, X., & Li, Z. (2020). A new quaternion-based kalman filter for human body motion tracking using the second estimator of the optimal quaternion algorithm and the joint angle constraint method with inertial and magnetic Sensors. *Sensors*, *20*(21), 6018-6037. https://doi.org/10.3390/s20216018
91. Duarte, M., & Freitas, S. M. (2010). Revision of posturography based on force plate for balance evaluation. *Revista brasileira de fisioterapia (Sao Carlos (Sao Paulo, Brazil))*, *14*(3), 183–192.
92. Dugan, E., Shilt, J., Masterson, C., & Ernest, K. (2021). The use of inertial measurement units to assess gait and postural control following concussion. *Gait & Posture*, *83*, 262-267. https://doi.org/10.1016/j.gaitpost.2020.10.004
93. Eastlack, M. E., Arvidson, J., Snyder-Mackler, L., Danoff, J. V., & McGarvey, C. L. (1991). Interrater reliability of videotaped observational gait-analysis assessments. *Physical therapy*, *71*(6), 465–472. https://doi.org/10.1093/ptj/71.6.465
94. Ellis, G. (2012). *Control system design guide: Using your computer to understand and diagnose feedback controllers Ed. 4* (pp. 165-183). Elsevier Science.
95. Elvan, A., & Ozyurek, S. (2020). Principles of kinesiology. In S. Angin & I. Şimşek, *Comparative Kinesiology of the Human Body: Normal and Pathological Conditions* (pp. 13-27). Academic Press. Retrieved 19 October 2021, from.
96. Emmert-Streib, F., & Dehmer, M. (2019). Understanding statistical hypothesis testing: The logic of statistical inference. *Machine Learning and Knowledge Extraction*, *1*(3), 945-961. https://doi.org/10.3390/make1030054
97. Ercan, S., Baskurt, Z., Baskurt, F., & Cetin, C. (2020). Balance disorder, falling risks and fear of falling in obese individuals: cross-sectional clinical research in Isparta. JPMA. The Journal of the Pakistan Medical Association, 70(1), 17–23. https://doi.org/10.5455/JPMA.293668
98. Estévez-Pedraza, Á., Martínez-Méndez, R., Portillo-Rodríguez, O., & Parra-Rodríguez, L. (2020). Portable device for the measurement and assessment of the human equilibrium. *Annals of Biomedical Engineering*, *49*(2), 933-945. https://doi.org/10.1007/s10439-020-02630-w
99. Fábrega-Cuadros, R., Aibar-Almazán, A., Martínez-Amat, A., & Hita-Contreras, F. (2020). Impact of psychological distress and sleep quality on balance confidence,

muscle strength, and functional balance in community-dwelling middle-aged and older people. *Journal of Clinical Medicine*, *9*(9), 3059-3016. https://doi. 10.3390/jcm9093059

100. Fernandez, C., & Goldberg, J. (1976). Physiology of peripheral neurons innervating otolith organs of the squirrel monkey. III. Response dynamics. *Journal of Neurophysiology*, *39*(5), 996-1008. https://doi.org/10.1152/jn.1976.39.5.996
101. Fisher, M., & Marshall, A. (2009). Understanding descriptive statistics. *Australian Critical Care*, *22*(2), 93-97. https://doi.org/10.1016/j.aucc.2008.11.003
102. Fitzpatrick, R., & McCloskey, D. (1994). Proprioceptive, visual and vestibular thresholds for the perception of sway during standing in humans. *The Journal of Physiology*, *478*(1), 173-186. https://doi.org/10.1113/jphysiol.1994.sp020240
103. Franco, F., & Di Napoli, A. (2017). Measures of association in medicine and epidemiology. *Giornale Di Tecniche Nefrologiche E Dialitiche*, *29*(2), 127-128. https://doi.org/10.5301/gtnd.2017.16951
104. Fujimoto, M., Bair, W. N., & Rogers, M. W. (2015). Centre of pressure control for balance maintenance during lateral waist-pull perturbations in older adults. *Journal of biomechanics*, *48*(6), 963–968. https://doi.org/10.1016/j.jbiomech.2015.02.012
105. Fukuoka, Y., Nagata, T., Ishida, A., & Minamitani, H. (2001). Characteristics of somatosensory feedback in postural control during standing. *IEEE transactions on neural systems and rehabilitation engineering: a publication of the IEEE Engineering in Medicine and Biology Society*, *9*(2), 145–153. https://doi.org/10.1109/7333.928574
106. Gage, W. H., Winter, D. A., Frank, J. S., & Adkin, A. L. (2004). Kinematic and kinetic validity of the inverted pendulum model in quiet standing. *Gait & posture*, *19*(2), 124–132. https://doi.org/10.1016/S0966-6362(03)00037-7
107. García-Liñeira, J., García-Soidán, J., Romo-Pérez, V., & Leirós-Rodríguez, R. (2020). Reliability of accelerometric assessment of balance in children aged 6–12 years. *BMC Pediatrics*, *20*(1), 1-8. https://doi.org/10.1186/s12887-020-02073-1
108. Gemperle, F., Kasabach, C., Stivoric, J., Bauer, M., & Martin, R. (1998). Design for wearability. In *Digest of Papers. Second International Symposium on Wearable Computers (Cat. No.98EX215)* (pp. 116–122). Pittsburgh, PA, USA; IEEE. Retrieved 18 October 2021, from.
109. Gerasimenko, Y., Sayenko, D., Gad, P., Liu, C. T., Tillakaratne, N., Roy, R. R., Kozlovskaya, I., & Edgerton, V. R. (2017). Feed-forwardness of spinal networks in

posture and locomotion. *The Neuroscientist: a review journal bringing neurobiology, neurology and psychiatry*, *23*(5), 441–453. https://doi.org/10.1177/1073858416683681

110. Gesicho, M., Were, M., & Babic, A. (2021). Evaluating performance of health care facilities at meeting HIV-indicator reporting requirements in Kenya: an application of K-means clustering algorithm. *BMC Medical Informatics and Decision Making*, *21*(1), 1-18. https://doi.org/10.1186/s12911-020-01367-9
111. Geuze, R. (2003). Static balance and developmental coordination disorder. *Human Movement Science*, *22*(4-5), 527-548. https://doi.org/10.1016/j.humov.2003.09.008
112. Ghanavati, T., Shaterzadeh Yazdi, M., Goharpey, S., & Arastoo, A. (2012). Functional balance in elderly with diabetic neuropathy. *Diabetes Research and Clinical Practice*, *96*(1), 24-28. https://doi.org/10.1016/j.diabres.2011.10.041
113. Ghislieri, M., Gastaldi, L., Pastorelli, S., Tadano, S., & Agostini, V. (2019). Wearable inertial sensors to assess standing balance: A systematic review. *Sensors*, *19*(19), 4075-4100. https://doi.org/10.3390/s19194075
114. Giavarina D. (2015). Understanding Bland Altman analysis. *Biochemia medica*, *25*(2), 141–151. https://doi.org/10.11613/BM.2015.015
115. Giersch, A., Boucart, M., Speeg-Schatz, C., Muller-Kauffmann, F., & Danion, J. (1996). Lorazepam impairs perceptual integration of visual forms: a central effect. *Psychopharmacology*, *126*(3), 260-270. https://doi.org/10.1007/bf02246456
116. Giladi, N., & Nieuwboer, A. (2008). Understanding and treating freezing of gait in parkinsonism, proposed working definition, and setting the stage. *Movement disorders: official journal of the Movement Disorder Society*, *23 Suppl 2*, S423–S425. https://doi.org/10.1002/mds.21927
117. Glasser, A., & Campbell, M. C. (1999). Biometric, optical and physical changes in the isolated human crystalline lens with age in relation to presbyopia. *Vision research*, *39*(11), 1991–2015. https://doi.org/10.1016/s0042-6989(98)00283-1
118. Gogtay, N. J., & Thatte, U. M. (2017). Principles of Correlation Analysis. *The Journal of the Association of Physicians of India*, *65*(3), 78–81.
119. Gogtay, N. J., Deshpande, S. P., & Thatte, U. M. (2017). Principles of regression analysis. *The Journal of the Association of Physicians of India*, *65*(4), 48–52.
120. Goldenberg M. M. (2012). Multiple sclerosis review. *P & T: a peer-reviewed journal for formulary management*, *37*(3), 175–184.

121. Gonzalez, S., Stegall, P., Edwards, H., Stirling, L., & Siu, H. (2020). Ablation analysis to select wearable sensors for classifying standing, walking, and running. *Sensors*, *21*(1), 194-214. https://doi.org/10.3390/s21010194
122. Graf, W., & Klam, F. (2006). Le système vestibulaire: anatomie fonctionnelle et comparée, évolution et développement. *Comptes Rendus Palevol*, *5*(3-4), 637-655. https://doi.org/10.1016/j.crpv.2005.12.009
123. Gray, J.R., Grove, S.K., & Sutherland, S. (2017). Burns and Grove's the practice of nursing research: Appraisal, synthesis, and generation of evidence (8th ed.). Elsevier.
124. Grimshaw, P., Cole, M., Burden, A., & Fowler, N. (2019). *Instant notes in sport and exercise biomechanics*. Taylor & Francis Group.
125. Hair, J.F., Anderson, R.E., et al. (1998) Multivariate data analysis with readings. Prentice-Hall, Englewood Cliffs, NJ.
126. Hall, E. A., Chomistek, A. K., Kingma, J. J., & Docherty, C. L. (2018). Balance- and strength-training protocols to improve chronic ankle instability deficits, Part I: Assessing clinical outcome measures. *Journal of athletic training*, *53*(6), 568–577. https://doi.org/10.4085/1062-6050-385-16
127. Hamill, J., Knutzen, K., & Derrick, T. (2021). *Biomechanical basis of human movement* (5th ed.). Wolters Kluwer Health.
128. Harrell, R., Manetta, C., & Gorgacz, M. (2021). Dizziness and balance disorders in a traumatic brain injury population: Current clinical approaches. *Current Physical Medicine and Rehabilitation Reports*, *9*(2), 41-46. https://doi.org/10.1007/s40141-021-00308-5
129. Hartigan, J., & Wong, M. (1979). Algorithm AS 136: A K-Means clustering algorithm. *Applied Statistics*, *28*(1), 100-108. https://doi.org/10.2307/2346830
130. Hasegawa, N., Maas, K., Shah, V., Carlson-Kuhta, P., Nutt, J., & Horak, F. et al. (2021). Functional limits of stability and standing balance in people with Parkinson's disease with and without freezing of gait using wearable sensors. *Gait & Posture*, *87*, 123-129. https://doi.org/10.1016/j.gaitpost.2021.04.023
131. Hasegawa, N., Shah, V. V., Carlson-Kuhta, P., Nutt, J. G., Horak, F. B., & Mancini, M. (2019). How to select balance measures sensitive to Parkinson's disease from body-worn inertial sensors-separating the trees from the forest. *Sensors (Basel, Switzerland)*, *19*(15), 3320-3338. https://doi.org/10.3390/s19153320

132. Herculano-Houzel, S. (2009). The human brain in numbers: a linearly scaled-up primate brain. *Frontiers in Human Neuroscience*, *3*, 1-11. https://doi.org/10.3389/neuro.09.031.2009
133. Hergenroeder, A., Wert, D., Hile, E., Studenski, S., & Brach, J. (2011). Association of body mass index with self-report and performance-based measures of balance and mobility. *Physical Therapy*, *91*(8), 1223-1234. https://doi.org/10.2522/ptj.20100214
134. Hess, A., & Hess, J. (2018). Analysis of variance. *Transfusion*, *58*(10), 2255-2256. https://doi.org/10.1111/trf.14790
135. Hill, M., Duncan, M., & Price, M. (2020). The emergence of age-related deterioration in dynamic, but not quiet standing balance abilities among healthy middle-aged adults. *Experimental Gerontology*, *140*, 111076-111087. https://doi.org/10.1016/j.exger.2020.111076
136. Hillier, S. L., Hiller, J. E., & Metzer, J. (1997). Epidemiology of traumatic brain injury in South Australia. *Brain injury*, *11*(9), 649–659. https://doi.org/10.1080/026990597123205
137. Hipsley, A., & Hall, B. (2021). Influence of ocular rigidity and ocular biomechanics on the pathogenesis of age-related presbyopia. In I. Pallikaris, M. Tsilimbaris & A. Dastiridou, *Ocular Rigidity, Biomechanics and Hydrodynamics of the Eye* (1st ed., pp. 27-146). Springer, Cham. Retrieved 5 December 2021, from.
138. Ho, R. (2006). *Handbook of univariate and multivariate data analysis and interpretation with SPSS*. Chapman & Hall/CRC.
139. Hof, A., Gazendam, M., & Sinke, W. (2005). The condition for dynamic stability. *Journal of Biomechanics*, *38*(1), 1-8. https://doi.org/10.1016/j.jbiomech.2004.03.025
140. Hoffman, J. (2019). *Biostatistics for medical and biomedical practitioners Ed. 2*. Elsevier Science.
141. *Home - Xsens 3D motion tracking*. Xsens.com. (2021). Retrieved 30 November 2021, from https://www.xsens.com/.
142. Honeine, J. L., & Schieppati, M. (2014). Time-interval for integration of stabilizing haptic and visual information in subjects balancing under static and dynamic conditions. *Frontiers in systems neuroscience*, *8*, 190-205. https://doi.org/10.3389/fnsys.2014.00190

143. Horak, F. B., & Nashner, L. M. (1986). Central programming of postural movements: adaptation to altered support-surface configurations. *Journal of neurophysiology*, *55*(6), 1369–1381. https://doi.org/10.1152/jn.1986.55.6.1369
144. Horak, F.B. (1987). Clinical measurement of postural control in adults. *Physical Therapy*, *67*(12), 1881-1885. https://doi.org/10.1093/ptj/67.12.1881
145. Horak, F.B. (1997). Clinical assessment of balance disorders. *Gait & Posture*, *6*(1), 76-84. https://doi.org/10.1016/s0966-6362(97)00018-0
146. Horak, F.B. (2006). Postural orientation and equilibrium: what do we need to know about neural control of balance to prevent falls?. *Age and Ageing*, *35*(suppl_2), ii7-ii11. https://doi.org/10.1093/ageing/afl077
147. Hou, Y., Chiu, Y., Chiang, S., Chen, H., & Sung, W. (2019). Development of a smartphone-based balance assessment system for subjects with stroke. *Sensors*, *20*(1), 88-97. https://doi.org/10.3390/s20010088
148. Htun, Z., Latt, M., New, C., & Mon, S. (2018). Performance comparison of experimental-based Kalman filter and complementary filter for IMU sensor fusion by applying quadrature encoder. *International Journal of Scientific and Research Publications (IJSRP)*, *8*(11), 1-8. https://doi.org/10.29322/ijsrp.8.11.2018.p8304
149. Huang, A. (2008) Similarity measures for text document clustering. In Proceedings of the Sixth New Zealand Computer Science Research Student Conference, Christchurch, New Zealand, 49–56.
150. Ibara, T., Takahashi, M., Shinkoda, K., Kawashima, M., & Anan, M. (2021). Hip sway in patients with hip osteoarthritis during one-leg standing with a focus on time series data. *Motor Control*, *25*(3), 502-518. https://doi.org/10.1123/mc.2020-0055
151. Ihlen, E. A., Skjæret, N., & Vereijken, B. (2013). The influence of centre-of-mass movements on the variation in the structure of human postural sway. *Journal of biomechanics*, *46*(3), 484–490. https://doi.org/10.1016/j.jbiomech.2012.10.016
152. Im, C., Kim, D., Yun, J., & Park, J. (2021). Compensatory postural responses to backward loss of balance in patients with cerebellar disease. *Gait & Posture*, *86*, 7-12. https://doi.org/10.1016/j.gaitpost.2021.02.027
153. Invensense.(n.d.). MPU-6050 six-axis (gyro + accelerometer) MEMs MotionTracking™ device. https://invensense.tdk.com/products/motion-tracking/6-axis/mpu-6050/

154. Irimia, A., & Van Horn, J. (2021). Mapping the rest of the human connectome: Atlasing the spinal cord and peripheral nervous system. *Neuroimage*, *225*, 117478-117496. https://doi.org/10.1016/j.neuroimage.2020.117478
155. Jacobs R. (1997). Control model of human stance using fuzzy logic. *Biological cybernetics*, *77*(1), 63–70. https://doi.org/10.1007/s004220050367
156. Jain, A. (2010). Data clustering: 50 years beyond K-means. *Pattern Recognition Letters*, *31*(8), 651-666. https://doi.org/10.1016/j.patrec.2009.09.011
157. Janc, M., Sliwinska-Kowalska, M., Jozefowicz-Korczynska, M., Marciniak, P., Rosiak, O., & Kotas, R. et al. (2021). A comparison of head movements tests in force plate and accelerometer based posturography in patients with balance problems due to vestibular dysfunction. *Scientific Reports*, *11*(1), 1-9. https://doi.org/10.1038/s41598-021-98695-1
158. Janse, R., Hoekstra, T., Jager, K., Zoccali, C., Tripepi, G., Dekker, F., & van Diepen, M. (2021). Conducting correlation analysis: important limitations and pitfalls. *Clinical Kidney Journal*, *14*(11), 2332-2337. https://doi.org/10.1093/ckj/sfab085
159. Jaworski, J., & Kołodziej, E. (2020). Assessment of postural stability using the Zebris Platform in women above the age of 60. *Journal of Kinesiology and Exercise Sciences*, *30*(92), 13-18. https://doi.org/10.5604/01.3001.0014.8210
160. Johansson, R., & Magnusson, M. (1991). Human postural dynamics. *Critical reviews in biomedical engineering*, *18*(6), 413–437.
161. Jolliffe, I., & Cadima, J. (2016). Principal component analysis: a review and recent developments. *Philosophical Transactions of the Royal Society A: Mathematical, Physical and Engineering Sciences*, *374*(2065), 20150202-20150218. https://doi.org/10.1098/rsta.2015.0202
162. Jun, J., & Yanling, L. (2021). The effect of physical activity intensity on the growth and development of 3–6 years old preschool children. *The International Journal of Electrical Engineering & Education*, 1-12. https://doi.org/10.1177/00207209211013464
163. Kabade, V., Hooda, R., Raj, C., Awan, Z., Young, A., Welgampola, M., & Prasad, M. (2021). Machine learning techniques for differential diagnosis of vertigo and dizziness: A review. *Sensors*, *21*(22), 7565-7582. https://doi.org/10.3390/s21227565
164. Kaiser, H. (1958). The varimax criterion for analytic rotation in factor analysis. *Psychometrika*, *23*(3), 187-200. https://doi.org/10.1007/bf02289233

165. Kamran, F., Harrold, K., Zwier, J., Carender, W., Bao, T., Sienko, K., & Wiens, J. (2021). Automatically evaluating balance using machine learning and data from a single inertial measurement unit. *Journal of Neuroengineering and Rehabilitation*, *18*(1), 1-7. https://doi.org/10.1186/s12984-021-00894-4
166. Kapteyn, T. S., Bles, W., Njiokiktjien, C. J., Kodde, L., Massen, C. H., & Mol, J. M. (1983). Standardization in platform stabilometry being a part of posturography. *Agressologie: revue internationale de physio-biologie et de pharmacologie appliquees aux effets de l'agression*, *24*(7), 321–326.
167. Karantonis, D. M., Narayanan, M. R., Mathie, M., Lovell, N. H., & Celler, B. G. (2006). Implementation of a real-time human movement classifier using a triaxial accelerometer for ambulatory monitoring. *IEEE transactions on information technology in biomedicine: a publication of the IEEE Engineering in Medicine and Biology Society*, *10*(1), 156–167. https://doi.org/10.1109/titb.2005.856864
168. Karimi, M. T., & Solomonidis, S. (2011). The relationship between parameters of static and dynamic stability tests. *Journal of Research in Medical Sciences*, *16*(4), 530-535.
169. Karthikbabu, S., & Verheyden, G. (2020). Relationship between trunk control, core muscle strength and balance confidence in community-dwelling patients with chronic stroke. *Topics in Stroke Rehabilitation*, *28*(2), 88-95. https://doi.org/10.1080/10749357.2020.1783896
170. Kashyap, B., Phan, D., Pathirana, P., Horne, M., Power, L., & Szmulewicz, D. (2020). Objective assessment of cerebellar ataxia: A comprehensive and refined approach. *Scientific Reports*, *10*(1), 1-17. https://doi.org/10.1038/s41598-020-65303-7
171. Kaufman, K., & An, K. (2017). Biomechanics. In G. Firestein, R. Budd, S. Gabriel, I. McInnes & J. O'Dell, *Kelley and Firestein's Textbook of Rheumatology* (10th ed., pp. 78-89). Elsevier. Retrieved 19 October 2021, from.
172. Kavanagh, J., & Menz, H. (2008). Accelerometry: A technique for quantifying movement patterns during walking. *Gait & Posture*, *28*(1), 1-15. https://doi.org/10.1016/j.gaitpost.2007.10.010
173. Khan, K., & Andersen, H. (2021). The impact of diabetic neuropathy on activities of daily living, postural balance and risk of falls - A systematic review. *Journal of Diabetes Science and Technology*, 193229682199792. https://doi.org/10.1177/1932296821997921

174. Khera, P., & Kumar, N. (2020). Role of machine learning in gait analysis: a review. *Journal of Medical Engineering & Technology*, *44*(8), 441-467. https://doi.org/10.1080/03091902.2020.1822940
175. Kim H. Y. (2014). Analysis of variance (ANOVA) comparing means of more than two groups. *Restorative dentistry & endodontics*, *39*(1), 74–77. https://doi.org/10.5395/rde.2014.39.1.74
176. Kim, C., Yu, I., & Song, Y. (2002). Kohonen neural network and wavelet transform based approach to short-term load forecasting. *Electric Power Systems Research*, *63*(3), 169-176. https://doi.org/10.1016/s0378-7796(02)00097-4
177. Kim, S.D., Allen, N.E., Canning, C.G., Fung, V.S.C. (2018). Parkinson disease. *Handbook of Clinical Neurology*, 159, 173-193.
178. Kim, T. (2015). T test as a parametric statistic. *Korean Journal of Anesthesiology*, *68*(6), 540-546. https://doi.org/10.4097/kjae.2015.68.6.540
179. Kingma, H., Gauchard, G. C., de Waele, C., van Nechel, C., Bisdorff, A., Yelnik, A., Magnusson, M., & Perrin, P. P. (2011). Stocktaking on the development of posturography for clinical use. *Journal of vestibular research: equilibrium & orientation*, *21*(3), 117–125. https://doi.org/10.3233/VES-2011-0397
180. Klingner, C., & Witte, O. (2018). Somatosensory deficits. In G. Vallar & H. Coslett, *The Parietal Lobe* (pp. 185-206). Elsevier. Retrieved 5 December 2021, from.
181. Klunk, D., Woost, T., Fricke, C., Classen, J., & Weise, D. (2021). Differentiating neurodegenerative parkinsonian syndromes using vestibular evoked myogenic potentials and balance assessment. *Clinical Neurophysiology*, *132*(11), 2808-2819. https://doi.org/10.1016/j.clinph.2021.08.012
182. Kodinariya, T. M., & Makwana, P. R. (2013). Review on determining number of cluster in K-means clustering. *International Journal*, *1*(6),90-95.
183. Kohonen T. (2013). Essentials of the self-organizing map. *Neural networks: The official journal of the International Neural Network Society*, *37*, 52–65. https://doi.org/10.1016/j.neunet.2012.09.018
184. Kohonen, T. (1990). The self-organizing map. *Proceedings of The IEEE*, *78*(9), 1464-1480. https://doi.org/10.1109/5.58325
185. Kováčiková, Z., Sarvestan, J., & Zemková, E. (2021). Age-related differences in stair descent balance control: Are women more prone to falls than men?. *PLOS ONE*, *16*(1), e0244990- e0245001. https://doi.org/10.1371/journal.pone.0244990

186. Krishna, K. V. S. (2021). Energy production by conservation of angular momentum (energy production in the scale of type-1 civilization from the rotation of a planet). *International Journal of Research in Engineering, Science and Management*, *4*(2), 73–77. Retrieved from https://www.journals.resaim.com/ijresm/article/view/505
187. Kristinsdottir, E. K., Fransson, P. A., & Magnusson, M. (2001). Changes in postural control in healthy elderly subjects are related to vibration sensation, vision and vestibular asymmetry. *Acta oto-laryngologica*, *121*(6), 700–706. https://doi.org/10.1080/00016480152583647
188. Lapointe, A., Ritchie, J., Vitali, R., Burma, J., Soroush, A., Oni, I., & Dunn, J. (2021). Internal consistency of sway measures via embedded head-mounted accelerometers: implications for neuromotor investigations. *Sensors*, *21*(13), 4492-4502. https://doi.org/10.3390/s21134492
189. Larose, D., & Larose, C. (2014). *Discovering knowledge in data* (2nd ed.). Wiley.
190. Lawrence, R. D., Almasi, G. S., & Rushmeier, H. E. (1999). A scalable parallel algorithm for self-organizing maps with applications to sparse data mining problems. *Data Mining and Knowledge Discovery*, *3*(2), 171-195.
191. Leirós-Rodríguez, R., García-Soidán, J., & Romo-Pérez, V. (2019). Analyzing the use of accelerometers as a method of early diagnosis of alterations in balance in elderly people: A systematic review. *Sensors*, *19*(18), 3883-3907. https://doi.org/10.3390/s19183883
192. Li, C., Hoffman, H., Ward, B., Cohen, H., & Rine, R. (2016). Epidemiology of dizziness and balance problems in children in the United States: A population-based study. *The Journal of Pediatrics*, *171*, 240-247. https://doi.org/10.1016/j.jpeds.2015.12.002
193. Li, T., Xue, T., Wang, B., & Zhang, J. (2018). Decoding voluntary movement of single hand based on analysis of brain connectivity by using EEG signals. *Frontiers in Human Neuroscience*, *12*, 381-395. https://doi.org/10.3389/fnhum.2018.00381
194. Liberson, W. T., Holmquest, H. J., & Halls, A. (1962). Accelerographic study of gait. *Archives of physical medicine and rehabilitation*, *43*, 547–551.
195. Lima Rebêlo, F., Fellipe de Souza Silva, L., Gomes de Araújo Filho, H., Sales Barreto, A., & Souza Siqueira Quintans, J. (2021). Dizziness is a predictor factor for the risk of falls in institutionalised older adults in Brazil. *Health & Social Care in the Community*, 1-9. https://doi.org/10.1111/hsc.13477

196. Lindemann, U., Hock, A., Stuber, M., Keck, W., & Becker, C. (2005). Evaluation of a fall detector based on accelerometers: A pilot study. *Medical & Biological Engineering & Computing*, *43*(5), 548-551. https://doi.org/10.1007/bf02351026
197. Liszka-Hackzell, J., & Martin, D. (2005). Analysis of nighttime activity and daytime pain in patients with chronic back pain using a self-organizing map neural network. *Journal of Clinical Monitoring and Computing*, *19*(6), 411-414. https://doi.org/10.1007/s10877-005-0392-8
198. Liu, K., Zhang, W., Chen, W., Li, K., Dai, F., & Cui, F. et al. (2009). The development of micro-gyroscope technology. *Journal of Micromechanics and Microengineering*, *19*(11), 113001-1130031. https://doi.org/10.1088/0960-1317/19/11/113001
199. Liu, Y., Mu, Y., Chen, K., Li, Y., & Guo, J. (2020). Daily activity feature selection in smart homes based on Pearson correlation coefficient. *Neural Processing Letters*, *51*(2), 1771-1787. https://doi.org/10.1007/s11063-019-10185-8
200. Lopez-Escamez, J. A., Carey, J., Chung, W. H., Goebel, J. A., Magnusson, M., Mandalà, M., Newman-Toker, D. E., Strupp, M., Suzuki, M., Trabalzini, F., Bisdorff, A., Classification Committee of the Barany Society, Japan Society for Equilibrium Research, European Academy of Otology and Neurotology (EAONO), Equilibrium Committee of the American Academy of Otolaryngology-Head and Neck Surgery (AAO-HNS), & Korean Balance Society (2015). Diagnostic criteria for Menière's disease. *Journal of vestibular research: equilibrium & orientation*, *25*(1), 1–7. https://doi.org/10.3233/VES-150549
201. Loram, I., & Lakie, M. (2002). Human balancing of an inverted pendulum: position control by small, ballistic-like, throw and catch movements. *The Journal of Physiology*, *540*(3), 1111-1124. https://doi.org/10.1113/jphysiol.2001.013077
202. Low, E., Sam, T. H., Tee, K. S., Abdul Rahim, R., Saim, H., Wan Zakaria, W. N., Mohd Khialdin, S., Isa, H., & Soon, C. F. (2020). Development of a wireless and ambulatory posture monitoring system. *International Journal of Integrated Engineering*, *12*(2), 170-176. Retrieved from https://publisher.uthm.edu.my/ojs/index.php/ijie/article/view/5702
203. Lu, T., & Chang, C. (2012). Biomechanics of human movement and its clinical applications. *The Kaohsiung Journal of Medical Sciences*, *28*(2), S13-S25. https://doi.org/10.1016/j.kjms.2011.08.004

204. Lyu, S., Piazza, S., Downs, D., & Freivalds, A. (2019). Validity of pendant-based IMU assessment of postural stability under varying balance conditions compared to a sensor positioned on the lower back. *Proceedings of The Human Factors and Ergonomics Society Annual Meeting*, *63*(1), 1159-1163. https://doi.org/10.1177/1071181319631296

205. Maas, A., Menon, D. K., Adelson, P. D., Andelic, N., Bell, M. J., Belli, A., Bragge, P., Brazinova, A., Büki, A., Chesnut, R. M., Citerio, G., Coburn, M., Cooper, D. J., Crowder, A. T., Czeiter, E., Czosnyka, M., Diaz-Arrastia, R., Dreier, J. P., Duhaime, A. C., Ercole, A., … InTBIR participants and investigators (2017). Traumatic brain injury: integrated approaches to improve prevention, clinical care, and research. *The Lancet. Neurology*, *16*(12), 987–1048. https://doi.org/10.1016/S1474-4422(17)30371-X

206. MacFarland, T. W., & Yates, J. M. (2016). *Mann–Whitney U Test. Introduction to nonparametric statistics for the biological sciences using R*. Berlin: Springer

207. Madigan, M. L., Davidson, B. S., & Nussbaum, M. A. (2006). Postural sway and joint kinematics during quiet standing are affected by lumbar extensor fatigue. *Human movement science*, *25*(6), 788–799. https://doi.org/10.1016/j.humov.2006.04.004

208. Madni, A., Costlow, L., & Knowles, S. (2003). Common design techniques for BEI GyroChip quartz rate sensors for both automotive and aerospace/defense markets. *IEEE Sensors Journal*, *3*(5), 569-578. https://doi.org/10.1109/jsen.2003.817728

209. Majcen Rosker, Z., Kristjansson, E., Vodicar, M., & Rosker, J. (2021). Postural balance and oculomotor control are influenced by neck kinaesthetic functions in elite ice hockey players. *Gait & Posture*, *85*, 145-150. https://doi.org/10.1016/j.gaitpost.2021.01.024

210. Maltese, P. E., Manara, E., Beccari, T., Dundar, M., Capodicasa, N., & Bertelli, M. (2020). Genetic testing for autonomic dysfunction or dysautonomias. *Acta bio-medica: Atenei Parmensis*, *91*(13-S), e2020002- e2020007. https://doi.org/10.23750/abm.v91i13-S.10518

211. Mancini, M., & Horak, F. B. (2010). The relevance of clinical balance assessment tools to differentiate balance deficits. *European journal of physical and rehabilitation medicine*, *46*(2), 239–248.

212. Mancini, M., Rocchi, L., Horak, F. B., & Chiari, L. (2008). Effects of Parkinson's disease and levodopa on functional limits of stability. *Clinical biomechanics (Bristol, Avon)*, *23*(4), 450–458. https://doi.org/10.1016/j.clinbiomech.2007.11.007
213. Mancini, M., Shah, V., Stuart, S., Curtze, C., Horak, F., Safarpour, D., & Nutt, J. (2021). Measuring freezing of gait during daily-life: an open-source, wearable sensors approach. *Journal of Neuroengineering and Rehabilitation*, *18*(1), 1-13. https://doi.org/10.1186/s12984-020-00774-3
214. Mann, H., & Whitney, D. (1947). On a test of whether one of two random variables is stochastically larger than the other. *The Annals of Mathematical Statistics*, *18*(1), 50-60. https://doi.org/10.1214/aoms/1177730491
215. Mansson, L., Bäckman, P., Öhberg, F., Sandlund, J., Selling, J., & Sandlund, M. (2021). Evaluation of concurrent validity between a smartphone self-test prototype and clinical instruments for balance and leg strength. *Sensors*, *21*(5), 1765-1782. https://doi.org/10.3390/s21051765
216. Manto, M., Bower, J., Conforto, A., Delgado-García, J., da Guarda, S., & Gerwig, M. et al. (2011). Consensus paper: Roles of the cerebellum in motor control—The diversity of ideas on cerebellar involvement in movement. *The Cerebellum*, *11*(2), 457-487. https://doi.org/10.1007/s12311-011-0331-9
217. Marengoni, A., Angleman, S., Melis, R., Mangialasche, F., Karp, A., Garmen, A., Meinow, B., & Fratiglioni, L. (2011). Aging with multimorbidity: a systematic review of the literature. *Ageing research reviews*, *10*(4), 430–439. https://doi.org/10.1016/j.arr.2011.03.003
218. Marié, S., Montés-Micó, R., Martínez-Albert, N., García-Marqués, J., & Cerviño, A. (2021). Evaluation of physiological parameters on discomfort glare thresholds using LUMIZ 100 tool. *Translational Vision Science & Technology*, *10*(8), 28-37. https://doi.org/10.1167/tvst.10.8.28
219. Masani, K., Popovic, M., Nakazawa, K., Kouzaki, M., & Nozaki, D. (2003). Importance of body sway velocity information in controlling ankle extensor activities during quiet stance. *Journal of Neurophysiology*, *90*(6), 3774-3782. https://doi.org/10.1152/jn.00730.2002
220. Masani, K., Vette, A. H., & Popovic, M. R. (2006). Controlling balance during quiet standing: proportional and derivative controller generates preceding motor command to body sway position observed in experiments. *Gait & posture*, *23*(2), 164–172. https://doi.org/10.1016/j.gaitpost.2005.01.006

221. Masani, K., Vette, A., Abe, M., & Nakazawa, K. (2014). Centre of pressure velocity reflects body acceleration rather than body velocity during quiet standing. *Gait & Posture*, *39*(3), 946-952. https://doi.org/10.1016/j.gaitpost.2013.12.008
222. Maskey, R., Fei, J., & Nguyen, H. (2018). Use of exploratory factor analysis in maritime research. *The Asian Journal of Shipping and Logistics*, *34*(2), 91-111. https://doi.org/10.1016/j.ajsl.2018.06.006
223. Matłosz, P., Wyszyńska, J., Podgórska-Bednarz, J., Leszczak, J., Rachwał, M., & Przednowek, K. et al. (2020). Agreement of three posturographic force plates in the assessment of postural stability. *International Journal of Environmental Research and Public Health*, *17*(9), 3188-3198. https://doi.org/10.3390/ijerph17093188
224. Mayagoitia, R. E., Lötters, J. C., Veltink, P. H., & Hermens, H. (2002). Standing balance evaluation using a triaxial accelerometer. *Gait & posture*, *16*(1), 55–59. https://doi.org/10.1016/s0966-6362(01)00199-0
225. Menz, H. B., Lord, S. R., & Fitzpatrick, R. C. (2003). Acceleration patterns of the head and pelvis when walking are associated with risk of falling in community-dwelling older people. *The journals of gerontology. Series A, Biological sciences and medical sciences*, *58*(5), M446–M452. https://doi.org/10.1093/gerona/58.5.m446
226. Menz, H., Lord, S.R., & Fitzpatrick, R.C. (2003). Age-related differences in walking stability. *Age and Ageing*, *32*(2), 137-142. https://doi.org/10.1093/ageing/32.2.137
227. Mesároš, P., Behúnová, A., Mandičák, T., Behún, M., & Krajníková, K. (2019). Impact of enterprise information systems on selected key performance indicators in construction project management: An empirical study. *Wireless Networks*, *27*(3), 1641-1648. https://doi.org/10.1007/s11276-019-02048-w
228. Mileti, I., Taborri, J., Rossi, S., Del Prete, Z., Paoloni, M., Suppa, A., & Palermo, E. (2019). Reactive postural responses to continuous yaw perturbations in healthy humans: The effect of aging. *Sensors*, *20*(1), 63-79. https://doi.org/10.3390/s20010063
229. Miller, D., Boyce, B., Dugger, M., Buchheit, T., & Gall, K. (2007). Characteristics of a commercially available silicon-on-insulator MEMS material. *Sensors and Actuators A: Physical*, *138*(1), 130-144. https://doi.org/10.1016/j.sna.2007.04.023
230. Milton J C, Hill-Smith I, Jackson S. H. D. (2008). Prescribing for older people. *BMJ*, 336(7644), 606-609. https://doi.org/10.1136/bmj.39503.424653.80

231. Miot HA (2017). Assessment of data normality in clinical and experimental studies. *Brazilian Vascular Journal*, *16* (2), 88–91. https://doi.org/10.1590/1677-5449.041117
232. Mishra, P., Pandey, C. M., Singh, U., Gupta, A., Sahu, C., & Keshri, A. (2019). Descriptive statistics and normality tests for statistical data. *Annals of cardiac anaesthesia*, *22*(1), 67–72. https://doi.org/10.4103/aca.ACA_157_18
233. Mishra, P., Singh, U., Pandey, C., Mishra, P., & Pandey, G. (2019). Application of student's t-test, analysis of variance, and covariance. *Annals of Cardiac Anaesthesia*, *22*(4), 407-411. https://doi.org/10.4103/aca.aca_94_19
234. Moe-Nilssen R. (1998). A new method for evaluating motor control in gait under real-life environmental conditions. Part 1: The instrument. *Clinical biomechanics (Bristol, Avon)*, *13*(4-5), 320–327. https://doi.org/10.1016/s0268-0033(98)00089-8
235. Mohammadi, M., Ghamkhar, L., Alizadeh, A., Shaabani, M., Salavati, M., & Kahlaee, A. (2021). Comparison of the reliance of the postural control system on the visual, vestibular and proprioceptive inputs in chronic low back pain patients and asymptomatic participants. *Gait & Posture*, *85*, 266-272. https://doi.org/10.1016/j.gaitpost.2021.02.010
236. Mohd-Yasin, F., Korman, C., & Nagel, D. (2003). Measurement of noise characteristics of MEMS accelerometers. *Solid-State Electronics*, *47*(2), 357-360. https://doi.org/10.1016/s0038-1101(02)00220-4
237. Moisan, G., Chayasit, P., Boonsinsukh, R., Nester, C., & Hollands, K. (2021). Postural control during quiet standing and voluntary stepping response tasks in individuals post-stroke: a case-control study. *Topics in Stroke Rehabilitation*, 1-8. https://doi.org/10.1080/10749357.2021.1943803
238. Morimoto, H., Asai, Y., Johnson, E., Koide, Y., Niki, J., & Sakai, S. et al. (2019). Objective measures of physical activity in patients with chronic unilateral vestibular hypofunction, and its relationship to handicap, anxiety and postural stability. *Auris Nasus Larynx*, *46*(1), 70-77. https://doi.org/10.1016/j.anl.2018.06.010
239. Mu, J., & Han, L. (2017). Performance analysis of the ZigBee networks in 5G environment and the nearest access routing for improvement. *Ad Hoc Networks*, *56*, 1-12. https://doi.org/10.1016/j.adhoc.2016.10.006
240. Mubashar, R., Siddique, M., Rehman, A., Asad, A., & Rasool, A. (2021). Comparative performance analysis of short-range wireless protocols for wireless

personal area network. *Iran Journal of Computer Science*, *4*(3), 201-210. https://doi.org/10.1007/s42044-021-00087-1

241. Mukhiya, R., Agarwal, P., Badjatya, S., Garg, M., Gaikwad, P., & Sinha, S. et al. (2019). Design, modelling and system level simulations of DRIE-based MEMS differential capacitive accelerometer. *Microsystem Technologies*, *25*(9), 3521-3532. https://doi.org/10.1007/s00542-018-04292-0
242. Mukhiya, R., Garg, M., Gaikwad, P., Sinha, S., Singh, A., & Gopal, R. (2020). Electrical equivalent modeling of MEMS differential capacitive accelerometer. *Microelectronics Journal*, *99*, 104770-104777. https://doi.org/10.1016/j.mejo.2020.104770
243. Mulas, I., Putzu, V., Asoni, G., Viale, D., Mameli, I., & Pau, M. (2020). Clinical assessment of gait and functional mobility in Italian healthy and cognitively impaired older persons using wearable inertial sensors. *Aging Clinical and Experimental Research*, *33*(7), 1853-1864. https://doi.org/10.1007/s40520-020-01715-9
244. Mustafazade, A., Pandit, M., Zhao, C., Sobreviela, G., Du, Z., Steinmann, P., Zou, X., Howe, R. and Seshia, A., 2020. A vibrating beam MEMS accelerometer for gravity and seismic measurements. *Scientific Reports*, 10(1), 1-8.
245. Myles, P. and Cui, J., 2007. I. Using the Bland–Altman method to measure agreement with repeated measures. *British Journal of Anaesthesia*, 99(3), 309-311.
246. Najafi, B., Aminian, K., Paraschiv-Ionescu, A., Loew, F., Bula, C., & Robert, P. (2003). Ambulatory system for human motion analysis using a kinematic sensor: monitoring of daily physical activity in the elderly. *IEEE Transactions On Biomedical Engineering*, *50*(6), 711-723. https://doi.org/10.1109/tbme.2003.812189
247. Narkhede, P., Poddar, S., Walambe, R., Ghinea, G., & Kotecha, K. (2021). Cascaded complementary filter architecture for sensor fusion in attitude estimation. *Sensors*, *21*(6), 1937-1954. https://doi.org/10.3390/s21061937
248. Nashner, L., & McCollum, G. (1985). The organization of human postural movements: A formal basis and experimental synthesis. *Behavioral and Brain Sciences*, *8*(1), 135-150. https://doi.org/10.1017/s0140525x00020008
249. Nations, U. (2012). World Population Prospects, the 2012 Revision | United Nations. Retrieved 21 February 2021, from https://www.un.org/en/desa/world-population-prospects-2012-revision

250. Neptune, R., & Vistamehr, A. (2019). Dynamic balance during human movement: measurement and control mechanisms. *Journal of Biomechanical Engineering*, *141(7)*,1-10. https://doi.org/10.1115/1.4042170
251. Ng, Y., Hill, K., Jacques, A., & Burton, E. (2021). Reliability and validity of a modified version of the community balance and mobility scale (CBMS-Home) for use in home assessment. *Physical Therapy*, *101*(8), 1-12. https://doi.org/10.1093/ptj/pzab134
252. Nguyen, G., MacLean, J., & Stirling, L. (2021). Quantification of compensatory torso motion in post-stroke patients using wearable inertial measurement units. *IEEE Sensors Journal*, 1-12. https://doi.org/10.1109/jsen.2021.3072010
253. Nicholas, S. C., Doxey-Gasway, D. D., & Paloski, W. H. (1998). A link-segment model of upright human posture for analysis of head-trunk coordination. *Journal of vestibular research: equilibrium & orientation*, *8*(3), 187–200.
254. Noamani, A., Nazarahari, M., Lewicke, J., Vette, A., & Rouhani, H. (2020). Validity of using wearable inertial sensors for assessing the dynamics of standing balance. *Medical Engineering & Physics*, *77*, 53-59. https://doi.org/10.1016/j.medengphy.2019.10.018
255. Noury, N., Dittmar, A., Corroy, C., Baghai, R., Weber, J. L., Blanc, D., Klefstat, F., Blinovska, A., Vaysse, S., & Comet, B. (2004). VTAMN--a smart clothe for ambulatory remote monitoring of physiological parameters and activity. *Conference proceedings: ... Annual International Conference of the IEEE Engineering in Medicine and Biology Society. IEEE Engineering in Medicine and Biology Society. Annual Conference*, *2004*, 3266–3269. https://doi.org/10.1109/IEMBS.2004.1403919
256. *Nrf24L01-2.4GHz-HowTo - ArduinoInfo*. Arduinoinfo.mywikis.net. (2021). Retrieved 17 November 2021, from https://arduinoinfo.mywikis.net/wiki/Nrf24L01-2.4GHz-HowTo.
257. Nutt, J. G., Bloem, B. R., Giladi, N., Hallett, M., Horak, F. B., & Nieuwboer, A. (2011). Freezing of gait: moving forward on a mysterious clinical phenomenon. *The Lancet. Neurology*, *10*(8), 734–744. https://doi.org/10.1016/S1474-4422(11)70143-0
258. Ojie, O, D., & Saatchi, R. (2020). Principal component analysis of the modified Clinical Test of Sensory Interaction in healthy adult humans. *WSEAS Transactions on Biology and Biomedicine*, *17*, 125-142. https://doi.org/10.37394/23208.2020.17.15

259. Ojie, O.D & Saatchi, R. (2020). Development and evaluation of an accelerometry system based on inverted pendulum to measure and analyse human balance. *Adv. Asset Manag. Cond. Monit*. 1129–1141.

260. Ojie, O.D, Saatchi, R., & Saatchi, M. (2020). Demonstration of the effect of centre of mass height on postural sway using accelerometry for balance analysis. *Technologies*, *8*(2), 20-33. https://doi.org/10.3390/technologies8020020

261. Ojie, O.D., & Saatchi, R. (2021). Kohonen neural network investigation of the effects of the visual, proprioceptive and vestibular systems to balance in young healthy adult subjects. *Healthcare*, *9*(9), 1219-1236. https://doi.org/10.3390/healthcare9091219

262. Olchowik, G., Tomaszewski, M., Olejarz, P., Warchoł, J., Różańska-Boczula, M., & Maciejewski, R. (2015). The human balance system and gender. *Acta of bioengineering and biomechanics*, *17*(1), 69–74.

263. Orcan, F. (2020). Parametric or non-parametric: Skewness to test normality for mean comparison. *International Journal of Assessment Tools in Education*, 236-246. https://doi.org/10.21449/ijate.656077

264. Ozinga, S., & Alberts, J. (2014). Quantification of postural stability in older adults using mobile technology. *Experimental Brain Research*, *232*(12), 3861-3872. https://doi.org/10.1007/s00221-014-4069-8

265. Pagano, G., Donisi, L., Marsico, V., Losavio, E., Cesarelli, M., & D'Addio, G. (2021). Reliability of kinematic parameters related to the Timed Up and Go Test in patients with gait impairments. In *2021 IEEE International Symposium on Medical Measurements and Applications (MeMeA)* (pp.1-5). Lausanne; Institute of Electrical and Electronics Engineers.

266. Paillard, T., & Noé, F. (2015). Techniques and methods for testing the postural function in healthy and pathological subjects. *Biomed Research International*, *2015*, 1-15. https://doi.org/10.1155/2015/891390

267. Pandit, S., & Gupta, S. (2011). A comparative study on distance measuring approaches for clustering. *International Journal of Research in Computer Science*, *2*(1), 29-31.

268. Panjan, A., & Sarabon, N. (2010). Review of methods for the evaluation of human body balance. Sport Science Review, 19(5), 1-33. https://doi.org/10.2478/v10237-011-0036-5

269. Papp, M. E., Grahn-Kronhed, A. C., Rauch Lundin, H., & Salminen, H. (2021). Changes in physical activity levels and relationship to balance performance, gait

speed, and self-rated health in older Swedish women: a longitudinal study. *Aging clinical and experimental research*, 1-9.

270. Pau, M., Leban, B., Deidda, M., Porta, M., Coghe, G., Cattaneo, D., & Cocco, E. (2021). Use of wrist-worn accelerometers to quantify bilateral upper limb activity and asymmetry under free-living conditions in people with multiple sclerosis. *Multiple Sclerosis and Related Disorders*, *53*, 103081-103087. https://doi.org/10.1016/j.msard.2021.103081
271. Pavão, S., Nunes, G., Santos, A., & Rocha, N. (2014). Relationship between static postural control and the level of functional abilities in children with cerebral palsy. *Brazilian Journal of Physical Therapy*, *18*(4), 300-307. https://doi.org/10.1590/bjpt-rbf.2014.0056
272. Pérennou, D., Decavel, P., Manckoundia, P., Penven, Y., Mourey, F., Launay, F., Pfitzenmeyer, P., & Casillas, J. M. (2005). Evaluation de l'équilibre en pathologie neurologique et gériatrique [Evaluation of balance in neurologic and geriatric disorders]. *Annales de readaptation et de medecine physique: revue scientifique de la Societe francaise de reeducation fonctionnelle de readaptation et de medecine physique*, *48*(6), 317–335. https://doi.org/10.1016/j.annrmp.2005.04.009
273. Perlmutter, M., & Breit, S. (2016). The future of the MEMS inertial sensor performance, design and manufacturing. In *DGON Intertial Sensors and Systems (ISS)*, 1-12. Karlsruhe, Germany; Institute of Electrical and Electronics Engineers. Retrieved 7 December 2021, from.
274. Peterka R. J. (2002). Sensorimotor integration in human postural control. *Journal of neurophysiology*, *88*(3), 1097–1118. https://doi.org/10.1152/jn.2002.88.3.1097
275. Peterka, R. J. (2000). Postural control model interpretation of stabilogram diffusion analysis. *Biological Cybernetics*, *82*(4), 335-343. https://doi.org/10.1007/s004220050587
276. Phillips, J., Newman, J., FitzGerald, J., & Cox, S. (2020). Implications of vestibular telemetry for the management of Ménière's Disease—Our experience with three adults. *Clinical Otolaryngology*, *46*(2), 425-429. https://doi.org/10.1111/coa.13676
277. Polechoński, J., Nawrocka, A., Wodarski, P., & Tomik, R. (2019). Applicability of smartphone for dynamic postural stability evaluation. *Biomed Research International*, *2019*, 1-6. https://doi.org/10.1155/2019/9753898

278. Pollind, M., & Soangra, R. (2020). Development and validation of wearable inertial sensor system for postural sway analysis. *Measurement*, *165*, 108101-108110. https://doi.org/10.1016/j.measurement.2020.108101
279. Pollock, A., Durward, B., Rowe, P., & Paul, J. (2000). What is balance?. *Clinical Rehabilitation*, *14*(4), 402-406. https://doi.org/10.1191/0269215500cr342oa
280. Porciuncula, F., Wasserman, P., Marder, K., & Rao, A. (2020). Quantifying postural control in premanifest and manifest Huntington disease using wearable sensors. *Neurorehabilitation and Neural Repair*, *34*(9), 771-783. https://doi.org/10.1177/1545968320939560
281. Prakash, C., Kumar, R., & Mittal, N. (2016). Recent developments in human gait research: parameters, approaches, applications, machine learning techniques, datasets and challenges. *Artificial Intelligence Review*, *49*(1), 1-40. https://doi.org/10.1007/s10462-016-9514-6
282. Prieto, T., Myklebust, J., Hoffmann, R., Lovett, E., & Myklebust, B. (1996). Measures of postural steadiness: differences between healthy young and elderly adults. *IEEE Transactions on Biomedical Engineering*, *43*(9), 956-966. https://doi.org/10.1109/10.532130
283. Proske, U., & Gandevia, S. C. (2012). The proprioceptive senses: their roles in signaling body shape, body position and movement, and muscle force. *Physiological reviews*, *92*(4), 1651–1697. https://doi.org/10.1152/physrev.00048.2011
284. Purves, D., & Williams, S. (2001). *Neuroscience. 2nd edition*. Sinauer Associates.
285. Purves, D., Augustine, G., Fitzpatrick, D., Katz, L., LaMantia, A., McNamara, J., & Williams, S. (2001). *Neuroscience* (2nd ed.). Sinauer Associates.
286. Quintana, C., Heebner, N., Olson, A., Abt, J., & Hoch, M. (2020). Sport-specific differences in dynamic visual acuity and gaze stabilization in division-I collegiate athletes. *Journal of Vestibular Research*, *30*(4), 249-257. https://doi.org/10.3233/ves-200710
287. Quinzi, F., Camomilla, V., Bratta, C., Piacentini, M., Sbriccoli, P., & Vannozzi, G. (2021). Hopping skill in individuals with down syndrome: A qualitative and quantitative assessment. *Human Movement Science*, *78*, 102821-102830. https://doi.org/10.1016/j.humov.2021.102821

288. Ranganathan, P., Pramesh, C. S., & Aggarwal, R. (2017). Common pitfalls in statistical analysis: Measures of agreement. *Perspectives in clinical research*, *8*(4), 187–191. https://doi.org/10.4103/picr.PICR_123_17

289. Raymakers, J., Samson, M., & Verhaar, H. (2005). The assessment of body sway and the choice of the stability parameter(s). *Gait & Posture*, *21*(1), 48-58. https://doi.org/10.1016/j.gaitpost.2003.11.006

290. Redfern, M., Yardley, L., & Bronstein, A. (2001). Visual influences on balance. *Journal of Anxiety Disorders*, *15*(1-2), 81-94. https://doi.org/10.1016/s0887-6185(00)00043-8

291. Rhea, C. K., Kiefer, A. W., Wright, W. G., Raisbeck, L. D., & Haran, F. J. (2015). Interpretation of postural control may change due to data processing techniques. *Gait & posture*, *41*(2), 731–735. https://doi.org/10.1016/j.gaitpost.2015.01.008

292. Ricci, M., Terribili, M., Giannini, F., Errico, V., Pallotti, A., & Galasso, C. et al. (2019). Wearable-based electronics to objectively support diagnosis of motor impairments in school-aged children. *Journal of Biomechanics*, *83*, 243-252. https://doi.org/10.1016/j.jbiomech.2018.12.005

293. Ricci, N., de Faria Figueiredo Gonçalves, D., Coimbra, A., & Coimbra, I. (2009). Sensory interaction on static balance: A comparison concerning the history of falls of community-dwelling elderly. *Geriatrics & Gerontology International*, *9*(2), 165-171. https://doi.org/10.1111/j.1447-0594.2009.00516.x

294. Richmond, S. B., Fling, B. W., Lee, H., & Peterson, D. S. (2021). The assessment of centre of mass and centre of pressure during quiet stance: Current applications and future directions. *Journal of biomechanics*, *123*, 110485-110489. https://doi.org/10.1016/j.jbiomech.2021.110485

295. Robinovitch, S. N., Feldman, F., Yang, Y., Schonnop, R., Leung, P. M., Sarraf, T., Sims-Gould, J., & Loughin, M. (2013). Video capture of the circumstances of falls in elderly people residing in long-term care: an observational study. *Lancet (London, England)*, *381*(9860), 47–54. https://doi.org/10.1016/S0140-6736(12)61263-X

296. Rodrigo, S., Lescano, C., & Rodrigo, R. (2012). Application of Kohonen maps to kinetic analysis of human gait. *Revista Brasileira De Engenharia Biomédica*, *28*(3), 217-226. https://doi.org/10.4322/rbeb.2012.027

297. Rodríguez-Rubio, P., Bagur-Calafat, C., López-de-Celis, C., Bueno-Gracía, E., Cabanas-Valdés, R., Herrera-Pedroviejo, E., & Girabent-Farrés, M. (2020). Validity and reliability of the Satel 40 Hz stabilometric force platform for measuring quiet

stance and dynamic standing balance in healthy subjects. *International Journal of Environmental Research and Public Health*, *17*(21), 7733-7746. https://doi.org/10.3390/ijerph17217733

298. Rogers, M. W., & Mille, M. L. (2018). Balance perturbations. *Handbook of clinical neurology*, *159*, 85–105. https://doi.org/10.1016/B978-0-444-63916-5.00005-7
299. Roh, M., Shin, E., & Lee, S. (2021). Relations between postural sway and cognitive workload during various gaze tasks in healthy young and old people. *Journal of Exercise Rehabilitation*, *17*(2), 131-137. https://doi.org/10.12965/jer.2142154.077
300. Rosenblatt, J., & Benjamini, Y. (2018). On mixture alternatives and Wilcoxon's signed-rank test. *The American Statistician*, *72*(4), 344-347. https://doi.org/10.1080/00031305.2017.1360795
301. Roughead, E., Vitry, A., Caughey, G., & Gilbert, A. (2011). Multimorbidity, care complexity and prescribing for the elderly. *Aging Health*, *7*(5), 695-705. https://doi.org/10.2217/ahe.11.64
302. Rovini, E., Maremmani, C., & Cavallo, F. (2020). A wearable system to objectify assessment of motor tasks for supporting Parkinson's disease diagnosis. *Sensors*, *20*(9), 2630-2656. https://doi.org/10.3390/s20092630
303. Rubin, G. S., West, S. K., Muñoz, B., Bandeen-Roche, K., Zeger, S., Schein, O., & Fried, L. P. (1997). A comprehensive assessment of visual impairment in a population of older Americans. The SEE Study. Salisbury Eye Evaluation Project. *Investigative ophthalmology & visual science*, *38*(3), 557–568.
304. Runge, C. F., Shupert, C. L., Horak, F. B., & Zajac, F. E. (1999). Ankle and hip postural strategies defined by joint torques. *Gait & posture*, *10*(2), 161–170. https://doi.org/10.1016/s0966-6362(99)00032-6
305. Saccenti, E., Hendriks, M., & Smilde, A. (2020). Corruption of the Pearson correlation coefficient by measurement error and its estimation, bias, and correction under different error models. *Scientific Reports*, *10*(1), 1-19. https://doi.org/10.1038/s41598-019-57247-4
306. Safavynia, S., & Ting, L. (2013). Sensorimotor feedback based on task-relevant error robustly predicts temporal recruitment and multidirectional tuning of muscle synergies. *Journal of Neurophysiology*, *109*(1), 31-45. https://doi.org/10.1152/jn.00684.2012
307. Saftari, L., & Kwon, O. (2018). Ageing vision and falls: a review. *Journal of Physiological Anthropology*, *37*(1), 1-14. https://doi.org/10.1186/s40101-018-0170-1

308. Saha, H., Mandal, S., Mitra, S., Banerjee, S., & Saha, U. (2017). Comparative performance analysis between nRF24L01+ and XBEE ZB module based wireless ad-hoc networks. *International Journal of Computer Network and Information Security*, *9*(7), 36-44. https://doi.org/10.5815/ijcnis.2017.07.05
309. Saha, K. (2021). Vertigo related to central nervous system disorders. *CONTINUUM: Lifelong Learning in Neurology*, *27*(2), 447-467. https://doi.org/10.1212/con.0000000000000933
310. Samanta, A., Mauntana, S., Barsi, Z., Yarlagadda, B., & Nelson, P. (2020). Is your vision blurry? A systematic review of home-based visual acuity for telemedicine. *Journal of Telemedicine and Telecare*, 1-10. https://doi.org/10.1177/1357633x20970398
311. Samsonova, E., Kok, J., & IJzerman, A. (2006). TreeSOM: Cluster analysis in the self-organizing map. *Neural Networks*, *19*(6-7), 935-949. https://doi.org/10.1016/j.neunet.2006.05.003
312. Saunders, J., Inman, V., & Eberhart, H. (1953). The major determinants in normal and pathological gait. *The Journal of Bone & Joint Surgery*, *35*(3), 543-558. https://doi.org/10.2106/00004623-195335030-00003
313. Savadkoohi, M., Oladunni, T., & Thompson, L. (2021). Deep neural networks for human's fall-risk prediction using force-plate time series signal. *Expert Systems with Applications*, *182*, 115220-115235. https://doi.org/10.1016/j.eswa.2021.115220
314. Sayal, K., Prasad, V., Daley, D., Ford, T., & Coghill, D. (2018). ADHD in children and young people: prevalence, care pathways, and service provision. *The lancet. Psychiatry*, *5*(2), 175–186. https://doi.org/10.1016/S2215-0366(17)30167-0
315. Scholz, J., Schöner, G., Hsu, W., Jeka, J., Horak, F., & Martin, V. (2007). Motor equivalent control of the center of mass in response to support surface perturbations. *Experimental Brain Research*, *180*(1), 163-179. https://doi.org/10.1007/s00221-006-0848-1
316. Senturia, S. (2001). *Microsystem design* (1st ed.). Springer.
317. Serrien, B., Hohenauer, E., Clijsen, R., Taube, W., Baeyens, J. P., & Küng, U. (2017). Changes in balance coordination and transfer to an unlearned balance task after slackline training: a self-organizing map analysis. *Experimental brain research*, *235*(11), 3427–3436. https://doi.org/10.1007/s00221-017-5072-7

318. Shafizadeh, M., Parvinpour, S., Balali, M., & Shabani, M. (2020). Effects of age and task difficulty on postural sway, variability and complexity. *Adaptive Behavior*, 105971232096397. https://doi.org/10.1177/1059712320963974
319. Shaikh, A., & Joshi, R. (2020). Influence of gender on static balance in healthy community dwelling elderly: a comparison using posturography. *International Journal of Research in Medical Sciences*, *8*(8), 2950-2953. https://doi.org/10.18203/2320-6012.ijrms20203444
320. *Shimmer wearable sensor technology | Wireless IMU | ECG | EMG | GSR*. Shimmer wearable sensor technology. (2021). Retrieved 30 November 2021, from https://shimmersensing.com/.
321. Shiraishi, Y., Niimi, N., Goda, A., Takei, M., Kimura, T., & Kohno, T. et al. (2021). Assessment of physical activity using waist-worn accelerometers in hospitalized heart failure patients and its relationship with Kansas City Cardiomyopathy Questionnaire. *Journal of Clinical Medicine*, *10*(18), 4103-4116. https://doi.org/10.3390/jcm10184103
322. Shiroma, E. J., Schrack, J. A., & Harris, T. B. (2018). Accelerating accelerometer research in aging. *The journals of gerontology. Series A, Biological sciences and medical sciences*, *73*(5), 619–621. https://doi.org/10.1093/gerona/gly033
323. Shumway-Cook, A., & Horak, F. B. (1986). Assessing the influence of sensory interaction of balance. Suggestion from the field. *Physical therapy*, *66*(10), 1548–1550. https://doi.org/10.1093/ptj/66.10.1548
324. Sinaga, K., & Yang, M. (2020). Unsupervised K-means clustering algorithm. *IEEE Access*, *8*, 80716-80727. https://doi.org/10.1109/access.2020.2988796
325. Siragy, T., & Nantel, J. (2020). Absent arm swing and dual tasking decreases trunk postural control and dynamic balance in people with Parkinson's disease. *Frontiers in Neurology*, *11*, 1-10. https://doi.org/10.3389/fneur.2020.00213
326. Smalheiser, N. (2017). *Data literacy: How to make your experiments robust and reproducible*. Elsevier Science.
327. Smith P. F. (2017). The vestibular system and cognition. *Current opinion in neurology*, *30*(1), 84–89. https://doi.org/10.1097/WCO.0000000000000403
328. Smith, B. I., Docherty, C. L., Simon, J., Klossner, J., & Schrader, J. (2012). Ankle strength and force sense after a progressive, 6-week strength-training program in people with functional ankle instability. *Journal of athletic training*, *47*(3), 282–288. https://doi.org/10.4085/1062-6050-47.3.06

329. Soangra, R., & Lockhart, T. E. (2013). Comparison of intra individual physiological sway complexity from force plate and inertial measurement unit - biomed 2013. *Biomedical sciences instrumentation*, *49*, 180–186.
330. Soltero, E. G., Navabi, N., Vander Wyst, K. B., Hernandez, E., Castro, F. G., Ayers, S. L., Mendez, J., & Shaibi, G. Q. (2021). Examining 24-hour activity and sleep behaviors and related determinants in Latino adolescents and young adults with obesity. *Health education & behavior: the official publication of the Society for Public Health Education*, 10901981211054789. Advance online publication. https://doi.org/10.1177/10901981211054789
331. Sorock, G. S., & Shimkin, E. E. (1988). Benzodiazepine sedatives and the risk of falling in a community-dwelling elderly cohort. Archives of internal medicine, 148(11), 2441–2444.
332. Spirduso, W., Francis, K., & MacRae, P. (2005). *Physical dimensions of aging*. Champaign, Ill.: Human Kinetics.
333. Stevens, J. (1992). *Applied multivariate statistics for the social sciences*. Lawrence Erlbaum Associates.
334. Sturnieks, D. L., St George, R., & Lord, S. R. (2008). Balance disorders in the elderly. *Neurophysiologie clinique /Clinical neurophysiology*, *38*(6), 467–478. https://doi.org/10.1016/j.neucli.2008.09.001
335. Sun, R., Hsieh, K., & Sosnoff, J. (2019). Fall risk prediction in Multiple Sclerosis using postural sway measures: A machine learning approach. *Scientific Reports*, *9*(1), 1-7. https://doi.org/10.1038/s41598-019-52697-2
336. Suvarna, T., Raj, J., & Prakash, N. (2021). Correlation between balance and BMI in collegiate students: A cross sectional study. *International Journal of Physiotherapy and Research*, *9*(1), 3759-3764. https://doi.org/10.16965/ijpr.2021.103
337. Taffé, P., Halfon, P., & Halfon, M. (2020). A new statistical methodology overcame the defects of the Bland–Altman method. *Journal of Clinical Epidemiology*, *124*, 1-7. https://doi.org/10.1016/j.jclinepi.2020.03.018
338. Tan, G., Tan, M., Luben, R., Wareham, N., Khaw, K., & Myint, P. (2021). The relationship between alcohol intake and falls hospitalization: Results from the EPIC-Norfolk. *Geriatrics & Gerontology International*, *21*(8), 657-663. https://doi.org/10.1111/ggi.14219
339. Thompson, M. (Ed.). (2014). Intuitive analog circuit design (2nd ed.) Retrieved from https://www-sciencedirect-com.hallam.idm.oclc.org/topics/engineering/magnitude-

340. Upload.wikimedia.org. (2021). Retrieved 7 December 2021, from https://upload.wikimedia.org/wikipedia/commons/4/45/Anatomical_Planes-en.svg.
341. Uppal, A. (2020). *Physical Education and Health* (6th ed., pp. 157-158). Friends Publications.
342. Van Buren, E., & Herring, A. (2020). To be parametric or non-parametric, that is the question. *BJOG: An International Journal of Obstetrics & Gynaecology*, *127*(5), 549-550. https://doi.org/10.1111/1471-0528.15545
343. van Emmerik, R., Ducharme, S., Amado, A., & Hamill, J. (2016). Comparing dynamical systems concepts and techniques for biomechanical analysis. *Journal of Sport and Health Science*, *5*(1), 3-13. https://doi.org/10.1016/j.jshs.2016.01.013
344. Vatcheva, K. P., Lee, M., McCormick, J. B., & Rahbar, M. H. (2016). Multicollinearity in regression analyses conducted in epidemiologic studies. *Epidemiology (Sunnyvale, Calif.)*, *6*(2), 227-235. https://doi.org/10.4172/2161-1165.1000227
345. Vesanto, J., & Alhoniemi, E. (2000). Clustering of the self-organizing map. *IEEE Transactions On Neural Networks*, *11*(3), 586-600. https://doi.org/10.1109/72.846731
346. Vidal, P. P., Degallaix, L., Josset, P., Gasc, J. P., & Cullen, K. E. (2004). Postural and locomotor control in normal and vestibularly deficient mice. *The Journal of physiology*, *559*(Pt 2), 625–638. https://doi.org/10.1113/jphysiol.2004.063883
347. Visser, J. E., Carpenter, M. G., van der Kooij, H., & Bloem, B. R. (2008). The clinical utility of posturography. *Clinical neurophysiology: official journal of the International Federation of Clinical Neurophysiology*, *119*(11), 2424–2436. https://doi.org/10.1016/j.clinph.2008.07.220
348. Visual Information for Advocacy. (2021). Processing. https://visualisingadvocacy.org/node/638.html
349. Wallisch, P., Lusignan, M., Benayoun, M., Baker, T., Dickey, A., & Hatsopoulos, N. (2014). *MATLAB for neuroscientists*. Elsevier.
350. Walsh, J. (1962). *Handbook of Nonparametric Statistics*. D. Van Nostrand Company, Inc.
351. Wang, F., Skubic, M., Abbott, C., & Keller, J. M. (2010). Body sway measurement for fall risk assessment using inexpensive webcams. *Annual International Conference of the IEEE Engineering in Medicine and Biology Society. IEEE Engineering in Medicine and Biology Society. Annual International Conference*, *2010*, 2225–2229. https://doi.org/10.1109/IEMBS.2010.5626100

352. Wardoyo, S., Hutajulu, P., & Togibasa, O. (2016). A development of force plate for biomechanics analysis of standing and walking. *Journal of Physics: Conference Series*, *739*, 012118-012123. https://doi.org/10.1088/1742-6596/739/1/012118
353. Watson, P., & Petrie, A. (2010). Method agreement analysis: A review of correct methodology. *Theriogenology*, *73*(9), 1167-1179. https://doi.org/10.1016/j.theriogenology.2010.01.003
354. *Wearable sensors - APDM wearable technologies*. APDM. (2021). Retrieved 30 November 2021, from https://apdm.com/wearable-sensors/.
355. Welniarz, Q., Worbe, Y., & Gallea, C. (2021). The forward model: a unifying theory for the role of the cerebellum in motor control and sense of agency. *Frontiers in Systems Neuroscience*, *15*,1-14. https://doi.org/10.3389/fnsys.2021.644059
356. Wilcoxon, F. (1945). Individual comparisons by ranking methods. *Biometrics Bulletin*, *1*(6), 80-83. https://doi.org/10.2307/3001968
357. Winter, D. (1995). Human balance and posture control during standing and walking. Gait & Posture, 3(4), 193-214. https://doi.org/10.1016/0966-6362(96)82849-9
358. Winter, D. A., Patla, A. E., Ishac, M., & Gage, W. H. (2003). Motor mechanisms of balance during quiet standing. *Journal of electromyography and kinesiology: official journal of the International Society of Electrophysiological Kinesiology*, *13*(1), 49–56. https://doi.org/10.1016/s1050-6411(02)00085-8
359. Winter, D. A., Patla, A. E., Prince, F., Ishac, M., & Gielo-Perczak, K. (1998). Stiffness control of balance in quiet standing. *Journal of neurophysiology*, *80*(3), 1211–1221. https://doi.org/10.1152/jn.1998.80.3.1211
360. Witvrouw, A., Tilmans, H., & De Wolf, I. (2004). Materials issues in the processing, the operation and the reliability of MEMS. *Microelectronic Engineering*, *76*(1-4), 245-257. https://doi.org/10.1016/j.mee.2004.07.001
361. Wright, J., & Jordanov, I. (2014). Intelligent approaches in locomotion - A review. *Journal of Intelligent & Robotic Systems*, *80*(2), 255-277. https://doi.org/10.1007/s10846-014-0149-z
362. Wrisley, D. M., & Whitney, S. L. (2004). The effect of foot position on the modified clinical test of sensory interaction and balance. *Archives of physical medicine and rehabilitation*, *85*(2), 335–338. https://doi.org/10.1016/j.apmr.2003.03.005

363. Wrisley, D. M., & Whitney, S. L. (2004). The effect of foot position on the modified clinical test of sensory interaction and balance. *Archives of physical medicine and rehabilitation*, *85*(2), 335–338. https://doi.org/10.1016/j.apmr.2003.03.005

364. Yan, F., Robert, M., & Li, Y. (2017). Statistical methods and common problems in medical or biomedical science research. *International journal of physiology, pathophysiology and pharmacology*, *9*(5), 157–163.

365. Yang, C., & Hsu, Y. (2010). A review of accelerometry-based wearable motion detectors for physical activity monitoring. *Sensors*, *10*(8), 7772-7788. https://doi.org/10.3390/s100807772

366. Yazdi, N., Ayazi, F., & Najafi, K. (1998). Micromachined inertial sensors. *Proceedings of The IEEE*, *86*(8), 1640-1659. https://doi.org/10.1109/5.704269

367. Yeh, T., Cluff, T., & Balasubramaniam, R. (2014). Visual reliance for balance control in older adults persists when visual information is disrupted by artificial feedback delays. *Plos ONE*, *9*(3), e91554-e91562. https://doi.org/10.1371/journal.pone.0091554

368. Young, A.S., Rosengren, S.M., Welgampola, M.S. (2018). Disorders of the inner-ear balance organs and their pathways. *Handbook of Clinical Neurology, 159*, 385–401

369. Yu, J., Capio, C., Abernethy, B., & Sit, C. (2021). Moderate-to-vigorous physical activity and sedentary behavior in children with and without developmental coordination disorder: Associations with fundamental movement skills. *Research in Developmental Disabilities*, *118*, 104070. https://doi.org/10.1016/j.ridd.2021.104070

370. Yu, L., Zhao, Y., Wang, H., Sun, T., Murphy, T., & Tsui, K. (2021). Assessing elderly's functional balance and mobility via analyzing data from waist-mounted tri-axial wearable accelerometers in timed up and go tests. *BMC Medical Informatics and Decision Making*, *21*(1), 1-14. https://doi.org/10.1186/s12911-021-01463-4

371. Zaki, M. & Meira, W. (2020). Data mining and machine learning: In Fundamental Concepts and Algorithms (2nd ed.). Cambridge University Press: Cambridge.

372. Zalewski C. K. (2015). Aging of the human vestibular system. *Seminars in hearing*, *36*(3), 175–196. https://doi.org/10.1055/s-0035-1555120

373. Zemková, E., Ďurinová, E., Džubera, A., Chochol, J., Koišová, J., Šimonová, M., & Zapletalová, L. (2021). Simultaneous measurement of centre of pressure and centre of mass in assessing postural sway in healthcare workers with non-specific back pain:

protocol for a cross-sectional study. *BMJ open*, *11*(8), e050014. https://doi.org/10.1136/bmjopen-2021-050014

374. Zhang, Y., Wang, H., Yao, Y., Liu, J., Sun, X., & Gu, D. (2021). Walking stability in patients with benign paroxysmal positional vertigo: an objective assessment using wearable accelerometers and machine learning. *Journal of Neuroengineering and Rehabilitation*, *18*(1), 1-9. https://doi.org/10.1186/s12984-021-00854-y
375. Guo, Z., Fucheng, C., Boyu, L., Le, C., Chao, L., & Ke, S. (2015). Research development of silicon MEMS gyroscopes: a review. *Microsystem Technologies*, *21*(10), 2053-2066. https://doi.org/10.1007/s00542-015-2645-x
376. Zhou, J., Jiang, X., Yu, W., Zhu, H., Lo, O., & Gouskova, N. et al. (2021). A smartphone app-based application enabling remote assessments of standing balance during the COVID-19 pandemic and beyond. *IEEE Internet of Things Journal*, *8*(21), 15818-15828. https://doi.org/10.1109/jiot.2021.3064442
377. Zhou, X., Armaghani, D., Ye, J., Khari, M., & Motahari, M. (2020). Hybridization of parametric and non-parametric techniques to predict air over-pressure induced by quarry blasting. *Natural Resources Research*, *30*(1), 209-224. https://doi.org/10.1007/s11053-020-09714-3
378. Zhu, W., Li, Y., Wang, B., Zhao, C., Wu, T., Liu, T., & Sun, F. (2021). Objectively measured physical activity is associated with static balance in young adults. *International Journal of Environmental Research and Public Health*, *18*(20), 10787-10797. https://doi.org/10.3390/ijerph182010787
379. Zijlstra, W., & Aminian, K. (2007). Mobility assessment in older people: new possibilities and challenges. *European Journal of Ageing*, *4*(1), 3-12. https://doi.org/10.1007/s10433-007-0041-9

Appendices

Appendix 1: Ethical approval from Sheffield Hallam University

Rodrigues, Marcos [redacted] Tue, Aug 22, 2017, 11:58 AM

to me, Marcos, Reza, !

Dear Ojie,

I have reviewed your application for ethical clearance re. accelerometer-based diagnostics of vestibular dysfunctions

Approval is granted for stage 1 of the research, involving collecting data from selected SHU students and staff. As yo correctly assumed, a new application is required for stage 2 of the research.

Wishing you good luck with your research,

Kind regards,

Marcos A Rodrigues
FREC Joint Chair

Appendix 2: Informed consent in paediatric research

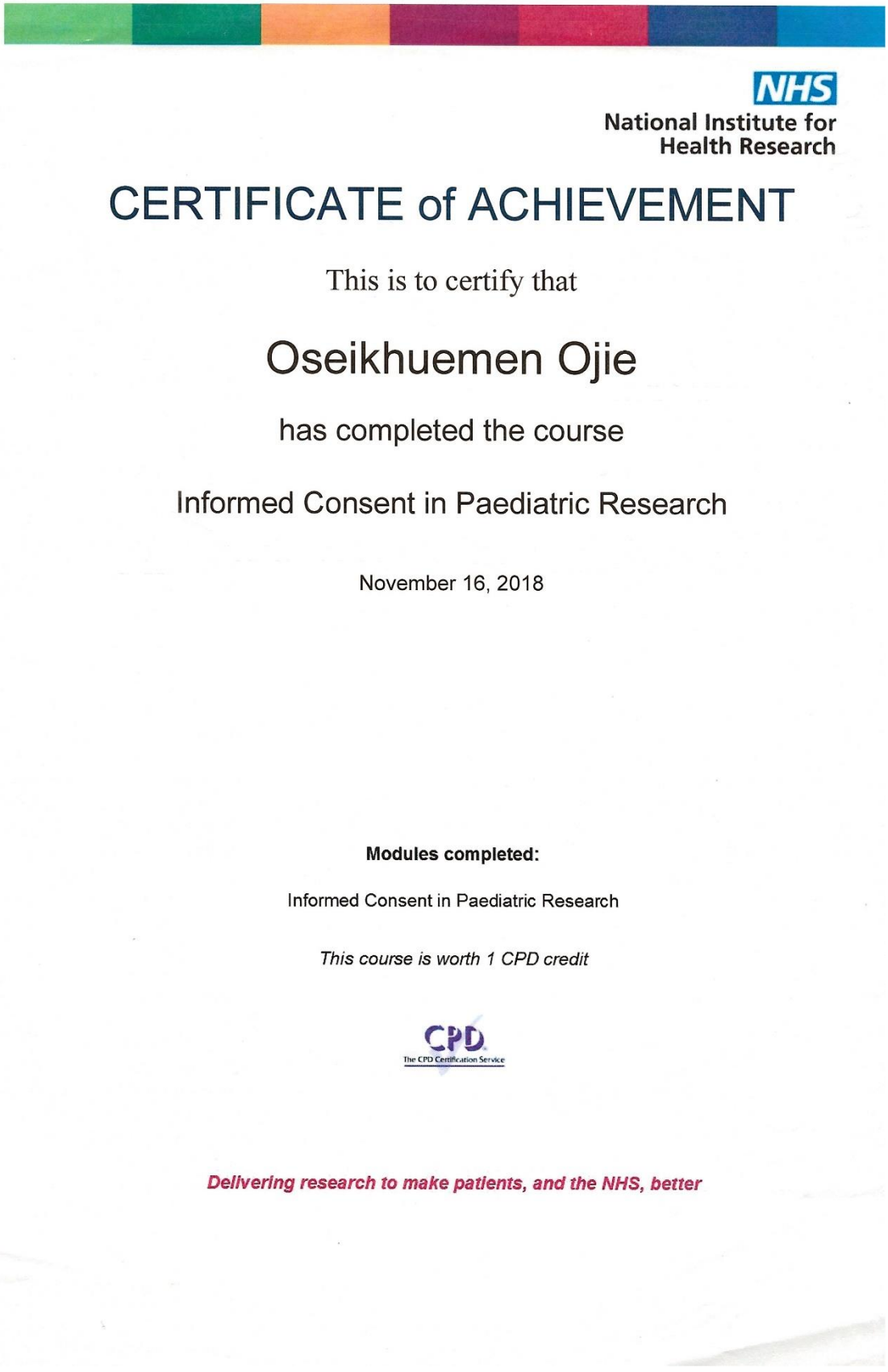

NHS
National Institute for Health Research

CERTIFICATE of ACHIEVEMENT

This is to certify that

Oseikhuemen Ojie

has completed the course

Informed Consent in Paediatric Research

November 16, 2018

Modules completed:

Informed Consent in Paediatric Research

This course is worth 1 CPD credit

CPD
The CPD Certification Service

Delivering research to make patients, and the NHS, better

Appendix 3: Introduction to good clinical practice eLearning (primary care)

NHS
National Institute for Health Research

CERTIFICATE of ACHIEVEMENT

This is to certify that

Oseikhuemen Ojie

has completed the course

Introduction to Good Clinical Practice eLearning (Primary Care)

November 16, 2018

A practical guide to ethical and scientific quality standards in clinical research

Including EU Directives, Medicines for Human Use (Clinical Trials) Regulations & the Department of Health UK Policy Framework for Health & Social Care Research, as applied to the conduct of Clinical Trials & other studies conducted in the NHS

Modules completed:

Introduction to Research and the GCP standards
Preparing to deliver your study
Identifying and recruiting participants: eligibility and informed consent
Ongoing study delivery and data collection
Safety Reporting
Study closure

This course is worth 4 CPD credits

CPD
The CPD Certification Service

Delivering research to make patients, and the NHS, better

Appendix 4: Research passport

CCRF children's clinical research facility
innovative & pioneering treatments for children

Sheffield Children's NHS Foundation Trust

D Floor Stephenson Wing
Sheffield Children's NHS Foundation Trust
Western Bank, Sheffield S10 2TH

Tel: 0114 226 7980 Fax: 0114 226 7844

www.sheffieldchildrenscrf.nhs.uk

22nd November 2018

Dear Davis Ojie

Letter of access for research: SCH-2335 – Vestibular Function Testing in Children Using Accelerometry

In accepting this letter, each participating organisation confirms your right of access to conduct research through their organisation for the purpose and on the terms and conditions set out below. This right of access commences on 22nd November 2018 and ends on 1st February 2021 unless terminated earlier in accordance with the clauses below.

You have a right of access to conduct such research as confirmed in writing in the letter of permission for research from Sheffield Children's Hospital. Please note that you cannot start the research until the Principal Investigator for the research projects you are involved with have received a letter from us giving confirmation from the individual organisation(s) of their agreement to conduct the research.

The information supplied about your role in research at the organisation(s) has been reviewed and you do not require an honorary research contract with the organisation(s). We are satisfied that such pre-engagement checks as we consider necessary have been carried out. Evidence of checks should be available on request to the organisation(s).

You are considered to be a legal visitor to the organisations premises. You are not entitled to any form of payment or access to other benefits provided by the organisation(s) or this organisation to employees and this letter does not give rise to any other relationship between you and the organisation(s), in particular that of an employee.

While undertaking research through the organisation(s) you will remain accountable to your substantive employer but you are required to follow the reasonable instructions of the organisation(s) or those instructions given on their behalf in relation to the terms of this right of access.

Where any third party claim is made, whether or not legal proceedings are issued, arising out of or in connection with your right of access, you are required to co-operate fully with any investigation by the organisation(s) in connection with any such claim and to give all such assistance as may reasonably be required regarding the conduct of any legal proceedings.

You must act in accordance with the organisations policies and procedures, which are available to you upon request, and the Research Governance Framework.

You are required to co-operate with the organisation(s) in discharging its/their duties under the Health and Safety at Work etc Act 1974 and other health and safety legislation and to take reasonable care for the health and safety of yourself and others while on the organisations premises. You must observe the same standards of care and propriety in dealing with patients, staff, visitors, equipment and premises as is expected of any other

contract holder and you must act appropriately, responsibly and professionally at all times.

If you have a physical or mental health condition or disability which may affect your research role and which might require special adjustments to your role, if you have not already done so, you must notify your employer and each organisation prior to commencing your research role at that organisation.

You are required to ensure that all information regarding patients or staff remains secure and *strictly confidential* at all times. You must ensure that you understand and comply with the requirements of the NHS Confidentiality Code of Practice and the Data Protection Act 1998. Furthermore you should be aware that under the Act, unauthorised disclosure of information is an offence and such disclosures may lead to prosecution.

You should ensure that, where you are issued with an identity or security card, a bleep number, email or library account, keys or protective clothing, these are returned upon termination of this arrangement. Please also ensure that while on the organisations premises you wear your ID badge at all times, or are able to prove your identity if challenged. Please note that the organisation(s) do not accept responsibility for damage to or loss of personal property.

This organisation may revoke this letter and any organisation(s) may terminate your right to attend at any time either by giving seven days' written notice to you or immediately without any notice if you are in breach of any of the terms or conditions described in this letter or if you commit any act that we reasonably consider to amount to serious misconduct or to be disruptive and/or prejudicial to the interests and/or business of the organisation(s) or if you are convicted of any criminal offence. You must not undertake regulated activity if you are barred from such work. If you are barred from working with adults or children this letter of access is immediately terminated. Your employer will immediately withdraw you from undertaking this or any other regulated activity and you MUST stop undertaking any regulated activity immediately.

Your substantive employer is responsible for your conduct during this research project and may in the circumstances described above instigate disciplinary action against you.

No organisation will indemnify you against any liability incurred as a result of any breach of confidentiality or breach of the Data Protection Act 1998. Any breach of the Data Protection Act 1998 may result in legal action against you and/or your substantive employer.

If your current role or involvement in research changes, or any of the information provided in your Research Passport changes, you must inform your employer through their normal procedures. You must also inform your nominated manager in each participating organisation and the R&D office in this organisation.

Yours sincerely

[redacted]

Dominic Nash
R&D Manager, Sheffield Children's NHS Foundation Trust

cc: HR department at Sheffield Children's NHS Foundation Trust
HR department of the substantive employer (and provider of honorary clinical contract, where applicable)

Appendix 5: Participant information sheet

Sheffield Hallam University

Participant Information Sheet

This information sheet is produced to outline the purpose of the study, why you were asked to participate, how you will be involved, what will happen to the recorded data and what will be the study's benefits. The information sheet highlights that participation in the study in completely on the voluntary basis and by no mean it will affect the way your injury is treated. You can ask questions before and after reading this information sheet.

1. **Study title**
   Computerised accelerometry for diagnosing vestibular dysfunctions

2. **Background to the study**
   We aim to develop a system to improve the assessment and diagnosis of human balance (vestibular) problems. These will lead to better understanding of the causes of the problems some people have in maintaining balance when standing still or walking.

   The current diagnosis methods are either subjective or require expensive equipment that are only available in specialised gait centres. In this study a portable and cost effective system to help clinicians better assess and diagnose balance problems will be developed. The system can be used in a larger number of centres as it is more cost effective and easier to operate. The system uses small sensors called inertia measurement units (IMUs). These sensors are placed on the body and measure the body's posture and movements.

   The test is harmless and does not cause any pain.

3. **Why you are asked me to take part?**
   Before we evaluate the system in a hospital, we need to have evidence of its suitability. We have collaboration for the study with a hospital. We would like to evaluate the system on adult volunteers in the University's laboratory before we carry out a more detailed evaluation in a hospital environment on patients. The university based evaluation will help us to be better prepared in the future hospital trials. You are approached as we thought you could help us with this study.

4. **What will you be required to do?**
   A member of research team (PhD student or his supervisor) will provide you with the study's information sheet to read. The researcher will also briefly summarises the content of the information sheet and invite you to ask any question you may have. If you are happy to participate, you are given a consent form. You need to read it carefully and if you still happy to participate, you need to sign it.

   The researcher places few (no more than 4), small (size of 1 pence coin) sensors on your body. You are then asked to make a few simple body movements for about 5 minutes and these movements are recorded. The sensors are then removed are you are free to go.

5. **Where will this take place?**
   The recording will take place in a SHU research laboratory.

6. **How often will I have to take part, and for how long?**
   You will only take part once. The recording is about 5 minutes. The complete test (including the time to explain the study, place and remove the sensors, etc.) will be about 20 minutes.

7. **When will I have the opportunity to discuss my participation?**
   Prior to signing the consent form you can ask any question you may have.

8. **Who will be responsible for all of the information when this study is over?**
   The study is subject to the University's Ethics regulations. The data are stored and processed in line with the University's Ethics guidance. Your identity will not be revealed in publications or reports emanating from this study. The person accountable for all issues related to this study is Prof. Reza Saatchi (Lecturer at SHU).

9. **Who will have access to it?**
   The data will be anonymised (by the PhD student or his director of studies), i.e. the recorded data are labelled by unique numbers. The researchers at SHU and authorised medical staff at the collaborating institution (Sheffield Children's Hospital) will have access to the anonymised data. The data will be analysed and published in various forms such as articles in journals, conferences, web sites, reports etc. In none of these publications your identity will be revealed.

10. **What will happen to the information when this study is over?**
    Once the data are analysed by the PhD student and his supervisory team based at Sheffield Hallam University and the collaborating institution, they will be published in various forms e.g. journals, conferences and reports.

    The data will be kept on a secure computer at Sheffield Hallam University for 10 years and then it will be destroyed.

11. **How will you use what you find out?**
    If we can demonstrate that the system is effective, we will further develop it so that it is ultimately commercialised and is used routinely by medical practitioners. If we find deficiencies in the system, we will develop ways to overcome them.

12. **Will anyone be able to contact me with what is recorded and reported?**
    No- all publications will be anonymised, i.e. your identity can not be determined from any of the publications.

13. **How long is the whole data recording is likely to last?**
    The actual data recording will be about 5 minutes, but by the time we go through the study with you, place the sensors and remove them etc. it will be about 20 minutes.

14. **How can I find out about the results of the study?**
    We will not directly inform you about the outcome of the study, but the findings will be published. Your identity however is not revealed. The test s not designed to provide diagnostic information and no diagnostic feedback will be provided to the participants with regard to the test outcome (however information can be published in an anonymised form).

15. **What if I do not wish to take part?**
    The participation in this study is completely voluntary.

16. **What if I change my mind during the study?**
    During the data recording we will immediately stop the recording if you tell us you desire to withdraw. After the recording, you can still tell us your wish to withdraw and we will do our best to realise this.

17. **Do you have any other questions?**
Please ask the staff handing out the information sheet if you have any question related to this study. They will be very happy to answer your questions.

18. **Details of who to contact with any concerns after the study.**

Prof. Reza Saatchi
Professor of Electronics (Medical Engineering)
Department of Engineering
Sheffield Hallam University
Sheaf Building
Howard Street
Sheffield
S1 1WB

Appendix 6: Participant consent form

Participant Consent forms

PARTICIPANT CONSENT FORM

Study title: Computerised accelerometry for diagnosing vestibular dysfunctions

To be completed by the participant:
Please answer the following questions by ticking the response box that applies or answering us verbally

	YES	NO
1. I have **read or listened** to the Information Sheet for this study and have had details of the study explained to me.	☐	☐
2. My questions about the study have been answered to my satisfaction and I understand that I may ask further questions at any point.	☐	☐
3. I understand that I am free to withdraw from the study within the time limits outlined in the Information Sheet, without giving a reason for my withdrawal or to decline to answer any particular questions in the study without any consequences to my future treatment by the researcher.	☐	☐
4. I agree to provide information to the researchers under the conditions of confidentiality set out in the Information Sheet.	☐	☐
5. I wish to participate in the study under the conditions set out in the Information Sheet.	☐	☐
6. I consent to the information collected for the purposes of this research study to be used for any other research purposes.	☐	☐
Personal data protection		
• I agree for the researcher to use my real name. I understand that in this case I will be identified as a participant in the research.	☐	☐
OR		
• I agree for the researcher to use a pseudonym when referring to the information I provide. I understand that in this case I won't be identified in the research.	☐	☐

Signature of participant: _____ **Date:** _____

Name of participant (block letters): _____

Signature of investigator(s): _____ **Date:** _____

Name of investigator(s) (block letters): _____

17/08/2017

Appendix 7: Filtering from the gyroscope and accelerometer sensor and sway parameters of some subjects.

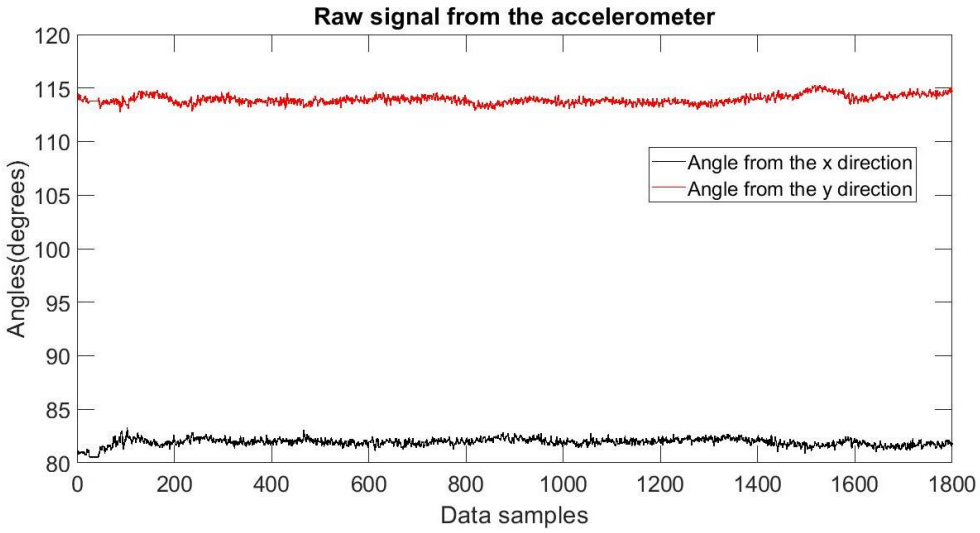

(a)

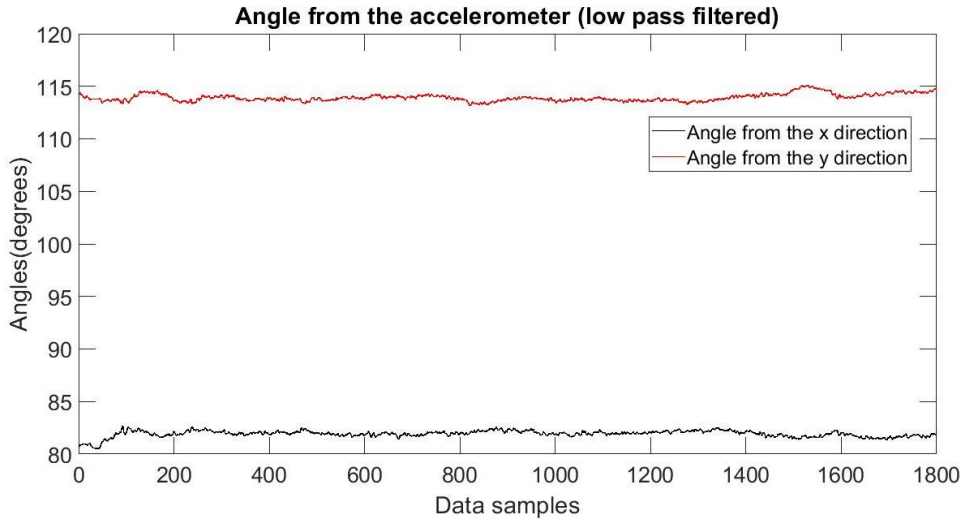

(b)

Figure 7.1. Angle of the accelerometer signal: (a) Raw signal (b) filtered signal.

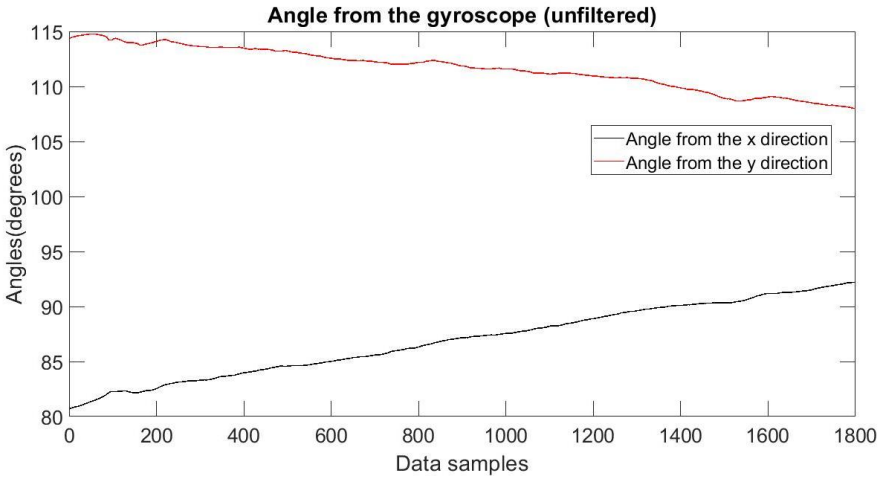

(a)

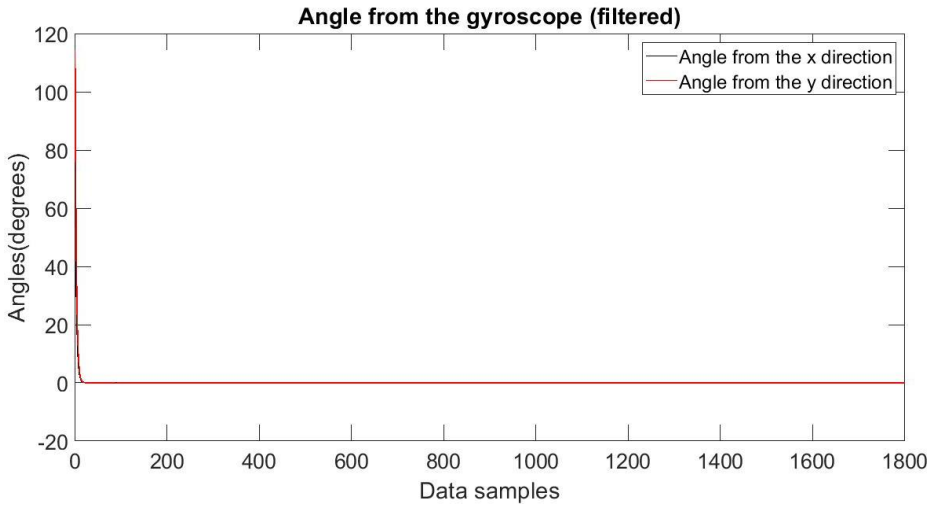

(b)

Figure 7.2. Angle of the gyroscope signal: (a) Raw integrated signal (b) filtered signal.

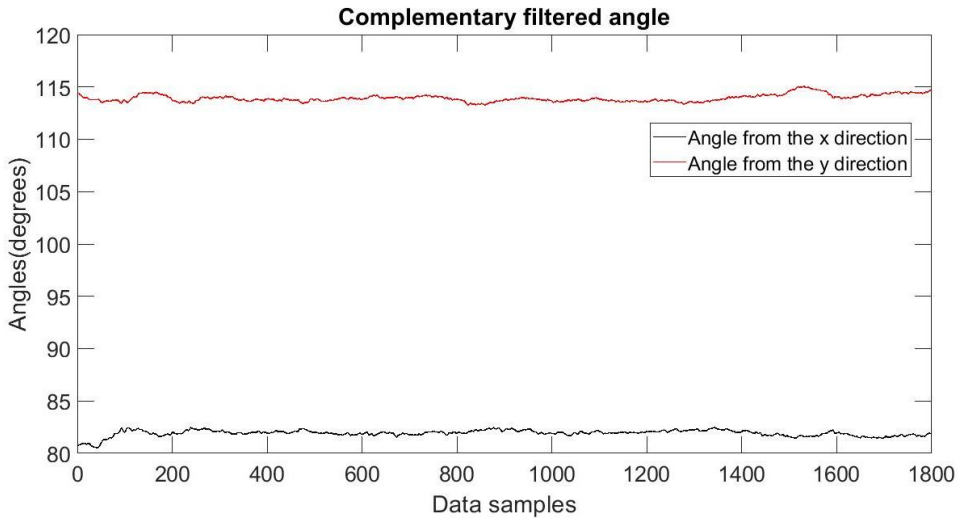

Figure 7.3. Angle of the complementary filter

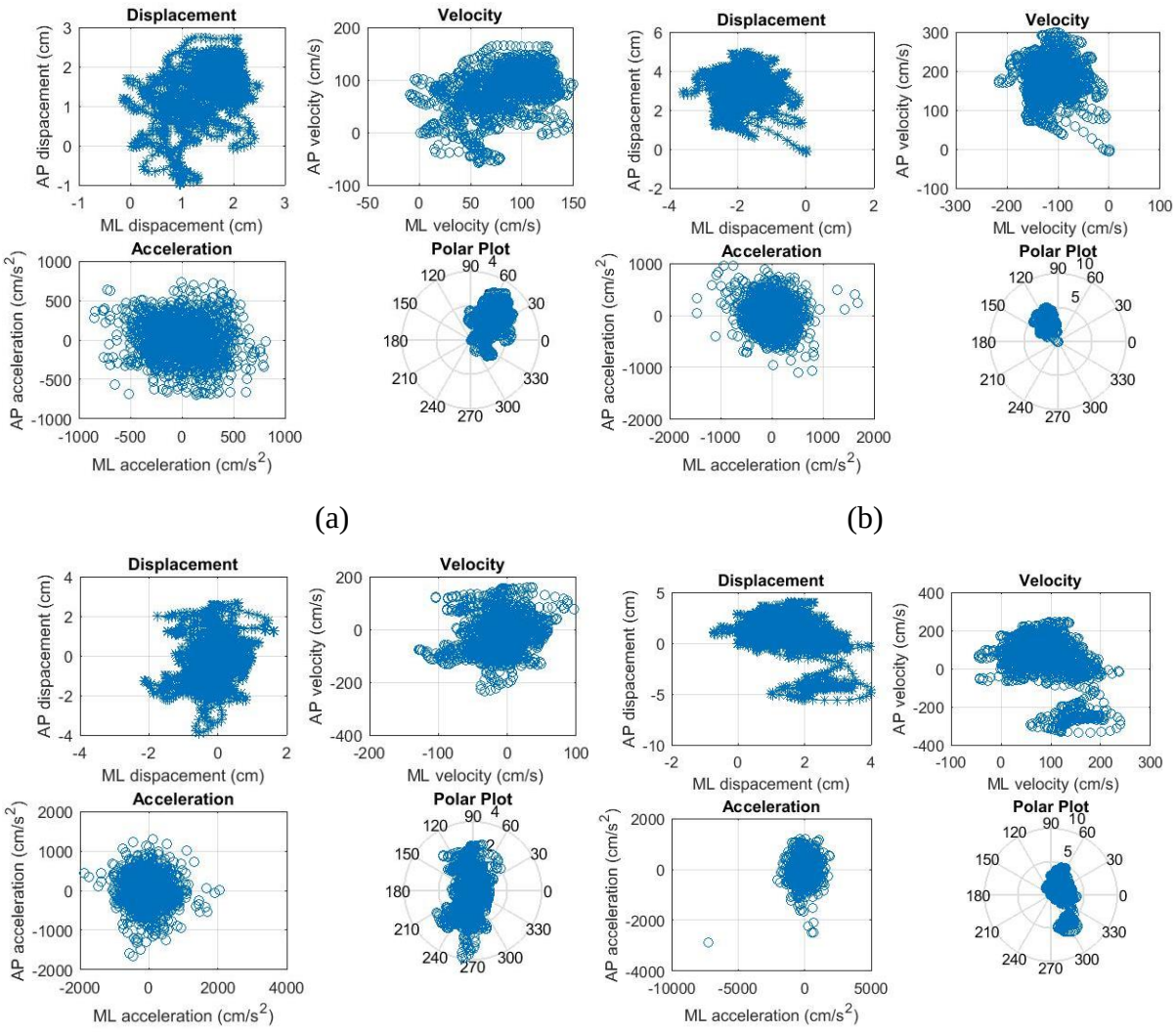

Figure 7.3. The mCTSIB conditions for subject 1: (a) condition 1, (b) condition 2, (c) condition 3 and (d) condition 4

The figure shows reduced values for the condition one, followed by condition two and three, with condition four showing the greatest amount of variation in values. There is more spread towards the ML direction for the displacement, velocity and acceleration in condition two than in condition three. This suggested that the removal of the visual system (condition 2) results in a greater change in the velocity of the ML direction. Similarly, more spread is seen in the AP direction for condition three than in condition two. This suggested that the proprioceptive system results in more AP spread.

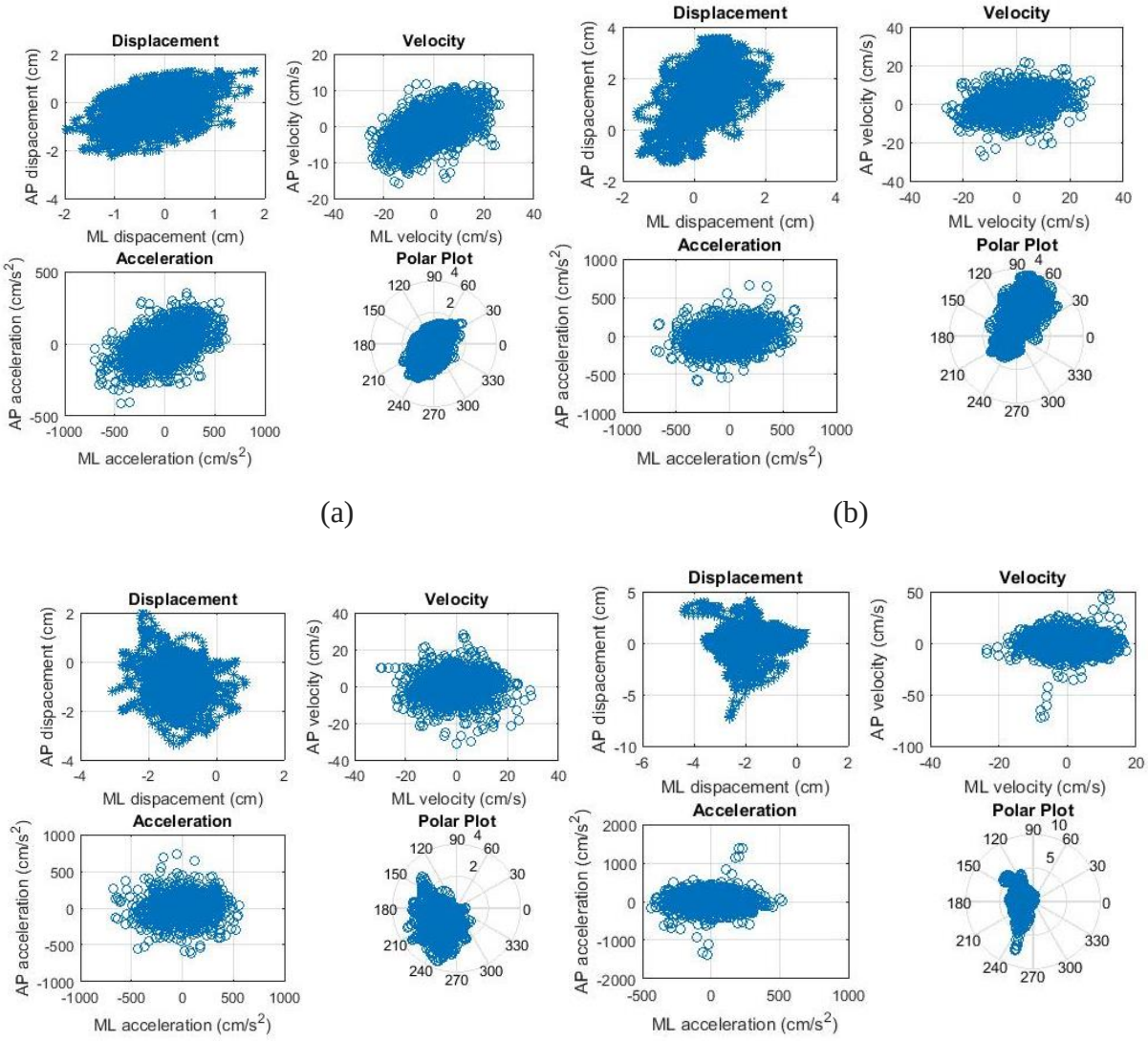

Figure 7.4. The mCTSIB conditions for subject 2: (a) condition 1, (b) condition 2, (c) condition 3 and (d) condition 4

Appendix 8: Box plot of the external measures for the clustering using the rms position and velocity

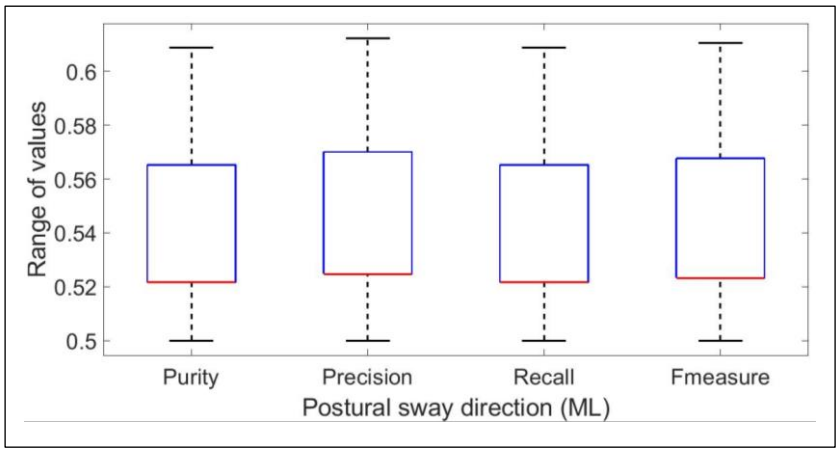

(a)

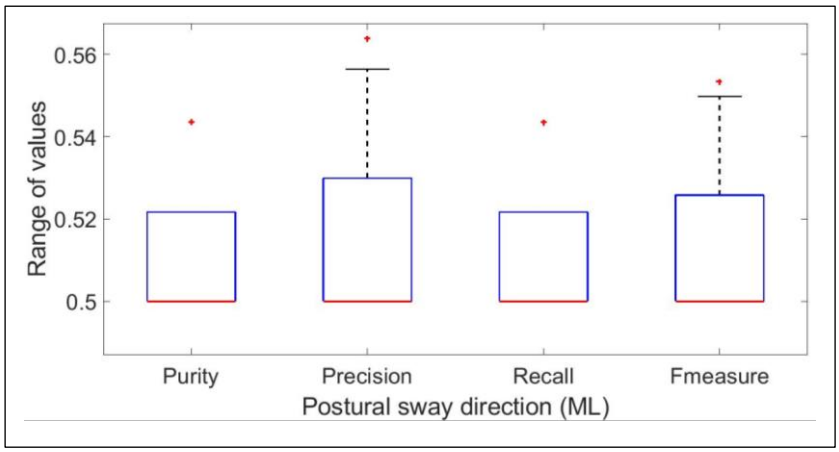

(b)

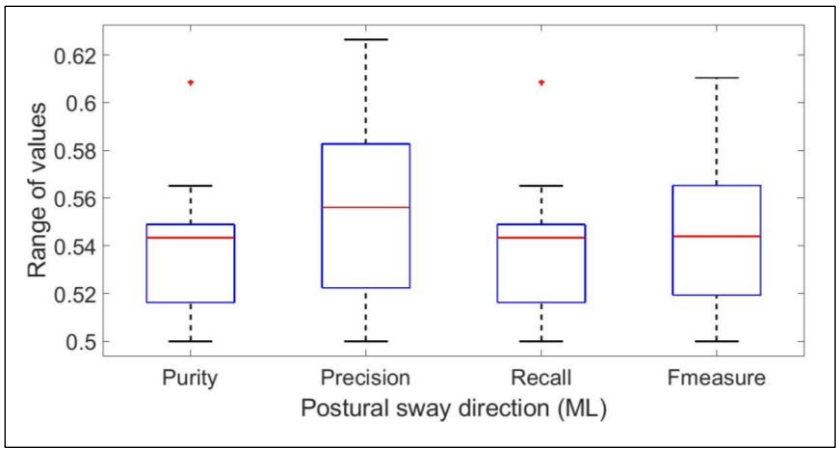

(c)

Figure 8.1. Box plot of the resulting clustering of the external measures for the ML direction, conditions: (a) 1 and 2 (b) 1 and 3 (c) 1 and 4. The red line indicates the median value

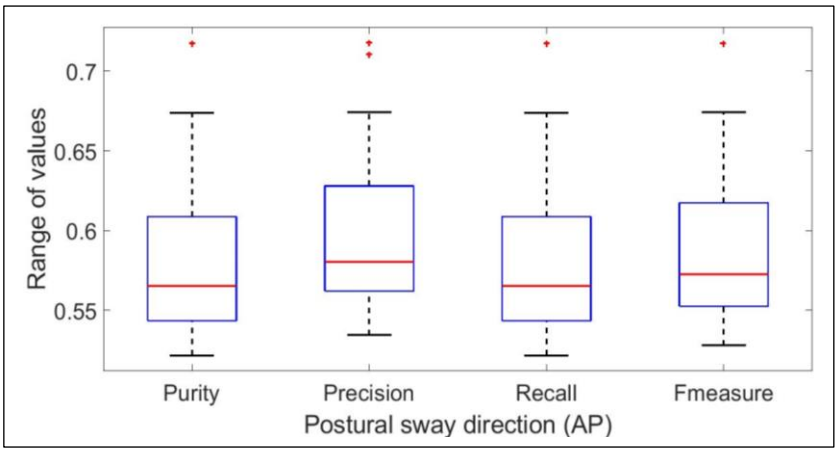

(a)

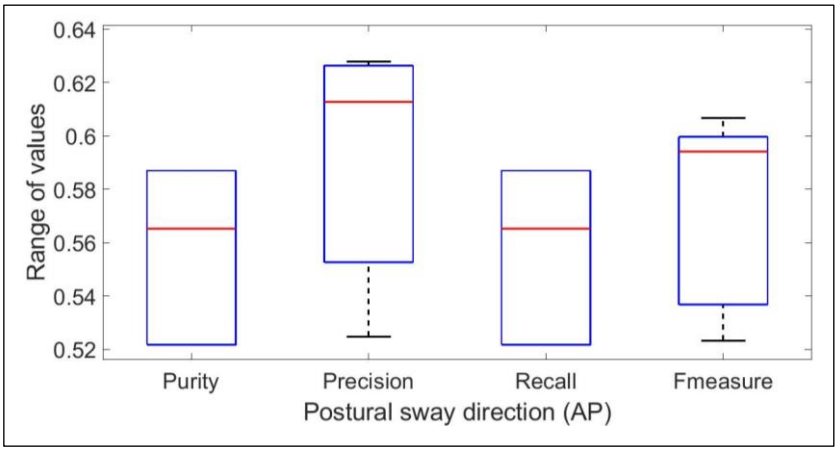

(b)

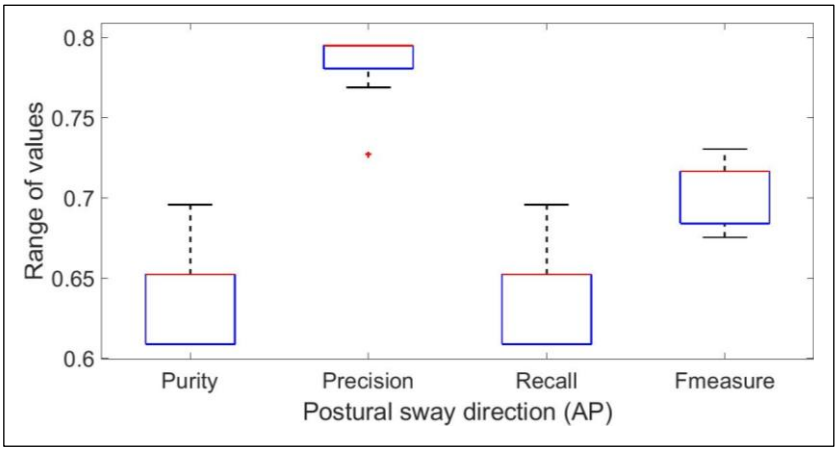

(c)

Figure 8.2. Box plot of the resulting clustering of the external measures for the AP direction conditions: (a) 1 and 2 (b) 1 and 3 (c) 1 and 4. The red line indicates the median value

Appendix 9: Kohonen clustering using rms position and velocity

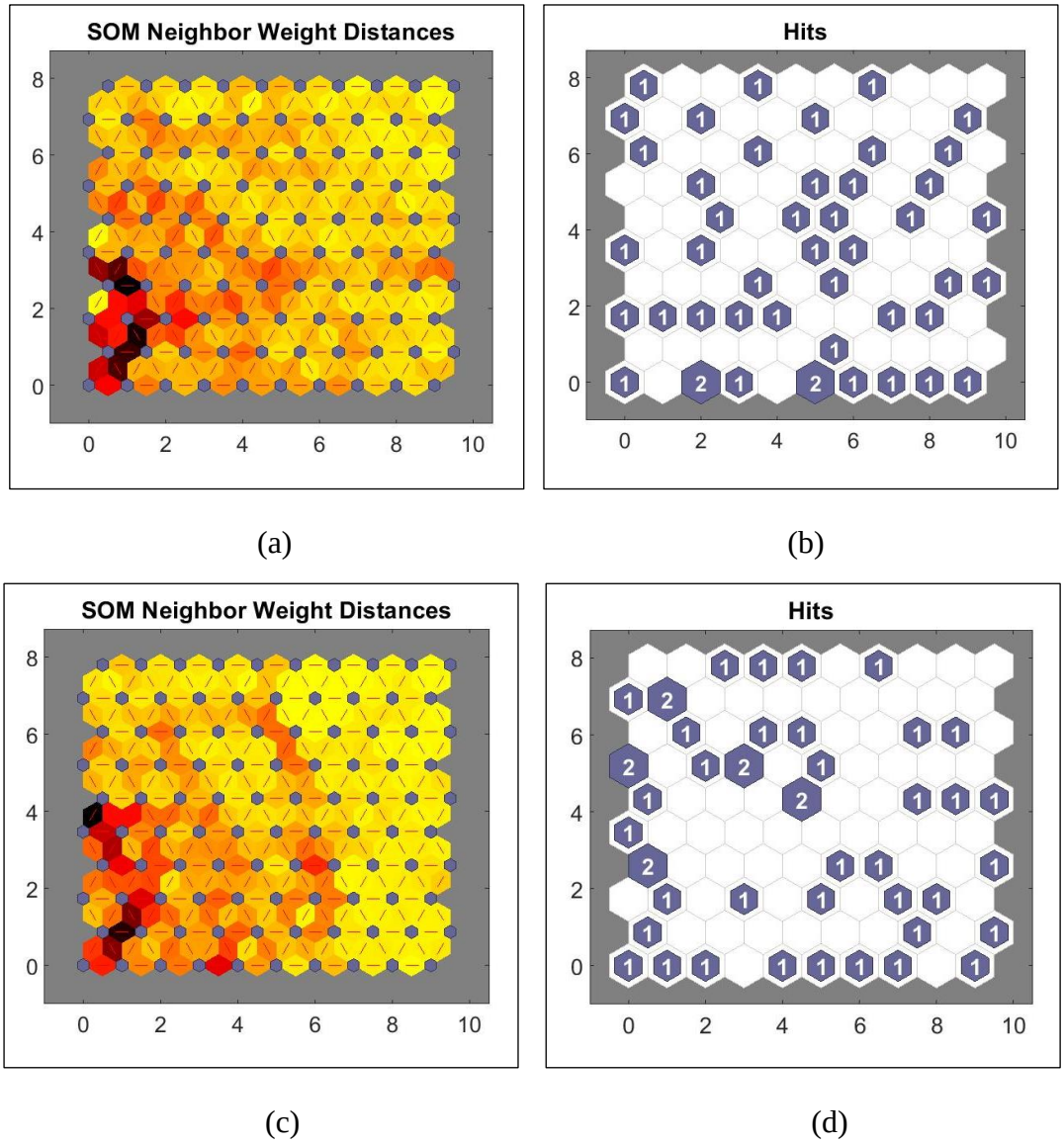

Figure 9.1. Plot of neighbourhood distance and input vector hits of conditions 1 and 2. (a,b) representing the AP direction, (c,d) representing the ML direction. The horizontal and vertical axes are neurons positions.

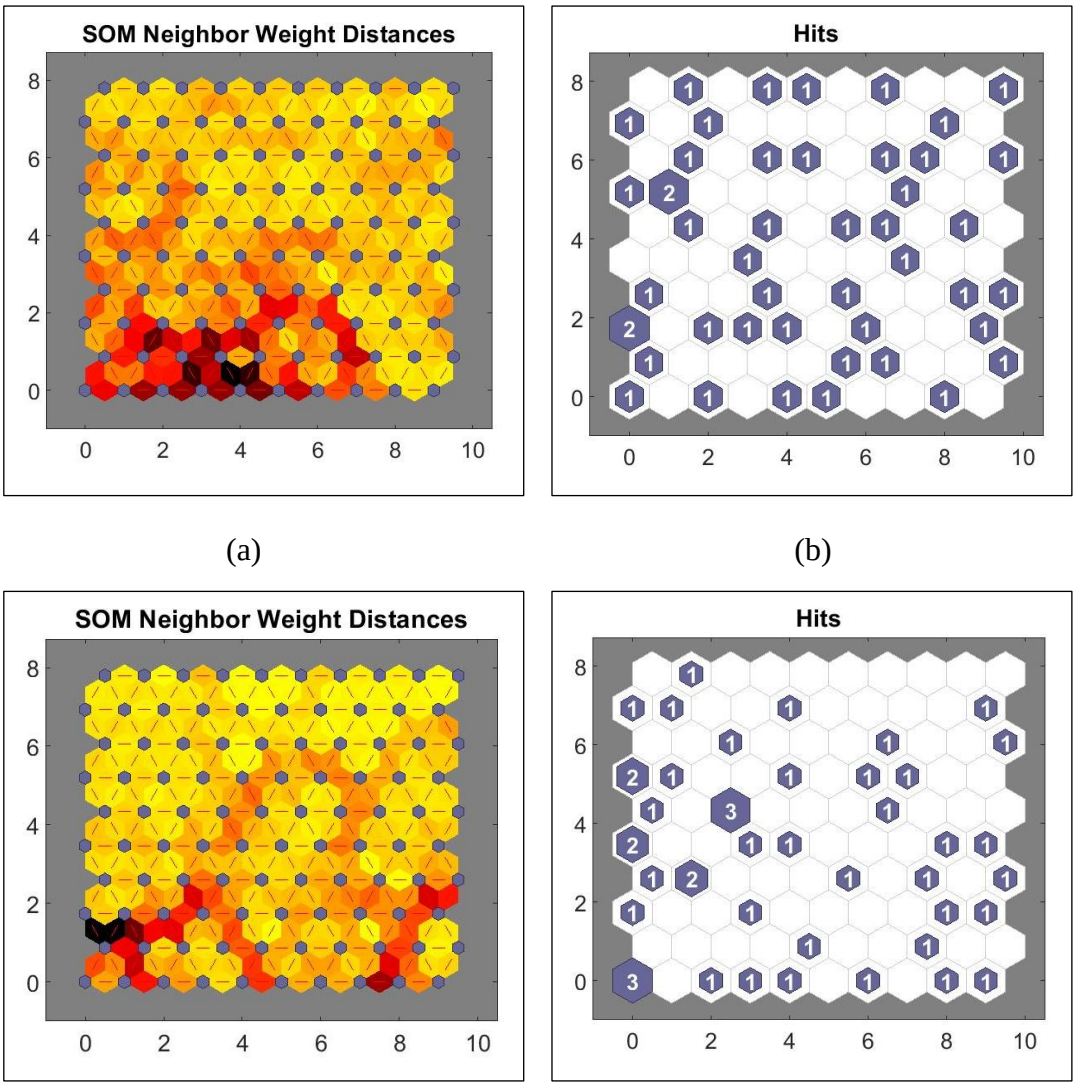

Figure 9.2. Plot of neighbourhood distance and input vector hits of conditions 1 and 3. (a,b) representing the AP direction, (c,d) representing the ML direction. The horizontal and vertical axes are neurons positions.

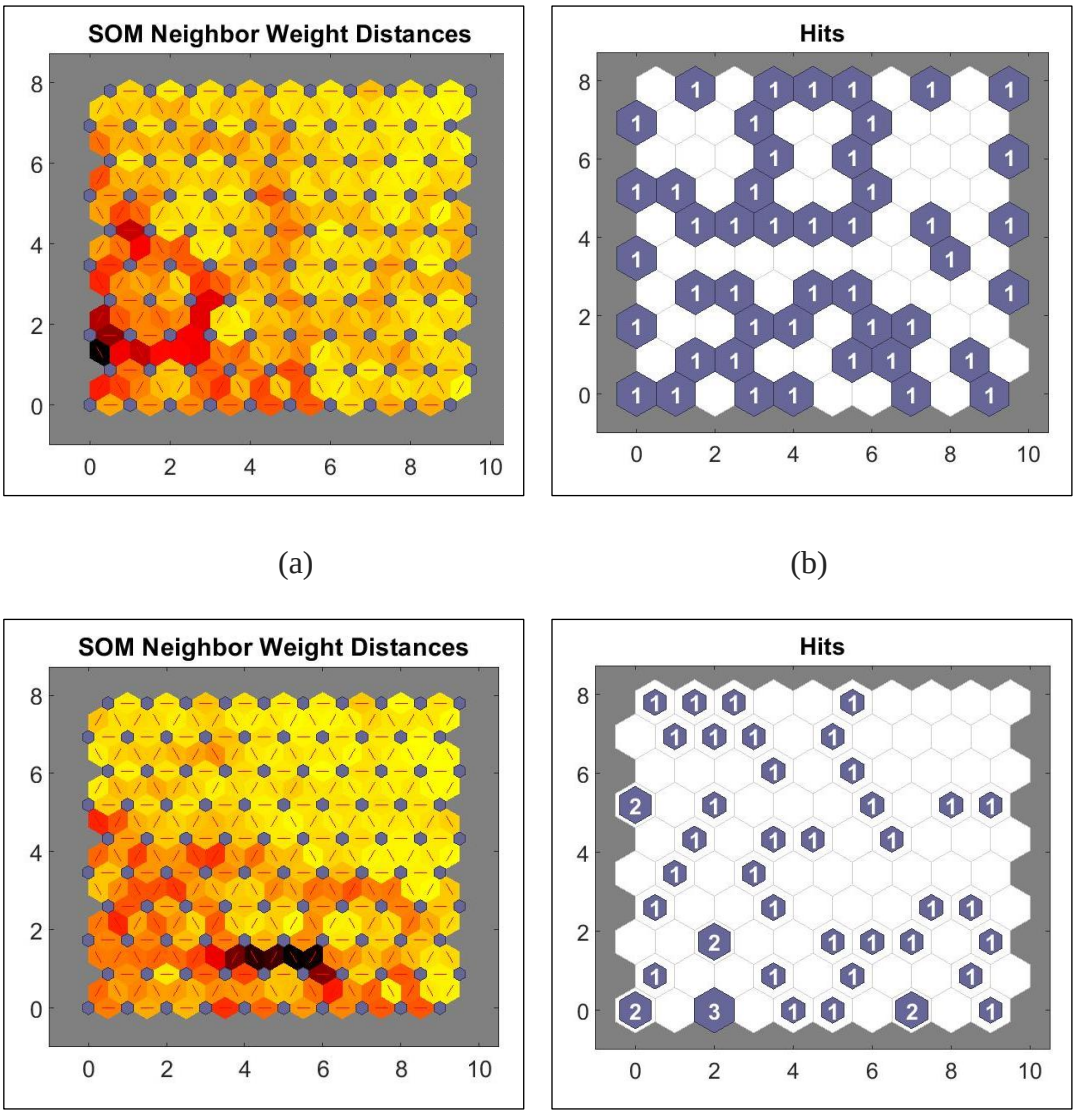

(a) (b)

(c) (d)

Figure 9.3. Plot of neighbourhood distance and input vector hits of conditions 1 and 4. (a,b) representing the AP direction, (c,d) representing the ML direction. The horizontal and vertical axes are neurons positions.